Die Bedeutung des Purinstoffwechsels auf die Proliferation von Gliazellen nach der neuronalen Schädigung

Dissertation

zur Erlangung des akademischen Grades
Doktor der Medizin (Dr. med.)

vorgelegt
der Medizinischen Fakultät
der Martin-Luther-Universität Halle-Wittenberg

von Joshua Marvin Kleine

Betreuer:	Prof. Dr. med. Faramarz Dehghani
	Prof. Dr. med. Julian Prell
Gutachter:	Prof. Dr. Thomas Arendt, Leipzig
	Prof. Dr. Lars Fester, Bonn

Datum der Verteidigung: 30.09.2024

Referat

Akute neuronale Schädigungen wie der Schlaganfall oder die Schädel-Hirn-Trauma führen oft zu bleibenden fokalen Defiziten der Betroffenen. Durch den primären Schaden einer akuten neuronalen Läsion kommt es zu einer Aktivierung von schädlichen wie auch protektiven zellulären und biochemischen Kaskaden. Diesen folgt ein Sekundärschaden mit inflammatorischen Komponenten, welcher zu einem Läsionswachstum beiträgt. Mycophenolat-Mofetil (MMF), als selektiver Inhibitor der Inosin-5'Monophosphatdehydrogenase 2 (IMPDH-Isoform 2) und ein Schlüsselenzym des Purinstoffwechsels, zeigte bereits in verschiedenen Modellen akuter neuronaler Läsionen einen positiven Einfluss auf den Verlauf der Schädigung. Es wurde hier geprüft, ob MMF die Neuroinflammation moduliert, einen Einfluss auf die Proliferation und Zytokinproduktion von Astrozyten und Mikroglia besitzt und seine Effekte zeitabhängig entfaltet. Des Weiteren erfolgten die nähere Charakterisierung des protektiven Zeitfensters, die Analyse der IMPDH-Isoform 2 als molekulare Zielstruktur sowie Untersuchungen Mikroglia-unabhängiger Effekte von MMF in organotypischen hippocampalen Schnittkulturen (OHSC) und primären Zellkulturen. Zur Analyse Mikroglia-unabhängiger Effekte wurden diese durch Bisphosphonat-Clodronat aus den OHSC depletiert. Darüber hinaus sollte das ermittelte Zeitfenster in einem traumatischen *in vivo* Modell überprüft werden. Es fand sich, dass die für MMF beschriebenen Effekte auf einer frühen Mikroglia-vermittelten Phase sowie einer späteren möglichen astrozytären Phase beruhen. Eine Applikation von MMF innerhalb der ersten 8-12 Stunden und bis höchstens 36 Stunden nach der Schädigung zeigte protektive Effekte in OHSC. Eine Stimulation durch Lipopolysaccharide in primären Mikroglia oder Astrozyten hatte keinen Einfluss auf die Expression der IMPDH-Isoform 2. Zwar konnte für MMF ein genereller Effekt *in vivo* nach 14 Tagen nachgewiesen werden, eine Translation des neurozytoprotektiven Zeitfensters von den OHSC zeigte *in vivo* jedoch keine signifikanten Effekte auf das Läsionsvolumen nach traumatischer Schädigung.

Zusammenfassend deckt sich die in den OHSC beschriebene Mikroglia-abhängige Phase mit dem nachgewiesenen effektiven Zeitfenster zwischen 8-36 Stunden. Ein zellspezifisches Wirkungsspektrum durch MMF in diesem Zeitfenster ist daher in den OHSC anzunehmen. Nach 72 Stunden scheinen Astrozyten hier ebenfalls eine zunehmende Rolle zu spielen.

Joshua Marvin Kleine: Die Bedeutung des Purinstoffwechsels auf die Proliferation von Gliazellen nach neuronaler Schädigung, Halle (Saale), Univ., Med. Fak., Diss., 30 Seiten, 2024

Inhaltsverzeichnis

Abkürzungsverzeichnis .....

1. Einleitung 1

1.1 Neuronaler Schaden 1

1.1.1 Mikroglia 3

1.1.2 Astrozyten 4

1.1.3 Exzitotoxizität 5

1.1.4 Oxidativer und nitrosaminer Stress 6

1.2 Neuroinflammation 7

1.2.1 Aktivierung von Mikroglia 8

1.2.2 Reaktive Astrogliose 9

1.3 Organotypische hippocampale Schnittkulturen (OHSC) 10

1.3.1 Anwendungsgebiete der OHSC 11

1.3.2 Neurozytoprotektion durch Endocannabinoide und Nimodipin 11

1.4 Purinstoffwechsel und die Zellteilung 13

1.4.1 Zellzyklus und Zellteilung 13

1.4.2 Purinstoffwechsel 14

1.4.3 Inosin-5'Monophosphatdehydrogenase (IMPDH) 15

1.4.4 Inhibition der IMPDH durch Mycophenolat-Mofetil (MMF) 15

1.5 Neurozytoprotektive Effekte von MMF 16

2. Diskussion 18

2.1 Das Modell der organotypischen hippocampalen Schnittkulturen (OHSC) 18

2.1.1 Vorteile, methodische Limitationen und neue Anwendungsgebiete der OHSC 18

2.1.2 Neurozytoprotektive Effekte von 2-AG, PEA und Nimodipin in OHSC 19

2.1.3 Translationale Forschung als Schlüsselstelle in der Neurozytoprotektion? 21

2.2 Immunmodulation als ein neurozytoprotektives Konzept 22

2.3 MMF und dessen neurozytoprotektive Eigenschaften 23

2.3.1 Mikroglia als vermittelnde Zellen der Effekte von MMF 24

2.3.2 Mikroglia-unabhängige Effekte von MMF 25

2.3.3 Der Einfluss von MMF auf NO und die Zytokinproduktion....26
2.3.4 Zeitabhängige Effekte von MMF....27
2.4 Die Bedeutung des Purinstoffwechsels auf die Proliferation von Gliazellen nach neuronaler Schädigung....28
3. Literaturverzeichnis....31
4. Thesen....52
5. Publikationen....53
5.1 Hinweis zur vorliegenden Genehmigung der Verlage....54
6. Erklärungen....
7. Danksagungen....

Abkürzungsverzeichnis

Δ9-THC	Tetrahydrocannabinol
2-AG	2-Arachidonylglycerol
Abn-CBDR	Abnormal-Cannabidiol-bezeichneter Rezeptor
ADP	Adenosindiphosphat
AEA	Arachidonylethanolamid
ALS	Amyotrophe Lateralsklerose
AMP	Adenosinmonophosphat
AMPA	α-amino-3-hydroxy-5-methyl-4-Isoxazolepropionische Säure
ATP	Adenosintriphosphat
BBB	Blut-Hirn-Schranke
BDNF	Hirneigene neutrotrophe Faktor
BrdU	Bromdesoxyuridin
CA	Cornu ammonis
Ca^{2+}	Calciumionen
CAPS	Cryoporin-assoziiertes periodisches Syndrom
CB	Cannabinoid
CBD	Cannabidiol
CCI	Standardisiertes kortikales Traumamodell
CDK	Cyclin-abhängige Kinasen
Clo	Bisphosphonat-Clodronat
DAMPS	Gefahrenassoziierte molekulare Muster
DG	Gyrus dentatus
EC	Entorhinaler Kortex
FAAH	Fettsäureamid-Hydrolase
FOXO	Forkhead-Box-Protein O
GABA	Gamma-Aminobuttersäure
GALST	Glutamat-Aspartat-Transporter
GFAP	Saures Gliafaserprotein
GLT-1	Glutamat-Transporter-1
GM-CSF	Granulozyten/Monozyten-Kolonie stimulierender Faktor
HMGB1	High-Mobility-Group-Protein B1
HSPs	Hitze-Schock-Protein
IB_4	Griffonia Simplicifolia Isolectin B_4
Iba1	Ionisiertes Calcium-bindende Adaptermolekül
IL-1	Interleukin-1
IL-6	Interleukin-6
IMP	Inosinmonophosphat
IMPDH	Inosin-5'Monophosphatdehydrogenase
IRF-1	Interferon regulierender Faktor 1
LPS	Lipopolysaccharide
M-CSF	Makrophagen-Kolonie stimulierender Faktor
MMF	Mycophenolat-Mofetil
MPS	Mycophenolatsäure
MS	Multiple Sklerose
mTOR	In Säugetieren vorkommendes Ziel von Rapamycin
MyD88	Primäres Antwortprotein 88 der myeloiden Differenzierung
NF-κB	Nukleärer Faktor kappa B
NGF	Nervenwachstumsfaktor
NLR	NOD-Like-Rezeptor
NMDA	N-Methyl-D-Aspartat
NO	Stickoxid
NOS	Stickoxid-Synthetase
Nrf2	Nukleärer erythroider Faktor 2
OHSC	Organotypische hippocampale Schnittkulturen

ORC	Oxidative regenerierte Zellulose
PAMPS	Pathologieassoziiertes molekulares Muster
PEA	Palmitoylethanolamid
PI	Propidium Iodid
PI3K	Phosphoinositid-3-Kinase
PPAR-Alpha	Peroxisomen Proliferations-aktivierender Rezeptor-Alpha
PRPP	Phosphoribosylpyrophosphat
PRR	Muster-Erkennungs-Rezeptoren
RNA	Ribonukleinsäure
SHT	Schädel-Hirn-Trauma
STAIR	Stroke Treatment Academic Industry Roundtable
STAT3	Signalgeber und Aktivator der Transkription 3
TGF-Beta	Transformierender Wachstumsfaktor-Beta
TLR	Toll-Like-Rezeptoren
TNF-Alpha	Tumornekrosefaktor Alpha
TRAPS	Tumornekrosefaktor-Alpha assoziiertes periodisches Syndrom
TrkA	Tropomyosinrezeptorkinase A
TRPV	Transiente Rezeptor-Potential-Kationenkänale der Unterfamilie V
UDP	Uridindiphosphat
UTP	Uridintriphosphat
XMP	Xanthosinmonophosphat
ZNS	Zentrales Nervensystem

1. Einleitung

Der Schlaganfall und traumatische Läsionen des zentralen Nervensystems (ZNS) stellen vorherrschende Ursachen für fokal-neurologische Ausfälle, kognitive Defizite sowie ein Hauptrisiko für eine eingeschränkte Partizipation im Alltag dar (Carandang et al., 2006; Maas et al., 2008). Global wurde der Schlaganfall als die zweithäufigste Todesursache im Jahr 2019 angegeben, und auch bei Menschen unter 70 Jahren steigt die Inzidenz zunehmend an (Feigin et al., 2021). Trotz großer Fortschritte in der Akutbehandlung profitieren nicht alle Patient:innen, so dass sie in Folge des Schlaganfalls oder Schädel-Hirn-Traumas (SHT) mit bleibenden neurologischen Defiziten sowie mit deutlichen Einschränkungen der Lebensqualität rechnen müssen (Nogueira et al., 2018; Feigin et al., 2021). Es ist deshalb wichtig, nach neuen potenziellen Möglichkeiten und therapeutischen Ansätzen zu suchen (Chamorro et al., 2016). Besonders zelluläre sowie interzelluläre Pathomechanismen neuronaler Läsionen und die dabei entstehende Neuroinflammation sind wichtige Ansatzpunkte für mögliche neurozytoprotektive Behandlungen (Nedergaard and Dirnagl, 2005). Die Entwicklung und Nutzung präklinischer Modelle spielt für das Verständnis der pathologischen Prozesse des neuronalen Schadens eine wichtige Rolle. Ein besonders etabliertes Modell für die Untersuchung der Zellen im Nervengewebe und der Prüfung verschiedener Medikamente und deren Wirkung stellen organotypische hippocampale Schnittkulturen (OHSC) dar (Grabiec et al., 2017).

1.1 Neuronaler Schaden

Bereits Cajal verstand Neurone als die grundlegende Funktionseinheit des ZNS. Diese Zellen sind großteils post-mitotisch, was einerseits die Voraussetzung zum Aufbau und zur Aufrechterhaltung der neuronalen Netzwerke bildet, andererseits aber eine eingeschränkte Regenerationsfähigkeit bedingt. Die neuronale Plastizität und die damit verbundene Eigenschaft, verlorene Funktionen durch benachbarte Areale zu übernehmen, stellt daher eine grundlegende Voraussetzung für den teilweisen Wiedergewinn zentraler Fähigkeiten dar (Holtmaat and Svoboda, 2009; Dimyan and Cohen, 2011; Qiao et al., 2023). Das therapeutische Dogma lautet daher, so viele neuronale Zellen wie möglich zu schützen und zu erhalten, um irreversible Schäden mit bleibenden Behinderungen der Patient:innen zu verhindern oder zu minimieren. Häufige Ursachen für akute neuronale Schädigungen stellen das SHT und der Schlaganfall dar (Maas et al., 2008; Feigin et al., 2016; Feigin et al., 2021). Aufgrund der ausgeprägten Heterogenität der Schädigung durch ein SHT erschwert dies reproduzierbare Studien wie auch eine adäquate Therapie (Balestreri et al., 2004; Mohammadifard et al., 2018). Zunehmend ist auch ein Anstieg der Inzidenz des Schlaganfalls zu beobachten (Kissela et al., 2012; Feigin et al., 2021). Die akute Schädigung durch solch ein Ereignis, sei es ischämischer oder traumatischer Natur, führt zu einem irreversiblen Verlust von Gliazellen und Neuronen, welcher unter dem Begriff des primären Schadens subsumiert wird (Dirnagl et al., 1999). Diesem folgt eine sehr

komplexe Antwort von intrinsischen und extrinsischen ineinandergreifenden zellulären wie biochemischen Kaskaden, welche unter dem Begriff des sekundären Schadens zusammengefasst werden (Chamorro et al., 2016; Cao et al., 2020). Sowohl der primäre als auch der sekundäre Schaden sind für den Schlaganfall und das SHT bereits detailliert beschrieben (Dirnagl et al., 1999; Jassam et al., 2017; Datta et al., 2023). Der sekundäre Schaden führt dabei zu einer Ausbreitung der Läsion durch Destruktion von bereits vulnerablen Neuronen in periläsionalen Arealen (Dirnagl et al., 1999; Jassam et al., 2017). Diese Progression entwickelt sich in einem Zeitraum von Stunden bis Wochen (**Abb. 1**). Zeitlich lassen sich bestimmte Elemente wie die Exzitotoxizität, die Entstehung von oxidativem Stress und die Aktivierung verschiedener Zellen des ZNS, unter anderem der Mikroglia und Astrozyten, infolge einer Neuroinflammation einordnen (Kunz et al., 2010).

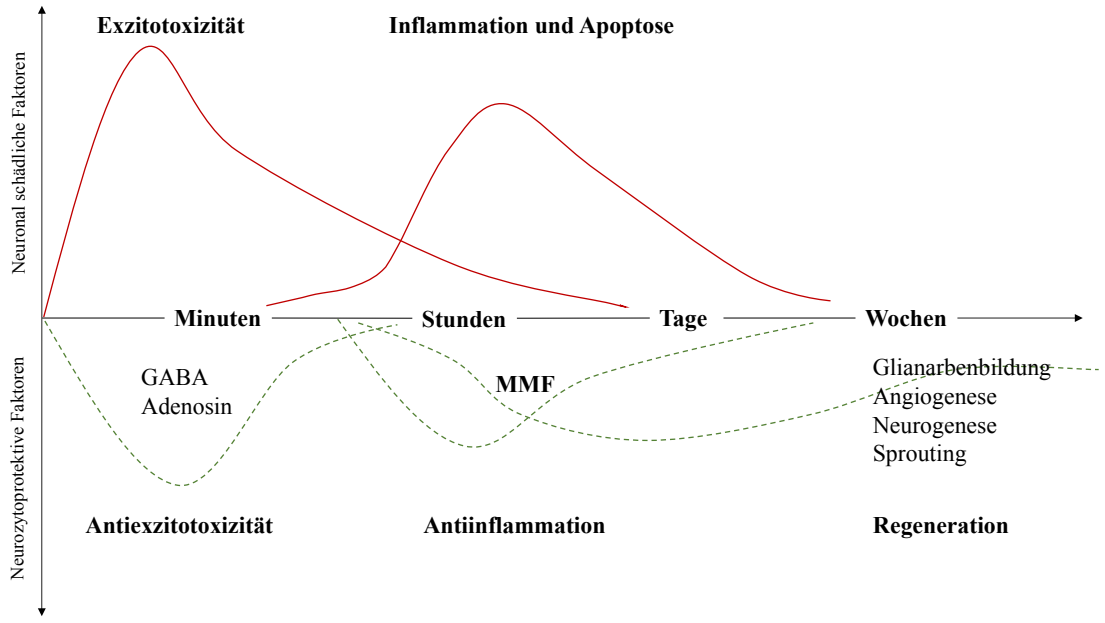

Abb. 1: Modifizierte Darstellung des sekundären Schadens nach Dirnagl et al. 1999. In Rot sind schädliche Einflüsse auf neuronale Zellen dargestellt. In Grün protektive Einflüsse, welche den schädlichen Prozessen entgegenwirken. Minuten nach der Schädigung überwiegt zu einem großen Teil die Exzitotoxizität gefolgt von oxidativem Stress. Es schließen sich neuroinflammatorische Prozesse an, welche Stunden bis Tage anhalten können.

Aufgrund der höheren Heterogenität des primären Schadens bei SHT variieren sekundäre Kaskaden mehr als bei einem ischämischen Schlaganfall (Maas et al., 2008; Ng and Lee, 2019). Der primäre Schaden wird hier maßgeblich durch eine begleitende Ischämie/Hypoxie, hämorrhagische Komponente, Hämatome sowie eine diffuse axonale Verletzung beeinflusst (Maas et al., 2008). Der folgenden inflammatorischen Komponente kommt insbesondere bei Kontusionsverletzungen, mit einem Anteil von 60% am sekundären Schaden, eine große Bedeutung zu (Maas et al., 2008). Durch eine Schädigung der Blut-Hirn-Schranke (BBB) und kleine Mikroblutungen kommt es neben der Migration peripherer Immunzellen zu einer

Expression von Hitze-Schock-Proteinen (HSPs) sowie dem High-Mobility-Group-Protein B1 (HMGB1) (Zheng et al., 2022). Eine Aktivierung der Mikroglia via nukleären Faktor kappa B (NF-κB) (Sun et al., 2020) und die Freisetzung von inflammatorischen Zytokinen sind die Folgen (Jassam et al., 2017). Neuroinflammatorische Prozesse finden sich in allen Phasen ischämischer oder traumatischer Schädigungen, angefangen bei einer frühen Freisetzung von Adenosintriphosphat (ATP) bis hin zu den späten regenerativen Prozessen (Jassam et al., 2017; Stoll and Nieswandt, 2019). Eine exakte Analyse der pathophysiologischen molekularen Kaskaden sowie der zellulären Integrationen von Mikroglia und Astrozyten am sekundären Schaden ist daher Grundlage für mögliche therapeutische Ansätze.

1.1.1 Mikroglia

Mikroglia machen ca. 5% der Gliapopulation aus und repräsentieren die ortsständigen Immunzellen des ZNS. Im Gegensatz zu anderen Gliazellen mit phylogenetischer neuroektodermaler Herkunft stellen Mikroglia nach aktuellem Stand eine sich eigenständig im ZNS regenerierende, aus dem Dottersack pränatal migrierende, Zellpopulation dar (Ginhoux et al., 2010; Ginhoux and Jung, 2014; Ginhoux and Garel, 2018). Unter physiologischen Bedingungen sind Mikroglia an zahlreichen Funktionen wie der Entwicklung des ZNS, der Neurogenese, dem Strukturerhalt der Synapsen und der Aufnahme immunologischer Aufgaben infolge diverser Pathologien beteiligt (Kettenmann et al., 2011; Casano and Peri, 2015; Wolf et al., 2017; Basilico et al., 2022; Whitelaw et al., 2023). Die Aktivierung durch eine pathologische Veränderung erfolgt über eine Vielzahl von Oberflächenrezeptoren der Mikroglia (Kettenmann et al., 2011; Jadhav et al., 2023; Wang et al., 2023b). Zum Großteil können diese unter dem Begriff der Muster-Erkennungs-Rezeptoren (PRRs) subsumiert werden. Zu dieser Gruppe lassen sich unter anderem die Familie der Toll-Like-Rezeptoren (TLR) (Bsibsi et al., 2002; Fitzgerald and Kagan, 2020) und die NOD-Like-Rezeptoren (NLR) (Shiau et al., 2013) zuordnen. Diese sind in der Lage, sogenannte gefahrenassoziierte molekulare Muster (DAMPS) wie Lipopolysaccharide (LPS) bei bakteriellen Infektionen oder auch pathologieassoziierte molekulare Muster (PAMPS) bei einem erhöhten zellulären Untergang zu erkennen (Jounai et al., 2013; Fitzgerald and Kagan, 2020). Dabei ist die Stimulation der Mikroglia durch LPS über den TLR-4 gut erforscht und stellt eine gängige Methode der Aktivierung in Zellkultur dar (Poltorak et al., 1998; Wu et al., 2022). Die Stimulation der TLR-4 erfolgt dabei unter anderem durch endogene Liganden wie HMGB1, HSPs und Protein S100 (Yu et al., 2010). An der Transduktion von TLR-4 unterscheidet man frühe von primärem Antwortprotein 88 der myeloiden Differenzierung (MyD88) abhängige Antworten und MyD88-unabhängige spätere Antworten (O'Neill, 2003; Leitner et al., 2019; Heidari et al., 2022; Wu et al., 2022). MyD88-abhängige Signalwege führen unter anderem zu einer Aktivierung von NF-κB, welche wiederum zu einer Erhöhung von Zytokinen wie Interleukin-1 (IL-1), Interleukin-6 (IL-6) oder Tumornekrosefaktor

(TNF)-Alpha führen kann (Trotta et al., 2014; Zaghloul et al., 2020; Carroll et al., 2021). Zu den DAMPS zählen jedoch auch Nukleotide wie ATP oder Uridintriphosphat (UTP), welche über purinerge Rezeptoren auf den Mikroglia erkannt werden (Davalos et al., 2005; Bianco et al., 2006; Wilmes et al., 2022; Schädlich et al., 2023). Der P2Y6, als Rezeptor von Uridindiphosphat (UDP), ist an der Regulierung der phagozytotischen Kapazität von Mikroglia beteiligt (Koizumi et al., 2007). Nach Antagonisierung oder Gen-Silencing des P2XR7, eines ionotropen ATP-Rezeptors, konnte in der Mikrogliazelllinie N9 eine reduzierte Proliferation nach LPS-Stimulation beobachtet werden (Bianco et al., 2006). Weiter zeigte sich in humanen Mikroglia nach Blockade des P2XR7 eine Inhibition der Phagozytose und Aktivierung der Caspase-1 (Janks et al., 2018). Caspase-1 spaltet die inaktive Vorstufe von IL-1-Beta in seine aktive Form (Allan et al., 2005). Darüber hinaus scheint eine Blockierung des P2XR7 in einem ischämischen arteriellen Okklusionsmodell *in vivo* zu einer reduzierten Caspase-1 Aktivität und IL-1-Beta zu führen (Wilmes et al., 2022). Denkbar ist auch ein Einfluss purinerger Rezeptoren auf die Bildung des Inflammasoms NLRP3 und somit auf Caspase-1 (Kahlenberg and Dubyak, 2004). Eine weitere Möglichkeit der Stimulation von Mikroglia stellen Neurotransmitter, beispielsweise Glutamat, dar (Pocock and Kettenmann, 2007). Bei ausreichendem variablen Stimulus kommt es zu einer funktionellen wie auch morphologischen Transformation der Mikroglia in einen „aktiveren" Zustand (Hanisch and Kettenmann, 2007; Deczkowska et al., 2018) (**Abb. 2**).

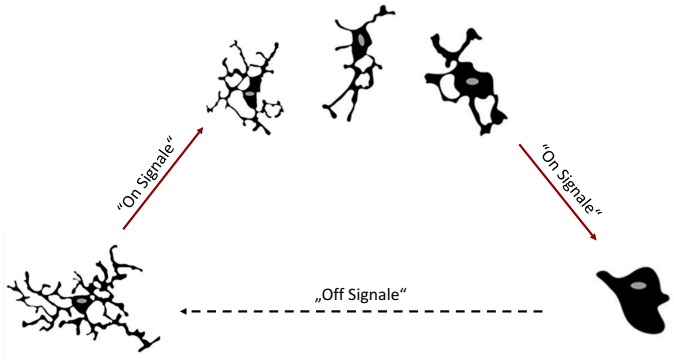

Abb. 2: Modifizierte Darstellung der Aktivierung der Mikroglia nach Wang et al. 2023:
Während die Mikroglia in ihrem „ramifizierten" Zustand ständig das neuronale Gewebe durchsuchen, führt das Auftreten von sogenannten „on-Signalen" (DAMPS oder PAMPS) wie zum Beispiel ATP oder auch das Wegfallen sogenannter „off-Signale" zu einer Veränderung des Aktivierungszustands. Die Zellen passen sich kontinuierlich der aktuellen Situation an und können hierbei verschiedene Phänotypen einnehmen (Wang et al., 2023a).

1.1.2 Astrozyten

Astrozyten machen im ZNS den größten Anteil aller Gliazellen aus. Dabei stellen sie eine morphologisch wie auch funktionell sehr heterogene ektodermale Zellpopulation dar (Molofsky and Deneen, 2015). Histologisch kann unter anderem zwischen protoplasmatischen Astrozyten mit vielen kurzen Ausläufern in der grauen Substanz und den fibrillären Astrozyten mit ihren langen, dünnen Ausläufern unterschieden werden (Miller and Raff, 1984; Bushong et al., 2002;

Lundgaard et al., 2014). Morphologisch sowie funktionell ist jedoch von einer ausgeprägten Heterogenität mit vielen weiteren Subgruppen und regionalen Unterschieden auszugehen (Khakh and Deneen, 2019). Eine wesentliche Aufgabe der Astrozyten besteht darin, ein ideales Milieu und die nötige Homöostase für neuronale Aktivität zu schaffen, diese aufrechtzuerhalten und strukturell wie auch funktionell von anderen Kompartimenten wie dem vaskulären System, dem Ependym und dem Ventrikelsystem zu separieren (Verkhratsky and Nedergaard, 2018). So übernehmen die Astrozyten eine Vielzahl wichtiger metabolischer Prozesse, welche zum Teil den neuronalen Stoffwechsel besonders im Hinblick auf den Gamma-Aminobuttersäure (GABA)/Glutamat-Metabolismus und den Energiespeicher komplementieren (Berkich et al., 2007; Brown and Ransom, 2007; Bittner et al., 2010; Liu et al., 2023). Durch ihren starken Bezug zu metabolischen Prozessen haben Astrozyten auch einen Einfluss auf die synaptische Aktivität (Halassa et al., 2007; Liu et al., 2023). Insgesamt sind die Astrozyten durch die Ausbildung zahlreicher Gap-Junctions als eine Art funktionelles Synzytium zu verstehen. Astrozyten sind an der Bildung der vaskulären Einheit beteiligt, welche die Gesamtheit der an der Regulierung des zerebralen Blutflusses beteiligten Astrozyten, Immunzellen und Endothelzellen, angepasst an die neuronale Aktivität oder Neuroinflammation, umfasst (Iadecola, 2017).

1.1.3 Exzitotoxizität

Die unkontrollierte Aktivierung von exzitatorischen Aminosäurerezeptoren und die damit verbundene Zellschädigung durch Calcium (Ca^{2+}) Überladung wird als Exzitotoxizität bezeichnet und stellt zeitlich eine frühe Komponente des sekundären Schadens dar (Olney et al., 1971; Rothstein et al., 1996; Dirnagl et al., 1999; Neves et al., 2023). Die dominierende Phase der Exzitotoxizität lässt sich innerhalb von Minuten bis Stunden nach einer primären Schädigung beobachten (Dirnagl et al., 1999). Durch eine unzureichende Sauerstoff- und Energieversorgung während eines SHT oder eines Schlaganfalls können weder Neurone noch Gliazellen ausreichend ATP generieren. Infolgedessen kommt es zu einem Zusammenbruch des Membranpotentials und zur Depolarisation mit unkontrollierter präsynaptischer Freisetzung von exzitatorischen Transmittern wie Glutamat (Dirnagl et al., 1999; Neves et al., 2023). Um eine Überstimulation an der Postsynapse zu verhindern, wird das freigesetzte Glutamat unter physiologischen Bedingungen unter hohem Energieaufwand präsynaptisch von den Neuronen durch ein Natrium-Glutamat-Kotransporter oder zu einem deutlich größeren Anteil von den Astrozyten (Andersen et al., 2021) durch den Glutamat-Transporter-1 (GLT-1) und den Glutamat-Aspartat-Transporter (GALST) wieder aufgenommen (Namura et al., 2002; Pawlak et al., 2005; Yalçın and Colak, 2020). Durch die spezifische Expression der Glutamin-Synthetase (GS) in den Astrozyten (Norenberg and Martinez-Hernandez, 1979; Mostafeezur et al., 2014) kommt diesen Zellen durch den Glutamat-Glutamin-Zyklus eine wichtige Bedeutung in der Transmitter-Homöostase zu (Hertz and Rothman, 2016). Unter pathologischen Bedingungen resultiert daher aus der

gesteigerten Glutamatfreisetzung und der eingeschränkten Wiederaufnahme eine Überstimulation ionotroper N-Methyl-D-Aspartat (NMDA)-Rezeptoren, α-amino-3-hydroxy-5-methyl-4-Isoxazolepropionische Säure (AMPA)-Rezeptoren und metabotroper Glutamat-Rezeptoren an der postsynaptischen Membran (Lai et al., 2014). Daraufhin kommt es zu einem Anstieg des intrazellulären Ca^{2+}. Der NMDA-Rezeptor übernimmt hierbei durch seine hohe Permeabilität für Ca^{2+} eine führende Rolle (Choi, 1987; 1988). Das intrazelluläre Ca^{2+} agiert als Second- oder Third-Messenger bei zahlreichen Signalkaskaden und aktiviert Phospholipasen, Proteasen und Stickoxid-Synthetasen (NOS) (Knowles and Moncada, 1994; Lipton, 1999). Diese Akkumulation von Ca^{2+} in der Zelle führt abschließend zur Destabilisierung von Membranen und einem Abbau von Proteinen (Kunz et al., 2010; Sorice, 2022). Zudem kommt es zu einem Einstrom von Natrium- und Chlorid-Ionen über ionotrope Kanäle wie die AMPA-Rezeptoren. Diesem Ionenfluss folgt osmotisch das Wasser und es kommt zur Schwellung der Nervenzellen. Je nach Konzentration und Dauer der Glutamatexposition kommt es entweder zur Apoptose oder zur Nekrose neuronaler Zellen (Lipton, 1999; Rivero-Segura et al., 2017).

1.1.4 Oxidativer und nitrosaminer Stress

Eine weitere wichtige Konsequenz der Exzitotoxizität ist die Aktivierung verschiedener Signalwege, welche zur Entstehung freier oxidativer Radikale und nitrosaminem Stress in Neuronen, Endothelzellen und Gliazellen führt (Lipton, 1999; Wu et al., 2020). An der Bildung von Stickoxid (NO) können drei verschiedene Formen der NOS beteiligt sein. Unter anderem die Ca^{2+}/Calmodulin-abhängige nNOS (neuronal) sowie die eNOS (endothelial), welche konstitutiv in Neuronen vorkommen können (Knowles and Moncada, 1994). Als dritte Form kann die iNOS (induzierbar) abgegrenzt werden (Hibbs et al., 1987; Dawson et al., 1991; Chao et al., 1992). Nach Läsionen im ZNS kommt es zu einer vermehrten Expression der iNOS mit konsekutiv erhöhter NO-Freisetzung (Endoh et al., 1994; Mizuma et al., 2018). In einem Mausmodell konnte ein Beginn der Expression nach 24 Stunden mit einem Maximum von 96 Stunden nach einer Läsion nachgewiesen werden (Iadecola et al., 1997). Die Expression der iNOS führte in einem ischämischen arteriellen Okklusionsmodell in Wildtyp-Mäusen nach 96 Stunden zu einem vergrößerten Läsionsvolumen im Vergleich zu Mäusen in einer iNOS-Knockout-Gruppe (Iadecola et al., 1997). Mikroglia und Astrozyten stellen die Hauptquellen für eine erhöhte Expression der iNOS und Produktion von NO nach einer Läsion dar (Possel et al., 2000; Dehghani et al., 2010). Insbesondere im Rahmen des Reperfusionsschadens sind die pathophysiologischen Prozesse des oxidativen Stresses eine wichtige molekulare Grundlage (Mizuma et al., 2018; Jurcau and Ardelean, 2022). Der oxidative Stress begünstigt zum einen neuroinflammatorische Prozesse, zum anderen ist er durch die iNOS oder durch periphere Immunzellen Teil der Neuroinflammation (Iadecola and Anrather, 2011; Chamorro et al., 2016; Stoll and Nieswandt, 2019).

1.2 Neuroinflammation

Das Gehirn gehört zu den immunprivilegierten Organen des Körpers und nimmt unter diesen eine besondere Rolle ein. Aufgrund der eingeschränkten Regenerationsfähigkeit stellt eine inflammatorische Antwort des ZNS immer ein Risiko für das neuronale Überleben dar. Ist die Immunantwort fehlreguliert, hat dies entscheidende Auswirkungen und Konsequenzen auf die Integrität und Funktion des ZNS. Trotz zahlreicher präklinischer Untersuchungen wurde bisher kein Durchbruch bei der Eindämmung des sekundären Schadens, insbesondere der Neuroinflammation, in klinischen Studien erzielt (Ghozy et al., 2022; Haupt et al., 2023). Die Neuroinflammation ist zum einen durch Zell-Zell-Interaktionen zwischen Mikroglia, Neuronen, Astrozyten, Endothelzellen und peripheren Immunzellen gekennzeichnet und zum anderen bestimmen zahlreiche verschiedene lösliche Faktoren wie Zytokine, Chemokine und reaktive Sauerstoffspezies den weiteren Verlauf (Nedergaard and Dirnagl, 2005; Hailer, 2008; Chamorro et al., 2012; Ahmad et al., 2013). Ein klassisches neuroinflammatorisches Zytokin stellt dabei das IL-1 dar (Allan et al., 2005). Nach ischämischen Läsionen tragen Gliazellen, Neurone sowie Endothelzellen und neutrophile Granulozyten zu einer erhöhten Expression und Freisetzung von IL-1 bei (Giulian et al., 1986; Pearson et al., 1999; Sobowale et al., 2016). IL-1-Beta und IL-1-Alpha sind dabei die Hauptvertreter in dieser Klasse (Allan et al., 2005). IL-1-Beta ist involviert in der Pathogenese und Behandlung teils neurologisch manifester autoinflammatorischer Erkrankungen wie dem familiären Mittelmeerfieber, dem Tumornekrosefaktor-Alpha assoziierten periodischen Syndrom (TRAPS) oder dem Cryoporin-assoziierten periodischen Syndrom (CAPS), sodass ein schädlicher Einfluss auf das Nervensystem angenommen werden kann (Kitley et al., 2010; Ozen and Bilginer, 2014; De Benedetti et al., 2018). Zwar ist eine direkte neuronale Schädigung durch IL-1 umstritten, jedoch zeigen tierexperimentelle Ergebnisse aus den OHSC sowie *in vivo* Experimente einen Einfluss auf die Progression der Schädigung und Beteiligung an der Pathogenese (Rothwell and Luheshi, 2000; Hailer et al., 2005). Weiter konnte für einen IL-1-Rezeptorantagonisten (IL-1-RA) ein neurozytoprotektiver Effekt auf solche Schädigungen nachgewiesen werden (Relton and Rothwell, 1992; Allan et al., 1998; Mulcahy et al., 2003). Daten aus einem *in vivo* arteriellen Okklusionsmodell deuten auf ein therapeutisches Zeitfenster von IL-1-RA innerhalb 12 Stunden nach der Schädigung hin (Xia et al., 2014). IL-1 besitzt dabei pleiotrope Effekte auf verschiedene Signalwege und Mediatoren (Allan et al., 2005). In primären hippocampalen neuronalen Zellkulturen konnte durch IL-1-Beta die Permeabilität des NMDA-Rezeptors erhöht und somit die Ca^{2+}-Überladung der Neurone verstärkt werden (Viviani et al., 2003). Auch besteht ein Einfluss auf das Endocannabinoidsystem, worin die Sensitivität für den Cannabinoid (CB)1-Rezeptor auf GABA-ergen Neuronen reduziert wird (Rossi et al., 2012; De Chiara et al., 2013). Neben IL-1-Beta kommt es zur Freisetzung von weiteren Zytokinen wie Tumornekrosefaktor TNF-Alpha oder IL-6 (Lambertsen et al., 2012). IL-

6 und weniger TNF-Alpha zeigten anders als IL-1 keinen eindeutigen destruktiven Effekt im ZNS (Bruce et al., 1996; Lambertsen et al., 2009; Erta et al., 2012; Probert, 2015). Neben zahlreichen löslichen Faktoren sind zelluläre Prozesse, welche insbesondere durch Mikroglia und Astrozyten vermittelt werden, maßgeblich an der Entstehung und Erhaltung der Neuroinflammation beteiligt (Qin et al., 2022). Der Verlauf der Neuroinflammation wird ebenfalls mitbestimmt von der Aktivierung und Rekrutierung weiterer peripherer Immunzellen.

1.2.1 Aktivierung von Mikroglia

Die Transformation der Mikroglia in einen „aktiveren Zustand" ist im Wesentlichen durch eine erhöhte Proliferation, Migration, Chemotaxis, Produktion und Freisetzung zellulärer und löslicher Zytokine sowie eine morphologische Transformation von einer ramifizierten zu einer amöboiden Zellstruktur gekennzeichnet (Streit et al., 1988; Carbonell et al., 2005; Deczkowska et al., 2018; van Weering et al., 2023). Erstmals wurde im Jahr 1978 die Proliferation von Mikroglia in hippocampalen Schnitten 20-30 Stunden nach Schädigung demonstriert und in Folge vielfach mit verschiedenen Markern, wie Ki67 und Bromdesoxyuridin (BrdU), bestätigt (Kitamura et al., 1978; Morshead and van der Kooy, 1990; Ebrahimi et al., 2012; Li et al., 2013). Charakteristisch ist eine rasche Steigerung der Proliferationsrate sowie ein schneller Abfall dieser nach 1-2 Wochen auf Normalwerte (Hailer et al., 1999). Die endogenen Faktoren, welche diese Prozesse steuern, sind derzeit noch nicht genau verstanden. In einem Mouse-Knockout-Modell des Makrophagen-Kolonie stimulierenden Faktor (M-CSF) konnte eine signifikante Reduktion der Proliferation von Mikroglia nachgewiesen werden (Raivich et al., 1994). Ebenso wie der M-CSF (Smith et al., 2013) scheinen andere Stimuli wie der Granulozyten/Monozyten-Kolonie stimulierende Faktor (GM-CSF), Hydrogenperoxid, der hirneigene neutrotrophe Faktor (BDNF) und der purinerge P2XR7 einen proliferativen Effekt auf Mikroglia zu haben (Bianco et al., 2006; Mander et al., 2006; Bureta et al., 2019; Dikmen et al., 2020; Onodera et al., 2021). Astrozyten nehmen via M-CFS, GM-CSF und transformierendem Wachstumsfaktor-Beta (TGF-Beta) Einfluss auf die Regulierung von Proliferation und Aktivierung der Mikroglia (Schilling et al., 2001; Matejuk and Ransohoff, 2020). Auch IL-1-Beta führte in den OHSC zwischen 4 und 72 Stunden nach einer Schädigung zu einer deutlichen Erhöhung der Anzahl an Mikroglia (Hailer et al., 2005). Etwa 24 Stunden nach der Schädigung zeigte sich neben der erhöhten Proliferation auch eine erhöhte Zellmigration der Mikroglia in Richtung der Läsion (Carbonell et al., 2005). Auf die Migration und Chemotaxis konnte neben zahlreichen weiteren Faktoren auch ein Einfluss für das Fractalkine-System mit seinem Liganden CX3CL-1 (Fractalkine) nachgewiesen werden. Fractalkine werden von Neuronen und Astrozyten freigesetzt und durch den auf Mikroglia vorkommenden Rezeptor CX3CR-1 erkannt (Poniatowski Ł et al., 2017). Weiterhin sind Faktoren wie ATP und Adenosindiphosphat (ADP) über P2Y-Rezeptoren und der Nervenwachstumsfaktor (NGF) durch den Tropomyosinrezeptorkinase A (TrkA)-Rezeptor an der

Migration der Mikroglia beteiligt (Honda et al., 2001; De Simone et al., 2007; Gómez Morillas et al., 2021).

1.2.2 Reaktive Astrogliose

Im Rahmen von akuten Pathologien kommt es zur Bildung einer sogenannten reaktiven Astrogliose, die mit einer Hypertrophie und Proliferation einhergeht (Sofroniew, 2009). Dies ist eine spezifische und evolutionär konservierte und zugleich heterogene Reaktion von Astrozyten auf polyätiologische Hirnschädigungen, von akuten traumatischen Läsionen und Infektionen bis hin zur Neurodegeneration (Escartin et al., 2021). Die Aktivierung von Astrozyten führt zur Entstehung mehrerer kontextspezifischer Phänotypen, die je nach Alter, Art der Pathologie und Hirnregion charakteristisch sind (Sofroniew, 2020). Diese vielfältigen Phänotypen unterscheiden sich durch ihr spezifisches molekulares Profil, ihre Funktionen und ihre unterschiedlichen Auswirkungen auf Krankheiten (Pekny and Nilsson, 2005; Endo et al., 2022). Allgemeine Kriterien einer astrozytären Reaktivität definieren ein kontinuierliches Spektrum von Veränderungen der molekularen Expression, zellulären Funktion, Hypertrophie sowie Proliferation. Diese können dabei abhängig von der Läsionsgröße und Ätiologie sein und zeichnen sich durch einen Verlust physiologischer Aufgaben oder durch eine Aktivierung bestimmter pathologischer Prozesse von protektivem als auch destruktivem Charakter aus (Sofroniew and Vinters, 2010). Bei der Entstehung einer reaktiven Astrogliose können insbesondere zwei wichtige Prozesse mit Beteiligung verschiedener astrozytärer Subtypen unterschieden werden. Zum einen Astrozyten, welche infolge einer gesteigerten Proliferation an der Bildung einer Barriere um die Läsion beteiligt sind („Glianarbe“), und zum anderen Astrozyten, welche sich durch eine Hypertrophie charakterisieren lassen, ohne ihre Struktur oder Integration grundlegend zu verändern (Bushong et al., 2002; Sofroniew, 2020). Auf transkriptioneller Ebene scheinen NF-κB, Signalgeber und Aktivator der Transkription 3 (STAT3) sowie das in Säugetieren vorkommende Ziel von Rapamycin (mTOR) vermehrt aktiviert zu sein (Herrmann et al., 2008; Codeluppi et al., 2009; Hu et al., 2022). Besonders in elongierten Astrozyten, welche an der Barrierebildung beteiligt sind, scheint STAT3 eine wichtige Rolle in der Organisation und Bildung dieser Kompartimentierung einzunehmen (Wanner et al., 2013). Eine Dysregulation oder ein Ausbleiben dieser Barrierebildung führt zu einer inadäquaten Regeneration der BBB, einer erhöhten Infiltration von Immunzellen sowie einer ausgeprägten neuronalen Schädigung (Faulkner et al., 2004). Die strukturellen und morphologischen Veränderungen in den Astrozyten beruhen auf einer erhöhten Expression verschiedener Intermediärfilamente wie dem sauren Gliafaserprotein (GFAP), Vimentin und Nestin (Sofroniew, 2009; Liu et al., 2014; Brenner and Messing, 2021). GFAP stellt nur etwa 15% des Volumens des Zytoskeletts dar und wird interessanterweise nicht von allen Astrozyten exprimiert (Bushong et al., 2002; Sofroniew and Vinters, 2010; Jurga et al., 2021).

Zu beachten ist ebenfalls, dass eine erhöhte Expression im Bereich der Schädigung zu möglichen Fehlinterpretationen der Läsionsgröße führen kann (Sofroniew, 2009). Durch die strukturellen und molekularen Veränderungen sowie die gesteigerte Proliferation kann es, in Abhängigkeit der Schwere einer Schädigung, zur Bildung einer „Glianarbe“ kommen, was aber keine zwingende Bedingung der reaktiven Astrogliose darstellt (Sofroniew, 2009). Zur Untersuchung von Astrozyten und Mikroglia *in vitro* eignen sich aufgrund ihrer spezifischen Heterogenität sowie ihrer komplexen multifaktoriellen Regulation Modelle, welche möglichst nahe an die *in vivo* Situation angepasst sind.

1.3 Organotypische hippocampale Schnittkulturen (OHSC)

OHSC sind ein Schnittkulturmodell der Hippocampusformation zusammen mit dem entorhinalem Kortex, in welchem Gliazellen, unter anderem Mikroglia, Astrozyten wie auch Neurone unter funktionell erhaltener Aktivität und intakten nervalen Schaltkreisen untersucht werden können (Heppner et al., 1998). In der Hippocampusformation (**Abb. 3**) findet sich das Stratum pyramidale und das Stratum granulare. Dabei sind die Pyramidenzellen im Bereich des Cornu ammonis (CA) mit seinen verschiedenen Regionen CA1-3 und die Körnerzellen im Gyrus dentatus (DG) lokalisiert. Funktionell projizieren als Tractus perforans bezeichnete exzitatorische Neurone aus dem entorhinalen Kortex (EC) zum DG. Von dort aus ziehen die als Moosfasern bezeichneten Axone der Körnerzellen in Richtung der CA3 Region, welche durch die Schaffer-Kollaterale mit der CA1 Region verbunden ist. CA1 Neurone projizieren in den entorhinalen Kortex (Woodhams and Atkinson, 1996). Dieser exzitatorische Schaltkreis wird durch Glutamat vermittelt und durch GABAerge Interneurone moduliert (Freund and Buzsáki, 1996). OHSC besitzen somit funktionell geschlossene neuronale Schaltkreise, welche das Überleben der Neurone bei einer *in vitro* Kultivierung sichert und die Untersuchungen von Einflüssen der peripheren Immunzellen und die genaue intrinsische Untersuchung der Gliazellen und ihrer Interaktionen ermöglicht (Grabiec et al., 2017).

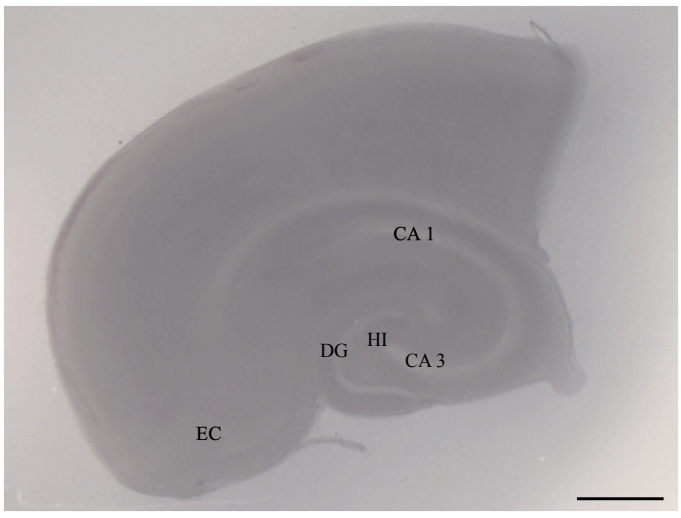

Abb. 3: Mikroskopische Aufnahme einer OHSC.
Dargestellt ist die Hippocampusformation der OHSC mit den Regionen des Cornu ammonis (CA), der Hilus (HI), Gyrus dentatus (DG) sowie der entorhinale Kortex (EC). Maßstab = 1mm.

1.3.1 Anwendungsgebiete der OHSC

Die Anwendungsgebiete des Modells sind sehr vielfältig. Zum einen kann in den OHSC ein reproduzierbarer mechanischer Schaden nachgebildet werden (Li et al., 2016). Zum anderen können durch Deprivation von Glucose und Sauerstoff ischämische Schäden erzeugt werden (Li et al., 2016; Cramer et al., 2022). Eine weitere Möglichkeit der neuronalen Schädigung stellt die exzitatorische Überstimulation mittels NMDA dar (Holopainen, 2005; Ebrahimi et al., 2010), welche die Exzitotoxizität modelliert (Choi, 1988). Besonders im Bereich des DG konnte in einem bestimmten Konzentrationsbereich eine lineare Beziehung zwischen NMDA und der neuronalen Schädigung nachgewiesen werden (Ebrahimi et al., 2010). Des Weiteren ist es möglich, durch den Einsatz des Bisphosphonat-Clodronat (Clo), eine zur Behandlung von Osteoporose eingesetzte Substanz, selektiv Mikroglia aus den OHSC zu depletieren (Kohl et al., 2003). Diese Eigenschaft ermöglicht die Untersuchung Mikroglia-unabhängiger Effekte. OHSC eignen sich ebenfalls als Modell zur Untersuchung von Effekten mannigfaltiger Substanzen und Materialien auf neuronales Gewebe, die zum Beispiel innerhalb neurochirurgischer Eingriffe verwendet werden (Kleine et al., 2021). Eine Möglichkeit dieser Testung stellt die Gruppe der oxidativen regenerierten Zellulosen (ORC) dar, die als gängige Hämostyptika nach neurochirurgischen Eingriffen zur Vermeidung eines Nachblutens verwendet werden (Kleine et al., 2021). ORC verbleiben dabei oft als Füllmittel in den entstandenen Kavitäten vor Ort. Für Tabotamp®, einen Vertreter der ORC, konnte bereits ein destruktiver Einfluss auf neuronale Zellen nachgewiesen werden (Leisz et al., 2020).

Zusammenfassend stellen OHSC ein ideales Modell zur Untersuchung des neuronalen Schadens mit seinen verschiedenen zellulären wie biochemischen Antworten sowie deren pharmakologischer Beeinflussung von beispielsweise intrinsischen Prozessen wie dem Endocannabinoidsystem oder durch Inhibition der Calciumkanäle dar.

1.3.2 Neurozytoprotektion durch Endocannabinoide und Nimodipin

Die Entdeckung des Endocannabinoidsystems begann insbesondere mit der Charakterisierung und Erforschung des erstmals 1988 beschriebenen CB1-Rezeptors (Devane et al., 1988). Dieser ist mit hoher Dichte im frontalen Cortex, in den Basalganglien, im Cerebellum, in der Substantia nigra und im Hippocampus zu finden (Wegener and Koch, 2009). Die Klonierung des CB2-Rezeptors gelang im Jahr 1993 (Munro et al., 1993; Grabon et al., 2023), welcher überwiegend auf verschiedenen Zellen des Immunsystems (Hiley and Kaup, 2007), einschließlich der Mikroglia, nachgewiesen wurde (Carlisle et al., 2002; Maresz et al., 2005; Lu and Mackie, 2021; Marinelli et al., 2023). Als Agonisten der Rezeptoren und als endogene Liganden wurde zuerst Arachidonylethanolamid (AEA) (Devane et al., 1992) und kurz darauf 2-Arachidonylglycerol (2-AG) entdeckt (Mechoulam et al., 1995). Neben den beiden klassischen CB1- und CB2-Rezeptoren lässt sich pharmakologisch einer in der Literatur als abnormal-Cannabidiol

bezeichneter Rezeptor (abn-CBDR) adressieren (Járai et al., 1999; Mackie and Stella, 2006; Cardinal von Widdern et al., 2020). Anders als die pflanzlichen Phytocannabinoide wie Tetrahydrocannabinol (Δ9-THC) oder Cannabidiol (CBD) handelt es sich bei den endogenen Cannabinoiden um Eicosanoide, welche insbesondere an der Zellmembran oder anderen intrazellulären Membranen gebildet werden können (Di Marzo, 1999; Muccioli, 2010; Oddi et al., 2023). Die Endocannabinoide fungieren im ZNS als Neuromodulatoren und werden anders als konventionelle Neurotransmitter nicht in Vesikeln gespeichert, sondern bei Bedarf aus Phospholipiden synthetisiert und sezerniert (De Petrocellis et al., 2004; Zhu et al., 2023). In Mäusen zeigte sich nach ischämischer Läsion für Palmitoylethanolamid (PEA) und nach einer traumatischen Läsion für 2-AG eine signifikant erhöhte endogene Bildung (Panikashvili et al., 2001; Franklin et al., 2003). Für diese beiden endogenen Cannabinoide konnte bereits in mehreren Publikationen ein positiver Effekt auf ischämische oder traumatische Läsionen gezeigt werden (Kreutz et al., 2007; Kreutz et al., 2009; Ahmad et al., 2012a; Ahmad et al., 2012b; Herrera et al., 2022; Beldarrain et al., 2023). Dieser neurozytoprotektive Effekt von 2-AG in OHSC von Ratten (Kreutz et al., 2007) scheint Mikroglia-abhängig und weniger über den CB2-Rezeptor als vielmehr über den abn-CBDR vermittelt zu sein (Kreutz et al., 2009). 2-AG nahm dabei Einfluss auf die Migration, Proliferation und Zytokinfreisetzung der Mikroglia (Facchinetti et al., 2003; Walter et al., 2003). Anders als 2-AG scheint PEA nicht über CB1-/CB2-Rezeptoren oder abn-CBDR zu wirken (Mackie and Stella, 2006). Angenommen wird eine Wirkung auf den Peroxisomen Proliferations-aktivierenden Rezeptor-Alpha (PPAR-Alpha) (Lo Verme et al., 2005; Rankin and Fowler, 2020) sowie ferner über eine Aktivierung von transienten Rezeptor-Potential-Kationenkänalen der Unterfamilie V (TRPV)1 und den G-Protein-gekoppelten Rezeptor GPR55 (Mackie and Stella, 2006; Ryberg et al., 2007; Ambrosino et al., 2013). Darüber hinaus führte PEA zu einer Inhibition der Fettsäureamid-Hydrolase (FAAH), welche bevorzugt am Abbau von AEA beteiligt ist, was wiederum zu einer Steigerung der Konzentrationen von AEA und 2-AG führte (Petrosino et al., 2016; Petrosino and Di Marzo, 2017). Die Applikation zweier Cannabinoide, welche durch ineinandergreifende molekulare Mechanismen zu einer Verstärkung ihrer Effekte führt, wird als Entourage-Effekt bezeichnet (Ben-Shabat et al., 1998; Hohmann et al., 2019). Neben Endocannabinoiden kann die Modulation des Calciumeinstroms eine Möglichkeit zur Abschwächung des neuronalen Schadens darstellen. Für Nimodipin, ein Calciumkanalblocker mit lipophilen Eigenschaften, konnten in zahlreichen Experimenten neurozytoprotektive Effekte nachgewiesen werden (Scriabine and van den Kerckhoff, 1988; Li et al., 2009; Sanz et al., 2012). Die Blockade von Calciumkanälen führte zu einer reduzierten intrazellulären Calciumaufnahme in kortikalen Synaptosomen/Neuronen bei gleichzeitiger reduzierter Glutamatfreisetzung (Scriabine and van den Kerckhoff, 1988; Abele et al., 1990; John R. McLeod et al., 1998; Carlson et al., 2020). Ein möglicher Einfluss von Nimodipin auf die NMDA vermittelte Exzitotoxizität durch Inhibition des intrazellulären Ca^{2+}-Einstroms liegt daher

nahe (Porter et al., 1997; Brewer et al., 2007). Genauere Wirkungsmechanismen der neurozytoprotektiven Effekte von Nimodipin sind jedoch noch nicht vollständig verstanden.
Zusammenfassend zeigte sich für die Endocannabinoide wie 2-AG und PEA sowie den Calciumkanalblocker Nimodipin in den OHSC ein neurozytoprotektiver Effekt (Hohmann et al., 2019; Hohmann et al., 2022). Zwar scheinen sich die molekularen Zielstrukturen beider Substanzen zu unterscheiden, jedoch konnte für die Endocannabinoide (Hohmann et al., 2019), weniger für Nimodipin (Chiozzi et al., 2019), ein Einfluss auf die Aktivierung und Zytokinfreisetzung von Mikroglia nachgewiesen werden. Der Purinstoffwechsel mit seiner De-novo-Synthese nimmt insbesondere in der Aktivierung und Proliferation von Immunzellen wie Mikroglia oder Astrozyten eine wichtige Rolle ein und stellt somit ein wichtiges Ziel für weitere neurozytoprotektive Ansätze dar.

1.4 Purinstoffwechsel und die Zellteilung

1.4.1 Zellzyklus und Zellteilung

Die Proliferation von Mikroglia und Astrozyten stellt ein wichtiges Charakteristikum der Aktivierung dieser Zellen dar (Hailer et al., 1999; Mitchison and Salmon, 2001; Wanner et al., 2013). Bei einer symmetrischen Teilung kommt es zu einer exakten Duplizierung des gesamten Chromosomensatzes und darüber hinaus zu einer Erhöhung der Zellmasse und des Zytoplasmas. Der typische eukaryotische Zellzyklus wird schematisch in eine G1-, G2-, S- und M-Phase unterteilt. Dabei werden die G1-, G2- und S-Phase unter dem Begriff der Interphase subsumiert. Unter der M-Phase versteht man die Mitose. Die G1-Phase ist durch Zellwachstum, Protein- sowie Nukleotidsynthese gekennzeichnet. In der S-Phase erfolgt die eigentliche Replikation der DNA und in der G2-Phase werden Proteine wie die Ribonukleinsäure (RNA) synthetisiert, die für die Zellteilung nötig sind (Löffler and Petrides, 2014; Matthews et al., 2022). Die Kontrolle des Zellzyklus wird über verschiedene Checkpoints realisiert. Die genaue Regulation dieser Checkpoints erfolgt über die Cycline und die Cyclin-abhängigen Kinasen (CDKs). Die Cycline und CDKs bilden aktive Komplexe, welche über Phosphorylierungen, Ubiquitinierungen, Translokationen in den Zellkern sowie Inhibitoren der Cycline von extern sowie intern reguliert werden können (Lukas and Bartek, 2004; Matthews et al., 2022). Für eine sichere Zellteilung ist es grundlegend wichtig, dass genügend Glucose, Aminosäuren, Lipide und auch Nukleotide zu Verfügung stehen (Zhu and Thompson, 2019). Die Nukleotide werden besonders bei der Replikation der DNA, der Synthese von ribosomaler (r)RNA und der Aufrechterhaltung des Transkriptoms (mRNA) benötigt. Die Glykolyse, der Pentosephosphatweg sowie der Purinstoffwechsel sind daher eng mit entscheidenden Schlüsselstellen der Proliferation und der Apoptose verknüpft (Buchakjian and Kornbluth, 2010; Pavlova and Thompson, 2016).

1.4.2 Purinstoffwechsel

Die De-novo-Synthese der Purine geht von der reaktionsfreudigen Verbindung Phosphoribosylpyrophosphat (PRPP) aus. Diese entsteht im Pentosephosphatweg und wird durch die PRPP-Synthetase katalysiert (**Abb. 4**). Anders als in der Pyrimidinsynthese, bei der die N-glykosidische Bindung zwischen Base und Ribose erst nach der Synthese des Pyrimidinrings geknüpft wird, erfolgt die Synthese an der Ribose zuerst offen, später dann als geschlossenes Ribonukleotid. Die Regulation erfolgt allosterisch, wobei das geschwindigkeitsbestimmende Enzym der Inosinmonophosphat (IMP)-Synthese die Glutamin-PRPP-Amidotransferase ist (**Abb. 4**) (Löffler and Petrides, 2014). Aus dem IMP entstehen über die Adenylsuccinat-Synthetase das Adenylsuccinat und unter der Abspaltung von Fumarat durch die Adenylsuccinat-Lyase das Adenosinmonophosphat (AMP) (**Abb. 4**). Durch die Inosin-5'Monophosphatdehydrogenase (IMPDH) entsteht aus IMP das Xanthosinmonophosphat (XMP) und dann unter Abspaltung von Glutamat durch die GMP-Synthetase das Guanosinmonophosphat (GMP, **Abb. 4**) (Yin et al., 2018). Besonders in schnell proliferierenden Zellen, wie beispielsweise in Immunzellen, B- und T-Lymphozyten, spielt die De-novo-Synthese von Purinen eine besondere Rolle (Allison et al., 1977; Sugiura et al., 2022). Neurone hingegen sind besonders in ihrer Entwicklung auf den Salvage-Pathway des Purinstoffwechsels angewiesen (Allison et al., 1975; Brosh et al., 1992). Das entscheidende Schlüsselenzym für die Generierung von GMP stellt die IMPDH dar. Daher bietet sich die IMPDH als eine ideale Zielstruktur zur Beeinflussung der GMP-Synthese und allosterisch des gesamten Purinstoffwechsels an (Burrell and Kollman, 2022).

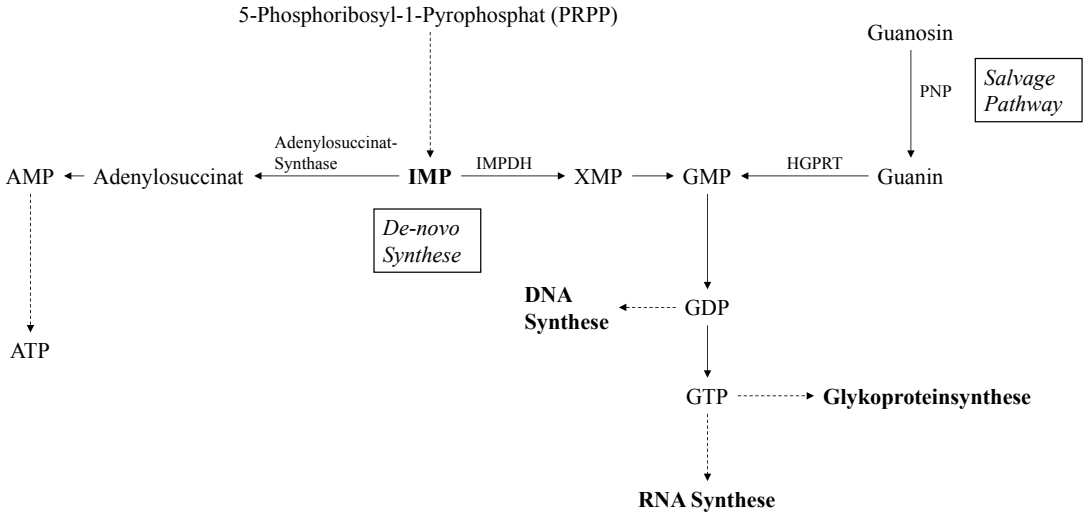

Abb. 4: Schema des Purinstoffwechsels. Die Purinsynthese wird bei Eukaryoten an multifaktoriellen Enzymen katalysiert (Pareek et al., 2021). Adenosinmonophosphat (AMP), Adenosintriphosphat (ATP), Desoxyribonukleinsäure (DNA), Guanosinmonophosphat (GMP), Guanosindiphosphat (GDP), Guanosintriphosphat (GTP), Hypoxanthin-Guanin-Phosphoribosyl-Transferase (HGPRT), Inosin-5'Monophosphatdehydrogenase (IMPDH), Purin-Nukleosid-Phosphorylase (PNP), Ribonukleinsäure (RNA), Xanthosinmonophosphat (XMP). Gestrichelte Pfeile = Zwischenschritte nicht dargestellt.

1.4.3 Inosin-5'Monophosphatdehydrogenase (IMPDH)

Die IMPDH katalysiert die Nicotinamidadenindinukleotid (NAD)- abhängige Oxidation von IMP zu XMP (**Abb. 4**). Dies ist die geschwindigkeitsbestimmende Reaktion im Guanosinstoffwechsel (Jackson et al., 1975). Es wurden zwei Isoformen beim Menschen identifiziert, die IMPDH-Isoform 1, welche in allen Zellen konstitutiv exprimiert wird, und die IMPDH-Isoform 2, die zusammen mit der IMPDH-Isoform 1 in proliferativen Zellen wie Leukozyten vermehrt exprimiert wird (Jain et al., 2004; Burrell and Kollman, 2022). Beide Isoformen sind 514 Aminosäuren lang, zu 84% identisch in ihrer Sequenz und fungieren als Homotetramer mit einem Molekulargewicht von 56-58 kDa (Carr et al., 1993). Das Gen für die humane IMPDH-Isoform 1 findet sich auf Chromosom 7 (7q31.3-q32) und das für die IMPDH-Isoform 2 auf Chromosom 3 (Glesne et al., 1993; Gu et al., 1994). Eine erhöhte Expression infolge einer Stimulation auf mRNA-Ebene konnte in T-Lymphozyten nach etwa 12-24 Stunden und auf Proteinebene nach 24-48 Stunden nachgewiesen werden (Dayton et al., 1994; Jain et al., 2004).

Die Regulation der IMPDH erfolgt zum Großteil allosterisch. Des Weiteren wird die Aktivität über posttranslationale Modifikationen, wie enzymatische Filamentation und spezifische Splice-Varianten mitbestimmt (Buey et al., 2022). Ein homozygoter Verlust der IMPDH-Isoform 2 in Mäusen führt zu einer frühen embryonalen Letalität (Gu et al., 2000). Die IMPDH ist zu einem Großteil zytoplasmatisch lokalisiert, wurde aber auch im Kern nachgewiesen (Kozhevnikova et al., 2012). So deutet eine Studie darauf hin, dass die IMPDH unabhängig von ihrer enzymatischen Funktion in E. coli und Drosophila-S2-Zellen auch die Fähigkeit eines transkriptionalen Repressors besitzt und hierdurch eine regulative Funktion im Zellzyklus einnehmen kann (Kozhevnikova et al., 2012). Der in T-Zellen nachgewiesene Einfluss auf die Proliferation und Aktivierung nach selektiver Inhibition der nicht enzymatischen CBS-Domäne der IMPDH-Isoform 2 legt einen Einfluss des Enzyms abseits der katalytischen Aktivität nahe (Pua et al., 2017). Sowohl in Makrophagen als auch in Mikroglia scheint die IMPDH-Isoform 2 einen Einfluss auf die Regulierung von inflammatorischen Zytokinen und die Proliferation zu nehmen (Jonsson and Carlsten, 2002; Dehghani et al., 2010; Ebrahimi et al., 2012). Genaue Mechanismen werden derzeit noch untersucht. Infolge der zentralen Funktion der IMPDH in der De-novo-Synthese des Purinstoffwechsels von Immunzellen, stellt diese eine interessante molekulare Struktur für mögliche pharmakologische Inhibitoren wie Mycophenolat-Mofetil (MMF, CellCept®), Ribavirin (Virazol®), Mizoribine (Bredinin®) oder selektive Inhibitoren der IMPDH-Isoform 2 wie Sappanone A dar (Cuny et al., 2017; Liao et al., 2017).

1.4.4 Inhibition der IMPDH durch Mycophenolat-Mofetil (MMF)

MMF wurde erstmals zur Behandlung der Psoriasis eingesetzt (Epinette et al., 1987; Broen and van Laar, 2020). In den 1990er Jahren gewann MMF immer mehr Bedeutung in der Transplantationsmedizin, wo es aufgrund seiner geringen nephrotoxischen Nebenwirkungen

gegenüber Cyclosporin A und Azathioprin zur Immunsuppression nach Nierentransplantationen eingesetzt wurde (Allison and Eugui, 2000). MMF ist ein Morpholinoethylester der Mycophenolatsäure (MPS) und wurde 1990 aufgrund seiner besseren Bioverfügbarkeit gegenüber MPS entwickelt (Lee et al., 1990; Broen and van Laar, 2020). MMF wird im Gewebe schnell zu MPS hydrolysiert, weshalb die meisten Studien mit MMF durchgeführt wurden. MMF als aktive Form ist ein nicht kompetitiver und reversibler Inhibitor der IMPDH. Es weist eine etwa 5-fach höhere Affinität zur IMPDH-Isoform 2 auf, welche vermehrt in aktivierten Leukozyten sowie Leukämiezellen und Ovarialkarzinomzellen exprimiert ist (Carr et al., 1993; Allison and Eugui, 2000). Diese Inhibition durch MMF scheint in B- oder T-Lymphozyten keinen Einfluss auf die Induktion der IMPDH-Isoform 1 oder IMPDH-Isoform 2 auf mRNA Ebene zu haben (Jain et al., 2004). In Untersuchungen der monozytären Zellreihe (Makrophagen Zelllinie IC-21) zeigte MMF einen reduzierenden Effekt auf die Zytokinproduktion sowie Proliferation (Jonsson and Carlsten, 2002). Auch in Mikroglia konnten analoge Ergebnisse von MMF auf die Zytokinproduktion und die Proliferation beobachtet werden (Dehghani et al., 2010; Ebrahimi et al., 2012). Für Sappanone A (Liao et al., 2017), einen sehr selektiven Inhibitor der IMPDH-Isoform 2, konnten ähnliche Beobachtungen gemacht werden. Die Bindung von Sappanone A erfolgt anders als bei MMF am nicht-katalytischen Cys140-Rest der regulatorischen Bateman-Domäne.

1.5 Neurozytoprotektive Effekte von MMF

Durch die bevorzugte Wirkung von MMF auf Leukozyten und monozytäre Zellen, welche aus der erhöhten Affinität zur IMPDH-Isoform 2 resultiert, entstand die Hypothese, dass MMF Einfluss auf die Mikroglia und auf den sekundären Schaden haben könnte (Jonsson and Carlsten, 2002). In primären mikrogliären und astrozytären Zellkulturen konnte ein hemmender Effekt von MMF auf die Proliferation sowie auf die Produktion von proinflammatorischen Zytokinen wie IL-1-Beta, TNF-Alpha und NO gezeigt werden (Miljkovic et al., 2002; Dehghani et al., 2010). Ähnliche Ergebnisse konnten nach selektiver Inhibition der IMPDH-Isoform 2 durch Sappanone A nachgewiesen werden (Liao et al., 2017). Sappanone A scheint diesen Prozess über den proinflammatorischen Transkriptionsfaktor nukleären erythroiden Faktor 2 (Nrf2) und NF-κB zu beeinflussen (Lee et al., 2015). Auch in OHSC wurde durch MMF neben einem neurozytoprotektiven Effekt ein solcher antiproliferativer Effekt für Mikroglia und Astrozyten beobachtet (Dehghani et al., 2003; Ebrahimi et al., 2012). Weiter scheint MMF auch einen protektiven Effekt auf die axonale Integrität von Projektionsneuronen nach mechanischer Schädigung in OHSC zu haben (Oest et al., 2006). Ein direkter protektiver Einfluss von MMF auf Neurone konnte in der Zellkultur nach Schädigung mittels NMDA nicht nachgewiesen werden (Dehghani et al., 2010). MMF scheint daher seine Effekte direkt über die Gliazellen oder über die Modulation ihrer Interaktionen zu vermitteln. Für die beobachteten Effekte durch MMF

konnte gezeigt werden, dass es ein spezifisches, besonders effektives Zeitfenster geben muss. Frühere Daten zeigten, dass die Applikation von MMF in einem Zeitintervall zwischen 12-36 Stunden nach der Schädigung zu einem wirksamen neurozytoprotektiven Effekt führte, außerdem konnte dieser Effekt bei einer kontinuierlichen Gabe innerhalb der ersten 12 Stunden nachgewiesen werden (Ebrahimi et al., 2012). Bei späterem Beginn zeigte sich kein protektiver Effekt mehr (Ebrahimi et al., 2012). Die Analysen des neuronalen Zelltods erfolgten hierbei nach 72 Stunden. Auch in verschiedenen *in vivo* Modellen gibt es weitere Hinweise auf einen neurozytoprotektiven Effekt von MMF (Chauhan et al., 2012; Dhande et al., 2017). Ein weiteres Verständnis über das genauere Zeitfenster sowie neurozytoprotektive Effekte von MMF auf die Schädigung und ihre Progression ist daher notwendig, um die genauere Wirkung von MMF und den Einfluss des Purinstoffwechsels in neuronalen Schädigungen zu verstehen. Hierzu gibt es weitere Ansätze, welche zum Beispiel die Beeinflussung von intrinsischen protektiven Systemen wie das Endocannabinoidsystem einschließen.

2. Diskussion

Akute Läsionen des ZNS führen oft zu anhaltenden Einschränkungen des täglichen Lebens. Der sekundäre Schaden stellt dabei, anders als der primäre Schaden, eine beeinflussbare Variable innerhalb einer akuten neuronalen Läsion dar und ist somit ein Ansatzpunkt für mögliche therapeutische Strategien. Im folgenden Abschnitt soll zuerst das Modell der OHSC in Bezug auf die neurozytoprotektiven Untersuchungen (Hohmann et al., 2019; Hohmann et al., 2022) und neue mögliche Anwendungsgebiete diskutiert werden (Kleine et al., 2021). Weiter werden die verschiedene Eigenschaften von MMF (Kleine et al., 2022) betrachtet und abschließend dessen Rolle als Inhibitor des Purinstoffwechsels auf Gliazellen nach neuronaler Schädigung dargelegt. Die Diskussion soll die Fragen nach Mikroglia-abhängigen und unabhängigen Effekten von MMF, einer Translation des Zeitfensters *in vivo* sowie die Bedeutung des Purinstoffwechsels auf die Proliferation von Gliazellen nach neuronaler Schädigung weiter beleuchten.

2.1 Das Modell der organotypischen hippocampalen Schnittkulturen (OHSC)

2.1.1 Vorteile, methodische Limitationen und neue Anwendungsgebiete der OHSC

OHSC stellen, wie bereits vorgestellt, aufgrund ihres morphologischen Aufbaus, ihrer intakten neuronalen Schaltkreise und ihrer organotypischen Verteilung von Gliazellen und Neuronen ein Modell dar, das den *in vivo* Bedingungen sehr nahe kommt. Die untereinander bestehenden neuronalen Verschaltungen des Tractus perforans mit seinen entorhinalen Efferenzen zum DG, die weiteren Verbindungen zur CA1 Region, Schaffer-Kollateralen zur CA3 Region und die Rückkopplung zum entorhinalen Cortex bleiben bei der Präparation und nach Kultivierung *in vitro* weitestgehend intakt (Holopainen, 2005; Grabiec et al., 2017). Auch die relativ frühe Präparation der OHSC aus Ratten am 9. Tag in Kultur scheint auf die neuronale Entwicklung, insbesondere im Hinblick auf die Anzahl der Synapsen, keinen relevanten Einfluss zu haben (De Simoni et al., 2003). Dennoch könnte diese frühe Kultivierung eine gewisse Limitation des Modells darstellen. Auf der einen Seite ist durch fehlende Einflüsse aus anderen Cortex-Regionen eine veränderte Modulation auf die Synapsenbildung und Plastizität durch das Fehlen von Neurotransmittern wie Dopamin, Serotonin und Acetylcholin denkbar (Ojeda and Ávila, 2019; Huber et al., 2022). Auf der anderen Seite kann jedoch auch keine gesicherte Äquivalenz zur *in vivo* Situation angenommen werden. Des Weiteren besteht generell das Problem, dass bei Gewinnung von Neuronen wie auch Gliazellen aus sehr jungen Tieren keine Einschätzung über den Einfluss neuronaler Wachstumsfaktoren und Hormone erfolgen kann (Donahue et al., 2006; Olivares-Hernández et al., 2022). Altersbezogene Veränderungen mit Einfluss auf die Funktion von Neuronen und Gliazellen werden nicht berücksichtigt und möglicherweise durch noch sehr junges neuronales Gewebe verzerrt (Bell et al., 2010; Niraula et al., 2017). Die Untersuchung von Erkrankungen wie dem Schlaganfall, dessen Inzidenz im Alter zunimmt, ist daher per se eine Limitation dieses Modells. Untersuchungen an erwachsenen Tieren (8-10 Wochen) zeigten, dass

die Kultivierung von OHSC aus diesem Alter bereits nach 6 Tagen in Kultur mit einer deutlich reduzierten Zellviabilität einherging (Legradi et al., 2011). Inwieweit eine analoge Kultivierung älterer Tiere durch veränderte Kulturmedien möglich ist, wird sich in weiteren Studien zeigen (Kim et al., 2013; Jang et al., 2018). Während sich Neurone der CA Region in einem postmitotischen Zustand befinden, scheint die Population im DG postnatal zwischen dem 5. bis 7. Tag noch mitotisch aktiv zu sein (Schlessinger et al., 1975). Eine Kultivierung bis zum 9. Tag postnatal ist daher sinnvoll. OHSC eignen sich als Modell ideal, um isoliert pharmakologische Effekte auf neuronale Zellen sowie Gliazellen zu untersuchen (Grabiec et al., 2017). Dabei kann in diesem Modell sowohl der Einfluss des Blutdrucks, des Perfusionsdrucks und die Steigerung des intrakraniellen Drucks als auch der Einfluss peripherer Immunzellen vernachlässigt werden (Chamorro et al., 2012). Das Modell hilft dabei, isolierte Effekte auf Mikroglia wie auch auf Astrozyten zu untersuchen und grundlegende Erkenntnisse über deren Eigenschaften zu gewinnen (Heppner et al., 1998; Kohl et al., 2003). Die Gewinnung mehrerer OHSC aus einem Tier ermöglicht zum einen eine Paralleltestung mehrerer Behandlungsgruppen, was wiederum zu einer verbesserten Vergleichbarkeit beiträgt. Zum anderen kann die Anzahl der Tiere gegenüber *in vivo* Experimenten reduziert werden. Neben der Analyse von diversen Medikamenten eignen sich OHSC zur Untersuchung von Effekten und Interaktionen verschiedener Materialien auf und mit Nervengewebe (Kleine et al., 2021). Bereits in einer vorangegangenen Studie konnte für Tabotamp®, einen Vertreter aus der Gruppe der ORC, ein schädlicher Effekt auf neuronale Zellen infolge eines sauren pH-Werts nachgewiesen werden (Leisz et al., 2020). Die OHSC eigneten sich hierbei zur weiteren Untersuchung dieser Gruppe von Hämostyptika und deren Einfluss auf neuronales Gewebe. In diesem Kontext konnten spezifische Eigenschaften für Tabotamp®, Equicel® und Equitamp® nachgewiesen und untereinander verglichen werden (Kleine et al., 2021). Die Applikation von Equicel® führte dabei zu einer signifikanten Zunahme der Mikroglia. Die Behandlung mit Tabotamp®, welches ausgeprägte saure Eigenschaften besitzt (Leisz et al., 2020), führte zu einer erschwerten immunhistochemischen Detektion der Mikroglia. Weiter zeigte sich für Tabotamp® und Equicel® eine deutlich destruktive Eigenschaft auf neuronales Gewebe, während der Schaden durch Equitamp® schwächer ausgeprägt war (Kleine et al., 2021). Dies könnte ein Hämostyptikum wie Tabotamp® oder Equicel® besonders bei großen Tumorresektionen attraktiv machen, um mögliche lokale Rezidive an den Resektionsrändern zu reduzieren. Equitamp® hingegen könnte insbesondere bei operativen Eingriffen an besonders eloquenten Regionen wie zum Beispiel einem Vestibularisschwannom einen Vorteil haben.

2.1.2 Neurozytoprotektive Effekte von 2-AG, PEA und Nimodipin in OHSC

Ein weiteres Anwendungsgebiet der OHSC ist die Untersuchung intrinsischer Systeme wie des Endocannabinoidsystems oder die weitere Erforschung von Medikamenten wie Nimodipin. Im Hinblick auf die Analyse von neurozytoprotektiven Effekten in den OHSC wurde sowohl die

zelluläre Schädigung im Bereich des DG als auch die Anzahl der Mikroglia betrachtet. Im Allgemeinen kann in Bezug auf die neuronale Schädigung zwischen Apoptose, Autophagie vermittelten Prozessen sowie nekrotischen Veränderungen unterschieden werden (Yuan et al., 2003). Bei Schädigungen durch NMDA in den OHSC ist sowohl das Vorhandensein von Anteilen einer Nekrose als auch der Apoptose denkbar (Bonfoco et al., 1995). Zur Quantifizierung des exakten Schadens und auch zur Lokalisation der Schädigung hat sich Propidium Iodid (PI) als Marker für Zelltod etabliert (Ebrahimi et al., 2010; Happ and Tasker, 2016). Intravital interkaliert PI infolge einer erhöhten Permeabilität der Zellmembran von geschädigten Zellen mit deren DNA. Dabei korreliert die NMDA Konzentration mit der Aufnahme von PI in den verschiedenen Bereichen des Hippocampus (Happ and Tasker, 2016). Die CA1 Region ist besonders vulnerabel bezüglich dieser Schädigung, sodass geringere Konzentrationsveränderungen größere Auswirkungen auf die Anzahl von PI positiven Zellen haben (Ebrahimi et al., 2010; Vinet et al., 2012; Happ and Tasker, 2016). Im DG hingegen besteht eine enge Beziehung zwischen NMDA Konzentration und Anzahl der PI positiven degenerierenden Zellen (Ebrahimi et al., 2010). Aus diesem Grund wurde der DG für die Analysen in den jeweiligen Arbeiten ausgewählt (Hohmann et al., 2019; Hohmann et al., 2022; Kleine et al., 2022). PEA, 2-AG wie auch Nimodipin zeigten einen positiven Einfluss auf die Schädigung durch NMDA im DG (Hohmann et al., 2019; Hohmann et al., 2022). Während für die Applikation von PEA oder 2-AG ein jeweiliger neurozytoprotektiver Effekt nachweisbar war, führte die gleichzeitige Gabe beider Substanzen zur Aufhebung dieser Effekte (Hohmann et al., 2019). Ähnliche Ergebnisse sind bereits für die gleichzeitige Behandlung durch 2-AG mit O-1918 (abn-CBDR Antagonist) oder CBD beschrieben (Kreutz et al., 2009). Eine mögliche Erklärung wären interferierende molekulare Mechanismen zwischen den durch 2-AG beeinflussten abn-CBDR-vermittelten Signalwegen und dem Einfluss von PEA auf PPAR-Alpha sowie TRPV1. Eine weitere Ursache der teils gegensätzlichen Effekte von PEA und 2-AG ist deren Einfluss auf die Lokalisation des PPAR-Alpha. Während PEA 6 Stunden nach LPS Stimulation primärer Mikroglia die nukleäre Lokalisation von PPAR-Alpha erhört, wirkt 2-AG dieser entgegen (Hohmann et al., 2019). Ein neurozytoprotektives Zeitfenster, analog zu den Ergebnissen mit MMF, wurde für PEA und 2-AG bislang nicht untersucht. Für die Applikation von Nimodipin 4 Stunden vor der Schädigung konnte ein protektiver Effekt auf Neurone im DG nachgewiesen werden. Eine Applikation 4 Stunden nach der Schädigung hatte keinen Effekt mehr auf das Überleben dieser Zellen (Hohmann et al., 2022). Diese Ergebnisse decken sich zum Großteil mit weiteren Studien *in vivo* und *in vitro* mit Nachweis eines zeitabhängigen neurozytoprotektiven Effekts von Nimodipin (Mattsson et al., 1999; Lecht et al., 2012). Daher eignet sich Nimodipin als eine Substanz, welche präoperativ vor neurochirurgischen Eingriffen an eloquenten Arealen eingesetzt werden könnte.
Neben der Analyse von PI positiven Zellen stellen die Mikroglia als spezifische Immunzellen im ZNS einen wichtigen Parameter einer neuronalen Schädigung dar. Die Visualisierung von

Mikroglia durch das Griffonia Simplicifolia Isolectin B_4 (IB_4) ist eine bereits länger etablierte Methode (Streit, 1990). IB_4 eignet sich, ähnlich wie das ionisierte Calcium-bindende Adaptermolekül (Iba1), als nicht selektiver Marker zur generellen Übersicht der Mikroglia und deren Morphologie (Schwabenland et al., 2021). Periventrikuläre und meningeale Makrophagen sowie das ZNS infiltrierende Monozyten oder Makrophagen können durch Iba1 und IB_4 nicht unterschieden werden (Jurga et al., 2020). Inwieweit selektivere Marker wie TMEM119 eindeutig zwischen Mikroglia und Makrophagen differenzieren können, wird in neueren Studien intensiv untersucht (Ruan and Elyaman, 2022; Vankriekelsvenne et al., 2022). Anders als Iba1, mit einer erhöhten Expression nach Aktivierung der Zellen (Imai and Kohsaka, 2002), ist für IB_4 eine erhöhte oder veränderte Struktur der Glykan-Gruppierungen derzeit noch unklar (Kettenmann et al., 2011). Zur generellen Analyse der Anzahl der Mikroglia ist somit IB_4 als Marker in den OHSC geeignet, da insbesondere in den OHSC periphere infiltrierende Immunzellen keine Rolle spielen. Für 2-AG oder PEA konnte neben dem neurozytoprotektiven Effekt eine Reduktion der Mikroglia beobachtet werden (Kreutz et al., 2007; Kreutz et al., 2009; Koch et al., 2011; Hohmann et al., 2019). Nach Depletion der Mikroglia konnte kein neurozytoprotektiver Effekt von 2-AG oder PEA mehr festgestellt werden, sodass hier ein Mikroglia-abhängiger Effekt anzunehmen ist (Hohmann et al., 2019). Darüber hinaus führte die Behandlung mit PEA oder PEA und 2-AG, jedoch nicht mit 2-AG, zu einer stärkeren Ramifizierung der Mikroglia (Hohmann et al., 2019). Die Applikation von PEA führte zu einer Reduktion von NO in primären Mikroglia, während eine Behandlung von 2-AG oder 2-AG und PEA zu einer erhöhten NO-Freisetzung führte (Hohmann et al., 2019). Anders als bei PEA und 2-AG (Hohmann et al., 2019) zeigte sich keine reduzierte Anzahl von Mikroglia nach der Behandlung mit Nimodipin (Hohmann et al., 2022). Ein Effekt von Nimodipin auf Mikroglia ist jedoch nicht ausgeschlossen. In einer Neuronalen-Gliazell-Mischkultur konnte ein Einfluss von Nimodipin auf die Aktivierung der Mikroglia sowie NO-Freisetzung, TNF-Alpha und IL-1-Beta Sekretion nachgewiesen werden (Li et al., 2009).

2.1.3 Translationale Forschung als Schlüsselstelle in der Neurozytoprotektion?

Wie die vorausgegangenen Untersuchungen zum Endocannabinoidsystem oder Nimodipin zeigen, gilt das Forschungsfeld der Neurozytoprotektion seit mehreren Jahrzehnten als ein wichtiges und innovatives Gebiet, bisher jedoch mit Ausbleiben von klinisch belastbaren Erfolgen (Edwards et al., 2005; Beauchamp et al., 2008; Chamorro et al., 2021). Eine wichtige Schlüsselstelle stellt die Translation präklinischer Daten in klinischen Studien dar. Insbesondere präklinische Probleme könnten hierbei eine unzureichende Randomisierung und Verblindung der verschiedenen Gruppen, eine unzureichende Power durch zu kleine Behandlungsgruppen, eine zu geringe Reproduzierbarkeit der verschiedenen Substanzen in ähnlichen Modellen und unabhängigen Laboren sowie eine unzureichende Generalisierbarkeit der Ergebnisse über mehrere Modelle hinweg sein (Endres et al., 2008; Chamorro et al., 2021). Der Einfluss von

Komorbiditäten, Alter oder Geschlecht wird in vielen Modellen ebenfalls nicht ausreichend berücksichtigt. Aus diesem Grund wurden hierfür die Stroke Treatment Academic Industry Roundtable (STAIR) –Empfehlungen für präklinische Experimente definiert (Lyden et al., 2021). Diese fordern unter anderem eine genaue Untersuchung der zugrundeliegenden Mechanismen, hierunter auch ein klar definiertes protektives Zeitfenster.

In den Untersuchungen zu MMF (Kleine et al., 2022) erfolgte eine Randomisierung der OHSC in die verschiedenen Behandlungsgruppen. Wir konnten die Ergebnisse aus vorausgegangen Arbeiten reproduzieren (Ebrahimi et al., 2012) und den STAIR-Empfehlungen folgend das protektive Zeitfenster weiter eingrenzen (Kleine et al., 2022). Zusätzlich wurden durch die Arbeitsgruppe Versuche in einem *in vivo* SHT-Modell durchgeführt, um eine Translation der neurozytoprotektiven Effekte von MMF zu testen. Hier konnte in einem standardisierten kortikalen Traumamodell (CCI) ein protektiver Effekt für MMF 14 Tage nach Schädigung nachgewiesen und ein Einfluss auf IL-1 aufgezeigt werden (*nicht publiziert*). Die Translation des in den OHSC definierten Zeitfensters von MMF in das *in vivo* CCI-Modell gelang jedoch nicht (**Abb. 5**, *nicht publiziert*). So ist im Allgemeinen eine Translation des neurozytoprotektiven Effekts durch MMF in ein *in vivo* Modell möglich. Denkbare Ursachen für ein anderes Behandlungszeitfenster *in vivo* wären unter anderem das unterschiedliche Alter der Tiere zwischen den beiden Modellen, eine komplexere Pharmakokinetik von MMF während eines SHT (Lee et al., 1990), der zusätzliche Effekt peripherer Immunzellen mit Einfluss auf die Aktivierung der Mikroglia und Astrozyten (Jassam et al., 2017) sowie die Auswirkungen von MMF auf Endothelzellen in Hinblick auf die Wiederherstellung der BBB (Huang et al., 2005). Zur weiteren Charakterisierung eines potenziellen Zeitfensters *in vivo* sind daher ergänzende Studien mit MMF notwendig.

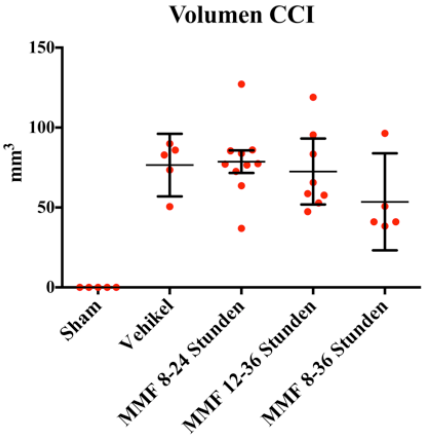

Abb. 5: Einfluss von MMF in verschiedenen Zeitfenstern *in vivo* nach CCI. Quantitative Analysen des Läsionsvolumens. Die MMF-Behandlung zwischen 8-24 Stunden (78,66 mm^3), 12-36 Stunden (72,52 mm^3) und 8-36 Stunden (53,52 mm^3) führte zu keiner signifikanten Reduktion des Läsionsvolumens im Vergleich zur Vehikel-Gruppe (76,55 mm^3, $p>0,05$). Die Werte sind als Mittelwert mit Standardfehler des Mittelwerts angegeben. Daten noch nicht publiziert.

2.2 Immunmodulation als ein neurozytoprotektives Konzept

Da die Neuroinflammation eher akut bis subakut nach einer Läsion auftritt, ist sie besonders zugänglich für mögliche therapeutische Ansätze (Dirnagl et al., 1999). Die derzeitige Entwicklung von einem festen 4,5 Stunden Therapiezeitfenster nach einem Schlaganfall zu einem gewebespezifischeren Zeitfenster (Nogueira et al., 2017) macht die Erforschung von

Immunmodulatoren wie MMF immer attraktiver (Lyden et al., 2021). Die Adressierung verschiedener Pathomechanismen und deren Modulation, wie zum Beispiel ein Mikroglia-abhängiges neurozytoprotektives Zeitfenster, könnte somit Ansatzpunkte für neue Therapiestrategien aufzeigen (Fisher and Savitz, 2022). Ein Wandel von einem gewebespezifischen Zeitfenster (Penumbra) zu einem sogenannten „Target-spezifischen Zeitfenster“ wäre in Zukunft hierdurch denkbar (Lyden et al., 2021). Bereits in den 90er Jahren wurden für diverse Immunsupressiva wie Cyclosporin A, Methylprednisolon oder FK506 (Tacrolimus) neurozytoprotektive Effekte nachgewiesen (Shiga et al., 1992; Behrmann et al., 1994; Sharkey and Butcher, 1994; Hailer, 2008). Auch MMF ist in diese Gruppe der Immunmodulatoren mit neurozytoprotektivem Potential einzuordnen (Miljkovic et al., 2002; Dehghani et al., 2003; Dehghani et al., 2010; Ebrahimi et al., 2012). Analog zu den Ergebnissen von MMF konnte für FK506 (Tacrolimus), neben dessen neurozytoprotektiver Wirkung in einem zerebralen Okklusionsmodell in Ratten, auch ein Einfluss auf die Aktivierung der Mikroglia wie Astrozyten und deren Zytokinproduktion gezeigt werden (Zawadzka and Kaminska, 2005). Weiterhin konnte für Roscovitin, ein CDK- Inhibitor nach einem *in vivo* SHT in Ratten eine reduzierte Aktivierung der Mikroglia wie verringerte NO-Freisetzung nachgewiesen werden (Hilton et al., 2008). MMF, wie auch andere Immunmodulatoren, zeigen hierbei ein multifaktorielles Wirkungsspektrum mit Einfluss auf die Aktivierung von Gliazellen (Zawadzka and Kaminska, 2005; Erlich et al., 2007; Wowro et al., 2019) und deren Zytokinproduktion (Muramoto et al., 2003; Zawadzka and Kaminska, 2005; Hilton et al., 2008).

2.3 MMF und dessen neurozytoprotektive Eigenschaften

Hauptsächlich in OHSC und Zellkulturen konnte für MMF ein neurozytoprotektiver Effekt nachgewiesen werden (Miljkovic et al., 2002; Dehghani et al., 2003; Dehghani et al., 2010; Ebrahimi et al., 2012). Eine Applikation von MMF innerhalb der ersten 4 Stunden hatte keinen Einfluss auf den neuronalen Schaden, eine Wirkung auf die Exzitotoxizität scheint daher unwahrscheinlich (Dehghani et al., 2003). Bei fehlenden Hinweisen auf eine direkte neuroprotektive Wirkung (Dehghani et al., 2010) besteht somit die Hypothese einer indirekten Wirkung durch Mikroglia und Astrozyten (Dehghani et al., 2003; Dehghani et al., 2010). Diese These wird durch ein späteres Zeitfenster und durch teilweise fehlende Effekte von MMF nach Depletion der Mikroglia aus den OHSC untermauert (Ebrahimi et al., 2012; Kleine et al., 2022). Die durch MMF nachgewiesene Reduktion der Proliferation und Zytokine wie IL-1, TNF-Alpha oder NO in primären Mikroglia und Astrozyten konnte durch die gleichzeitige Gabe von Guanosin antagonisiert werden. Dies deutet auf die spezifische Wirkung von MMF als Inhibitor des Purinstoffwechsels in Gliazellen hin (Dehghani et al., 2010). Eine zentrale Rolle des Purinstoffwechsels in der Vermittlung dieser Effekte ist daher weiter zu diskutieren. Für hohe Konzentrationen von MMF (10µg/ml) in primären Mikroglia konnte eine erhöhte Apoptoserate

nachgewiesen werden (Dehghani et al., 2010). Per se wäre daher eine geringe zytotoxische Wirkung durch MMF infolge erhöhter Konzentrationen denkbar. Für neuronale Zellen zeigte MMF (0,75µM) keinen schädlichen Einfluss (Brosh et al., 1992). Dies ist übereinstimmend mit einer untergeordneten Rolle der De-novo-Synthese in Neuronen (Giblett et al., 1972). Auch *in vivo* gibt es Hinweise auf eine neurozytoprotektive Wirkung. So konnte für MMF, nach arterieller Okklusion in einem Rattenmodell, eine Reduktion der kernspintomographisch gemessenen ischämischen Läsionen und eine Verbesserung bei neurologischen Funktionstests nachgewiesen werden (Chauhan et al., 2012). Auch in einem Modell an hypertensiven Mäusen zeigte MMF sowohl eine geringere Anzahl zerebraler Läsionen, ein reduziertes Hirnödem als auch bessere Endergebnisse bei Funktionstests auf (Dhande et al., 2017). In Bezug auf klinische Daten gibt es derzeit keine belastbaren Studien zur neurozytoprotektiven Wirkung nach einem Schlaganfall oder einem SHT. Die Therapie mit MMF im Rahmen einer primären zerebralen Vaskulitis mit dadurch einhergehenden Ischämien führte zu einer guten Remissionskontrolle (Rosati et al., 2017; Van Driessche et al., 2019). Auch in weiteren Modellen von Erkrankungen wie der Amyotrophen Lateralsklerose (ALS), Morbus Parkinson und der Multiplen Sklerose (MS) konnte für MMF ein positiver Einfluss auf das neuronale Überleben sowie die neuronale Regeneration nachgewiesen werden (Mowzoon et al., 2001; Vermersch et al., 2005; Yan et al., 2006; Michel et al., 2014). Abschließend bleibt der Anteil eines neurozytoprotektiven Einflusses in diesen Studien neben dem anzunehmenden Effekt der Immunsuppression durch MMF jedoch unklar (Ahrens et al., 2001; Mowzoon et al., 2001; Vermersch et al., 2005; Yan et al., 2006; Michel et al., 2014).

2.3.1 Mikroglia als vermittelnde Zellen der Effekte von MMF

MMF besitzt einen sehr starken Einfluss auf die Proliferation und somit auf die Anzahl der Mikroglia nach einer Schädigung (Dehghani et al., 2010; Ebrahimi et al., 2012; Kleine et al., 2022). Bereits eine geringe Dosis (1µg/ml) zeigte in der Zellkultur einen ausgeprägten antiproliferativen Effekt (Dehghani et al., 2010). Analog führte eine kurze (4-20 Stunden) wie auch frühe (ab 4 Stunden) Behandlung in den OHSC mit MMF (100µg/ml) zu einer deutlich reduzierten Anzahl und Proliferation der Mikroglia und Astrozyten (Ebrahimi et al., 2012). Diese Reduktion an Mikroglia korrelierte dabei nur teilweise mit einem neurozytoprotektiven Effekt in den OHSC (Dehghani et al., 2003; Ebrahimi et al., 2012; Kleine et al., 2022). Insbesondere bei einem frühen oder zu kurzen Behandlungszeitfenster (4-8 Stunden, 4-24 Stunden, 8-24 Stunden) oder zu späten Beginn der Behandlung (ab 16 Stunden) war in mehreren Studien eine signifikant reduzierte Anzahl der Mikroglia ohne neurozytoprotektiven Effekt nachweisbar (Ebrahimi et al., 2012; Kleine et al., 2022). Die Reduktion der Mikroglia scheint daher eher eine Komponente des protektiven Effektes von MMF als der führende Mediator zu sein. Dies bedeutet, dass (i) die Anzahl der Mikroglia kein direkter Parameter für einen neurozytoprotektiven Effekt ist und (ii) der neurozytoprotektive Effekt durch MMF nicht auf eine absolute Reduktion der Mikroglia zurückzuführen ist. Unabhängig von der reduzierten Anzahl der Mikroglia legen Untersuchungen

von Mikroglia-abhängigen und -unabhängigen Effekten eine frühe Mikroglia-abhängige Phase für die neurozytoprotektiven Effekte in den OHSC nahe (Kleine et al., 2022). Nach einer Depletion der Mikroglia durch Clodronat konnte folglich in den ersten 48 Stunden kein neurozytoprotektiver Effekt durch MMF nachgewiesen werden (Kleine et al., 2022). Darüber hinaus wurde nach der Depletion dieser Zellen in den OHSC eine deutliche Zunahme der neuronalen Schädigung beobachtet (Kohl et al., 2003; Kreutz et al., 2009; Kleine et al., 2022). Dies legt eine potenziell protektive Eigenschaft der Mikroglia auf neuronales Gewebe nahe (Streit, 2002). Die Exazerbation der Schädigung wäre zum einen durch das Fehlen einiger antiinflammatorischer Zytokine der Mikroglia erklärbar (Colton, 2009). Zum anderen sind Mikroglia in der Lage, über Faktoren wie dem Insulin-ähnlichen Wachstumsfaktor-1 (IGF-1) Einfluss auf die Neurogenese zu nehmen (Thored et al., 2009; Chen and Trapp, 2016). Weiter leisten Mikroglia über die Phagozytose, insbesondere nach neuronaler Schädigung, einen wichtigen Beitrag zur Homöostase im ZNS (Takahashi et al., 2005; Prinz et al., 2019). *In vivo* zeigt sich weitestgehend eine vergleichbare Datenlage zum Einfluss einer Depletion der Mikroglia auf die neuronale Läsion. Analysen von *in vivo* Studien in einem Mausmodell bei Läsionen des Myelons sowie nach zerebraler arterieller Okklusion zeigten eine Exazerbation des neuronalen Schadens nach Depletion der Mikroglia (Fu et al., 2020; Marino Lee et al., 2021). Jedoch ist die Datenlage *in vivo* heterogener, da zwei Studien in Mäusen nach Depletion der Mikroglia durch Gabe eines Kolonie-stimulierenden Faktor 1 Rezeptor (CSF1R)-Inhibitors keinen signifikanten Einfluss auf die Infarktgröße nach arterieller Okklusion aufwiesen (Cramer et al., 2022; Stojiljkovic et al., 2022). Abschließend ist jedoch die alleinige Reduktion der Anzahl der Mikroglia oder gar deren komplette Depletion kein sinnvoller neurozytoprotektiver Ansatz. Vielmehr scheint eine zeitspezifische Modulation der Mikroglia eine aussichtsreichere Möglichkeit zu sein.

2.3.2 Mikroglia-unabhängige Effekte von MMF

Anders als für 2-AG oder PEA (Hohmann et al., 2019) zeigte sich für MMF neben einer frühen Mikroglia-abhängigen Phase eine spätere Mikroglia-unabhängige Phase (Kleine et al., 2022). In OHSC ohne Mikroglia konnte 72 Stunden nach der Behandlung mit MMF ein neurozytoprotektiver Effekt nachgewiesen werden (Kleine et al., 2022). Ein Einfluss in dieser späten Phase von MMF auf Astrozyten und auf die Astrogliose scheint dabei denkbar (Miljkovic et al., 2002; Dehghani et al., 2010; Ebrahimi et al., 2012). So konnte ein Effekt von MMF auf die mRNA-Expression auf des Interferon regulierenden Faktor 1 (IRF-1), der iNOS und NO-Produktion in Astrozyten gefunden werden (Miljkovic et al., 2002). Auch zeigte sich in einer Studie in astrozytären Kulturen eine Reduktion der Proliferation und Produktion von TNF-Alpha sowie NO (Dehghani et al., 2010). In einem „Scratch-wound"-Modell konnte insbesondere nach 24 und 48 Stunden eine Wirkung auf die Bildung der Astrogliose nachgewiesen werden

(Ebrahimi et al., 2012). Auch in *in vivo* Versuchen in der Arbeitsgruppe in einem CCI-Modell bestätigte sich ein Einfluss auf die Proliferation der Astrozyten (*nicht publiziert*). Darüber hinaus scheint MMF *in vivo* einen Einfluss auf die IL-1-Beta-Expression in Astrozyten zu haben (**Abb. 6**, *nicht publiziert*). Hierbei wäre sowohl ein direkter Einfluss auf die Astrozyten (Dehghani et al., 2010) als auch eine indirekte Wirkung über die antiinflammatorischen Effekte der Mikroglia wahrscheinlich (Liddelow et al., 2017). Nach Aktivierung der Astrozyten durch Mikroglia-konditioniertes Medium konnte insbesondere eine starke Erhöhung von proinflammatorischen Zytokinen wie IL-1-Beta oder TNF-Alpha nachgewiesen werden, sodass eine indirekte Aktivierung der Astrozyten durch Mikroglia angenommen werden kann (Liddelow et al., 2017). Der Nachweis eines neurozytoprotektiven Effekts in Mikroglia depletierten OHSC 72 Stunden nach Schädigung spricht jedoch eher für einen direkten Effekt durch Astrozyten (Kleine et al., 2022). Welchen abschließenden Effekt MMF jedoch auf die Bildung der reaktiven Astrogliose und auf das Überleben von neuronalen Zellen hat, ist derzeit noch nicht sicher geklärt. Generell besitzt die Bildung einer reaktiven Astrogliose und die damit einhergehende Kompartimentalisierung einer Läsion teils auch neurozytoprotektive Eigenschaften (Myer et al., 2006; Shimada et al., 2011; Cekanaviciute et al., 2014; Liu et al., 2014). Sollte die Glianarbe das Ausmaß der Schädigung begrenzen, würde eine komplette Inhibition dieser Reaktion durch MMF wohl eher zu einer Zunahme der Schädigung führen (Sofroniew, 2009; Becerra-Calixto and Cardona-Gomez, 2017). Weitere Untersuchungen sind daher nötig, um die genaue Wirkung von MMF in dieser späteren Phase weiter zu klären. Spannend bleibt daher die Frage, welchen Einfluss MMF auf die neuronale Schädigung weit über den beobachteten Zeitraum nimmt.

2.3.3 Der Einfluss von MMF auf NO und die Zytokinproduktion

Generell kann angenommen werden, dass eine akute neuronale Schädigung in Mikroglia und Astrozyten zu einer Hochregulierung und Freisetzung von verschiedenen Zytokinen führt (Lee et al., 1993; Gourin and Shackford, 1997; Dehghani et al., 2010). Diese Zytokine können wiederum den sekundären Schaden beeinflussen. Für MMF konnte eine Reduktion von NO und Zytokine wie IL-1 und TNF-Alpha nachgewiesen werden (Miljkovic et al., 2002; Dehghani et al., 2010; Roth et al., 2021). Insbesondere wurde die Menge des sezernierten IL-1-Beta in primären Mikroglia durch MMF nach LPS-Stimulation reduziert (Dehghani et al., 2010). Auch *in vivo* konnte, in Übereinstimmung mit den bisherigen Ergebnissen, in einem CCI-Modell ein positiver Einfluss auf die IL-1-Beta-Expression im periläsionalen Bereich in Astrozyten nach MMF-Behandlung nachgewiesen werden (**Abb. 6**, *nicht publiziert)*. IL-1 führt durch seine pleiotrope Wirkung unter anderem zur Freisetzung weiterer Zytokine in Mikroglia und Astrozyten (Zhu et al., 2022) und beeinflusst das neuronale Überleben durch die Modulierung der Migration weiterer peripherer Immunzellen und Disruption der BBB (Wang et al., 2014; Wong et al., 2019; Roth et al., 2021).

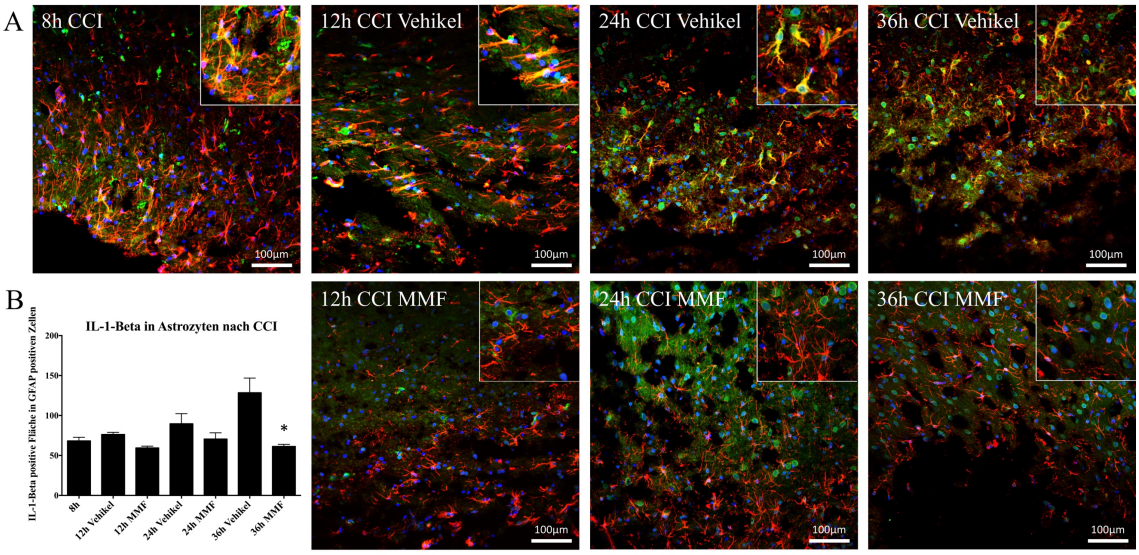

Abb. 6 IL-1-Beta Expression in Astrozyten ipsilateral des CCI. (A) Konfokale Laser-Scanning-Mikroskopie (CLSM) mit Darstellung von IL-1-Beta (Grün), GFAP in Astrozyten (Rot) und DAPI in Zellkernen (Blau) der ipsilateralen Seite zu verschiedenen Zeitpunkten mit und ohne MMF-Behandlung. (B) Quantitative Analysen der mittleren IL-1-Beta Fläche in GFAP positiven Zellen des ipsilateralen Kortex (* $p<0,05$ gegenüber 36h Vehikel). Die Werte sind als Mittelwert mit Standardfehler des Mittelwerts angegeben. Skalenbalken = 100 µm.

2.3.4 Zeitabhängige Effekte von MMF

Die durch MMF nachgewiesenen neurozytoprotektiven Effekte unterliegen einem spezifischen Behandlungszeitfenster (Ebrahimi et al., 2012). Dieses weist besonders zwischen 8-36 Stunden nach der Schädigung neben dem antiproliferativen auch einen neurozytoprotektiven Effekt auf (Ebrahimi et al., 2012; Kleine et al., 2022). Für MMF konnte gezeigt werden, dass die Applikation innerhalb der ersten 8-12 Stunden nach der Schädigung in OHSC begonnen und für 24 Stunden andauern sollte, um einen neurozytoprotektiven Effekt zu erzielen (Kleine et al., 2022). Ein Beginn 16 Stunden nach der Schädigung in den OHSC zeigte keinen nachweisbaren neurozytoprotektiven Effekt (Ebrahimi et al., 2012). Eine Behandlung durch MMF sollte daher nicht später als 16 Stunden nach der Läsion begonnen werden und nicht kürzer als 24 Stunden anhalten. Es soll trotzdem bedacht werden, dass Infektionen in der akuten Phase eine ernstzunehmende Komplikation von Patient:innen nach ischämischem Schlaganfall oder SHT darstellen. Ein kurzes Zeitfenster für eine mögliche Therapie im Rahmen einer Immunmodulation ohne das Risiko einer systemischen Immunsuppression wäre daher wünschenswert (Westendorp et al., 2011). Die volle systemische immunsuppressive Wirkung durch MMF ist allerdings erst nach 21-30 Tagen anzunehmen (Allison and Eugui, 2005).

Die frühe Mikroglia-abhängige Phase von MMF scheint generell mit dem Zeitfenster sowie einem Maximum der Proliferationsrate nach 24 Stunden übereinzustimmen (Ebrahimi et al., 2012; Kleine et al., 2022). Interessanterweise konnte nachgewiesen werden, dass eine Behandlung mit MMF zwischen 8-24 Stunden nach der Schädigung mit Fixierung der Schnitte nach 72 Stunden keinen protektiven Einfluss hat. Bei früherer Fixierung der Schnitte nach 24

Stunden konnte jedoch ein neurozytoprotektiver Effekt aufgezeigt werden (Kleine et al., 2022). Das bedeutet, dass auch in einem früheren und kürzeren Zeitintervall eine Wirkung durch MMF möglich ist, jedoch nicht ausreicht, um die destruktiven Prozesse, die danach folgen, hinreichend zu modulieren. Weiter unklar bleibt, welchen Effekt die spätere Mikroglia-unabhängige Phase nach 72 Stunden auf den neuronalen Schaden hat (Kleine et al., 2022).

2.4 Die Bedeutung des Purinstoffwechsels auf die Proliferation von Gliazellen nach neuronaler Schädigung

Das Zusammenspiel von Metabolismus wie dem Purinstoffwechsel, der Proliferation von Gliazellen und deren inflammatorischen Kaskaden legt die Grundlage für mögliche dysregulierte Prozesse, welche durch Substanzen wie MMF therapeutisch beeinflussbar sind (Kleine et al., 2022). Dieses Zusammenspiel des zellulären Stoffwechsels und der Aktivierung von Immunzellen ist insbesondere in Lymphozyten gut erforscht. Eine T-Zell-Aktivierung führte unter anderem zu einer gleichzeitigen Stimulation der zellulären Glucose-Aufnahme sowie der Glykolyse (Frauwirth et al., 2002; Chapman et al., 2020). Der Phosphoinositid-3-Kinase (PI3K)/Akt-Signalweg scheint dabei eine grundlegende Funktion in dieser Regulation zu haben (Zhu and Thompson, 2019). Dabei können weitere Faktoren wie mTOR (Zeng and Chi, 2017) und Forkhead-Box-Protein O (FOXO) (Luo and Li, 2018) an der Kontrolle zwischen dem metabolischen Zustand und der inflammatorischen Antwort von T-Zellen beteiligt sein. Eine besondere Bedeutung bei der Zellteilung kommt dem Nukleotidmetabolismus von Immunzellen zu. Bei T-Zellen, weniger bei B-Zellen, hat die De-novo-Synthese von Purinen eine zentrale Bedeutung für die Proliferation und Aktivität (Allison et al., 1977). In humanen Leukozyten führt Guanosin (GMP, GDP und GTP) zu einer Aktivierung der PRPP-Synthetase, während Adenosin eine hemmende Wirkung auf die De-novo-Synthese hat (Allison and Eugui, 2000). MMF ist, wie bereits erwähnt, durch die Inhibition der IMPDH in der Lage, den Guanosin-Pool zu depletieren und hat daher allosterisch einen Einfluss auf die gesamte De-novo-Synthese (Allison and Eugui, 2000; Liao et al., 2017). Die Hemmung der IMPDH mit hieraus folgender Reduktion des intrazellulären GMP resultiert daher in einer Inhibition der PRPP-Synthetase und damit des gesamten Purinstoffwechsels. Das Ergebnis ist eine reduzierte Proliferation von T- und B-Zellen (Allison et al., 1993), Mikroglia und Astrozyten (Ebrahimi et al., 2012). Durch die zusätzliche Gabe von Guanosin konnten die durch MMF ausgelösten antiproliferativen Effekte auf die Mikroglia antagonisiert werden (Ebrahimi et al., 2012). In aus dem Thymus gewonnenen T-Lymphozyten konnte gezeigt werden, dass die De-novo-Synthese besonders abhängig vom Zellzyklus ist und ein Großteil der De-novo-Synthese in der S-Phase erfolgt. MMF führt daher vor allem zu einer Hemmung in der S-Phase (Cohn et al., 1999). Aufgrund des ausgeprägten Einflusses von MMF auf die Mikroglia scheint die De-novo-Synthese auch in diesen Zellen eine zentrale Bedeutung zu spielen (Dehghani et al., 2010; Ebrahimi et al., 2012).

Die Inhibition des Purinstoffwechsels durch MMF könnte zu einem erhöhten metabolischen Stress in Mikroglia führen. Eine typische Reaktion auf metabolischen Stress in Zellen stellt die Autophagie dar (Zhu and Thompson, 2019; Klionsky et al., 2021). Autophagie definiert einen Prozess infolge eines Nährstoff- oder Energiemangels, bei dem es zum Abbau von zellulären Komponenten kommt, um grundlegende Funktionen und letztendlich das Überleben der Zelle zu sichern. Dies wird zum Großteil über Autophagosomen und die Lysosomen realisiert und als Makroautophagie bezeichnet (Rabinowitz and White, 2010; Klionsky et al., 2021). Die Signalwege der DAMPS und PAMPS können durch ineinandergreifende Kaskaden die Autophagie regulieren (Levine et al., 2011). Diese wird unter anderem über den Unc-51 ähnliche Autophagie aktivierende Kinase (ULK1)/mTOR Komplex1 realisiert. Die zur Autophagie zugehörigen Gene (Atg) und deren Proteine sind an der Modulation der Prozesse beteiligt (Rabinowitz and White, 2010; Klionsky et al., 2021). Als erste Verbindung zwischen der Autophagie und der Zytokinproduktion konnte Atg 5 nachgewiesen werden (Lee et al., 2007; Virgin and Levine, 2009; Yamamoto et al., 2023). In Makrophagen konnte nach einem Knockout-Modell des Gens Atg16L1 eine erhöhte Aktivität der Caspase-1 und hierdurch eine erhöhte IL-1-Beta-Aktivierung beobachtet werden (Saitoh et al., 2008). In einer Analyse des Transkriptoms in einer Magenkarzinom Zelllinie konnte ein Einfluss von MMF auf den mit der Autophagie eng verknüpften PI3K/AKT/mTOR Signalweg sowie verschiedene Cycline und CDKs beobachtet werden (Rabinowitz and White, 2010; Dun et al., 2013). Dies könnte eine veränderte Expression der Nukleotidsynthese wie auch Glykolyse in Jurkat-T-Zellen durch MMF erklären (Fernández-Ramos et al., 2016; Zhu and Thompson, 2019). Diese Verbindung zwischen Autophagie und der Inhibition des Purinstoffwechsels durch MMF stellt somit eine mögliche Hypothese der zugrunde liegenden molekularen Mechanismen einer reduzierten Zytokinproduktion von Astrozyten und Mikroglia dar (Dehghani et al., 2010). Neben dieser Hypothese stellt die IMPDH selbst eine molekulare Struktur dar, welche neurozytoprotektive Effekte vermitteln könnte (Kozhevnikova et al., 2012). Die Regulation der IMPDH erfolgt zum Teil allosterisch. Für GMP wie auch XMP und Nicotinamidadenindinukleotid (NAD)H konnte ein inhibitorischer Effekt auf die IMPDH-Isoformen 1 und 2 nachgewiesen werden (Carr et al., 1993). Neben dieser allosterischen Regulation war nach Aktivierung von Lymphozyten eine vermehrte Expression der IMPDH-Isoform 2 nachweisbar (Allison et al., 1993). In OHSC zeigte sich nach Schädigung durch NMDA eine signifikante erhöhte Expression der IMPDH-Isoform 2 nach 12 Stunden gegenüber 36 und 48 Stunden (Ebrahimi et al., 2012). Allerdings konnten in Zellkulturen von Astrozyten und Mikroglia keine signifikanten Veränderungen der IMPDH-Isoform 2 nachgewiesen werden (Kleine et al., 2022). In der monozytären Zelllinie (Jukart-Zellen) war eine erhöhte Expression der mRNA der IMPDH-Isoform 2 nach 12 Stunden, wie in OHSC beobachtet, nachweisbar. Ein Einfluss auf die Expression konnte durch MMF in dieser Studie nicht aufgezeigt werden (Jain et al., 2004). Die Regulation der IMPDH-Isoform 2 ist wahrscheinlich zu einem großen Teil auf

Protein-Protein-Interaktionen oder posttranslationale Modifikationen zurückzuführen (Jain et al., 2004). Weiter konnte nachgewiesen werden, dass die IMPDH zytoplasmatisch wie auch nukleär lokalisiert ist. Dabei scheint die IMPDH in Eukaryoten auch eine Rolle als Transkriptionsfaktor im Sinne eines Repressors in der Regulation der Histongene und E2F zu spielen (Kozhevnikova et al., 2012). Auch deuten mehrere Studien darauf hin, dass eine gewisse Regulation der IMPDH durch eine Polymerisation in Filamente realisiert wird (Calise et al., 2018; Buey et al., 2022). Für die Behandlung mit MMF in HeLa-Zellen konnte eine vermehrte Polymerisation der IMPDH in Makrostrukturen nachgewiesen werden (Thomas et al., 2012). Die duale Funktion als metabolisches Schlüsselenzym des Purinstoffwechsels und auch die Funktion als ein Trankskriptionsfaktor im Sinne eines Repressors mit hieraus antiproliferativer Wirkung legt eine übergeordnete regulatorische Funktion der IMPDH mit Verknüpfung des Metabolismus und der Genexpression insbesondere in der späten S-Phase nahe. IMPDH kann sich des Weiteren in sogenannten Makrostrukturen organisieren und im Sinne eines Sensors Nukleotide binden (Thomas et al., 2012). Diese Integration der IMPDH als Enzym und als Transkriptionsfaktor wäre die Grundlage für einen weiteren hypothetischen Wirkungsmechanismus von MMF. Auch für weitere Inhibitoren von IMPDH konnte ein neurozytoprotektiver Effekt und ein Einfluss auf die Proliferation von Mikroglia nachgewiesen werden (Liao et al., 2017). Für Sappanone A konnte in Übereinstimmung mit den Ergebnissen von MMF eine Reduktion von proinflammatorischen Zytokinen wie TNF-Alpha, IL-1-Beta und IL-6 sowie der iNOS und auch ein Effekt auf die Proliferation von Mikroglia sowie die Integrität von Neuronen nach LPS Gabe in der CA1 Region nachgewiesen werden (Liao et al., 2017). Sappanone A zeigte auch *in vivo* bereits neurozytoprotektive Effekte (Wang et al., 2021). Für Ribavirin, einem Nukleosid-Analogon und Inhibitor der IMPDH, zeigten sich Hinweise auf eine Reduktion der Proliferation von Mikroglia wie auch auf neurozytoprotektive Eigenschaften (Solbrig et al., 2002).

Die enge Verbindung zwischen Metabolismus, Proliferation und Differenzierung von Immunzellen stellt eine wichtige Basis für das Verständnis komplexer neuroinflammatorischer Antworten im Rahmen eines Schlaganfalls oder eines SHT dar. Abschließend bleibt das Bild zwischen den genauen molekularen Mechanismen des Purinstoffwechsels, dem Einfluss von MMF und dessen Verschaltung mit immunologischen Prozessen sowie der Autophagie und Zytokinproduktion in Gliazellen inkomplett. Die vorgelegten Arbeiten unterstreichen dabei die weitere Notwenigkeit, molekulare Prozesse im Zusammenspiel von Mikroglia und Astrozyten im Hinblick auf den Purinstoffwechsel weiter zu untersuchen und sie zeigen eine eindeutiges zeitliches Mikroglia-abhängiges neurozytoprotektives Wirkspektrum für MMF auf.

3. Literaturverzeichnis

Abele, A.E., Scholz, K.P., Scholz, W.K., and Miller, R.J. (1990). Excitotoxicity induced by enhanced excitatory neurotransmission in cultured hippocampal pyramidal neurons. *Neuron* 4(3)**,** 413-419. doi: 10.1016/0896-6273(90)90053-I.

Ahmad, A., Crupi, R., Campolo, M., Genovese, T., Esposito, E., and Cuzzocrea, S. (2013). Absence of TLR4 reduces neurovascular unit and secondary inflammatory process after traumatic brain injury in mice. *PloS one* 8(3)**,** e57208-e57208. doi: 10.1371/journal.pone.0057208.

Ahmad, A., Crupi, R., Impellizzeri, D., Campolo, M., Marino, A., Esposito, E., et al. (2012a). Administration of palmitoylethanolamide (PEA) protects the neurovascular unit and reduces secondary injury after traumatic brain injury in mice. *Brain Behav Immun* 26(8)**,** 1310-1321. doi: 10.1016/j.bbi.2012.07.021.

Ahmad, A., Genovese, T., Impellizzeri, D., Crupi, R., Velardi, E., Marino, A., et al. (2012b). Reduction of ischemic brain injury by administration of palmitoylethanolamide after transient middle cerebral artery occlusion in rats. *Brain Res* 1477**,** 45-58. doi: 10.1016/j.brainres.2012.08.006.

Ahrens, N., Salama, A., and Haas, J. (2001). Mycophenolate-mofetil in the treatment of refractory multiple sclerosis. *J Neurol* 248(8)**,** 713-714. doi: 10.1007/s004150170122.

Allan, S.M., Lawrence, C.B., and Rothwell, N.J. (1998). Interleukin-1 beta and interleukin-1 receptor antagonist do not affect glutamate release or calcium entry in rat striatal synaptosomes. *Mol Psychiatry* 3(2)**,** 178-182. doi: 10.1038/sj.mp.4000351.

Allan, S.M., Tyrrell, P.J., and Rothwell, N.J. (2005). Interleukin-1 and neuronal injury. *Nat Rev Immunol* 5(8)**,** 629-640. doi: 10.1038/nri1664.

Allison, A.C., and Eugui, E.M. (2000). Mycophenolate mofetil and its mechanisms of action. *Immunopharmacology* 47(2-3)**,** 85-118.

Allison, A.C., and Eugui, E.M. (2005). Mechanisms of action of mycophenolate mofetil in preventing acute and chronic allograft rejection. *Transplantation* 80(2 Suppl)**,** S181-190. doi: 10.1097/01.tp.0000186390.10150.66.

Allison, A.C., Hovi, T., Watts, R.W., and Webster, A.D. (1975). Immunological observations on patients with Lesch-Nyhan syndrome, and on the role of de-novo purine synthesis in lymphocyte transformation. *Lancet (London, England)* 2(7946)**,** 1179-1183. doi: 10.1016/s0140-6736(75)92661-6.

Allison, A.C., Hovi, T., Watts, R.W., and Webster, A.D. (1977). The role of de novo purine synthesis in lymphocyte transformation. *Ciba Found Symp* (48)**,** 207-224. doi: 10.1002/9780470720301.ch13.

Allison, A.C., Kowalski, W.J., Muller, C.D., and Eugui, E.M. (1993). Mechanisms of action of mycophenolic acid. *Ann N Y Acad Sci* 696**,** 63-87. doi: 10.1111/j.1749-6632.1993.tb17143.x.

Ambrosino, P., Soldovieri, M.V., Russo, C., and Taglialatela, M. (2013). Activation and desensitization of TRPV1 channels in sensory neurons by the PPARα agonist palmitoylethanolamide. *Br J Pharmacol* 168(6)**,** 1430-1444. doi: 10.1111/bph.12029.

Andersen, J.V., Markussen, K.H., Jakobsen, E., Schousboe, A., Waagepetersen, H.S., Rosenberg, P.A., et al. (2021). Glutamate metabolism and recycling at the excitatory synapse in health and neurodegeneration. *Neuropharmacology* 196**,** 108719. doi: https://doi.org/10.1016/j.neuropharm.2021.108719.

Balestreri, M., Czosnyka, M., Chatfield, D.A., Steiner, L.A., Schmidt, E.A., Smielewski, P., et al. (2004). Predictive value of Glasgow Coma Scale after brain trauma: change in trend over the past ten years. *J Neurol Neurosurg Psychiatry* 75(1)**,** 161-162.

Basilico, B., Ferrucci, L., Ratano, P., Golia, M.T., Grimaldi, A., Rosito, M., et al. (2022). Microglia control glutamatergic synapses in the adult mouse hippocampus. *Glia* 70(1)**,** 173-195. doi: 10.1002/glia.24101.

Beauchamp, K., Mutlak, H., Smith, W.R., Shohami, E., and Stahel, P.F. (2008). Pharmacology of traumatic brain injury: where is the "golden bullet"? *Mol Med* 14(11-12)**,** 731-740. doi: 10.2119/2008-00050.Beauchamp.

Becerra-Calixto, A., and Cardona-Gomez, G.P. (2017). The Role of Astrocytes in Neuroprotection after Brain Stroke: Potential in Cell Therapy. *Front Mol Neurosci* 10**,** 88. doi: 10.3389/fnmol.2017.00088.

Behrmann, D.L., Bresnahan, J.C., and Beattie, M.S. (1994). Modeling of acute spinal cord injury in the rat: neuroprotection and enhanced recovery with methylprednisolone, U-74006F and YM-14673. *Exp Neurol* 126(1)**,** 61-75. doi: 10.1006/exnr.1994.1042.

Beldarrain, G., Hilario, E., Lara-Celador, I., Chillida, M., Catalan, A., Álvarez-Diaz, A., et al. (2023). The Long-Term Neuroprotective Effect of the Endocannabinoid 2-AG and Modulation of the SGZ's Neurogenic Response after Neonatal Hypoxia-Ischemia. *Pharmaceutics* 15(6). doi: 10.3390/pharmaceutics15061667.

Bell, R.D., Winkler, E.A., Sagare, A.P., Singh, I., LaRue, B., Deane, R., et al. (2010). Pericytes control key neurovascular functions and neuronal phenotype in the adult brain and during brain aging. *Neuron* 68(3)**,** 409-427. doi: 10.1016/j.neuron.2010.09.043.

Ben-Shabat, S., Fride, E., Sheskin, T., Tamiri, T., Rhee, M.H., Vogel, Z., et al. (1998). An entourage effect: inactive endogenous fatty acid glycerol esters enhance 2-arachidonoyl-glycerol cannabinoid activity. *Eur J Pharmacol* 353(1)**,** 23-31. doi: 10.1016/s0014-2999(98)00392-6.

Berkich, D.A., Ola, M.S., Cole, J., Sweatt, A.J., Hutson, S.M., and LaNoue, K.F. (2007). Mitochondrial transport proteins of the brain. *Journal of neuroscience research* 85(15)**,** 3367-3377. doi: 10.1002/jnr.21500.

Bianco, F., Ceruti, S., Colombo, A., Fumagalli, M., Ferrari, D., Pizzirani, C., et al. (2006). A role for P2X7 in microglial proliferation. *Journal of neurochemistry* 99(3)**,** 745-758. doi: 10.1111/j.1471-4159.2006.04101.x.

Bittner, C.X., Loaiza, A., Ruminot, I., Larenas, V., Sotelo-Hitschfeld, T., Gutiérrez, R., et al. (2010). High resolution measurement of the glycolytic rate. *Frontiers in neuroenergetics* 2**,** 26. doi: 10.3389/fnene.2010.00026.

Bonfoco, E., Krainc, D., Ankarcrona, M., Nicotera, P., and Lipton, S.A. (1995). Apoptosis and necrosis: two distinct events induced, respectively, by mild and intense insults with N-methyl-D-aspartate or nitric oxide/superoxide in cortical cell cultures. *Proc Natl Acad Sci U S A* 92(16)**,** 7162-7166.

Brenner, M., and Messing, A. (2021). Regulation of GFAP Expression. *ASN Neuro* 13**,** 1759091420981206. doi: 10.1177/1759091420981206.

Brewer, L.D., Thibault, O., Staton, J., Thibault, V., Rogers, J.T., Garcia-Ramos, G., et al. (2007). Increased vulnerability of hippocampal neurons with age in culture: Temporal association with increases in NMDA receptor current, NR2A subunit expression and recruitment of L-type calcium channels. *Brain Research* 1151**,** 20-31. doi: https://doi.org/10.1016/j.brainres.2007.03.020.

Broen, J.C.A., and van Laar, J.M. (2020). Mycophenolate mofetil, azathioprine and tacrolimus: mechanisms in rheumatology. *Nat Rev Rheumatol* 16(3)**,** 167-178. doi: 10.1038/s41584-020-0374-8.

Brosh, S., Sperling, O., Dantziger, E., and Sidi, Y. (1992). Metabolism of guanine and guanine nucleotides in primary rat neuronal cultures. *J Neurochem* 58(4)**,** 1485-1490. doi: 10.1111/j.1471-4159.1992.tb11368.x.

Brown, A.M., and Ransom, B.R. (2007). Astrocyte glycogen and brain energy metabolism. *Glia* 55(12)**,** 1263-1271. doi: 10.1002/glia.20557.

Bruce, A.J., Boling, W., Kindy, M.S., Peschon, J., Kraemer, P.J., Carpenter, M.K., et al. (1996). Altered neuronal and microglial responses to excitotoxic and ischemic brain injury in mice lacking TNF receptors. *Nature medicine* 2(7)**,** 788-794. doi: 10.1038/nm0796-788.

Bsibsi, M., Ravid, R., Gveric, D., and van Noort, J.M. (2002). Broad Expression of Toll-Like Receptors in the Human Central Nervous System. *Journal of Neuropathology & Experimental Neurology* 61(11)**,** 1013-1021. doi: 10.1093/jnen/61.11.1013.

Buchakjian, M.R., and Kornbluth, S. (2010). The engine driving the ship: metabolic steering of cell proliferation and death. *Nature Reviews Molecular Cell Biology* 11(10)**,** 715-727. doi: 10.1038/nrm2972.

Buey, R.M., Fernández-Justel, D., Jiménez, A., and Revuelta, J.L. (2022). The gateway to guanine nucleotides: Allosteric regulation of IMP dehydrogenases. *Protein Sci* 31(9)**,** e4399. doi: 10.1002/pro.4399.

Bureta, C., Setoguchi, T., Saitoh, Y., Tominaga, H., Maeda, S., Nagano, S., et al. (2019). TGF-β Promotes the Proliferation of Microglia In Vitro. *Brain Sci* 10(1). doi: 10.3390/brainsci10010020.

Burrell, A.L., and Kollman, J.M. (2022). IMPDH dysregulation in disease: a mini review. *Biochem Soc Trans* 50(1)**,** 71-82. doi: 10.1042/bst20210446.

Bushong, E.A., Martone, M.E., Jones, Y.Z., and Ellisman, M.H. (2002). Protoplasmic astrocytes in CA1 stratum radiatum occupy separate anatomical domains. *The Journal of neuroscience : the official journal of the Society for Neuroscience* 22(1)**,** 183-192. doi: 10.1523/JNEUROSCI.22-01-00183.2002.

Calise, S.J., Abboud, G., Kasahara, H., Morel, L., and Chan, E.K.L. (2018). Immune Response-Dependent Assembly of IMP Dehydrogenase Filaments. *Front Immunol* 9**,** 2789. doi: 10.3389/fimmu.2018.02789.

Cao, Z., Harvey, S.S., Bliss, T.M., Cheng, M.Y., and Steinberg, G.K. (2020). Inflammatory Responses in the Secondary Thalamic Injury After Cortical Ischemic Stroke. *Front Neurol* 11**,** 236. doi: 10.3389/fneur.2020.00236.

Carandang, R., Seshadri, S., Beiser, A., Kelly-Hayes, M., Kase, C.S., Kannel, W.B., et al. (2006). Trends in Incidence, Lifetime Risk, Severity, and 30-Day Mortality of Stroke Over the Past 50 Years. *JAMA* 296(24)**,** 2939-2946. doi: 10.1001/jama.296.24.2939.

Carbonell, W.S., Murase, S., Horwitz, A.F., and Mandell, J.W. (2005). Migration of perilesional microglia after focal brain injury and modulation by CC chemokine receptor 5: an in situ time-lapse confocal imaging study. *J Neurosci* 25(30)**,** 7040-7047. doi: 10.1523/jneurosci.5171-04.2005.

Cardinal von Widdern, J., Hohmann, T., and Dehghani, F. (2020). Abnormal Cannabidiol Affects Production of Pro-Inflammatory Mediators and Astrocyte Wound Closure in Primary Astrocytic-Microglial Cocultures. *Molecules* 25(3). doi: 10.3390/molecules25030496.

Carlisle, S.J., Marciano-Cabral, F., Staab, A., Ludwick, C., and Cabral, G.A. (2002). Differential expression of the CB2 cannabinoid receptor by rodent macrophages and macrophage-like cells in relation to cell activation. *Int Immunopharmacol* 2(1)**,** 69-82. doi: 10.1016/s1567-5769(01)00147-3.

Carlson, A.P., Hänggi, D., Macdonald, R.L., and Shuttleworth, C.W. (2020). Nimodipine Reappraised: An Old Drug With a Future. *Curr Neuropharmacol* 18(1)**,** 65-82. doi: 10.2174/1570159x17666190927113021.

Carr, S.F., Papp, E., Wu, J.C., and Natsumeda, Y. (1993). Characterization of human type I and type II IMP dehydrogenases. *J Biol Chem* 268(36)**,** 27286-27290.

Carroll, J.A., Race, B., Williams, K., Striebel, J.F., and Chesebro, B. (2021). Innate immune responses after stimulation with Toll-like receptor agonists in ex vivo microglial cultures and an in vivo model using mice with reduced microglia. *J Neuroinflammation* 18(1)**,** 194. doi: 10.1186/s12974-021-02240-w.

Casano, A.M., and Peri, F. (2015). Microglia: multitasking specialists of the brain. *Dev Cell* 32(4)**,** 469-477. doi: 10.1016/j.devcel.2015.01.018.

Cekanaviciute, E., Fathali, N., Doyle, K.P., Williams, A.M., Han, J., and Buckwalter, M.S. (2014). Astrocytic transforming growth factor-beta signaling reduces subacute neuroinflammation after stroke in mice. *Glia* 62(8)**,** 1227-1240. doi: 10.1002/glia.22675.

Chamorro, A., Dirnagl, U., Urra, X., and Planas, A.M. (2016). Neuroprotection in acute stroke: targeting excitotoxicity, oxidative and nitrosative stress, and inflammation. *Lancet Neurol* 15(8)**,** 869-881. doi: 10.1016/S1474-4422(16)00114-9.

Chamorro, Á., Lo, E.H., Renú, A., van Leyen, K., and Lyden, P.D. (2021). The future of neuroprotection in stroke. *J Neurol Neurosurg Psychiatry* 92(2)**,** 129-135. doi: 10.1136/jnnp-2020-324283.

Chamorro, A., Meisel, A., Planas, A.M., Urra, X., van de Beek, D., and Veltkamp, R. (2012). The immunology of acute stroke. *Nat Rev Neurol* 8(7)**,** 401-410. doi: 10.1038/nrneurol.2012.98.

Chao, C.C., Hu, S., Molitor, T.W., Shaskan, E.G., and Peterson, P.K. (1992). Activated microglia mediate neuronal cell injury via a nitric oxide mechanism. *J Immunol* 149(8)**,** 2736-2741.

Chapman, N.M., Boothby, M.R., and Chi, H. (2020). Metabolic coordination of T cell quiescence and activation. *Nat Rev Immunol* 20(1)**,** 55-70. doi: 10.1038/s41577-019-0203-y.

Chauhan, A., Sharma, U., Reeta, K.H., Jagannathan, N.R., Mehra, R.D., and Gupta, Y.K. (2012). Neuroimaging, biochemical and cellular evidence of protection by mycophenolate mofetil on middle cerebral artery occlusion induced injury in rats. *Eur J Pharmacol* 684(1-3)**,** 71-78. doi: 10.1016/j.ejphar.2012.03.037.

Chen, Z., and Trapp, B.D. (2016). Microglia and neuroprotection. *J Neurochem* 136 Suppl 1**,** 10-17. doi: 10.1111/jnc.13062.

Chiozzi, P., Sarti, A.C., Sanz, J.M., Giuliani, A.L., Adinolfi, E., Vultaggio-Poma, V., et al. (2019). Amyloid β-dependent mitochondrial toxicity in mouse microglia requires P2X7 receptor expression and is prevented by nimodipine. *Scientific Reports* 9(1)**,** 6475. doi: 10.1038/s41598-019-42931-2.

Choi, D.W. (1987). Ionic dependence of glutamate neurotoxicity. *The Journal of neuroscience : the official journal of the Society for Neuroscience* 7(2)**,** 369-379. doi: 10.1523/JNEUROSCI.07-02-00369.1987.

Choi, D.W. (1988). Glutamate neurotoxicity and diseases of the nervous system. *Neuron* 1(8)**,** 623-634.

Codeluppi, S., Svensson, C.I., Hefferan, M.P., Valencia, F., Silldorff, M.D., Oshiro, M., et al. (2009). The Rheb-mTOR pathway is upregulated in reactive astrocytes of the injured spinal cord. *The Journal of neuroscience : the official journal of the Society for Neuroscience* 29(4)**,** 1093-1104. doi: 10.1523/JNEUROSCI.4103-08.2009.

Cohn, R.G., Mirkovich, A., Dunlap, B., Burton, P., Chiu, S.H., Eugui, E., et al. (1999). Mycophenolic acid increases apoptosis, lysosomes and lipid droplets in human lymphoid and monocytic cell lines. *Transplantation* 68(3)**,** 411-418. doi: 10.1097/00007890-199908150-00014.

Colton, C.A. (2009). Heterogeneity of microglial activation in the innate immune response in the brain. *J Neuroimmune Pharmacol* 4(4)**,** 399-418. doi: 10.1007/s11481-009-9164-4.

Cramer, T., Gill, R., Thirouin, Z.S., Vaas, M., Sampath, S., Martineau, F., et al. (2022). Cross-talk between GABAergic postsynapse and microglia regulate synapse loss after brain ischemia. *Sci Adv* 8(9)**,** eabj0112. doi: 10.1126/sciadv.abj0112.

Cuny, G.D., Suebsuwong, C., and Ray, S.S. (2017). Inosine-5'-monophosphate dehydrogenase (IMPDH) inhibitors: a patent and scientific literature review (2002-2016). *Expert Opin Ther Pat* 27(6)**,** 677-690. doi: 10.1080/13543776.2017.1280463.

Datta, S., Lin, F., Jones, L.D., Pingle, S.C., Kesari, S., and Ashili, S. (2023). Traumatic brain injury and immunological outcomes: the double-edged killer. *Future Sci OA* 9(6)**,** Fso864. doi: 10.2144/fsoa-2023-0037.

Davalos, D., Grutzendler, J., Yang, G., Kim, J.V., Zuo, Y., Jung, S., et al. (2005). ATP mediates rapid microglial response to local brain injury in vivo. *Nat Neurosci* 8(6)**,** 752-758. doi: 10.1038/nn1472.

Dawson, V.L., Dawson, T.M., London, E.D., Bredt, D.S., and Snyder, S.H. (1991). Nitric oxide mediates glutamate neurotoxicity in primary cortical cultures. *Proc Natl Acad Sci U S A* 88(14)**,** 6368-6371.

Dayton, J.S., Lindsten, T., Thompson, C.B., and Mitchell, B.S. (1994). Effects of human T lymphocyte activation on inosine monophosphate dehydrogenase expression. *J Immunol* 152(3)**,** 984-991.

De Benedetti, F., Gattorno, M., Anton, J., Ben-Chetrit, E., Frenkel, J., Hoffman, H.M., et al. (2018). Canakinumab for the Treatment of Autoinflammatory Recurrent Fever Syndromes. *New England Journal of Medicine* 378(20)**,** 1908-1919. doi: 10.1056/NEJMoa1706314.

De Chiara, V., Motta, C., Rossi, S., Studer, V., Barbieri, F., Lauro, D., et al. (2013). Interleukin-1beta alters the sensitivity of cannabinoid CB1 receptors controlling glutamate transmission in the striatum. *Neuroscience* 250**,** 232-239. doi: 10.1016/j.neuroscience.2013.06.069.

De Petrocellis, L., Cascio, M.G., and Di Marzo, V. (2004). The endocannabinoid system: a general view and latest additions. *British journal of pharmacology* 141(5)**,** 765-774. doi: 10.1038/sj.bjp.0705666.

De Simone, R., Ambrosini, E., Carnevale, D., Ajmone-Cat, M.A., and Minghetti, L. (2007). NGF promotes microglial migration through the activation of its high affinity receptor: modulation by TGF-beta. *Journal of neuroimmunology* 190(1-2)**,** 53-60. doi: 10.1016/j.jneuroim.2007.07.020.

De Simoni, A., Griesinger, C.B., and Edwards, F.A. (2003). Development of rat CA1 neurones in acute versus organotypic slices: role of experience in synaptic morphology and activity. *J Physiol* 550(Pt 1)**,** 135-147. doi: 10.1113/jphysiol.2003.039099.

Deczkowska, A., Amit, I., and Schwartz, M. (2018). Microglial immune checkpoint mechanisms. *Nature Neuroscience* 21(6)**,** 779-786. doi: 10.1038/s41593-018-0145-x.

Dehghani, F., Hischebeth, G.T.R., Wirjatijasa, F., Kohl, A., Korf, H.-W., and Hailer, N.P. (2003). The immunosuppressant mycophenolate mofetil attenuates neuronal damage after excitotoxic injury in hippocampal slice cultures. *European Journal of Neuroscience* 18(5)**,** 1061-1072. doi: 10.1046/j.1460-9568.2003.02821.x.

Dehghani, F., Sayan, M., Conrad, A., Evers, J., Ghadban, C., Blaheta, R., et al. (2010). Inhibition of microglial and astrocytic inflammatory responses by the immunosuppressant mycophenolate mofetil. *Neuropathol Appl Neurobiol* 36(7)**,** 598-611. doi: 10.1111/j.1365-2990.2010.01104.x.

Devane, W.A., Dysarz, F.A., 3rd, Johnson, M.R., Melvin, L.S., and Howlett, A.C. (1988). Determination and characterization of a cannabinoid receptor in rat brain. *Mol Pharmacol* 34(5)**,** 605-613.

Devane, W.A., Hanus, L., Breuer, A., Pertwee, R.G., Stevenson, L.A., Griffin, G., et al. (1992). Isolation and structure of a brain constituent that binds to the cannabinoid receptor. *Science* 258(5090)**,** 1946-1949. doi: 10.1126/science.1470919.

Dhande, I.S., Zhu, Y., Braun, M.C., Hicks, M.J., Wenderfer, S.E., and Doris, P.A. (2017). Mycophenolate mofetil prevents cerebrovascular injury in stroke-prone spontaneously hypertensive rats. *Physiol Genomics* 49(3)**,** 132-140. doi: 10.1152/physiolgenomics.00110.2016.

Di Marzo, V. (1999). Biosynthesis and inactivation of endocannabinoids: relevance to their proposed role as neuromodulators. *Life Sci* 65(6-7)**,** 645-655. doi: 10.1016/s0024-3205(99)00287-8.

Dikmen, H.O., Hemmerich, M., Lewen, A., Hollnagel, J.-O., Chausse, B., and Kann, O. (2020). GM-CSF induces noninflammatory proliferation of microglia and disturbs electrical neuronal network rhythms in situ. *Journal of Neuroinflammation* 17(1)**,** 235. doi: 10.1186/s12974-020-01903-4.

Dimyan, M.A., and Cohen, L.G. (2011). Neuroplasticity in the context of motor rehabilitation after stroke. *Nat Rev Neurol* 7(2)**,** 76-85. doi: 10.1038/nrneurol.2010.200.

Dirnagl, U., Iadecola, C., and Moskowitz, M.A. (1999). Pathobiology of ischaemic stroke: an integrated view. *Trends Neurosci* 22(9)**,** 391-397.

Donahue, C.P., Kosik, K.S., and Shors, T.J. (2006). Growth hormone is produced within the hippocampus where it responds to age, sex, and stress. *Proc Natl Acad Sci U S A* 103(15)**,** 6031-6036. doi: 10.1073/pnas.0507776103.

Dun, B., Sharma, A., Xu, H., Liu, H., Bai, S., Zeng, L., et al. (2013). Transcriptomic changes induced by mycophenolic acid in gastric cancer cells. *Am J Transl Res* 6(1)**,** 28-42.

Ebrahimi, F., Hezel, M., Koch, M., Ghadban, C., Korf, H.W., and Dehghani, F. (2010). Analyses of neuronal damage in excitotoxically lesioned organotypic hippocampal slice cultures. *Ann Anat* 192(4)**,** 199-204. doi: 10.1016/j.aanat.2010.06.002.

Ebrahimi, F., Koch, M., Pieroh, P., Ghadban, C., Hobusch, C., Bechmann, I., et al. (2012). Time dependent neuroprotection of mycophenolate mofetil: effects on temporal dynamics in glial proliferation, apoptosis, and scar formation. *J Neuroinflammation* 9**,** 89. doi: 10.1186/1742-2094-9-89.

Edwards, P., Arango, M., Balica, L., Cottingham, R., El-Sayed, H., Farrell, B., et al. (2005). Final results of MRC CRASH, a randomised placebo-controlled trial of intravenous corticosteroid in adults with head injury-outcomes at 6 months. *Lancet* 365(9475)**,** 1957-1959. doi: 10.1016/s0140-6736(05)66552-x.

Endo, F., Kasai, A., Soto, J.S., Yu, X., Qu, Z., Hashimoto, H., et al. (2022). Molecular basis of astrocyte diversity and morphology across the CNS in health and disease. *Science* 378(6619)**,** eadc9020. doi: 10.1126/science.adc9020.

Endoh, M., Maiese, K., and Wagner, J. (1994). Expression of the inducible form of nitric oxide synthase by reactive astrocytes after transient global ischemia. *Brain research* 651(1-2)**,** 92-100. doi: 10.1016/0006-8993(94)90683-1.

Endres, M., Engelhardt, B., Koistinaho, J., Lindvall, O., Meairs, S., Mohr, J.P., et al. (2008). Improving outcome after stroke: overcoming the translational roadblock. *Cerebrovasc Dis* 25(3)**,** 268-278. doi: 10.1159/000118039.

Epinette, W.W., Parker, C.M., Jones, E.L., and Greist, M.C. (1987). Mycophenolic acid for psoriasis: A review of pharmacology, long-term efficacy, and safety. *Journal of the American Academy of Dermatology* 17(6)**,** 962-971. doi: https://doi.org/10.1016/S0190-9622(87)70285-0.

Erlich, S., Alexandrovich, A., Shohami, E., and Pinkas-Kramarski, R. (2007). Rapamycin is a neuroprotective treatment for traumatic brain injury. *Neurobiol Dis* 26(1)**,** 86-93. doi: 10.1016/j.nbd.2006.12.003.

Erta, M., Quintana, A., and Hidalgo, J. (2012). Interleukin-6, a major cytokine in the central nervous system. *Int J Biol Sci* 8(9)**,** 1254-1266. doi: 10.7150/ijbs.4679.

Escartin, C., Galea, E., Lakatos, A., O'Callaghan, J.P., Petzold, G.C., Serrano-Pozo, A., et al. (2021). Reactive astrocyte nomenclature, definitions, and future directions. *Nature Neuroscience* 24(3)**,** 312-325. doi: 10.1038/s41593-020-00783-4.

Facchinetti, F., Del Giudice, E., Furegato, S., Passarotto, M., and Leon, A. (2003). Cannabinoids ablate release of TNFalpha in rat microglial cells stimulated with lypopolysaccharide. *Glia* 41(2)**,** 161-168. doi: 10.1002/glia.10177.

Faulkner, J.R., Herrmann, J.E., Woo, M.J., Tansey, K.E., Doan, N.B., and Sofroniew, M.V. (2004). Reactive astrocytes protect tissue and preserve function after spinal cord injury. *J Neurosci* 24(9)**,** 2143-2155. doi: 10.1523/jneurosci.3547-03.2004.

Feigin, V.L., Roth, G.A., Naghavi, M., Parmar, P., Krishnamurthi, R., Chugh, S., et al. (2016). Global burden of stroke and risk factors in 188 countries, during 1990-2013: a systematic analysis for the Global Burden of Disease Study 2013. *Lancet Neurol* 15(9)**,** 913-924. doi: 10.1016/S1474-4422(16)30073-4.

Feigin, V.L., Stark, B.A., Johnson, C.O., Roth, G.A., Bisignano, C., Abady, G.G., et al. (2021). Global, regional, and national burden of stroke and its risk factors, 1990–2019: a systematic analysis for the Global Burden of Disease Study 2019. *The Lancet Neurology* 20(10)**,** 795-820. doi: 10.1016/S1474-4422(21)00252-0.

Fernández-Ramos, A.A., Poindessous, V., Marchetti-Laurent, C., Pallet, N., and Loriot, M.A. (2016). The effect of immunosuppressive molecules on T-cell metabolic reprogramming. *Biochimie* 127**,** 23-36. doi: 10.1016/j.biochi.2016.04.016.

Fisher, M., and Savitz, S.I. (2022). Pharmacological brain cytoprotection in acute ischaemic stroke - renewed hope in the reperfusion era. *Nat Rev Neurol* 18(4)**,** 193-202. doi: 10.1038/s41582-021-00605-6.

Fitzgerald, K.A., and Kagan, J.C. (2020). Toll-like Receptors and the Control of Immunity. *Cell* 180(6)**,** 1044-1066. doi: 10.1016/j.cell.2020.02.041.

Franklin, A., Parmentier-Batteur, S., Walter, L., Greenberg, D.A., and Stella, N. (2003). Palmitoylethanolamide increases after focal cerebral ischemia and potentiates microglial cell motility. *J Neurosci* 23(21)**,** 7767-7775. doi: 10.1523/jneurosci.23-21-07767.2003.

Frauwirth, K.A., Riley, J.L., Harris, M.H., Parry, R.V., Rathmell, J.C., Plas, D.R., et al. (2002). The CD28 signaling pathway regulates glucose metabolism. *Immunity* 16(6)**,** 769-777. doi: 10.1016/s1074-7613(02)00323-0.

Freund, T.F., and Buzsáki, G. (1996). Interneurons of the hippocampus. *Hippocampus* 6(4)**,** 347-470. doi: 10.1002/(sici)1098-1063(1996)6:4<347::Aid-hipo1>3.0.Co;2-i.

Fu, H., Zhao, Y., Hu, D., Wang, S., Yu, T., and Zhang, L. (2020). Depletion of microglia exacerbates injury and impairs function recovery after spinal cord injury in mice. *Cell Death Dis* 11(7)**,** 528. doi: 10.1038/s41419-020-2733-4.

Ghozy, S., Reda, A., Varney, J., Elhawary, A.S., Shah, J., Murry, K., et al. (2022). Neuroprotection in Acute Ischemic Stroke: A Battle Against the Biology of Nature. *Front Neurol* 13**,** 870141. doi: 10.3389/fneur.2022.870141.

Giblett, E.R., Anderson, J.E., Cohen, F., Pollara, B., and Meuwissen, H.J. (1972). Adenosine-deaminase deficiency in two patients with severely impaired cellular immunity. *Lancet (London, England)* 2(7786)**,** 1067-1069. doi: 10.1016/s0140-6736(72)92345-8.

Ginhoux, F., and Garel, S. (2018). The mysterious origins of microglia. *Nat Neurosci* 21(7)**,** 897-899. doi: 10.1038/s41593-018-0176-3.

Ginhoux, F., Greter, M., Leboeuf, M., Nandi, S., See, P., Gokhan, S., et al. (2010). Fate mapping analysis reveals that adult microglia derive from primitive macrophages. *Science* 330(6005)**,** 841-845. doi: 10.1126/science.1194637.

Ginhoux, F., and Jung, S. (2014). Monocytes and macrophages: developmental pathways and tissue homeostasis. *Nat Rev Immunol* 14(6)**,** 392-404. doi: 10.1038/nri3671.

Giulian, D., Baker, T.J., Shih, L.C., and Lachman, L.B. (1986). Interleukin 1 of the central nervous system is produced by ameboid microglia. *J Exp Med* 164(2)**,** 594-604. doi: 10.1084/jem.164.2.594.

Glesne, D., Collart, F., Varkony, T., Drabkin, H., and Huberman, E. (1993). Chromosomal localization and structure of the human type II IMP dehydrogenase gene (IMPDH2). *Genomics* 16(1)**,** 274-277. doi: 10.1006/geno.1993.1177.

Gómez Morillas, A., Besson, V.C., and Lerouet, D. (2021). Microglia and Neuroinflammation: What Place for P2RY12? *Int J Mol Sci* 22(4). doi: 10.3390/ijms22041636.

Gourin, C.G., and Shackford, S.R. (1997). Production of tumor necrosis factor-alpha and interleukin-1beta by human cerebral microvascular endothelium after percussive trauma. *The Journal of trauma* 42(6)**,** 1101-1107. doi: 10.1097/00005373-199706000-00020.

Grabiec, U., Hohmann, T., Hammer, N., and Dehghani, F. (2017). Organotypic Hippocampal Slice Cultures As a Model to Study Neuroprotection and Invasiveness of Tumor Cells. *J Vis Exp* (126). doi: 10.3791/55359.

Grabon, W., Rheims, S., Smith, J., Bodennec, J., Belmeguenai, A., and Bezin, L. (2023). CB2 receptor in the CNS: From immune and neuronal modulation to behavior. *Neurosci Biobehav Rev* 150**,** 105226. doi: 10.1016/j.neubiorev.2023.105226.

Gu, J.J., Kaiser-Rogers, K., Rao, K., and Mitchell, B.S. (1994). Assignment of the human type I IMP dehydrogenase gene (IMPDH1) to chromosome 7q31.3-q32). *Genomics* 24(1)**,** 179-181. doi: 10.1006/geno.1994.1597.

Gu, J.J., Stegmann, S., Gathy, K., Murray, R., Laliberte, J., Ayscue, L., et al. (2000). Inhibition of T lymphocyte activation in mice heterozygous for loss of the IMPDH II gene. *J Clin Invest* 106(4)**,** 599-606. doi: 10.1172/jci8669.

Hailer, N.P. (2008). Immunosuppression after traumatic or ischemic CNS damage: it is neuroprotective and illuminates the role of microglial cells. *Prog Neurobiol* 84(3)**,** 211-233. doi: 10.1016/j.pneurobio.2007.12.001.

Hailer, N.P., Grampp, A., and Nitsch, R. (1999). Proliferation of microglia and astrocytes in the dentate gyrus following entorhinal cortex lesion: a quantitative bromodeoxyuridine-labelling study. *Eur J Neurosci* 11(9)**,** 3359-3364. doi: 10.1046/j.1460-9568.1999.00808.x.

Hailer, N.P., Vogt, C., Korf, H.W., and Dehghani, F. (2005). Interleukin-1beta exacerbates and interleukin-1 receptor antagonist attenuates neuronal injury and microglial activation after excitotoxic damage in organotypic hippocampal slice cultures. *Eur J Neurosci* 21(9)**,** 2347-2360. doi: 10.1111/j.1460-9568.2005.04067.x.

Halassa, M.M., Fellin, T., and Haydon, P.G. (2007). The tripartite synapse: roles for gliotransmission in health and disease. *Trends in molecular medicine* 13(2)**,** 54-63. doi: 10.1016/j.molmed.2006.12.005.

Hanisch, U.K., and Kettenmann, H. (2007). Microglia: active sensor and versatile effector cells in the normal and pathologic brain. *Nat Neurosci* 10(11)**,** 1387-1394. doi: 10.1038/nn1997.

Happ, D.F., and Tasker, R.A. (2016). A method for objectively quantifying propidium iodide exclusion in organotypic hippocampal slice cultures. *Journal of neuroscience methods* 269**,** 1-5. doi: 10.1016/j.jneumeth.2016.05.006.

Haupt, M., Gerner, S.T., Bähr, M., and Doeppner, T.R. (2023). Neuroprotective Strategies for Ischemic Stroke-Future Perspectives. *Int J Mol Sci* 24(5). doi: 10.3390/ijms24054334.

Heidari, A., Yazdanpanah, N., and Rezaei, N. (2022). The role of Toll-like receptors and neuroinflammation in Parkinson's disease. *Journal of Neuroinflammation* 19(1)**,** 135. doi: 10.1186/s12974-022-02496-w.

Heppner, F.L., Skutella, T., Hailer, N.P., Haas, D., and Nitsch, R. (1998). Activated microglial cells migrate towards sites of excitotoxic neuronal injury inside organotypic hippocampal slice cultures. *Eur J Neurosci* 10(10)**,** 3284-3290. doi: 10.1046/j.1460-9568.1998.00379.x.

Herrera, M.I., Udovin, L.D., Kobiec, T., Toro-Urrego, N., Kusnier, C.F., Kölliker-Frers, R.A., et al. (2022). Palmitoylethanolamide attenuates neurodevelopmental delay and early hippocampal damage following perinatal asphyxia in rats. *Front Behav Neurosci* 16**,** 953157. doi: 10.3389/fnbeh.2022.953157.

Herrmann, J.E., Imura, T., Song, B., Qi, J., Ao, Y., Nguyen, T.K., et al. (2008). STAT3 is a critical regulator of astrogliosis and scar formation after spinal cord injury. *The Journal of neuroscience : the official journal of the Society for Neuroscience* 28(28)**,** 7231-7243. doi: 10.1523/JNEUROSCI.1709-08.2008.

Hertz, L., and Rothman, D.L. (2016). Glucose, Lactate, β-Hydroxybutyrate, Acetate, GABA, and Succinate as Substrates for Synthesis of Glutamate and GABA in the Glutamine-Glutamate/GABA Cycle. *Adv Neurobiol* 13**,** 9-42. doi: 10.1007/978-3-319-45096-4_2.

Hibbs, J.B., Jr., Vavrin, Z., and Taintor, R.R. (1987). L-arginine is required for expression of the activated macrophage effector mechanism causing selective metabolic inhibition in target cells. *J Immunol* 138(2)**,** 550-565.

Hiley, C.R., and Kaup, S.S. (2007). GPR55 and the vascular receptors for cannabinoids. *Br J Pharmacol* 152(5)**,** 559-561. doi: 10.1038/sj.bjp.0707421.

Hilton, G.D., Stoica, B.A., Byrnes, K.R., and Faden, A.I. (2008). Roscovitine Reduces Neuronal Loss, Glial Activation, and Neurologic Deficits after Brain Trauma. *Journal of Cerebral Blood Flow & Metabolism* 28(11)**,** 1845-1859. doi: 10.1038/jcbfm.2008.75.

Hohmann, U., Ghadban, C., Hohmann, T., Kleine, J., Schmidt, M., Scheller, C., et al. (2022). Nimodipine Exerts Time-Dependent Neuroprotective Effect after Excitotoxical Damage in Organotypic Slice Cultures. *Int J Mol Sci* 23(6). doi: 10.3390/ijms23063331.

Hohmann, U., Pelzer, M., Kleine, J., Hohmann, T., Ghadban, C., and Dehghani, F. (2019). Opposite Effects of Neuroprotective Cannabinoids, Palmitoylethanolamide, and 2-Arachidonoylglycerol on Function and Morphology of Microglia. *Front Neurosci* 13**,** 1180. doi: 10.3389/fnins.2019.01180.

Holopainen, I.E. (2005). Organotypic hippocampal slice cultures: a model system to study basic cellular and molecular mechanisms of neuronal cell death, neuroprotection, and synaptic plasticity. *Neurochem Res* 30(12)**,** 1521-1528. doi: 10.1007/s11064-005-8829-5.

Holtmaat, A., and Svoboda, K. (2009). Experience-dependent structural synaptic plasticity in the mammalian brain. *Nat Rev Neurosci* 10(9)**,** 647-658. doi: 10.1038/nrn2699.

Honda, S., Sasaki, Y., Ohsawa, K., Imai, Y., Nakamura, Y., Inoue, K., et al. (2001). Extracellular ATP or ADP induce chemotaxis of cultured microglia through Gi/o-coupled P2Y receptors. *The Journal of neuroscience : the official journal of the Society for Neuroscience* 21(6)**,** 1975-1982. doi: 10.1523/JNEUROSCI.21-06-01975.2001.

Hu, S., Chen, Y., Huang, S., Liu, M., Liu, Y., and Huang, S. (2022). Sodium Danshensu protects against oxygen glucose deprivation/reoxygenation-induced astrocytes injury through regulating NOD-like receptor pyrin domain containing 3 (NLRP3) inflammasome and tuberous sclerosis complex-2 (TSC2)/mammalian target of rapamycin (mTOR) pathways. *Ann Transl Med* 10(20)**,** 1097. doi: 10.21037/atm-22-2143.

Huang, Y., Liu, Z., Huang, H., Liu, H., and Li, L. (2005). Effects of mycophenolic acid on endothelial cells. *Int Immunopharmacol* 5(6)**,** 1029-1039. doi: 10.1016/j.intimp.2005.01.015.

Huber, N., Korhonen, S., Hoffmann, D., Leskelä, S., Rostalski, H., Remes, A.M., et al. (2022). Deficient neurotransmitter systems and synaptic function in frontotemporal lobar degeneration—Insights into disease mechanisms and current therapeutic approaches. *Molecular Psychiatry* 27(3)**,** 1300-1309. doi: 10.1038/s41380-021-01384-8.

Iadecola, C. (2017). The Neurovascular Unit Coming of Age: A Journey through Neurovascular Coupling in Health and Disease. *Neuron* 96(1)**,** 17-42. doi: 10.1016/j.neuron.2017.07.030.

Iadecola, C., and Anrather, J. (2011). The immunology of stroke: from mechanisms to translation. *Nat Med* 17(7)**,** 796-808. doi: 10.1038/nm.2399.

Iadecola, C., Zhang, F., Casey, R., Nagayama, M., and Ross, M.E. (1997). Delayed reduction of ischemic brain injury and neurological deficits in mice lacking the inducible nitric oxide synthase gene. *J Neurosci* 17(23)**,** 9157-9164.

Imai, Y., and Kohsaka, S. (2002). Intracellular signaling in M-CSF-induced microglia activation: role of Iba1. *Glia* 40(2)**,** 164-174. doi: 10.1002/glia.10149.

Jackson, R.C., Weber, G., and Morris, H.P. (1975). IMP dehydrogenase, an enzyme linked with proliferation and malignancy. *Nature* 256(5515)**,** 331-333. doi: 10.1038/256331a0.

Jadhav, P., Karande, M., Sarkar, A., Sahu, S., Sarmah, D., Datta, A., et al. (2023). Glial Cells Response in Stroke. *Cell Mol Neurobiol* 43(1)**,** 99-113. doi: 10.1007/s10571-021-01183-3.

Jain, J., Almquist, S.J., Ford, P.J., Shlyakhter, D., Wang, Y., Nimmesgern, E., et al. (2004). Regulation of inosine monophosphate dehydrogenase type I and type II isoforms in human lymphocytes. *Biochemical pharmacology* 67(4)**,** 767-776. doi: 10.1016/j.bcp.2003.09.043.

Jang, S., Kim, H., Kim, H.J., Lee, S.K., Kim, E.W., Namkoong, K., et al. (2018). Long-Term Culture of Organotypic Hippocampal Slice from Old 3xTg-AD Mouse: An ex vivo Model of Alzheimer's Disease. *Psychiatry Investig* 15(2)**,** 205-213. doi: 10.30773/pi.2017.04.02.

Janks, L., Sharma, C.V.R., and Egan, T.M. (2018). A central role for P2X7 receptors in human microglia. *J Neuroinflammation* 15(1)**,** 325. doi: 10.1186/s12974-018-1353-8.

Járai, Z., Wagner, J.A., Varga, K., Lake, K.D., Compton, D.R., Martin, B.R., et al. (1999). Cannabinoid-induced mesenteric vasodilation through an endothelial site distinct from CB1 or CB2 receptors. *Proc Natl Acad Sci U S A* 96(24)**,** 14136-14141. doi: 10.1073/pnas.96.24.14136.

Jassam, Y.N., Izzy, S., Whalen, M., McGavern, D.B., and El Khoury, J. (2017). Neuroimmunology of Traumatic Brain Injury: Time for a Paradigm Shift. *Neuron* 95(6)**,** 1246-1265. doi: 10.1016/j.neuron.2017.07.010.

John R. McLeod, J., Shen, M., Kim, D.J., and Thayer, S.A. (1998). Neurotoxicity Mediated by Aberrant Patterns of Synaptic Activity Between Rat Hippocampal Neurons in Culture. *Journal of Neurophysiology* 80(5)**,** 2688-2698. doi: 10.1152/jn.1998.80.5.2688.

Jonsson, C.A., and Carlsten, H. (2002). Mycophenolic acid inhibits inosine 5'-monophosphate dehydrogenase and suppresses production of pro-inflammatory cytokines, nitric oxide, and LDH in macrophages. *Cell Immunol* 216(1-2)**,** 93-101. doi: 10.1016/s0008-8749(02)00502-6.

Jounai, N., Kobiyama, K., Takeshita, F., and Ishii, K.J. (2013). Recognition of damage-associated molecular patterns related to nucleic acids during inflammation and vaccination. *Frontiers in cellular and infection microbiology* 2**,** 168-168. doi: 10.3389/fcimb.2012.00168.

Jurcau, A., and Ardelean, A.I. (2022). Oxidative Stress in Ischemia/Reperfusion Injuries following Acute Ischemic Stroke. *Biomedicines* 10(3). doi: 10.3390/biomedicines10030574.

Jurga, A.M., Paleczna, M., Kadluczka, J., and Kuter, K.Z. (2021). Beyond the GFAP-Astrocyte Protein Markers in the Brain. *Biomolecules* 11(9). doi: 10.3390/biom11091361.

Jurga, A.M., Paleczna, M., and Kuter, K.Z. (2020). Overview of General and Discriminating Markers of Differential Microglia Phenotypes. *Front Cell Neurosci* 14**,** 198. doi: 10.3389/fncel.2020.00198.

Kahlenberg, J.M., and Dubyak, G.R. (2004). Mechanisms of caspase-1 activation by P2X7 receptor-mediated K+ release. *American Journal of Physiology-Cell Physiology* 286(5)**,** C1100-C1108. doi: 10.1152/ajpcell.00494.2003.

Kettenmann, H., Hanisch, U.K., Noda, M., and Verkhratsky, A. (2011). Physiology of microglia. *Physiol Rev* 91(2)**,** 461-553. doi: 10.1152/physrev.00011.2010.

Khakh, B.S., and Deneen, B. (2019). The Emerging Nature of Astrocyte Diversity. *Annu Rev Neurosci* 42**,** 187-207. doi: 10.1146/annurev-neuro-070918-050443.

Kim, H., Kim, E., Park, M., Lee, E., and Namkoong, K. (2013). Organotypic hippocampal slice culture from the adult mouse brain: a versatile tool for translational neuropsychopharmacology. *Prog Neuropsychopharmacol Biol Psychiatry* 41**,** 36-43. doi: 10.1016/j.pnpbp.2012.11.004.

Kissela, B.M., Khoury, J.C., Alwell, K., Moomaw, C.J., Woo, D., Adeoye, O., et al. (2012). Age at stroke: temporal trends in stroke incidence in a large, biracial population. *Neurology* 79(17)**,** 1781-1787. doi: 10.1212/WNL.0b013e318270401d.

Kitamura, T., Tsuchihashi, Y., and Fujita, S. (1978). Initial response of silver-impregnated "resting microglia" to stab wounding in rabbit hippocampus. *Acta Neuropathol* 44(1)**,** 31-39. doi: 10.1007/bf00691636.

Kitley, J.L., Lachmann, H.J., Pinto, A., and Ginsberg, L. (2010). Neurologic manifestations of the cryopyrin-associated periodic syndrome. *Neurology* 74(16)**,** 1267-1270. doi: 10.1212/WNL.0b013e3181d9ed69.

Kleine, J., Hohmann, U., Hohmann, T., Ghadban, C., Schmidt, M., Laabs, S., et al. (2022). Microglia-Dependent and Independent Brain Cytoprotective Effects of Mycophenolate Mofetil During Neuronal Damage. *Frontiers in Aging Neuroscience* 14. doi: 10.3389/fnagi.2022.863598.

Kleine, J., Leisz, S., Ghadban, C., Hohmann, T., Prell, J., Scheller, C., et al. (2021). Variants of Oxidized Regenerated Cellulose and Their Distinct Effects on Neuronal Tissue. *Int J Mol Sci* 22(21). doi: 10.3390/ijms222111467.

Klionsky, D.J., Abdel-Aziz, A.K., Abdelfatah, S., Abdellatif, M., Abdoli, A., Abel, S., et al. (2021). Guidelines for the use and interpretation of assays for monitoring autophagy (4th edition)(1). *Autophagy* 17(1)**,** 1-382. doi: 10.1080/15548627.2020.1797280.

Knowles, R.G., and Moncada, S. (1994). Nitric oxide synthases in mammals. *Biochem J* 298 (Pt 2)(Pt 2)**,** 249-258. doi: 10.1042/bj2980249.

Koch, M., Kreutz, S., Böttger, C., Benz, A., Maronde, E., Ghadban, C., et al. (2011). Palmitoylethanolamide protects dentate gyrus granule cells via peroxisome proliferator-activated receptor-α. *Neurotox Res* 19(2)**,** 330-340. doi: 10.1007/s12640-010-9166-2.

Kohl, A., Dehghani, F., Korf, H.W., and Hailer, N.P. (2003). The bisphosphonate clodronate depletes microglial cells in excitotoxically injured organotypic hippocampal slice cultures. *Experimental Neurology* 181(1)**,** 1-11. doi: 10.1016/s0014-4886(02)00049-3.

Koizumi, S., Shigemoto-Mogami, Y., Nasu-Tada, K., Shinozaki, Y., Ohsawa, K., Tsuda, M., et al. (2007). UDP acting at P2Y6 receptors is a mediator of microglial phagocytosis. *Nature* 446(7139)**,** 1091-1095. doi: 10.1038/nature05704.

Kozhevnikova, E.N., van der Knaap, J.A., Pindyurin, A.V., Ozgur, Z., van Ijcken, W.F., Moshkin, Y.M., et al. (2012). Metabolic enzyme IMPDH is also a transcription factor regulated by cellular state. *Mol Cell* 47(1)**,** 133-139. doi: 10.1016/j.molcel.2012.04.030.

Kreutz, S., Koch, M., Böttger, C., Ghadban, C., Korf, H.W., and Dehghani, F. (2009). 2-Arachidonoylglycerol elicits neuroprotective effects on excitotoxically lesioned dentate gyrus granule cells via abnormal-cannabidiol-sensitive receptors on microglial cells. *Glia* 57(3)**,** 286-294. doi: 10.1002/glia.20756.

Kreutz, S., Koch, M., Ghadban, C., Korf, H.W., and Dehghani, F. (2007). Cannabinoids and neuronal damage: differential effects of THC, AEA and 2-AG on activated microglial cells and degenerating neurons in excitotoxically lesioned rat organotypic hippocampal slice cultures. *Exp Neurol* 203(1)**,** 246-257. doi: 10.1016/j.expneurol.2006.08.010.

Kunz, A., Dirnagl, U., and Mergenthaler, P. (2010). Acute pathophysiological processes after ischaemic and traumatic brain injury. *Best Pract Res Clin Anaesthesiol* 24(4)**,** 495-509. doi: 10.1016/j.bpa.2010.10.001.

Lai, T.W., Zhang, S., and Wang, Y.T. (2014). Excitotoxicity and stroke: identifying novel targets for neuroprotection. *Prog Neurobiol* 115**,** 157-188. doi: 10.1016/j.pneurobio.2013.11.006.

Lambertsen, K.L., Biber, K., and Finsen, B. (2012). Inflammatory cytokines in experimental and human stroke. *J Cereb Blood Flow Metab* 32(9)**,** 1677-1698. doi: 10.1038/jcbfm.2012.88.

Lambertsen, K.L., Clausen, B.H., Babcock, A.A., Gregersen, R., Fenger, C., Nielsen, H.H., et al. (2009). Microglia protect neurons against ischemia by synthesis of tumor necrosis factor. *The Journal of neuroscience : the official journal of the Society for Neuroscience* 29(5)**,** 1319-1330. doi: 10.1523/JNEUROSCI.5505-08.2009.

Lecht, S., Rotfeld, E., Arien-Zakay, H., Tabakman, R., Matzner, H., Yaka, R., et al. (2012). Neuroprotective effects of nimodipine and nifedipine in the NGF-differentiated PC12 cells exposed to oxygen-glucose deprivation or trophic withdrawal. *International Journal of Developmental Neuroscience* 30(6)**,** 465-469. doi: https://doi.org/10.1016/j.ijdevneu.2012.05.007.

Lee, H.K., Lund, J.M., Ramanathan, B., Mizushima, N., and Iwasaki, A. (2007). Autophagy-dependent viral recognition by plasmacytoid dendritic cells. *Science* 315(5817)**,** 1398-1401. doi: 10.1126/science.1136880.

Lee, S., Choi, S.-Y., Choo, Y.-Y., Kim, O., Tran, P.T., Dao, C.T., et al. (2015). Sappanone A exhibits anti-inflammatory effects via modulation of Nrf2 and NF-κB. *International immunopharmacology* 28(1)**,** 328-336. doi: 10.1016/j.intimp.2015.06.015.

Lee, S.C., Liu, W., Dickson, D.W., Brosnan, C.F., and Berman, J.W. (1993). Cytokine production by human fetal microglia and astrocytes. Differential induction by lipopolysaccharide and IL-1 beta. *J Immunol* 150(7)**,** 2659-2667.

Lee, W.A., Gu, L., Miksztal, A.R., Chu, N., Leung, K., and Nelson, P.H. (1990). Bioavailability improvement of mycophenolic acid through amino ester derivatization. *Pharmaceutical research* 7(2)**,** 161-166. doi: 10.1023/a:1015828802490.

Legradi, A., Varszegi, S., Szigeti, C., and Gulya, K. (2011). Adult rat hippocampal slices as in vitro models for neurodegeneration: Studies on cell viability and apoptotic processes. *Brain Res Bull* 84(1)**,** 39-44. doi: 10.1016/j.brainresbull.2010.10.008.

Leisz, S., Trutschel, M.-L., Mäder, K., Scheller, C., Strauss, C., and Simmermacher, S. (2020). Tabotamp®, Respectively, Surgicel®, Increases the Cell Death of Neuronal and Glial Cells In Vitro. *Materials* 13(11)**,** 2453.

Leitner, G.R., Wenzel, T.J., Marshall, N., Gates, E.J., and Klegeris, A. (2019). Targeting toll-like receptor 4 to modulate neuroinflammation in central nervous system disorders. *Expert Opin Ther Targets* 23(10)**,** 865-882. doi: 10.1080/14728222.2019.1676416.

Levine, B., Mizushima, N., and Virgin, H.W. (2011). Autophagy in immunity and inflammation. *Nature* 469(7330)**,** 323-335. doi: 10.1038/nature09782.

Li, Q., Han, X., and Wang, J. (2016). Organotypic Hippocampal Slices as Models for Stroke and Traumatic Brain Injury. *Mol Neurobiol* 53(6)**,** 4226-4237. doi: 10.1007/s12035-015-9362-4.

Li, T., Pang, S., Yu, Y., Wu, X., Guo, J., and Zhang, S. (2013). Proliferation of parenchymal microglia is the main source of microgliosis after ischaemic stroke. *Brain* 136(Pt 12)**,** 3578-3588. doi: 10.1093/brain/awt287.

Li, Y., Hu, X., Liu, Y., Bao, Y., and An, L. (2009). Nimodipine protects dopaminergic neurons against inflammation-mediated degeneration through inhibition of microglial activation. *Neuropharmacology* 56(3)**,** 580-589. doi: 10.1016/j.neuropharm.2008.10.016.

Liao, L.X., Song, X.M., Wang, L.C., Lv, H.N., Chen, J.F., Liu, D., et al. (2017). Highly selective inhibition of IMPDH2 provides the basis of antineuroinflammation therapy. *Proc Natl Acad Sci U S A* 114(29)**,** E5986-E5994. doi: 10.1073/pnas.1706778114.

Liddelow, S.A., Guttenplan, K.A., Clarke, L.E., Bennett, F.C., Bohlen, C.J., Schirmer, L., et al. (2017). Neurotoxic reactive astrocytes are induced by activated microglia. *Nature* 541(7638)**,** 481-487. doi: 10.1038/nature21029.

Lipton, P. (1999). Ischemic cell death in brain neurons. *Physiol Rev* 79(4)**,** 1431-1568. doi: 10.1152/physrev.1999.79.4.1431.

Liu, Y., Shen, X., Zhang, Y., Zheng, X., Cepeda, C., Wang, Y., et al. (2023). Interactions of glial cells with neuronal synapses, from astrocytes to microglia and oligodendrocyte lineage cells. *Glia* 71(6)**,** 1383-1401. doi: 10.1002/glia.24343.

Liu, Z., Li, Y., Cui, Y., Roberts, C., Lu, M., Wilhelmsson, U., et al. (2014). Beneficial effects of gfap/vimentin reactive astrocytes for axonal remodeling and motor behavioral recovery in mice after stroke. *Glia* 62(12)**,** 2022-2033. doi: 10.1002/glia.22723.

Lo Verme, J., Fu, J., Astarita, G., La Rana, G., Russo, R., Calignano, A., et al. (2005). The nuclear receptor peroxisome proliferator-activated receptor-alpha mediates the anti-inflammatory actions of palmitoylethanolamide. *Mol Pharmacol* 67(1)**,** 15-19. doi: 10.1124/mol.104.006353.

Löffler, and Petrides (2014). *Biochemie und Pathobiochemie.* Springer Berlin Heidelberg.

Lu, H.C., and Mackie, K. (2021). Review of the Endocannabinoid System. *Biol Psychiatry Cogn Neurosci Neuroimaging* 6(6)**,** 607-615. doi: 10.1016/j.bpsc.2020.07.016.

Lukas, J., and Bartek, J. (2004). Cell division: the heart of the cycle. *Nature* 432(7017)**,** 564-567. doi: 10.1038/432564a.

Lundgaard, I., Osorio, M.J., Kress, B.T., Sanggaard, S., and Nedergaard, M. (2014). White matter astrocytes in health and disease. *Neuroscience* 276**,** 161-173. doi: 10.1016/j.neuroscience.2013.10.050.

Luo, C.T., and Li, M.O. (2018). Foxo transcription factors in T cell biology and tumor immunity. *Seminars in cancer biology* 50**,** 13-20. doi: 10.1016/j.semcancer.2018.04.006.

Lyden, P., Buchan, A., Boltze, J., and Fisher, M. (2021). Top Priorities for Cerebroprotective Studies-A Paradigm Shift: Report From STAIR XI. *Stroke* 52(9)**,** 3063-3071. doi: 10.1161/strokeaha.121.034947.

Maas, A.I., Stocchetti, N., and Bullock, R. (2008). Moderate and severe traumatic brain injury in adults. *Lancet Neurol* 7(8)**,** 728-741. doi: 10.1016/S1474-4422(08)70164-9.

Mackie, K., and Stella, N. (2006). Cannabinoid receptors and endocannabinoids: evidence for new players. *Aaps j* 8(2)**,** E298-306. doi: 10.1007/bf02854900.

Mander, P.K., Jekabsone, A., and Brown, G.C. (2006). Microglia proliferation is regulated by hydrogen peroxide from NADPH oxidase. *J Immunol* 176(2)**,** 1046-1052. doi: 10.4049/jimmunol.176.2.1046.

Maresz, K., Carrier, E.J., Ponomarev, E.D., Hillard, C.J., and Dittel, B.N. (2005). Modulation of the cannabinoid CB2 receptor in microglial cells in response to inflammatory stimuli. *J Neurochem* 95(2)**,** 437-445. doi: 10.1111/j.1471-4159.2005.03380.x.

Marinelli, S., Marrone, M.C., Di Domenico, M., and Marinelli, S. (2023). Endocannabinoid signaling in microglia. *Glia* 71(1)**,** 71-90. doi: 10.1002/glia.24281.

Marino Lee, S., Hudobenko, J., McCullough, L.D., and Chauhan, A. (2021). Microglia depletion increase brain injury after acute ischemic stroke in aged mice. *Exp Neurol* 336**,** 113530. doi: 10.1016/j.expneurol.2020.113530.

Matejuk, A., and Ransohoff, R.M. (2020). Crosstalk Between Astrocytes and Microglia: An Overview. *Front Immunol* 11**,** 1416. doi: 10.3389/fimmu.2020.01416.

Matthews, H.K., Bertoli, C., and de Bruin, R.A.M. (2022). Cell cycle control in cancer. *Nat Rev Mol Cell Biol* 23(1)**,** 74-88. doi: 10.1038/s41580-021-00404-3.

Mattsson, P., Aldskogius, H., and Svensson, M. (1999). Nimodipine-induced survival rate of facial motor neurons following intracranial transection of the facial nerve in the adult rat. *Journal of Neurosurgery* 90(4)**,** 760-765. doi: 10.3171/jns.1999.90.4.0760.

Mechoulam, R., Ben-Shabat, S., Hanus, L., Ligumsky, M., Kaminski, N.E., Schatz, A.R., et al. (1995). Identification of an endogenous 2-monoglyceride, present in canine gut, that binds to cannabinoid receptors. *Biochem Pharmacol* 50(1)**,** 83-90. doi: 10.1016/0006-2952(95)00109-d.

Michel, L., Vukusic, S., De Seze, J., Ducray, F., Ongagna, J.C., Lefrère, F., et al. (2014). Mycophenolate mofetil in multiple sclerosis: a multicentre retrospective study on 344 patients. *J Neurol Neurosurg Psychiatry* 85(3)**,** 279-283. doi: 10.1136/jnnp-2013-305298.

Miljkovic, D., Samardzic, T., Cvetkovic, I., Mostarica Stojkovic, M., and Trajkovic, V. (2002). Mycophenolic acid downregulates inducible nitric oxide synthase induction in astrocytes. *Glia* 39(3)**,** 247-255. doi: 10.1002/glia.10089.

Miller, R.H., and Raff, M.C. (1984). Fibrous and protoplasmic astrocytes are biochemically and developmentally distinct. *J Neurosci* 4(2)**,** 585-592. doi: 10.1523/jneurosci.04-02-00585.1984.

Mitchison, T.J., and Salmon, E.D. (2001). Mitosis: a history of division. *Nature cell biology* 3(1)**,** E17-E21. doi: 10.1038/35050656.

Mizuma, A., You, J.S., and Yenari, M.A. (2018). Targeting Reperfusion Injury in the Age of Mechanical Thrombectomy. *Stroke* 49(7)**,** 1796-1802. doi: 10.1161/strokeaha.117.017286.

Mohammadifard, M., Ghaemi, K., Hanif, H., Sharifzadeh, G., and Haghparast, M. (2018). Marshall and Rotterdam Computed Tomography scores in predicting early deaths after brain trauma. *European journal of translational myology* 28(3)**,** 7542-7542. doi: 10.4081/ejtm.2018.7542.

Molofsky, A.V., and Deneen, B. (2015). Astrocyte development: A Guide for the Perplexed. *Glia* 63(8)**,** 1320-1329. doi: 10.1002/glia.22836.

Morshead, C.M., and van der Kooy, D. (1990). Separate blood and brain origins of proliferating cells during gliosis in adult brains. *Brain Res* 535(2)**,** 237-244. doi: 10.1016/0006-8993(90)91606-h.

Mostafeezur, R.M., Shinoda, M., Unno, S., Zakir, H.M., Takatsuji, H., Takahashi, K., et al. (2014). Involvement of astroglial glutamate-glutamine shuttle in modulation of the jaw-opening reflex following infraorbital nerve injury. *Eur J Neurosci* 39(12)**,** 2050-2059. doi: 10.1111/ejn.12562.

Mowzoon, N., Sussman, A., and Bradley, W.G. (2001). Mycophenolate (CellCept) treatment of myasthenia gravis, chronic inflammatory polyneuropathy and inclusion body myositis. *J Neurol Sci* 185(2)**,** 119-122. doi: 10.1016/s0022-510x(01)00478-6.

Muccioli, G.G. (2010). Endocannabinoid biosynthesis and inactivation, from simple to complex. *Drug Discov Today* 15(11-12)**,** 474-483. doi: 10.1016/j.drudis.2010.03.007.

Mulcahy, N.J., Ross, J., Rothwell, N.J., and Loddick, S.A. (2003). Delayed administration of interleukin-1 receptor antagonist protects against transient cerebral ischaemia in the rat. *Br J Pharmacol* 140(3)**,** 471-476. doi: 10.1038/sj.bjp.0705462.

Munro, S., Thomas, K.L., and Abu-Shaar, M. (1993). Molecular characterization of a peripheral receptor for cannabinoids. *Nature* 365(6441)**,** 61-65. doi: 10.1038/365061a0.

Muramoto, M., Yamazaki, T., Nishimura, S., and Kita, Y. (2003). Detailed in vitro pharmacological analysis of FK506-induced neuroprotection. *Neuropharmacology* 45(3)**,** 394-403. doi: 10.1016/s0028-3908(03)00168-0.

Myer, D.J., Gurkoff, G.G., Lee, S.M., Hovda, D.A., and Sofroniew, M.V. (2006). Essential protective roles of reactive astrocytes in traumatic brain injury. *Brain* 129(Pt 10)**,** 2761-2772. doi: 10.1093/brain/awl165.

Namura, S., Maeno, H., Takami, S., Jiang, X.F., Kamichi, S., Wada, K., et al. (2002). Inhibition of glial glutamate transporter GLT-1 augments brain edema after transient focal cerebral ischemia in mice. *Neurosci Lett* 324(2)**,** 117-120.

Nedergaard, M., and Dirnagl, U. (2005). Role of glial cells in cerebral ischemia. *Glia* 50(4)**,** 281-286. doi: 10.1002/glia.20205.

Neves, D., Salazar, I.L., Almeida, R.D., and Silva, R.M. (2023). Molecular mechanisms of ischemia and glutamate excitotoxicity. *Life Sci***,** 121814. doi: 10.1016/j.lfs.2023.121814.

Ng, S.Y., and Lee, A.Y.W. (2019). Traumatic Brain Injuries: Pathophysiology and Potential Therapeutic Targets. *Frontiers in Cellular Neuroscience* 13(528). doi: 10.3389/fncel.2019.00528.

Niraula, A., Sheridan, J.F., and Godbout, J.P. (2017). Microglia Priming with Aging and Stress. *Neuropsychopharmacology* 42(1)**,** 318-333. doi: 10.1038/npp.2016.185.

Nogueira, R.G., Jadhav, A.P., Haussen, D.C., Bonafe, A., Budzik, R.F., Bhuva, P., et al. (2017). Thrombectomy 6 to 24 Hours after Stroke with a Mismatch between Deficit and Infarct. *New England Journal of Medicine* 378(1)**,** 11-21. doi: 10.1056/NEJMoa1706442.

Nogueira, R.G., Jadhav, A.P., Haussen, D.C., Bonafe, A., Budzik, R.F., Bhuva, P., et al. (2018). Thrombectomy 6 to 24 Hours after Stroke with a Mismatch between Deficit and Infarct. *N Engl J Med* 378(1)**,** 11-21. doi: 10.1056/NEJMoa1706442.

Norenberg, M.D., and Martinez-Hernandez, A. (1979). Fine structural localization of glutamine synthetase in astrocytes of rat brain. *Brain Res* 161(2)**,** 303-310. doi: 10.1016/0006-8993(79)90071-4.

O'Neill, L.A.J. (2003). The role of MyD88-like adapters in Toll-like receptor signal transduction. *Biochemical Society transactions* 31(Pt 3)**,** 643-647. doi: 10.1042/bst0310643.

Oddi, S., Fiorenza, M.T., and Maccarrone, M. (2023). Endocannabinoid signaling in adult hippocampal neurogenesis: A mechanistic and integrated perspective. *Prog Lipid Res***,** 101239. doi: 10.1016/j.plipres.2023.101239.

Oest, T.M., Dehghani, F., Korf, H.W., and Hailer, N.P. (2006). The immunosuppressant mycophenolate mofetil improves preservation of the perforant path in organotypic hippocampal slice cultures: a retrograde tracing study. *Hippocampus* 16(5)**,** 437-442. doi: 10.1002/hipo.20182.

Ojeda, J., and Ávila, A. (2019). Early Actions of Neurotransmitters During Cortex Development and Maturation of Reprogrammed Neurons. *Front Synaptic Neurosci* 11**,** 33. doi: 10.3389/fnsyn.2019.00033.

Olivares-Hernández, J.D., Carranza, M., Balderas-Márquez, J.E., Epardo, D., Baltazar-Lara, R., Ávila-Mendoza, J., et al. (2022). Neuroprotective and Regenerative Effects of Growth Hormone (GH) in the Embryonic Chicken Cerebral Pallium Exposed to Hypoxic-Ischemic (HI) Injury. *Int J Mol Sci* 23(16). doi: 10.3390/ijms23169054.

Olney, J.W., Ho, O.L., and Rhee, V. (1971). Cytotoxic effects of acidic and sulphur containing amino acids on the infant mouse central nervous system. *Experimental Brain Research* 14(1)**,** 61-76. doi: 10.1007/BF00234911.

Onodera, J., Nagata, H., Nakashima, A., Ikegaya, Y., and Koyama, R. (2021). Neuronal brain-derived neurotrophic factor manipulates microglial dynamics. *Glia* 69(4)**,** 890-904. doi: 10.1002/glia.23934.

Ozen, S., and Bilginer, Y. (2014). A clinical guide to autoinflammatory diseases: familial Mediterranean fever and next-of-kin. *Nature Reviews Rheumatology* 10(3)**,** 135-147. doi: 10.1038/nrrheum.2013.174.

Panikashvili, D., Simeonidou, C., Ben-Shabat, S., Hanuš, L., Breuer, A., Mechoulam, R., et al. (2001). An endogenous cannabinoid (2-AG) is neuroprotective after brain injury. *Nature* 413(6855), 527-531. doi: 10.1038/35097089.

Pareek, V., Pedley, A.M., and Benkovic, S.J. (2021). Human de novo purine biosynthesis. *Critical Reviews in Biochemistry and Molecular Biology* 56(1), 1-16. doi: 10.1080/10409238.2020.1832438.

Pavlova, N.N., and Thompson, C.B. (2016). The Emerging Hallmarks of Cancer Metabolism. *Cell Metab* 23(1), 27-47. doi: 10.1016/j.cmet.2015.12.006.

Pawlak, J., Brito, V., Küppers, E., and Beyer, C. (2005). Regulation of glutamate transporter GLAST and GLT-1 expression in astrocytes by estrogen. *Brain Res Mol Brain Res* 138(1), 1-7. doi: 10.1016/j.molbrainres.2004.10.043.

Pearson, V.L., Rothwell, N.J., and Toulmond, S. (1999). Excitotoxic brain damage in the rat induces interleukin-1beta protein in microglia and astrocytes: correlation with the progression of cell death. *Glia* 25(4), 311-323.

Pekny, M., and Nilsson, M. (2005). Astrocyte activation and reactive gliosis. *Glia* 50(4), 427-434. doi: 10.1002/glia.20207.

Petrosino, S., and Di Marzo, V. (2017). The pharmacology of palmitoylethanolamide and first data on the therapeutic efficacy of some of its new formulations. *Br J Pharmacol* 174(11), 1349-1365. doi: 10.1111/bph.13580.

Petrosino, S., Schiano Moriello, A., Cerrato, S., Fusco, M., Puigdemont, A., De Petrocellis, L., et al. (2016). The anti-inflammatory mediator palmitoylethanolamide enhances the levels of 2-arachidonoyl-glycerol and potentiates its actions at TRPV1 cation channels. *Br J Pharmacol* 173(7), 1154-1162. doi: 10.1111/bph.13084.

Pocock, J.M., and Kettenmann, H. (2007). Neurotransmitter receptors on microglia. *Trends Neurosci* 30(10), 527-535. doi: 10.1016/j.tins.2007.07.007.

Poltorak, A., He, X., Smirnova, I., Liu, M.Y., Van Huffel, C., Du, X., et al. (1998). Defective LPS signaling in C3H/HeJ and C57BL/10ScCr mice: mutations in Tlr4 gene. *Science (New York, N.Y.)* 282(5396), 2085-2088. doi: 10.1126/science.282.5396.2085.

Poniatowski Ł, A., Wojdasiewicz, P., Krawczyk, M., Szukiewicz, D., Gasik, R., Kubaszewski, Ł., et al. (2017). Analysis of the Role of CX3CL1 (Fractalkine) and Its Receptor CX3CR1 in Traumatic Brain and Spinal Cord Injury: Insight into Recent Advances in Actions of Neurochemokine Agents. *Mol Neurobiol* 54(3), 2167-2188. doi: 10.1007/s12035-016-9787-4.

Porter, N.M., Thibault, O., Thibault, V., Chen, K.-C., and Landfield, P.W. (1997). Calcium Channel Density and Hippocampal Cell Death with Age in Long-Term Culture. *The Journal of Neuroscience* 17(14), 5629. doi: 10.1523/JNEUROSCI.17-14-05629.1997.

Possel, H., Noack, H., Putzke, J., Wolf, G., and Sies, H. (2000). Selective upregulation of inducible nitric oxide synthase (iNOS) by lipopolysaccharide (LPS) and cytokines in microglia: in vitro and in vivo studies. *Glia* 32(1), 51-59. doi: 10.1002/1098-1136(200010)32:1<51::aid-glia50>3.0.co;2-4.

Prinz, M., Jung, S., and Priller, J. (2019). Microglia Biology: One Century of Evolving Concepts. *Cell* 179(2), 292-311. doi: 10.1016/j.cell.2019.08.053.

Probert, L. (2015). TNF and its receptors in the CNS: The essential, the desirable and the deleterious effects. *Neuroscience* 302, 2-22. doi: 10.1016/j.neuroscience.2015.06.038.

Pua, K.H., Stiles, D.T., Sowa, M.E., and Verdine, G.L. (2017). IMPDH2 Is an Intracellular Target of the Cyclophilin A and Sanglifehrin A Complex. *Cell Rep* 18(2), 432-442. doi: 10.1016/j.celrep.2016.12.030.

Qiao, C., Liu, Z., and Qie, S. (2023). The Implications of Microglial Regulation in Neuroplasticity-Dependent Stroke Recovery. *Biomolecules* 13(3). doi: 10.3390/biom13030571.

Qin, C., Yang, S., Chu, Y.H., Zhang, H., Pang, X.W., Chen, L., et al. (2022). Signaling pathways involved in ischemic stroke: molecular mechanisms and therapeutic interventions. *Signal Transduct Target Ther* 7(1)**,** 215. doi: 10.1038/s41392-022-01064-1.

Rabinowitz, J.D., and White, E. (2010). Autophagy and metabolism. *Science* 330(6009)**,** 1344-1348. doi: 10.1126/science.1193497.

Raivich, G., Moreno-Flores, M.T., Moller, J.C., and Kreutzberg, G.W. (1994). Inhibition of posttraumatic microglial proliferation in a genetic model of macrophage colony-stimulating factor deficiency in the mouse. *Eur J Neurosci* 6(10)**,** 1615-1618. doi: 10.1111/j.1460-9568.1994.tb00552.x.

Rankin, L., and Fowler, C.J. (2020). The Basal Pharmacology of Palmitoylethanolamide. *Int J Mol Sci* 21(21). doi: 10.3390/ijms21217942.

Relton, J.K., and Rothwell, N.J. (1992). Interleukin-1 receptor antagonist inhibits ischaemic and excitotoxic neuronal damage in the rat. *Brain Res Bull* 29(2)**,** 243-246. doi: 10.1016/0361-9230(92)90033-t.

Rivero-Segura, N.A., Flores-Soto, E., García de la Cadena, S., Coronado-Mares, I., Gomez-Verjan, J.C., Ferreira, D.G., et al. (2017). Prolactin-induced neuroprotection against glutamate excitotoxicity is mediated by the reduction of [Ca2+]i overload and NF-κB activation. *PLoS One* 12(5)**,** e0176910. doi: 10.1371/journal.pone.0176910.

Rosati, A., Cosi, A., Basile, M., Brambilla, A., Guerrini, R., Cimaz, R., et al. (2017). Mycophenolate mofetil as induction and long-term maintaining treatment in childhood: Primary angiitis of the central nervous system. *Joint Bone Spine* 84(3)**,** 353-356. doi: 10.1016/j.jbspin.2016.12.004.

Rossi, S., Sacchetti, L., Napolitano, F., De Chiara, V., Motta, C., Studer, V., et al. (2012). Interleukin-1beta causes anxiety by interacting with the endocannabinoid system. *J Neurosci* 32(40)**,** 13896-13905. doi: 10.1523/JNEUROSCI.1515-12.2012.

Roth, S., Cao, J., Singh, V., Tiedt, S., Hundeshagen, G., Li, T., et al. (2021). Post-injury immunosuppression and secondary infections are caused by an AIM2 inflammasome-driven signaling cascade. *Immunity* 54(4)**,** 648-659.e648. doi: 10.1016/j.immuni.2021.02.004.

Rothstein, J.D., Dykes-Hoberg, M., Pardo, C.A., Bristol, L.A., Jin, L., Kuncl, R.W., et al. (1996). Knockout of glutamate transporters reveals a major role for astroglial transport in excitotoxicity and clearance of glutamate. *Neuron* 16(3)**,** 675-686.

Rothwell, N.J., and Luheshi, G.N. (2000). Interleukin 1 in the brain: biology, pathology and therapeutic target. *Trends Neurosci* 23(12)**,** 618-625. doi: 10.1016/s0166-2236(00)01661-1.

Ruan, C., and Elyaman, W. (2022). A New Understanding of TMEM119 as a Marker of Microglia. *Front Cell Neurosci* 16**,** 902372. doi: 10.3389/fncel.2022.902372.

Ryberg, E., Larsson, N., Sjögren, S., Hjorth, S., Hermansson, N.O., Leonova, J., et al. (2007). The orphan receptor GPR55 is a novel cannabinoid receptor. *Br J Pharmacol* 152(7)**,** 1092-1101. doi: 10.1038/sj.bjp.0707460.

Saitoh, T., Fujita, N., Jang, M.H., Uematsu, S., Yang, B.G., Satoh, T., et al. (2008). Loss of the autophagy protein Atg16L1 enhances endotoxin-induced IL-1beta production. *Nature* 456(7219)**,** 264-268. doi: 10.1038/nature07383.

Sanz, J.M., Chiozzi, P., Colaianna, M., Zotti, M., Ferrari, D., Trabace, L., et al. (2012). Nimodipine inhibits IL-1β release stimulated by amyloid β from microglia. *Br J Pharmacol* 167(8)**,** 1702-1711. doi: 10.1111/j.1476-5381.2012.02112.x.

Schädlich, I.S., Winzer, R., Stabernack, J., Tolosa, E., Magnus, T., and Rissiek, B. (2023). The role of the ATP-adenosine axis in ischemic stroke. *Seminars in Immunopathology*. doi: 10.1007/s00281-023-00987-3.

Schilling, T., Nitsch, R., Heinemann, U., Haas, D., and Eder, C. (2001). Astrocyte-released cytokines induce ramification and outward K+ channel expression in microglia via distinct signalling pathways. *The European journal of neuroscience* 14(3)**,** 463-473. doi: 10.1046/j.0953-816x.2001.01661.x.

Schlessinger, A.R., Cowan, W.M., and Gottlieb, D.I. (1975). An autoradiographic study of the time of origin and the pattern of granule cell migration in the dentate gyrus of the rat. *J Comp Neurol* 159(2)**,** 149-175. doi: 10.1002/cne.901590202.

Schwabenland, M., Brück, W., Priller, J., Stadelmann, C., Lassmann, H., and Prinz, M. (2021). Analyzing microglial phenotypes across neuropathologies: a practical guide. *Acta Neuropathol* 142(6)**,** 923-936. doi: 10.1007/s00401-021-02370-8.

Scriabine, A., and van den Kerckhoff, W. (1988). Pharmacology of Nimodipine. *Annals of the New York Academy of Sciences* 522(1)**,** 698-706. doi: https://doi.org/10.1111/j.1749-6632.1988.tb33415.x.

Sharkey, J., and Butcher, S.P. (1994). Immunophilins mediate the neuroprotective effects of FK506 in focal cerebral ischaemia. *Nature* 371(6495)**,** 336-339. doi: 10.1038/371336a0.

Shiau, Celia E., Monk, Kelly R., Joo, W., and Talbot, William S. (2013). An Anti-inflammatory NOD-like Receptor Is Required for Microglia Development. *Cell Reports* 5(5)**,** 1342-1352. doi: https://doi.org/10.1016/j.celrep.2013.11.004.

Shiga, Y., Onodera, H., Matsuo, Y., and Kogure, K. (1992). Cyclosporin A protects against ischemia-reperfusion injury in the brain. *Brain Res* 595(1)**,** 145-148. doi: 10.1016/0006-8993(92)91465-q.

Shimada, I.S., Borders, A., Aronshtam, A., and Spees, J.L. (2011). Proliferating reactive astrocytes are regulated by Notch-1 in the peri-infarct area after stroke. *Stroke* 42(11)**,** 3231-3237. doi: 10.1161/STROKEAHA.111.623280.

Smith, A.M., Gibbons, H.M., Oldfield, R.L., Bergin, P.M., Mee, E.W., Curtis, M.A., et al. (2013). M-CSF increases proliferation and phagocytosis while modulating receptor and transcription factor expression in adult human microglia. *Journal of Neuroinflammation* 10(1)**,** 859. doi: 10.1186/1742-2094-10-85.

Sobowale, O.A., Parry-Jones, A.R., Smith, C.J., Tyrrell, P.J., Rothwell, N.J., and Allan, S.M. (2016). Interleukin-1 in Stroke: From Bench to Bedside. *Stroke* 47(8)**,** 2160-2167. doi: 10.1161/strokeaha.115.010001.

Sofroniew, M.V. (2009). Molecular dissection of reactive astrogliosis and glial scar formation. *Trends Neurosci* 32(12)**,** 638-647. doi: 10.1016/j.tins.2009.08.002.

Sofroniew, M.V. (2020). Astrocyte Reactivity: Subtypes, States, and Functions in CNS Innate Immunity. *Trends Immunol* 41(9)**,** 758-770. doi: 10.1016/j.it.2020.07.004.

Sofroniew, M.V., and Vinters, H.V. (2010). Astrocytes: biology and pathology. *Acta Neuropathol* 119(1)**,** 7-35. doi: 10.1007/s00401-009-0619-8.

Solbrig, M.V., Schlaberg, R., Briese, T., Horscroft, N., and Lipkin, W.I. (2002). Neuroprotection and reduced proliferation of microglia in ribavirin-treated bornavirus-infected rats. *Antimicrob Agents Chemother* 46(7)**,** 2287-2291. doi: 10.1128/aac.46.7.2287-2291.2002.

Sorice, M. (2022). Crosstalk of Autophagy and Apoptosis. *Cells* 11(9). doi: 10.3390/cells11091479.

Stojiljkovic, M.R., Schmeer, C., and Witte, O.W. (2022). Pharmacological Depletion of Microglia Leads to a Dose-Dependent Reduction in Inflammation and Senescence in the Aged Murine Brain. *Neuroscience* 488**,** 1-9. doi: 10.1016/j.neuroscience.2022.02.018.

Stoll, G., and Nieswandt, B. (2019). Thrombo-inflammation in acute ischaemic stroke - implications for treatment. *Nat Rev Neurol* 15(8)**,** 473-481. doi: 10.1038/s41582-019-0221-1.

Streit, W.J. (1990). An improved staining method for rat microglial cells using the lectin from Griffonia simplicifolia (GSA I-B4). *Journal of Histochemistry & Cytochemistry* 38(11)**,** 1683-1686. doi: 10.1177/38.11.2212623.

Streit, W.J. (2002). Microglia as neuroprotective, immunocompetent cells of the CNS. *Glia* 40(2)**,** 133-139. doi: 10.1002/glia.10154.

Streit, W.J., Graeber, M.B., and Kreutzberg, G.W. (1988). Functional plasticity of microglia: a review. *Glia* 1(5)**,** 301-307. doi: 10.1002/glia.440010502.

Sugiura, A., Andrejeva, G., Voss, K., Heintzman, D.R., Xu, X., Madden, M.Z., et al. (2022). MTHFD2 is a metabolic checkpoint controlling effector and regulatory T cell fate and function. *Immunity* 55(1)**,** 65-81.e69. doi: 10.1016/j.immuni.2021.10.011.

Sun, Z., Nyanzu, M., Yang, S., Zhu, X., Wang, K., Ru, J., et al. (2020). VX765 Attenuates Pyroptosis and HMGB1/TLR4/NF-κB Pathways to Improve Functional Outcomes in TBI Mice. *Oxid Med Cell Longev* 2020**,** 7879629. doi: 10.1155/2020/7879629.

Takahashi, K., Rochford, C.D., and Neumann, H. (2005). Clearance of apoptotic neurons without inflammation by microglial triggering receptor expressed on myeloid cells-2. *J Exp Med* 201(4)**,** 647-657. doi: 10.1084/jem.20041611.

Thomas, E.C., Gunter, J.H., Webster, J.A., Schieber, N.L., Oorschot, V., Parton, R.G., et al. (2012). Different Characteristics and Nucleotide Binding Properties of Inosine Monophosphate Dehydrogenase (IMPDH) Isoforms. *PLOS ONE* 7(12)**,** e51096. doi: 10.1371/journal.pone.0051096.

Thored, P., Heldmann, U., Gomes-Leal, W., Gisler, R., Darsalia, V., Taneera, J., et al. (2009). Long-term accumulation of microglia with proneurogenic phenotype concomitant with persistent neurogenesis in adult subventricular zone after stroke. *Glia* 57(8)**,** 835-849. doi: 10.1002/glia.20810.

Trotta, T., Porro, C., Calvello, R., and Panaro, M.A. (2014). Biological role of Toll-like receptor-4 in the brain. *J Neuroimmunol* 268(1-2)**,** 1-12. doi: 10.1016/j.jneuroim.2014.01.014.

Van Driessche, B., Verloo, P., Herregods, N., Mondelaers, V., Dehoorne, J., Van Coster, R., et al. (2019). Recurrent arterial ischemic stroke with good response to mycophenolate mofetil. *Eur J Paediatr Neurol* 23(1)**,** 222-227. doi: 10.1016/j.ejpn.2018.11.003.

van Weering, H.R.J., Nijboer, T.W., Brummer, M.L., Boddeke, E., and Eggen, B.J.L. (2023). Microglia morphotyping in the adult mouse CNS using hierarchical clustering on principal components reveals regional heterogeneity but no sexual dimorphism. *Glia*. doi: 10.1002/glia.24427.

Vankriekelsvenne, E., Chrzanowski, U., Manzhula, K., Greiner, T., Wree, A., Hawlitschka, A., et al. (2022). Transmembrane protein 119 is neither a specific nor a reliable marker for microglia. *Glia* 70(6)**,** 1170-1190. doi: 10.1002/glia.24164.

Verkhratsky, A., and Nedergaard, M. (2018). Physiology of Astroglia. *Physiol Rev* 98(1)**,** 239-389. doi: 10.1152/physrev.00042.2016.

Vermersch, P., Stojkovic, T., and de Seze, J. (2005). Mycophenolate mofetil and neurological diseases. *Lupus* 14 Suppl 1**,** s42-45. doi: 10.1191/0961203305lu2117oa.

Vinet, J., van Weering, H.R.J., Heinrich, A., Kälin, R.E., Wegner, A., Brouwer, N., et al. (2012). Neuroprotective function for ramified microglia in hippocampal excitotoxicity. *Journal of Neuroinflammation* 9(1)**,** 27. doi: 10.1186/1742-2094-9-27.

Virgin, H.W., and Levine, B. (2009). Autophagy genes in immunity. *Nat Immunol* 10(5)**,** 461-470. doi: 10.1038/ni.1726.

Viviani, B., Bartesaghi, S., Gardoni, F., Vezzani, A., Behrens, M.M., Bartfai, T., et al. (2003). Interleukin-1beta enhances NMDA receptor-mediated intracellular calcium increase through activation of the Src family of kinases. *J Neurosci* 23(25)**,** 8692-8700.

Walter, L., Franklin, A., Witting, A., Wade, C., Xie, Y., Kunos, G., et al. (2003). Nonpsychotropic cannabinoid receptors regulate microglial cell migration. *J Neurosci* 23(4)**,** 1398-1405. doi: 10.1523/jneurosci.23-04-01398.2003.

Wang, H., Li, J., Zhang, H., Wang, M., Xiao, L., Wang, Y., et al. (2023a). Regulation of microglia polarization after cerebral ischemia. *Front Cell Neurosci* 17**,** 1182621. doi: 10.3389/fncel.2023.1182621.

Wang, H., Li, X., Wang, Q., Ma, J., Gao, X., and Wang, M. (2023b). TREM2, microglial and ischemic stroke. *J Neuroimmunol* 381**,** 578108. doi: 10.1016/j.jneuroim.2023.578108.

Wang, M., Chen, Z., Yang, L., and Ding, L. (2021). Sappanone A Protects Against Inflammation, Oxidative Stress and Apoptosis in Cerebral Ischemia-Reperfusion Injury by Alleviating Endoplasmic Reticulum Stress. *Inflammation* 44(3)**,** 934-945. doi: 10.1007/s10753-020-01388-6.

Wang, Y., Jin, S., Sonobe, Y., Cheng, Y., Horiuchi, H., Parajuli, B., et al. (2014). Interleukin-1β induces blood-brain barrier disruption by downregulating Sonic hedgehog in astrocytes. *PLoS One* 9(10)**,** e110024. doi: 10.1371/journal.pone.0110024.

Wanner, I.B., Anderson, M.A., Song, B., Levine, J., Fernandez, A., Gray-Thompson, Z., et al. (2013). Glial scar borders are formed by newly proliferated, elongated astrocytes that interact to corral inflammatory and fibrotic cells via STAT3-dependent mechanisms after spinal cord injury. *J Neurosci* 33(31)**,** 12870-12886. doi: 10.1523/jneurosci.2121-13.2013.

Wegener, N., and Koch, M. (2009). Neurobiology and systems physiology of the endocannabinoid system. *Pharmacopsychiatry* 42 Suppl 1**,** S79-86. doi: 10.1055/s-0029-1216346.

Westendorp, W.F., Nederkoorn, P.J., Vermeij, J.D., Dijkgraaf, M.G., and van de Beek, D. (2011). Post-stroke infection: a systematic review and meta-analysis. *BMC Neurol* 11**,** 110. doi: 10.1186/1471-2377-11-110.

Whitelaw, B.S., Stoessel, M.B., and Majewska, A.K. (2023). Movers and shakers: Microglial dynamics and modulation of neural networks. *Glia* 71(7)**,** 1575-1591. doi: 10.1002/glia.24323.

Wilmes, M., Pinto Espinoza, C., Ludewig, P., Stabernack, J., Liesz, A., Nicke, A., et al. (2022). Blocking P2X7 by intracerebroventricular injection of P2X7-specific nanobodies reduces stroke lesions. *J Neuroinflammation* 19(1)**,** 256. doi: 10.1186/s12974-022-02601-z.

Wolf, S.A., Boddeke, H.W., and Kettenmann, H. (2017). Microglia in Physiology and Disease. *Annu Rev Physiol* 79**,** 619-643. doi: 10.1146/annurev-physiol-022516-034406.

Wong, R., Lénárt, N., Hill, L., Toms, L., Coutts, G., Martinecz, B., et al. (2019). Interleukin-1 mediates ischaemic brain injury via distinct actions on endothelial cells and cholinergic neurons. *Brain Behav Immun* 76**,** 126-138. doi: 10.1016/j.bbi.2018.11.012.

Woodhams, P.L., and Atkinson, D.J. (1996). Entorhinal axons perforate hippocampal field CA3 in organotypic slice culture. *Brain Res Dev Brain Res* 95(1)**,** 144-147. doi: 10.1016/0165-3806(96)00111-3.

Wowro, S.J., Tong, G., Krech, J., Rolfs, N., Berger, F., and Schmitt, K.R.L. (2019). Combined Cyclosporin A and Hypothermia Treatment Inhibits Activation of BV-2 Microglia but Induces an Inflammatory Response in an Ischemia/Reperfusion Hippocampal Slice Culture Model. *Frontiers in cellular neuroscience* 13**,** 273-273. doi: 10.3389/fncel.2019.00273.

Wu, L., Xian, X., Xu, G., Tan, Z., Dong, F., Zhang, M., et al. (2022). Toll-Like Receptor 4: A Promising Therapeutic Target for Alzheimer's Disease. *Mediators of Inflammation* 2022**,** 7924199. doi: 10.1155/2022/7924199.

Wu, L., Xiong, X., Wu, X., Ye, Y., Jian, Z., Zhi, Z., et al. (2020). Targeting Oxidative Stress and Inflammation to Prevent Ischemia-Reperfusion Injury. *Front Mol Neurosci* 13**,** 28. doi: 10.3389/fnmol.2020.00028.

Xia, Y.Y., Song, S.W., Min, Y., Zhong, Y., Sheng, Y.C., Li, R.P., et al. (2014). The effects of anakinra on focal cerebral ischemic injury in rats. *CNS Neurosci Ther* 20(9)**,** 879-881. doi: 10.1111/cns.12310.

Yalçın, G.D., and Colak, M. (2020). SIRT4 prevents excitotoxicity via modulating glutamate metabolism in glioma cells. *Hum Exp Toxicol* 39(7)**,** 938-947. doi: 10.1177/0960327120907142.

Yamamoto, H., Zhang, S., and Mizushima, N. (2023). Autophagy genes in biology and disease. *Nat Rev Genet* 24(6)**,** 382-400. doi: 10.1038/s41576-022-00562-w.

Yan, J., Xu, L., Welsh, A.M., Chen, D., Hazel, T., Johe, K., et al. (2006). Combined Immunosuppressive Agents or CD4 Antibodies Prolong Survival of Human Neural Stem Cell Grafts and Improve Disease Outcomes in Amyotrophic Lateral Sclerosis Transgenic Mice. *STEM CELLS* 24(8)**,** 1976-1985. doi: https://doi.org/10.1634/stemcells.2005-0518.

Yin, J., Ren, W., Huang, X., Deng, J., Li, T., and Yin, Y. (2018). Potential Mechanisms Connecting Purine Metabolism and Cancer Therapy. *Front Immunol* 9**,** 1697. doi: 10.3389/fimmu.2018.01697.

Yu, L., Wang, L., and Chen, S. (2010). Endogenous toll-like receptor ligands and their biological significance. *J Cell Mol Med* 14(11)**,** 2592-2603. doi: 10.1111/j.1582-4934.2010.01127.x.

Yuan, J., Lipinski, M., and Degterev, A. (2003). Diversity in the mechanisms of neuronal cell death. *Neuron* 40(2)**,** 401-413. doi: 10.1016/s0896-6273(03)00601-9.

Zaghloul, N., Kurepa, D., Bader, M.Y., Nagy, N., and Ahmed, M.N. (2020). Prophylactic inhibition of NF-κB expression in microglia leads to attenuation of hypoxic ischemic injury of the immature brain. *Journal of Neuroinflammation* 17(1)**,** 365. doi: 10.1186/s12974-020-02031-9.

Zawadzka, M., and Kaminska, B. (2005). A novel mechanism of FK506-mediated neuroprotection: downregulation of cytokine expression in glial cells. *Glia* 49(1)**,** 36-51. doi: 10.1002/glia.20092.

Zeng, H., and Chi, H. (2017). mTOR signaling in the differentiation and function of regulatory and effector T cells. *Current Opinion in Immunology* 46**,** 103-111. doi: https://doi.org/10.1016/j.coi.2017.04.005.

Zheng, R.Z., Lee, K.Y., Qi, Z.X., Wang, Z., Xu, Z.Y., Wu, X.H., et al. (2022). Neuroinflammation Following Traumatic Brain Injury: Take It Seriously or Not. *Front Immunol* 13**,** 855701. doi: 10.3389/fimmu.2022.855701.

Zhu, D., Zhang, J., Hashem, J., Gao, F., and Chen, C. (2023). Inhibition of 2-arachidonoylglycerol degradation enhances glial immunity by single-cell transcriptomic analysis. *J Neuroinflammation* 20(1)**,** 17. doi: 10.1186/s12974-023-02701-4.

Zhu, H., Hu, S., Li, Y., Sun, Y., Xiong, X., Hu, X., et al. (2022). Interleukins and Ischemic Stroke. *Front Immunol* 13**,** 828447. doi: 10.3389/fimmu.2022.828447.

Zhu, J., and Thompson, C.B. (2019). Metabolic regulation of cell growth and proliferation. *Nature Reviews Molecular Cell Biology* 20(7)**,** 436-450. doi: 10.1038/s41580-019-0123-5.

4. Thesen

1. OHSC stellen ein geeignetes Modell zur Untersuchung von verschiedenen Materialien auf neuronales Gewebe dar.
2. Eine generelle Übertragung der neurozytoprotektiven Ergebnisse aus den OHSC in ein *in vivo* Modell scheint prinzipiell möglich, jedoch ist die exakte Translation des spezifischen Zeitfensters von den OHSC auf ein CCI-Modell wegen der Effekte einwandernder Immunzellen nur teilweise möglich.
3. Die Translation der Ergebnisse zwischen verschiedenen tierexperimentellen Modellen und klinischen Studien stellt einen wichtigen Baustein in der neurozytoprotektiven Forschung dar.
4. Der neurozytoprotektive Effekt von MMF in OHSC ist zeitabhängig, die Behandlung sollte innerhalb der ersten 16 Stunden begonnen werden und mindestens 24 Stunden anhalten.
5. MMF zeigt eine frühe Mikroglia-abhängige neurozytoprotektive Phase, welche in Übereinstimmung mit dem nachgewiesenen Zeitfenster in den OHSC ist.
6. Die reduzierte Anzahl der Mikroglia ist eine Komponente des multimodalen neurozytoprotektiven Effekts von MMF und kann nicht als der einzige Mediator angesehen werden.
7. Nach 72 Stunden scheinen sich auch Astrozyten an der Neurozytoprotektion durch MMF zu beteiligen.

5. Publikationen

***Kleine J**, Leisz S, Ghadban C, Hohmann T, Prell J, Scheller C, Strauss C, Simmermacher S, Dehghani F (**2021**) Variants of Oxidized Regenerated Cellulose and Their Distinct Effects on Neuronal Tissue. Int. J. Mol. Sci. 2021,22,11467. https://doi.org/ 10.3390/ijms222111467*

***Kleine J**, Hohmann U, Hohmann T, Ghadban C, Schmidt M, Laabs S, Alessandri B and Dehghani F (**2022**) Microglia-Dependent and Independent Brain Cytoprotective Effects of Mycophenolate Mofetil During Neuronal Damage. Front. Aging Neurosci. 14:863598. doi: 10.3389/fnagi.2022.863598*

*Hohmann U, Pelzer M, **Kleine J**, Hohmann T, Ghadban C and Dehghani F (**2019**) Opposite Effects of Neuroprotective Cannabinoids, Palmitoylethanolamide, and 2-Arachidonoylglycerol on Function and Morphology of Microglia. Front. Neurosci. 13:1180. doi: 10.3389/fnins.2019.01180*

*Hohmann U, Ghadban C, Hohmann T, **Kleine J**, Schmidt M, Scheller C, Strauss C, Dehghani, F (**2022**) Nimodipine Exerts Time-Dependent Neuroprotective Effect after Excitotoxical Damage in Organotypic Slice Cultures. Int. J. Mol. Sci. 2022, 23,3331. https://doi.org/10.3390/ ijms23063331*

International Journal of
Molecular Sciences

MDPI

Article

Variants of Oxidized Regenerated Cellulose and Their Distinct Effects on Neuronal Tissue

Joshua Kleine [1,†], Sandra Leisz [2,*,†], Chalid Ghadban [1], Tim Hohmann [1], Julian Prell [2], Christian Scheller [2], Christian Strauss [2], Sebastian Simmermacher [2,‡] and Faramarz Dehghani [1,‡]

[1] Medical Faculty, Institute of Anatomy and Cell Biology, Martin Luther University Halle-Wittenberg, 06112 Halle (Saale), Germany; Joshua.kleine@student.uni-halle.de (J.K.); Chalid.ghadban@medizin.uni-halle.de (C.G.); Tim.hohmann@medizin.uni-halle.de (T.H.); Faramarz.dehghani@medizin.uni-halle.de (F.D.)
[2] Department of Neurosurgery, Medical Faculty, Martin Luther University Halle-Wittenberg, 06120 Halle (Saale), Germany; Julian.prell@uk-halle.de (J.P.); Christian.scheller@uk-halle.de (C.S.); Christian.strauss@uk-halle.de (C.S.); Sebastian.simmermacher@uk-halle.de (S.S.)
* Correspondence: Sandra.leisz@uk-halle.de; Tel.: +49-(0)-345-557-7014
† Both authors contributed equally.
‡ Both authors contributed equally.

Abstract: Based on oxidized regenerated cellulose (ORC), several hemostyptic materials, such as Tabotamp®, Equicel® and Equitamp®, have been developed to approach challenging hemostasis in neurosurgery. The present study compares ORC that differ in terms of compositions and properties, regarding their structure, solubility, pH values and effects on neuronal tissue. Cytotoxicity was detected via DNA-binding fluorescence dye in Schwann cells, astrocytes, and neuronal cells. Additionally, organotypic hippocampal slice cultures (OHSC) were analyzed, using propidium iodide, hematoxylin-eosin, and isolectin B_4 staining to investigate the cellular damage, cytoarchitecture, and microglia activation. Whereas Equicel® led to a neutral pH, Tabotamp® (pH 2.8) and Equitamp® (pH 4.8) caused a significant reduction of pH ($p < 0.001$). Equicel® and Tabotamp® increased cytotoxicity significantly in several cell lines ($p < 0.01$). On OHSC, Tabotamp® and Equicel® led to a stronger and deeper damage to the neuronal tissue than Equitamp® or gauze ($p < 0.01$). Equicel® increased strongly the number of microglia cells after 24 h ($p < 0.001$). Microglia cells were not detectable after Tabotamp® treatment, presumably due to an artifact caused by strong pH reduction. In summary, our data imply the use of Equicel®, Tabotamp® or Equitamp® for specific applications in distinct clinical settings depending on their localization or tissue properties.

Keywords: cellulose applications; oxidized regenerated cellulose; Tabotamp®; Equicel®; Equitamp®; cell death; organotypic hippocampal slice cultures

check for updates

Citation: Kleine, J.; Leisz, S.; Ghadban, C.; Hohmann, T.; Prell, J.; Scheller, C.; Strauss, C.; Simmermacher, S.; Dehghani, F. Variants of Oxidized Regenerated Cellulose and Their Distinct Effects on Neuronal Tissue. *Int. J. Mol. Sci.* **2021**, *22*, 11467. https://doi.org/10.3390/ijms222111467

Academic Editor: Suresh Valiyaveettil

Received: 4 October 2021
Accepted: 20 October 2021
Published: 25 October 2021

Publisher's Note: MDPI stays neutral with regard to jurisdictional claims in published maps and institutional affiliations.

Copyright: © 2021 by the authors. Licensee MDPI, Basel, Switzerland. This article is an open access article distributed under the terms and conditions of the Creative Commons Attribution (CC BY) license (https://creativecommons.org/licenses/by/4.0/).

1. Introduction

Intraoperative bleeding, especially during neurosurgical interventions, can lead to massive secondary complications. The rising number of neurosurgical patients under anticoagulative therapy increases the risk of perioperative hemorrhage [1]. Consequently, the application of hemostatic agents is an important option to handle intraoperative bleeding. Oxidized regenerated cellulose (ORC) is a commonly used absorbable hemostatic product that prevents bleeding and controls epidural oozing [2]. In a comprehensive review of topical hemostatic agents, ORC showed only moderate hemostatic effects, but good handling properties [3]. It did not stick to instruments, could easily be fitted to the tissue [2] and was completely absorbable within weeks [4]. Chemically, ORC consist of homo-polysaccharides and dinitrogen tetroxide. The oxidation of their hydroxyl groups to carboxyl acid groups forms a polyuronic acid [5]. Depending on the oxidized molecular position, different physico-chemical properties result and the efficiency of oxidation is influenced by factors like temperature and pressure [3]. The carboxylic acid groups are responsible for decrease

in the pH value with additional bactericidal properties [6,7]. Hemostasis is achieved via different mechanisms. Absorption of blood results in slightly swelling and formation of a plug at the injury site. Furthermore, the acidity causes erythrocyte cell lysis, and the released hemoglobin reacts with acid to form hematin [3,8,9]. Over the last few decades, several absorbable hemostyptic materials have been developed based on natural and artificial sources. Cellulose is a natural source of ORC. In comparison, viscose is a semi-artificial regenerated cellulose, which is chemically identical to the native fiber, but has a different ordered surface in the elementary lattice (hydrate cellulose). Regardless their source, all products are subsumed as ORC. Several approved ORC are offered on the European market including Tabotamp® (Ethicon, Johnson & Johnson, respectively Surgicel® as its brand name in USA), Equicel® and Equitamp® (Equimedical). Tabotamp® is established since 1959, whereas Equicel® and Equitamp® have been approved according to the EN ISO 10993 as a medical device since 2012. Recently, we demonstrated for Tabotamp® a strong and local cytotoxic effect in several monolayer cell culture systems. pH-sensitive fluorescence microscope analyses revealed a strong pH gradient between the local pH drop and the surrounding media [10].

Based on these data, the present study was designed to compare the effects of Tabotamp®, Equitamp® and Equicel® on pH values, properties in aqueous solution, cell detachment, glial cell response, cell death and the extension of cellular damage in monolayer cell systems and in the dentate gyrus of the organotypic hippocampal slice cultures.

2. Results

2.1. ORC Products Showed Different Structures and Properties in Aqueous Solution

ORC showed strong structural differences. While gauze and Equicel® consist of an ordered network based on frayed natural cotton fibers, Equitamp® and Tabotamp® were structured like a loose woven knit of smooth fibers. Equitamp® had a higher density than Tabotamp® (Figure 1A).

To compare the absorbability, gauze and ORC were incubated for 48 h in aqueous solution (Figure 1B). The non-absorbable gauze showed no dissolution, whereas Equitamp® and Tabotamp® were nearly completely dissolved. Equicel® formed a gelatin-like plug, which did not dissolve after 48 h.

The different oxidation of ORC caused changes in pH value in aqueous solution (Figure 1C). Non-oxidized gauze led to an increase in pH value from 7.50 ± 0.02 without gauze to 7.73 ± 0.01 with 500 mm^2/mL gauze. Even with large amounts of Equicel®, the pH value remained stable (pH 7.53 ± 0.01 without Equicel® to 7.52 ± 0.04 with 500 mm^2/mL Equicel®; $p = 0.88$). With smaller amounts of Equitamp®, the pH was stable (7.51 ± 0.04 with 40 mm^2/mL and 7.52 ± 0.13 with 75 mm^2/mL; $p = 1.00$). However, Equitamp® reduced pH from 7.49 ± 0.02 to 6.43 ± 0.23, 6.22 ± 0.05 and 4.78 ± 0.10 with amounts of 190, 250 and 500 mm^2/mL medium ($p < 0.001$). The strongest pH reduction was caused by Tabotamp®. Already amounts of 40 and 75 mm^2 Tabotamp® decreased the pH from 7.77 ± 0.02 to 7.28 ± 0.04 ($p < 0.001$) and 6.62 ± 0.10 ($p < 0.001$), respectively. Larger amounts of 190, 250, and 500 mm^2/mL Tabotamp® led to a strong acidic pH of 3.92 ± 0.09, 3.40 ± 0.09 and 2.84 ± 0.01 ($p < 0.001$) (Figure 1C).

Cell Detachment Analysis

Previously published results of cell detachment after incubation with Tabotamp®, gauze and untreated controls [10] were extended by experiments after incubation with Equicel® and Equitamp®. Crystal violet staining was applied after incubation with the different ORC for 24 h (Figure 2A). The quantification of cell detachment after incubation of ORC on Schwann cells revealed that Equitamp® (56.19% ± 8.55%) and Tabotamp® (89.25% ± 4.74%) caused an increased damage of the cell monolayers compared to gauze (19.59% ± 12.30%, $p < 0.05$) (Figure 2B). In case of immortalized neuronal cells, astrocytes and primary astrocytes, Tabotamp®, Equicel®, and Equitamp® showed no significant difference of cell detachment when compared to the gauze (Figure 2C–E; $p > 0.05$).

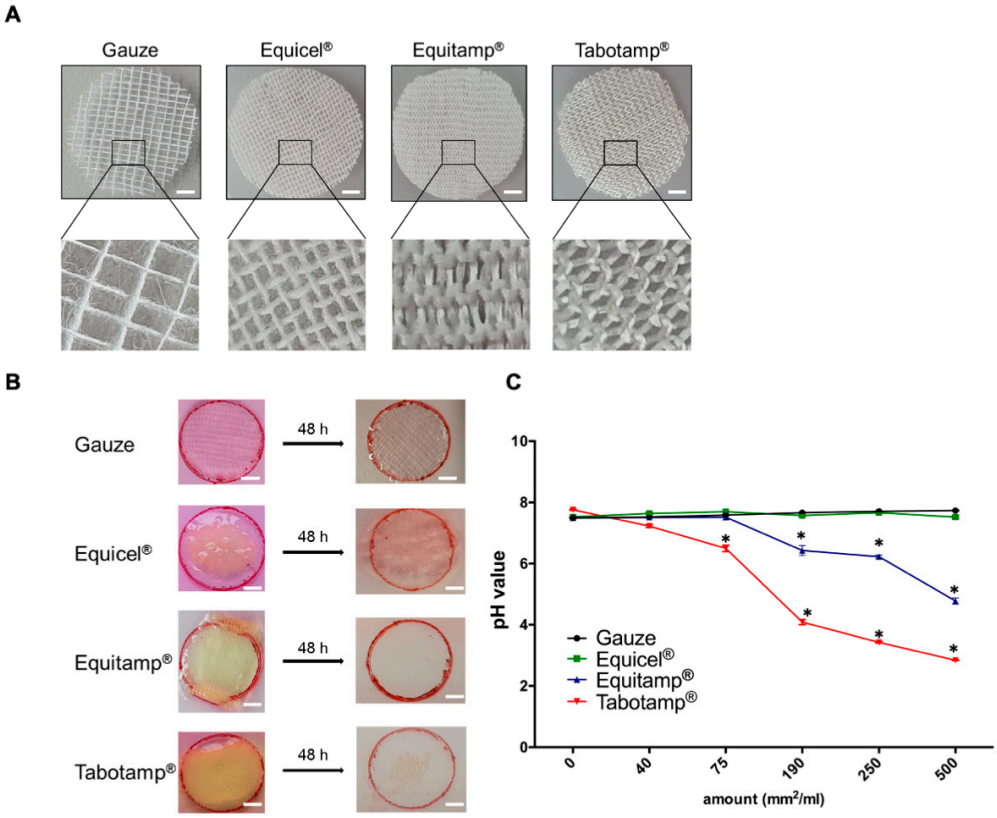

Figure 1. Comparison of ORC properties. Treatment materials with 22 mm diameter. In all experiments gauze served as non-oxidized, non-absorbable control. Gauze and Equicel® contain frayed organized fibers, which are arranged in a square network structure. Equicel® is an ORC based on natural cotton and contains collagen and fibrin. Equitamp® and Tabotamp® have a woven mesh structure. The viscose-based mesh of Equitamp® has a higher density compared to Tabotamp®. Bar = 3 mm (**A**). Samples were wetted with DMEM to compare the dissolution and absorbability. Bar = 5 mm (**B**). The pH values of increasing amounts of gauze or ORC per milliliter supplemented DMEM. The graph shows the mean and SEM of three independent analyses. The significance was tested to the same amount of gauze (* $p < 0.001$) (**C**).

2.2. Effect of Non-Oxidized Cellulose and ORC on Cell Viability

ORC-mediated cytotoxicity was measured via a fluorescence marked DNA-binding dye in Schwann cells, neuronal cells and astrocytes. Previously, we published the results for Tabotamp® and included the data in the figures for a better comparison between the ORC [10].

Compared to gauze, Equitamp® and Equicel® did not significantly affect cell death rates of Schwann cells. The highest cell death rates of Schwann cells were shown after incubation with Tabotamp® (100% coverage, Figure 3A). Comparison of Equitamp® with Equicel® (100% coverage) caused a significantly higher cytotoxicity of Equicel® ($p = 0.018$, Table S1).

Coverage with Equicel® and Tabotamp® showed an impaired neuronal cell survival, compared to gauze (55% and 100% coverage, $p < 0.05$, Figure 3B). Equitamp® induced cell death rates were equivalent to gauze and significantly reduced compared to higher values of Equicel® in neuronal cells ($p < 0.05$, Table S1).

Astrocytic cells demonstrated a high sensitivity to the treatment with ORC and even gauze (Figure 3C,D). Comparison between the ORC and gauze showed the highest cell death rates of immortalized astrocytes after incubation with Equicel® (33%, 55% and 100% coverage, $p < 0.002$) and Tabotamp® (55%, 100% coverage, $p < 0.05$, Figure 4C). In addition, for primary astrocytes Equicel® increased cell death (55% coverage, $p = 0.002$,

100% coverage, $p < 0.001$) in comparison to gauze (Figure 3D), whereas Equitamp® reduced cell death of primary astrocytes in comparison to gauze (55% and 100% coverage, $p < 0.001$).

Except for 33% coverage on immortalized astrocytes (C8D1A) the depicted Tabotamp® data showed cell death rates that were comparable to or even exceeded those caused by Equicel® (Figure 3C,D).

Incubation with gauze caused a significant increase in cytotoxicity of astrocytes (C8D1A) in comparison to untreated cells (control, CTL) (55% coverage, $p = 0.042$). However, the cell death rates of Equitamp® treated cells were comparable to CTL (Figure 3C, Table S1).

In addition, for primary astrocytes incubation with gauze increased cytotoxicity (55% and 100% coverage, $p < 0.05$, Figure 3D, Table S1).

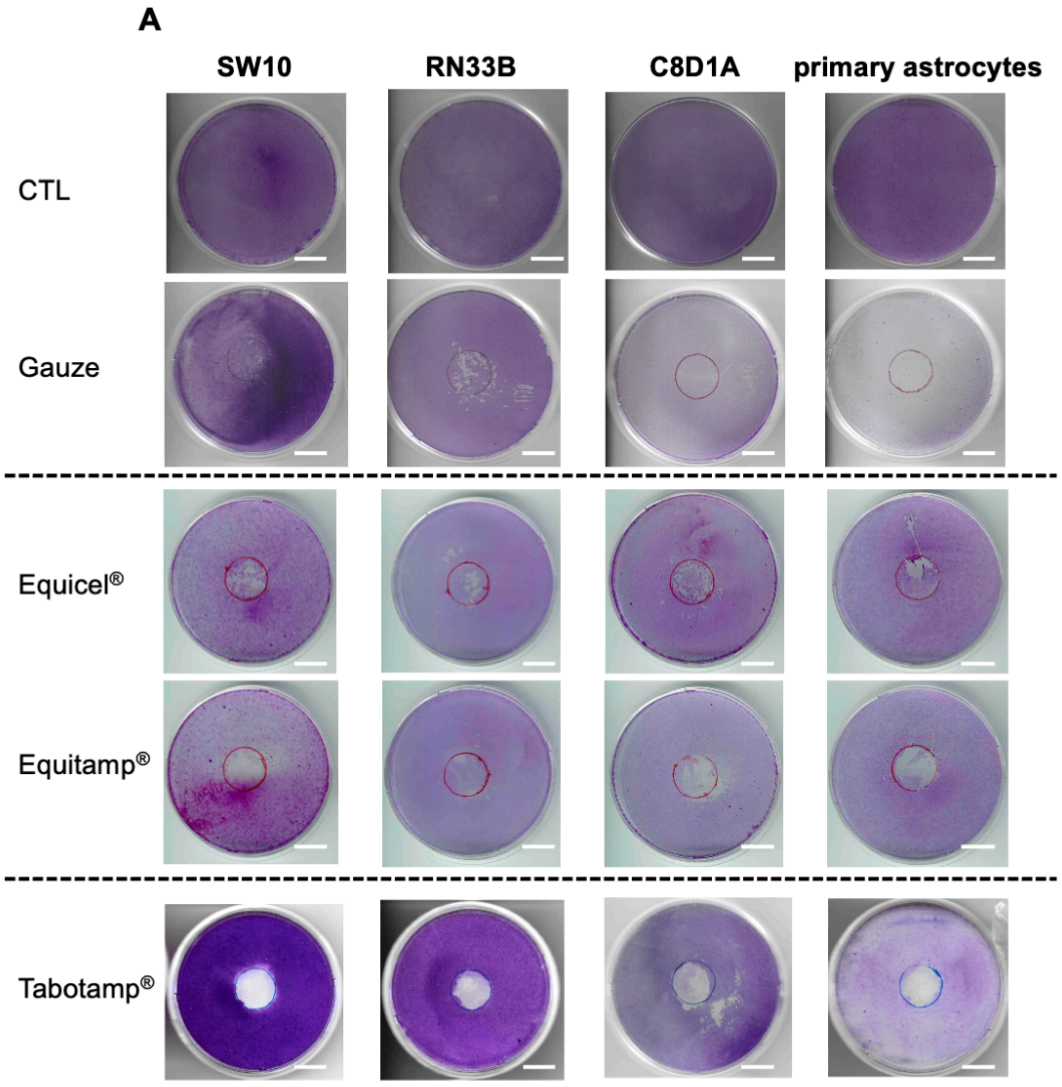

Figure 2. *Cont.*

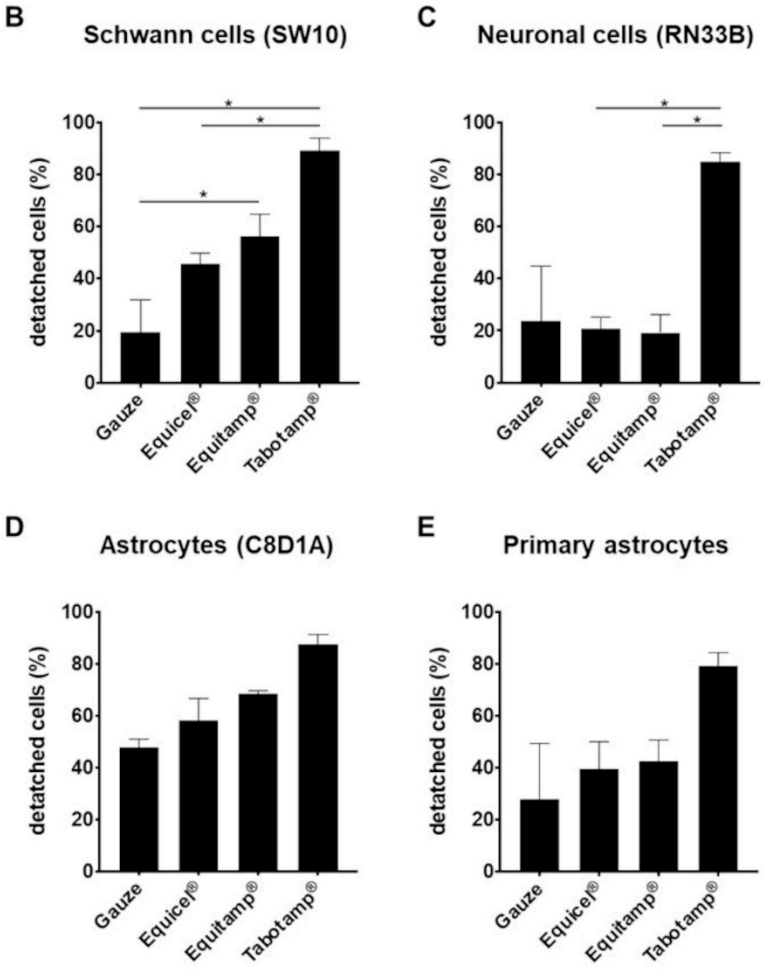

Figure 2. Detachment of cell monolayer after incubation with Equicel® and Equitamp®. Exemplary crystal violet staining of each ORC and cell line or primary cells. The results of untreated cells (control, CTL) and after incubation with gauze and Tabotamp® have already been published and are shown for comparison [10]. Cells were grown to complete confluence in 60 cm^2 cell culture dishes and incubated with Equicel® or Equitamp®. Bar = 2 cm (**A**). In addition, the means and SEM of quantified cell detachment analysis of three independent stained dishes from Schwann cells (**B**), neuronal cells (**C**), immortalized astrocytes (**D**) and primary astrocytic cultures (**E**) are shown (* $p < 0.05$).

2.3. Equicel® and Tabotamp® Generated Cellular Damage in the Dentate Gyrus of Organotypic Hippocampal Slice Cultures after 24 h

Untreated organotypic hippocampal slice cultures (OHSC) as well as slices treated with gauze displayed an excellent preservation of their cytoarchitecture. In CLSM only a few pycnotic propidium iodide (PI) positive nuclei were detected in granular cell layer (GCL) of the dentate gyrus (DG) (CTL: 5.4 PI positive cells/GCL, gauze: 42.8 PI positive cells/GCL) (Figure 4A,C). Treatment with Equicel® and Tabotamp® significantly increased the number of PI positive cells compared to gauze (Equicel®: 256.2 PI positive cells/GCL, $p < 0.001$; Tabotamp®: 230.4 PI positive cells/GCL, $p < 0.01$) (Figure 4A,C). No significant increase in the number of PI positive cells was found after treatment with Equitamp® compared to gauze (Equitamp®: 108.3 PI positive cells/GCL, $p > 0.05$) (Figure 4A,C).

To validate the extent of the overall damage indicated by the PI staining, the sections were assessed after staining with hematoxylin and eosin (HE). Treatment with Equicel® and Tabotamp® showed a clearly destroyed cytoarchitecture with pycnotic cell nuclei in the DG (Figure S1). The damage not only included superficial cell layers but also reached deep. The neuronal injury was consistently present in the z-stacks across all OHSC sectional images for both Equicel® and Tabotamp®. With a distance between the optical sections

of 5 µm and about 10–12 cuts per OHSC, a local, trans-sectional damage of at least 60 µm depth into the neuronal tissue was found.

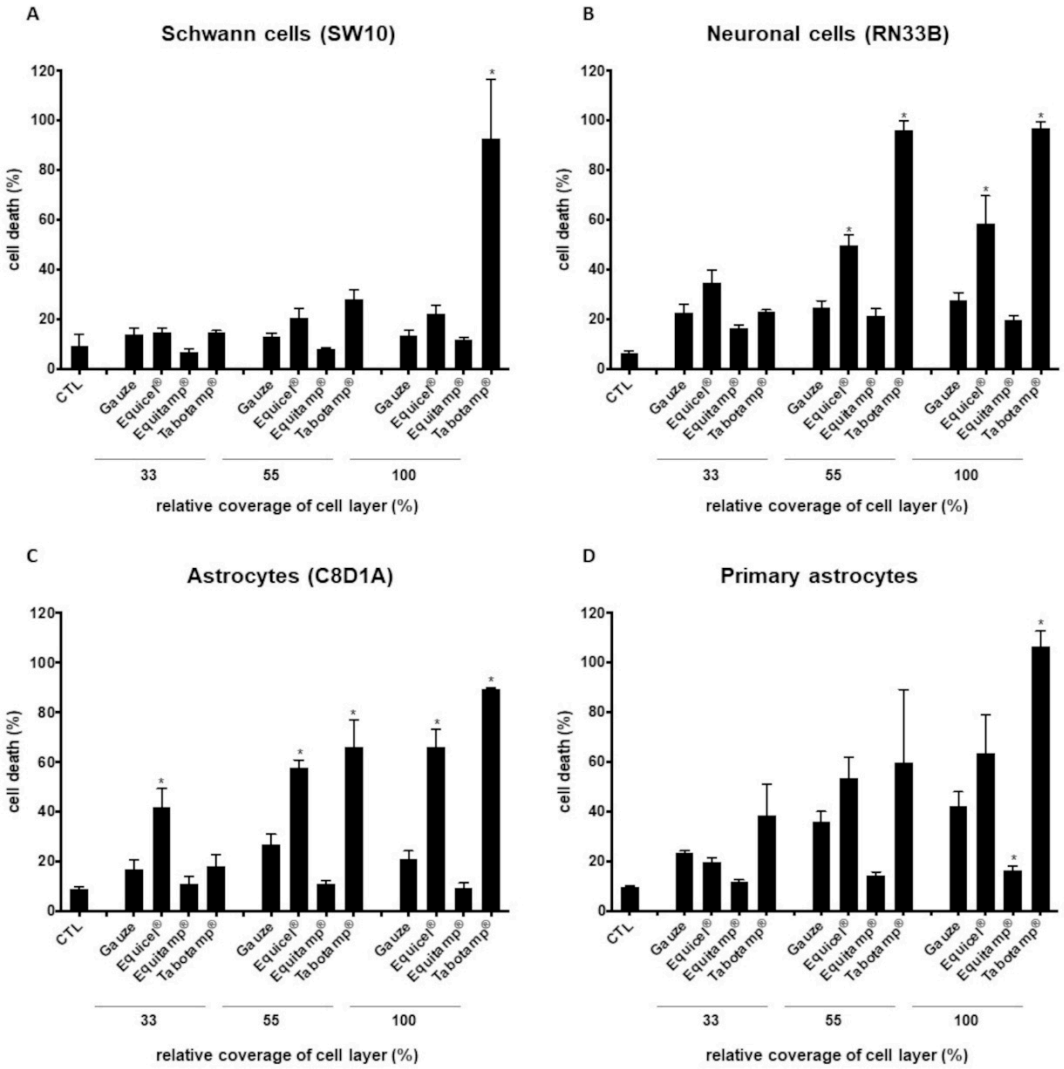

Figure 3. Detachment of cell monolayer after incubation with Equicel® and Equitamp®. Equicel® induced cell death of Schwann cells, neuronal cells and astrocytic cells. Quantification of cell death after 24 h using the CellTox Green assay. Schwann cells (SW10) (**A**), neuronal cells (RN33B) (**B**) and astrocytes (C8D1A and primary astrocytes) (**C**,**D**). ø 4 mm of non–oxidized cellulose (gauze), Equicel® or Equitamp® pieces correspond to 33% cell coverage, 5 mm pieces correspond to 55% cell coverage and 6 mm pieces correspond to 100% cell coverage. Signal of totally lysed cells of each cell type was set to 100% cell death. Cell culture medium without cells served as background control. Values are presented as means and SEM of four independent experiments. Statistical significance was analyzed with one-way ANOVA followed by Bonferroni's test. Significance was accepted with $p < 0.05$: * significant to same amount gauze treated cells. For multiple statistical comparison of all groups, see Table S1. For better comparability the published Tabotamp® cell death rates were included into the figures [10].

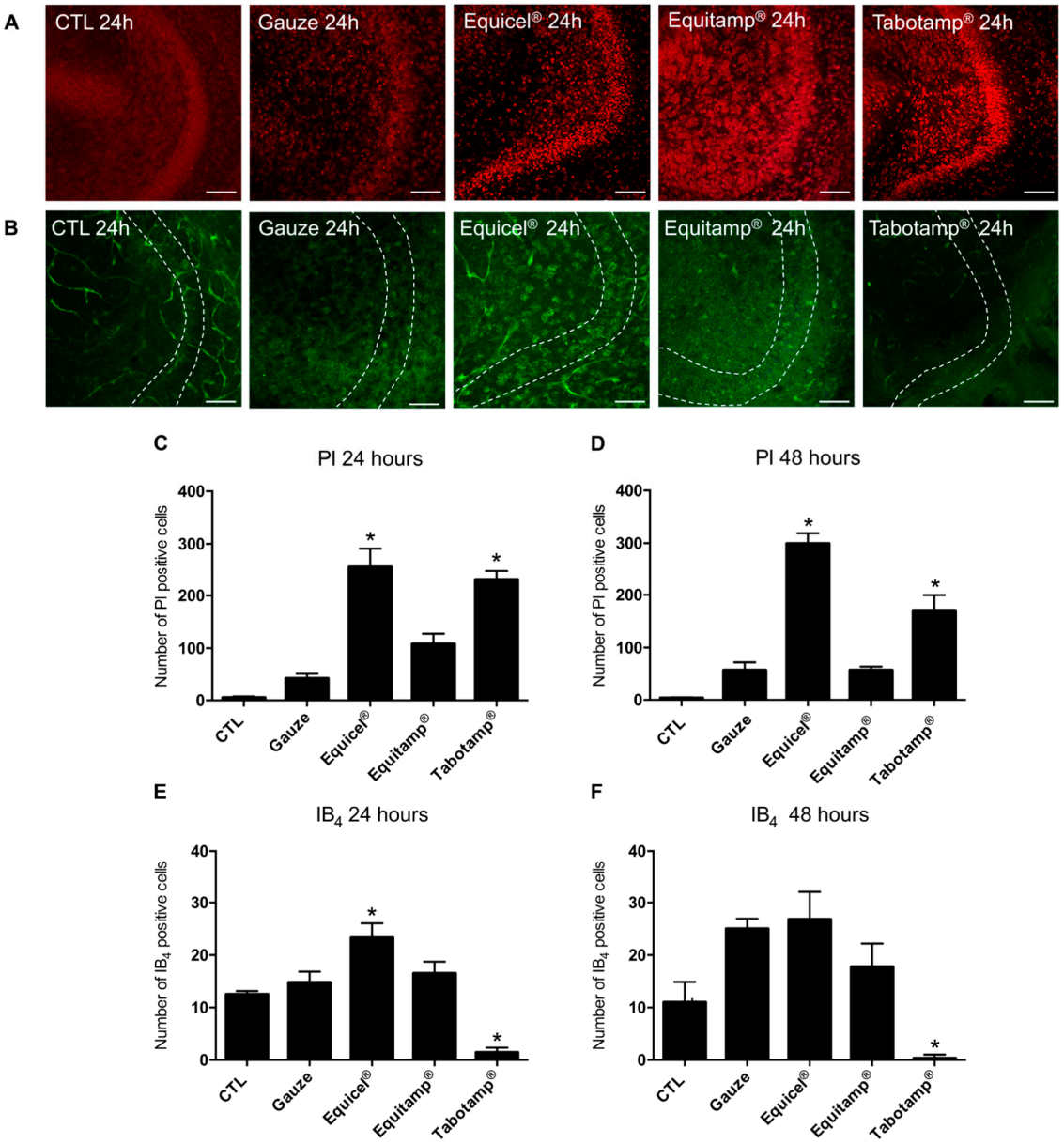

Figure 4. Effects of treatment with Equicel®, Equitamp® and Tabotamp® on cell viability and microglia activation in OHSC after 24 and 48 h. PI staining (red) of OHSC as recorded by confocal laser scanning microscopy representing dentate gyrus (DG) with granule cells (24 h results displayed) (**A**). Treatment with Equicel® and Tabotamp® led to intense red stained PI positive nuclei in DG regions. Equitamp® caused a mild accumulation of PI in the cells of the DG. IB_4 staining (green) of OHSC recorded by confocal laser scanning microscopy representing microglia cells and remaining vessels. In CTL, only isolated ramified microglia cells were visible. Treatment with Equicel® led to increase of amoeboid microglia cells in the DG. Dotted lines mark the borders of GCL (**B**). Quantitative analysis of the number of PI positive degenerating cells in GCL (**C**,**D**). Equicel® (* $p < 0.001$) and Tabotamp® (* $p < 0.01$) induced a significant increase of PI positive cells in GCL 24 h after treatment compared gauze (**C**). Similar results were obtained for Equicel® (* $p < 0.001$) and Tabotamp® (* $p < 0.01$) compared to the OHSC treated with gauze after 48 h (**D**). Quantitative analysis of the number of IB_4 positive microglia cells in GCL (**E**,**F**). After 24 h incubation with Equicel®, a significant increase in IB_4 positive microglia in the DG compared to the gauze was observed (*, $p < 0.05$). A clearly reduced number of IB_4 positive microglia was detected for Tabotamp® compared to gauze (* $p < 0.001$) (**E**). After 48 h no significant difference in IB_4 positive microglia cells between Equicel® and gauze was detectable (**F**). A general increase in the number of microglia was found in treated groups compared to the results after 24 h (CTL compared to gauze: * $p < 0.001$ after 48 h). For Tabotamp®, a significant reduction of microglia was present after 48 h compared to gauze (* $p < 0.001$). For a statistical comparison of all groups, see Table S2. Bar = 100 µm.

2.4. The Increased Cellular Damage of Equicel® and Tabotamp® Persisted after 48 h in OHSC

To investigate the extent of the damage over time, the number of PI positive cells was analyzed after 48 h. In case of the untreated control and after incubation with gauze, a well-preserved cytoarchitecture and a low number of PI positive cells (CTL: 3.4 PI positive cells/GCL, gauze: 57.6 PI positive cells/GCL) were detected (Figure 4D). Equicel® and Tabotamp® caused a rising number of PI positive cells compared to gauze (Equicel®: 299.4 PI positive cells/GCL, $p < 0.001$; Tabotamp®: 170.4 PI positive cells/GCL, $p < 0.01$) (Figure 4D). Equitamp® showed no significant change in PI positive cells after 48 h compared to gauze (Equitamp®: 57.3 PI positive cells/GCL, $p > 0.05$) (Figure 4D).

The number of PI positive cells showed a consistency of the damage compared to the results after 24 h ($p > 0.05$) (Figure 4C). The damage caused by Equicel® or Tabotamp® affected all sectional images of the z-stacks.

2.5. Equicel® Increased the Number of Isolectin B_4 Positive Microglia Cells after 24 h

To study ORC related reactions of microglia cells, the number of fluorescein isothiocyanate (FICT)-conjugated isolectin B_4 (IB_4) positive cells in the DG was quantified. In untreated controls, microglia cells were occasionally detected with typical ramified morphology after 24 h and 48 h (CTL 24 h: 12.5 IB_4 positive cells/GCL, CTL 48 h: 11.0 IB_4 positive cells/GCL) (Figure 4B,E,F). Treatment with gauze slightly increased the number of microglia over time (gauze 24 h: 14.8 IB_4 positive cells/GCL, gauze 48 h: 25.0 IB_4 positive cells/GCL) (Figure 4E,F). In contrast to 24 h, significantly more microglia cells were present in the gauze group than in controls after 48 h ($p < 0.001$). Equicel® induced a significant increase in the number of microglia cells compared to gauze after 24 h (Equicel® 24 h: 23.3 IB_4 positive cells/GCL, $p < 0.05$) (Figure 4E). No significant difference between Equicel® and gauze was found after 48 h (Equicel® 48 h: 26.8 IB_4 positive cells/GCL, $p > 0.05$) (Figure 4F). Comparable to PI results, there was no significant difference for Equitamp® treatment after 24 or 48 h. In contrast to all other results, a significant reduced number of microglia cells was measured in the Tabotamp® group (Tabotamp® 24 h: 1.4 IB_4 positive cells/GCL, $p < 0.001$; Tabotamp 48 h: 0.3 IB_4 positive cells/GCL, $p < 0.001$) (Figure 4B,E,F).

2.6. Tabotamp® Interfered with Immunofluorescence Staining

Limited to the areas covered with Tabotamp®, OHSC showed an almost complete depletion of IB_4 fluorescence signals. Inside the non-covered neuronal tissue, a clear accumulation of microglia cells was observed (Figure 5). Additional immunofluorescence staining against Iba1, an established marker for microglia cells, and further markers like NeuN and GFAP (Figure S2) showed no immunoreaction in all regions beneath Tabotamp® covered areas. These results strongly supported a methodical bias related to Tabotamp®.

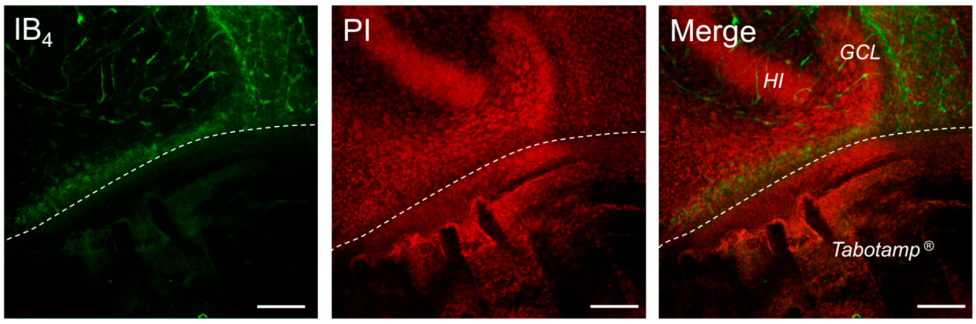

Figure 5. Exemplary image of an OHSC after half-side Tabotamp® treatment. Damaged neuronal cells were stained with PI (red) and microglia cells as well as vascular structures with IB_4 (green). The Tabotamp® covered area was clearly distinguished (below the dotted line) from the granule cell layer (GCL) of the DG and hilus region (HI), which was still well preserved above. Notably, a clearly reduced number of IB_4 positive cells is visible, while at the border a distinct increase of microglia cells could be observed. Bar = 100 µm.

3. Discussion

ORC has been frequently used in neurosurgery since the 1960s, especially to stop oozing in the brain resection cavity. In clinical practice, the walls of the resection cavities are typically covered with ORC to prevent rebleeding. Whereas Equicel® should be left in place after stopping the bleeding, removal of Equitamp® and Tabotamp® are recommended. Detachment of hemostats in intracerebral surgery strongly increases the risk of rebleeding. Therefore, in neurosurgery ORC often remain in place. However, little is known about the local effects of various ORC on neuronal tissue. Recently, we demonstrated on several monolayer cell culture systems that Tabotamp® causes a strong and local cytotoxic effect and induces a strong pH drop [10].

Our here presented results show that ORC are strongly diverse in their properties and have different effects on the cells or the tissue in their vicinity. Whereas Equitamp® and Tabotamp® were almost completely dissolved after 48 h, Equicel® swelled to a gelatine-like clot. This swelling might generate mechanical force, lead to compression and damage neuronal tissue. Even the formation of so-called textilomas was described after application of ORC during neurosurgical procedures [11–13]. Notably, these induced foreign body reactions in the brain can mimic recurrent intracranial tumors on MRI scans [14]. Histologically, these mass lesions were composed of not absorbed hemostat surrounded by inflammatory cellular infiltration [12]. Of the ORC investigated in this study, Equicel® appeared to more likely induce a foreign body reaction due to its slower dissolution, collagen content and microglia activation in OHSC. Some of ORC reduced the pH of solutions, depending on the chemical composition and oxidation grade [15]. The bactericide and hemostatic properties of Tabotamp® were associated with the strong pH reduction [3,7–9]. Equicel® and Equitamp® were proven bactericidal against gram positive and negative organisms (manufacturer's specification). Notably and despite bactericidal effects, comparable strong pH reduction was not achieved by Equitamp®, and Equicel® did not change the pH at all. Therefore, the bactericidal mode should be questioned for Equitamp® and Equicel® or parameters other than pH might be involved in bactericidal effects of these ORC.

Previously, we showed for Tabotamp® a local detachment of all tested cell types paralleled by a dose dependent increase of cytotoxicity [10]. Equitamp® and Equicel® also caused cell detachment albeit at a lower level indicating a decrease not only in pH value, but also in mechanical properties or other surface properties affect cell death. Cell death rates of Schwann cells increased only slightly after incubation with Equicel®, whereas astrocytes displayed a dose dependent enhancement of cell death rates. In contrast to the aforementioned results on Equicel®, incubation with Equitamp® decreased cell death in all analyzed cells compared to gauze. The data hints to a pH and material dependent variable cellular response and asks for a specific use of ORC under diverse clinical situations. Depending on the localization, neuronal damage caused by ORC had far-reaching clinical consequences [16–19]. As a further step of analysis, tissue cultures such as OHSC are suitable models for studying tissue-damaging processes and neuron glia interactions [20]. Therefore, the influence of Tabotamp®, Equitamp® and Equicel® application was analyzed on cell death, microglia activation and tissue structure alterations. With PI staining [21] the damage of neuronal cells was followed in the GCL after treatment with Tabotamp® and Equicel® 24 and 48 h post application. Former publications reported on neuronal damage by oxidized cellulose-mediated acidity [10,22]. In contrast to these findings and in our study, the pH value remained stable even with large quantities of Equicel®. Probably, swelling to a gelatinous mass might be an additional reason for causing neuronal damage. This property has already been described for Tabotamp® [19]. Here, the cellular damage was not only confined to the superficial cell layers but also visible in deeper layers of OHSC. However, it should be considered that tissue processing e.g., fixation or slice covering etc. might lead to a reduction of the OHSC height and therefore no reliable statement about the damage depth can be made. In contrast to Tabotamp® and Equicel®, the cellular damage was less pronounced after incubation with gauze and Equitamp®. These results from OHSC underline the importance of adaptation of the ORC to the specific properties of

different products by clinicians. Further examinations will be needed to evaluate whether the targeted use after gross total resection of gliomas has an influence on the development of a local recurrence. As mentioned before, so-called textilomas have been described after application of ORC. They showed a tissue reaction with accompanying phagocytic involvement and could have a damaging effect on neuronal structures [12,14,23–25]. Therefore, analysis of microglia reaction might be a useful parameter in context of ORC mediated neuronal injury [26,27]. In comparison to the other tested materials, Equicel® led to significant increase of microglia cells after 24 h. For Equicel®, the manufacturer declares the addition of collagen and fibrin. These additives might affect the mechanical properties, and the rapid and massive swelling of the material might be a trigger for the microglia response. In case of gauze and Equicel®, the number of microglia cells grew until 48 h putatively because of the direct interaction between the material and microglia cells. However, no significant difference was observed after Equitamp® treatment when compared to application of gauze after either 24 or 48 h. In contrast to the substantial neuronal damage observed after incubation with Tabotamp®, significantly lower numbers of microglia cells were measured. Nevertheless, a clear accumulation of microglia cells was visible at the border between the Tabotamp® covered area and the non-covered area. Therefore, we asked whether a depletion of microglia cells due to the reduced pH value or other unknown mechanisms might explain this unusual phenomenon. Since no signal was detected using the additionally analyzed microglial, astroglial and neuronal markers, we concluded that Tabotamp®-specific factors like strong local pH drop might interfere with binding epitopes, making them more difficult or even impossible to access for lectins or antibodies. Therefore, results for Tabotamp® must be viewed with caution regarding the number of microglia cells.

4. Materials and Methods

All animal experiments were performed in accordance with the Policy on Ethics and the Policy on the Use by the directive 2010/63/EU of the European Parliament and of the Council of the European Union. The preparations were approved by the local authorities for care and use of laboratory animals (permission numbers: K11M1 and I11M27).

4.1. Cellulose Samples

Non-oxidized cellulose (cotton gauze, Fink & Walter GmbH, Merchweiler, Germany) and oxidized regenerated cellulose (ORC) samples (Equicel® and Equitamp®, Equimedical BV, Zwaneburg, Netherlands; Tabotamp®, Johnson & Johnson Medical, Ethicon, Neuchâtel, Switzerland) were stamped into the specified sizes using sterile punches (Stiefel, GSK Consumer Healthcare, Dungarvan, Ireland).

4.2. Analysis of Cellulose Samples in Aqueous Solution

The 22 mm diameter samples (gauze, Equicel®, Equitamp®, Tabotamp®) were placed on cell culture dishes (60 cm^2, TPP, Trasadingen, Switzerland) with 10 mL Dulbecco's Modified Eagle's Medium (DMEM, Thermo Fisher Scientific, Waltham, MA, USA) completed with 10% fetal calf serum (FCS, Gibco, Thermo Fisher Scientific), 2 mmol/L glutamine (Biochrom AG, Merck, Darmstadt, Germany), 100 U/mL penicillin and 100 µg/mL streptomycin (Thermo Fisher Scientific). After taking pictures, the dishes were incubated for 48 h at 37 °C and imaged again. The same composition of cell culture medium was used for cultivation of the cells, for pH measurements and for cell death analyses. Then, the dishes were incubated for 48 h at 37 °C.

4.3. pH Measurement

The pH measurement with increasing amounts of the different ORC was carried out in culture medium containing 44 mmol/L sodium bicarbonate with the FiveGo pH meter (Mettler Toledo, Schwerzenbach, Switzerland) at room temperature.

4.4. Cell Lines

The immortalized cells C8D1A (CRL-254, Astrocytes), RN33B (CRL-2825, Neurons) and SW10 (CRL-2766, Schwann cells) were purchased from the American Type Culture Collection (Manassas, VA, USA). SW10 and C8D1A cells were cultured in supplemented DMEM at 75 cm^2 cell culture flasks (Sarstedt, Nümbrecht, Germany) under humidified atmosphere with 5% CO_2 at 37 °C. RN33B cells were cultured in DMEM/F12 (1:1, Thermo Fisher Scientific) with identical supplements and conditions. The passage number of all analyzed cells was below 20.

4.5. Primary Cultures

Primary astrocytic cultures were prepared from p0-2 Wistar rat brains as described before [28]. Wistar neonates were purchased from the central animal facility of the medical faculty of the Martin Luther University Halle-Wittenberg.

4.6. Crystal Violet Staining

SW10, RN33B, C8D1A cells or primary astrocytes were incubated in culture medium for 24 h with non-oxidized cotton gauze or ORC samples. Subsequently, cell culture dishes were washed with phosphate-buffered saline (PBS, Thermo Fisher Scientific), fixed with methanol and stained with 0.5% (*w*/*v*) Crystal violet (Merck), as described recently [10]. Dishes were scanned at 600 dpi and the covered area analyzed to determine the percentage of detached cells using ImageJ/Fiji software (NIH, Bethesda, MD, USA). The ORC-covered area was set to 100%.

4.7. Cytotoxicity Measurement

The 1×10^4 SW10, RN33B, C8D1A cells or primary astrocytes were seeded in triplicates in black 96 well cell culture plates (Greiner Bio-One, Frickenhausen, Germany). After 24 h, different areas of cellulose samples (gauze, Equicel® or Equitamp®; 0, 33, 55 or 100% coverage of cell layer) and the fluorescence marked DNA-binding dye CellTox-Green (1:1000, Promega, Mannheim, Germany), diluted in 200 µL culture medium were added. The fluorescence signals were measured at $485_{Ex}/535_{Em}$ with Tecan Reader (F200PRO, Tecan, Männedorf, Switzerland) after 24 h, and the relative cell death was calculated as described previously [10]. The fluorescence signals of the completely lysed untreated cells (lysis buffer, Promega) were set to 100%.

4.8. Organotypic Hippocampal Slice Cultures (OHSC)

OHSC were prepared under aseptic conditions from p8-9 Wistar rats as reported earlier [20,29] and kept in a fully humidified atmosphere with 5% (*v*/*v*) CO_2 at 35 °C. Culture medium was replaced every second day. After six days of incubation, the slices were divided into five different treatment groups (Figure 6). OHSC were covered by 4 mm diameter pieces of Equicel®, Equitamp®, Tabotamp® and gauze as a control or left uncovered as negative control (Figure 1A,B, CTL). Fixation was performed after 24 or 48 h. For all groups the culture medium was changed before starting the experiments and kept until fixation.

4.9. Confocal Laser Scanning Microscopy (CLSM) and Analysis of PI, NeuN, GFAP and IB_4 Positive Cells

Degenerated neurons were stained with 5 µg/mL of PI (Merck) 2 h before fixation. Afterwards, the OHSC were washed in PBS/Triton and incubated in normal goat serum (Sigma-Aldrich, Merck) diluted 1:20 in phosphate buffer (PB, 0.2 mol/L). Microglia cells were stained with IB_4 (Vector Laboratories, Burlingame, CA, USA) diluted 1:50 in PBS/Triton. To validate the IB_4 results some slices were labelled with ionized calcium binding adaptor molecule 1 antibody (Iba1, Polyclonal rabbit IgG; Thermo Fisher Scientific) diluted 1:200 in PBS/Triton and 0.5% bovine serum albumin (BSA, Sigma-Aldrich, Merck, St. Louis, MO, USA) followed by incubation with an Alexa 488 goat anti-rabbit antibody

(Thermo Fisher Scientific). To investigate the effects of Tabotamp® on immunofluorescence, neuronal cells were labelled with the neuronal marker (NeuN, Merck) and astrocytic cells with glial fibrillary acid protein (GFAP, BD Biosciences, CA, USA) and visualized by an Alexa 633 goat anti-mouse antibody. After staining, the slices were washed with PBS/Triton and cover slipped with fluorescent mounting medium (DAKO, Hamburg, Germany). The imaging of the OHSC was performed using a confocal laser scanning microscope (DMi8; Leica Microsystems, Wetzlar, Germany) with an excitation wavelength of 488 nm for IB_4 and Iba1 and an emission bandpass filter of 505 to 530 nm for IB_4 and 505 to 560 nm for Iba1, an excitation wavelength of 543 nm and an emission bandpass filter of 585 to 615 nm for PI and an excitation wavelength of 633 nm and an emission long pass filter of 650 nm for GFAP and NeuN. The images were taken using a z-scan with a section distance of 5 µm. Using Diamidine-2-phenylindol dihydrochloride (DAPI, Sigma-Aldrich) staining, the total mesh depth was displayed and thus the limits for the z-stack were determined. On average, 10–11 optical sections were obtained from one OHSC. For PI and IB_4 analyses, only the three middle sections of an OHSC were evaluated at 200-fold magnification with a resolution of 1024 × 1024 pixels. The number of PI and IB_4 positive cells in the DG was analyzed with MATLAB (MathWorks, Natick, MA, USA).

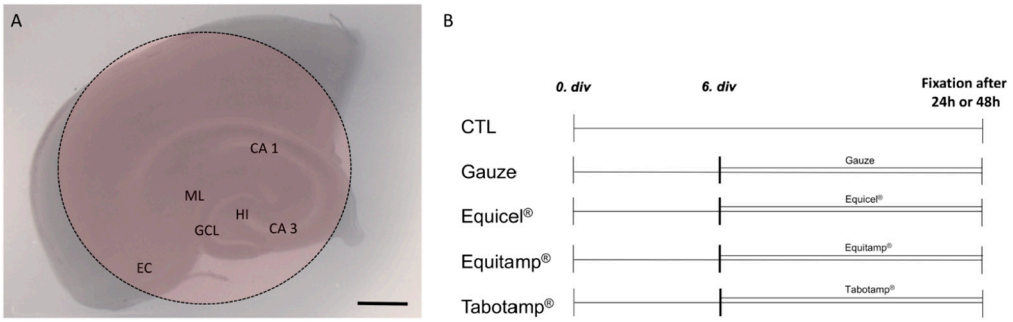

Figure 6. Schematic representation of an OHSC with ORC and treatment protocol. Schematic visualization of OHSC in culture. Intact cytoarchitecture of the OHSC is demonstrated with the entorhinal cortex (EC), the hippocampus with cornu ammonis (CA) subfields CA 1 and CA 3, the hilus re-gion (HI) and the dentate gyrus with the molecular layer (ML) and the granule cell layer (GCL). The red area indicates the location of the ORC (**A**). Treatment protocol of the OHSC (**B**). Bar = 1 mm.

4.10. Bright-Field Microscopy

Cellular damage and cytoarchitecture were qualitatively validated by hematoxylin labelling (Roth, Karlsruhe, Germany). OHSC were washed with PBS/Triton and stained with hematoxylin, dehydrated and placed on a coverslip with Entellan (Merck). Specimens were analyzed with NanoZoomer-SQ (Hamamatsu, Iwata City, Japan).

4.11. Statistical Analysis

Statistical analysis was performed with Prism 6 (GraphPad Software, San Diego, CA, USA) or SPSS software (version 25.0, IBM, Ehningen, Germany). The one-way ANOVA was used followed by Bonferroni's test for multiple comparisons between the groups. The data are presented as mean and SEM. $p < 0.05$ was considered statistically significant. All analyses were carried out after at least three independent experiments.

5. Conclusions

The frequent clinical application of ORC as a heterogeneous group should consider their dramatically different impact on local pH values, dissolution time, as well as their cytotoxic properties. Equicel® and Tabotamp® led to a pronounced cellular damage of OHSC, whereas Equitamp® causes the lowest cellular damage and cell death rate. The fast-rising number of microglia cells after incubation with Equicel® indicates an early immune response. Overall, our data support a specific use of ORC in distinct clinical settings

depending on its different properties. For better understanding of clinical implications of ORC further clinical studies are needed to verify and compare their complications especially in eloquent areas.

Supplementary Materials: The following are available online at https://www.mdpi.com/article/10.3390/ijms222111467/s1.

Author Contributions: Conceptualization, S.L., C.S. (Christian Strauss), S.S. and F.D.; methodology, J.K., C.G. and S.L.; software, J.K., S.L. and T.H.; investigation, J.K., C.G. and S.L.; resources, C.S. (Christian Strauss), J.P. and F.D.; data curation, J.K. and S.L.; writing—original draft preparation, J.K., S.L., S.S. and F.D.; writing—review and editing, all authors; visualization, J.K. and S.L.; supervision, S.L., T.H. and F.D.; project administration, C.S. (Christian Strauss), C.S. (Christian Scheller), S.S. and F.D. All authors have read and agreed to the published version of the manuscript.

Funding: This research received no external funding.

Institutional Review Board Statement: All animal experiments were performed in accordance with the Policy on Ethics and the Policy on the Use by the directive 2010/63/EU of the European Parliament and of the Council of the European Union. The preparations were approved by the local authorities for care and use of laboratory animals (permission numbers: K11M1 and I11M27).

Informed Consent Statement: Not applicable.

Data Availability Statement: Data is contained within the article and Supplementary Material (Tables S1 and S2).

Acknowledgments: We would like to thank Justine Werner for her excellent technical assistance.

Conflicts of Interest: The authors declare no conflict of interest.

References

1. Gerlach, R.; Krause, M.; Seifert, V.; Goerlinger, K. Hemostatic and hemorrhagic problems in neurosurgical patients. *Acta Neurochir.* **2009**, *151*, 873–900. [CrossRef] [PubMed]
2. Keshavarzi, S.; MacDougall, M.; Lulic, D.; Kasasbeh, A.; Levy, M. Clinical experience with the surgicel family of absorbable hemostats (oxidized regenerated cellulose) in neurosurgical applications: A review. *Wounds* **2013**, *25*, 160–167.
3. Másová, L.; Rysavá, J.; Krízová, P.; Suttnar, J.; Salaj, P.; Dyr, J.E.; Homola, J.; Dostálek, J.; Myska, K.; Pecka, M. Hemostyptic effect of oxidized cellulose on blood platelets. *Sb. Lek.* **2003**, *104*, 231–236.
4. Hutchinson, R.W.; George, K.; Johns, D.; Craven, L.; Zhang, G.; Shnoda, P. Hemostatic efficacy and tissue reaction of oxidized regenerated cellulose hemostats. *Cellulose* **2013**, *20*, 537–545. [CrossRef]
5. Miller, J.M.; Jackson, D.A.; Collier, C.S. An investigation of the chemical reactions of oxidized regenerated cellulose. *Exp. Med. Surg.* **1961**, *19*, 196–201. [PubMed]
6. Lewis, K.M.; Spazierer, D.; Urban, M.D.; Lin, L.; Redl, H.; Goppelt, A. Comparison of regenerated and non-regenerated oxidized cellulose hemostatic agents. *Eur. Surg.* **2013**, *45*, 213–220. [CrossRef]
7. Spangler, D.; Rothenburger, S.; Nguyen, K.; Jampani, H.; Weiss, S.; Bhende, S. In vitro antimicrobial activity of oxidized regenerated cellulose against antibiotic-resistant microorganisms. *Surg. Infect.* **2003**, *4*, 255–262. [CrossRef] [PubMed]
8. Achauer, B.M.; Black, K.S.; Grosmark, D.M.; Hayamizu, T.F. A comparison of hemostatic agents in microvascular surgery. *J. Microsurg.* **1982**, *3*, 242–247. [CrossRef]
9. Schonauer, C.; Tessitore, E.; Barbagallo, G.; Albanese, V.; Moraci, A. The use of local agents: Bone wax, gelatin, collagen, oxidized cellulose. *Eur. Spine J.* **2004**, *13* (Suppl. S1), S89–S96. [CrossRef] [PubMed]
10. Leisz, S.; Trutschel, M.L.; Mäder, K.; Scheller, C.; Strauss, C.; Simmermacher, S. Tabotamp®, Respectively, Surgicel®, Increases the Cell Death of Neuronal and Glial Cells In Vitro. *Materials* **2020**, *13*, 2453. [CrossRef]
11. Jaramillo-Jiménez, E.; Gupta, M.; Snipes, G.; Cheek, B.S.; Michael, C.B.; Navarro-Montoya, A.M.; Gómez-Escobar, T.; Jiménez-Villegas, J.; Rodríguez-Márquez, I.; Melguizo-Gavilanes, I. Textiloma Mimicking a Recurrent High-Grade Astrocytoma: A Case Report. *J. Neurol. Surg. Rep.* **2020**, *81*, e7–e9. [CrossRef]
12. Ribalta, T.; McCutcheon, I.E.; Neto, A.G.; Gupta, D.; Kumar, A.J.; Biddle, D.A.; Langford, L.A.; Bruner, J.M.; Leeds, N.E.; Fuller, G.N. Textiloma (gossypiboma) mimicking recurrent intracranial tumor. *Arch. Pathol. Lab. Med.* **2004**, *128*, 749–758. [CrossRef]
13. Lin, B.; Yang, H.; Cui, M.; Li, Y.; Yu, J. Surgicel application in intracranial hemorrhage surgery contributed to giant-cell granuloma in a patient with hypertension: Case report and review of the literature. *World J. Surg. Oncol.* **2014**, *12*, 101. [CrossRef] [PubMed]
14. Kothbauer, K.F.; Jallo, G.I.; Siffert, J.; Jimenez, E.; Allen, J.C.; Epstein, F.J. Foreign body reaction to hemostatic materials mimicking recurrent brain tumor. Report of three cases. *J. Neurosurg.* **2001**, *95*, 503–506. [CrossRef]
15. Coseri, S.; Biliuta, G.; Simionescu, B.C.; Stana-Kleinschek, K.; Ribitsch, V.; Harabagiu, V. Oxidized cellulose–survey of the most recent achievements. *Carbohydr. Polym.* **2013**, *93*, 207–215. [CrossRef]

16. Menovsky, T.; Plazier, M.; Rasschaert, R.; Maas, A.I.; Parizel, P.M.; Verbeke, S. Massive swelling of Surgicel® Fibrillar™ hemostat after spinal surgery. Case report and a review of the literature. *Minim. Invasive Neurosurg.* **2011**, *54*, 257–259. [CrossRef] [PubMed]
17. Boeris, D.; Evins, A.I.; Lanotte, M.M.; Zeme, S.; Ducati, A. Pontine compression caused by "surgiceloma" after trigeminal decompression: Case report and literature review. *Acta Neurol. Belg.* **2014**, *114*, 229–231. [CrossRef] [PubMed]
18. Awwad, E.E.; Smith, K.R., Jr. MRI of marked dural sac compression by surgicel in the immediately postoperative period after uncomplicated lumbar laminectomy. *J. Comput. Assist. Tomogr.* **1999**, *23*, 969–975. [CrossRef]
19. Brodbelt, A.R.; Miles, J.B.; Foy, P.M.; Broome, J.C. Intraspinal oxidised cellulose (Surgicel) causing delayed paraplegia after thoracotomy—A report of three cases. *Ann. R Coll. Surg. Engl.* **2002**, *84*, 97–99. [PubMed]
20. Grabiec, U.; Hohmann, T.; Hammer, N.; Dehghani, F. Organotypic Hippocampal Slice Cultures as a Model to Study Neuroprotection and Invasiveness of Tumor Cells. *J. Vis. Exp.* **2017**, *27*, e55359. [CrossRef]
21. Ebrahimi, F.; Hezel, M.; Koch, M.; Ghadban, C.; Korf, H.W.; Dehghani, F. Analyses of neuronal damage in excitotoxically lesioned organotypic hippocampal slice cultures. *Ann. Anat.* **2010**, *192*, 199–204. [CrossRef] [PubMed]
22. Nagamatsu, M.; Podratz, J.; Windebank, A.J.; Low, P.A. Acidity is involved in the development of neuropathy caused by oxidized cellulose. *J. Neurol. Sci.* **1997**, *146*, 97–102. [CrossRef]
23. Menovsky, T.; Bosshart, S.L.; Lukes, A. Surgicel for microvascular decompression of the trigeminal nerve. *Acta Neurol. Belg.* **2015**, *115*, 831–832. [CrossRef] [PubMed]
24. Sandhu, G.S.; Elexpuru-Camiruaga, J.A.; Buckley, S. Oxidized cellulose (Surgicel) granulomata mimicking tumour recurrence. *Br. J. Neurosurg.* **1996**, *10*, 617–619. [CrossRef] [PubMed]
25. Oto, A.; Remer, E.M.; O'Malley, C.M.; Tkach, J.A.; Gill, I.S. MR characteristics of oxidized cellulose (Surgicel). *AJR Am. J. Roentgenol.* **1999**, *172*, 1481–1484. [CrossRef] [PubMed]
26. Dimitrijevich, S.D.; Tatarko, M.; Gracy, R.W.; Wise, G.E.; Oakford, L.X.; Linsky, C.B.; Kamp, L. In vivo degradation of oxidized, regenerated cellulose. *Carbohydr. Res.* **1990**, *198*, 331–341. [CrossRef]
27. Pierce, A.; Wilson, D.; Wiebkin, O. Surgicel: Macrophage processing of the fibrous component. *Int. J. Oral Maxillofac. Surg.* **1987**, *16*, 338–345. [CrossRef]
28. Dehghani, F.; Conrad, A.; Kohl, A.; Korf, H.W.; Hailer, N.P. Clodronate inhibits the secretion of proinflammatory cytokines and NO by isolated microglial cells and reduces the number of proliferating glial cells in excitotoxically injured organotypic hippocampal slice cultures. *Exp. Neurol.* **2004**, *189*, 241–251. [CrossRef]
29. Grabiec, U.; Koch, M.; Kallendrusch, S.; Kraft, R.; Hill, K.; Merkwitz, C.; Ghadban, C.; Lutz, B.; Straiker, A.; Dehghani, F. The endocannabinoid N-arachidonoyldopamine (NADA) exerts neuroprotective effects after excitotoxic neuronal damage via cannabinoid receptor 1 (CB(1)). *Neuropharmacology* **2012**, *62*, 1797–1807. [CrossRef] [PubMed]

frontiers | Frontiers in Aging Neuroscience

ORIGINAL RESEARCH
published: 29 April 2022
doi: 10.3389/fnagi.2022.863598

Microglia-Dependent and Independent Brain Cytoprotective Effects of Mycophenolate Mofetil During Neuronal Damage

Joshua Kleine[1†], Urszula Hohmann[1†], Tim Hohmann[1], Chalid Ghadban[1], Miriam Schmidt[1], Sebastian Laabs[1], Beat Alessandri[2] and Faramarz Dehghani[1]*

[1] Department of Anatomy and Cell Biology, Medical Faculty, Martin-Luther-University Halle-Wittenberg, Halle (Saale), Germany, [2] Institute for Neurosurgical Pathophysiology, University Medical Center, Johannes Gutenberg University, Mainz, Germany

OPEN ACCESS

Edited by:
Alberto Javier Ramos, Consejo Nacional de Investigaciones Científicas y Técnicas (CONICET), Argentina

Reviewed by:
Angeliki Maria Nikolakopoulou, University of Southern California, United States
Johannes Boltze, University of Warwick, United Kingdom

***Correspondence:**
Faramarz Dehghani
faramarz.dehghani@medizin.uni-halle.de

[†] These authors have contributed equally to this work

Specialty section:
This article was submitted to Neuroinflammation and Neuropathy, a section of the journal Frontiers in Aging Neuroscience

Received: 27 January 2022
Accepted: 11 April 2022
Published: 29 April 2022

Citation:
Kleine J, Hohmann U, Hohmann T, Ghadban C, Schmidt M, Laabs S, Alessandri B and Dehghani F (2022) Microglia-Dependent and Independent Brain Cytoprotective Effects of Mycophenolate Mofetil During Neuronal Damage. Front. Aging Neurosci. 14:863598. doi: 10.3389/fnagi.2022.863598

Acute lesions of the central nervous system often lead to permanent limiting deficits. In addition to the initial primary damage, accompanying neuroinflammation is responsible for progression of damage. Mycophenolate mofetil (MMF) as a selective inhibitor of inosine 5-monophosphate dehydrogenase (IMPDH) was shown to modulate the inflammatory response and promote neuronal survival when applied in specific time windows after neuronal injury. The application of brain cytoprotective therapeutics early after neuronal damage is a fundamental requirement for a successful immunomodulation approach. This study was designed to evaluate whether MMF can still mediate brain cytoprotection when applied in predefined short time intervals following CNS injury. Furthermore, the role of microglia and changes in IMPDH2 protein expression were assessed. Organotypic hippocampal slice cultures (OHSC) were used as an *in vitro* model and excitotoxically lesioned with *N*-methyl-aspartate (NMDA). Clodronate (Clo) was used to deplete microglia and analyze MMF mediated microglia independent effects. The temporal expression of IMPDH2 was studied in primary glial cell cultures treated with lipopolysaccharide (LPS). In excitotoxically lesioned OHSC a significant brain cytoprotective effect was observed between 8 and 36 h but not within 8 and 24 h after the NMDA damage. MMF mediated effects were mainly microglia dependent at 24, 36, 48 h after injury. However, further targets like astrocytes seem to be involved in protective effects 72 h post-injury. IMPDH2 expression was detected in primary microglia and astrocyte cell cultures. Our data indicate that MMF treatment in OHSC should still be started no later than 8–12 h after injury and should continue at least until 36 h post-injury. Microglia seem to be an essential mediator of the observed brain cytoprotective effects. However, a microglia-independent effect was also found, indicating involvement of astrocytes.

Keywords: microglia, astrocytes, OHSC, neuroinflammation, IMPDH2, mycophenolate mofetil (MMF), brain cytoprotection

INTRODUCTION

Acute events like cerebral ischemia or traumatic brain injury (TBI) represent a major challenge in the acute clinical treatment, since lesions of the central nervous system (CNS) are often irreversible and cause severe impairments (Carandang et al., 2006; Maas et al., 2008). In turn, the irreversible primary damage leads to an activation of cellular and biochemical cascades that harm already vulnerable neurons in the perilesional area, inducing and increasing the initial damage (Dirnagl et al., 1999; Jassam et al., 2017). The resulting secondary damage is target of current therapies and the starting point for new treatment approaches (Hailer, 2008; Chamorro et al., 2016; Nogueira et al., 2018). The progression of secondary damage is characterized by the inflammatory response, which sets the level of further specific immunological reactions (Chamorro et al., 2012; Jassam et al., 2017). At cellular level, cell-cell interactions determine the responses between microglia, neurons, astrocytes, endothelial cells, and infiltrated peripheral immune cells (Nedergaard and Dirnagl, 2005; Ahmad et al., 2013; Burda and Sofroniew, 2014). In addition, different soluble factors such as cytokines, chemokines, and reactive oxygen species seem to play an essential role in secondary damage (Hailer, 2008; Dirnagl and Endres, 2014). The reduction of inflammation and secretion of proinflammatory factors by immunosuppressive agents is believed to be an effective strategy. Mycophenolate mofetil (MMF) was first used for immunosuppression after kidney transplantations (Allison et al., 1993). After administration, MMF is rapidly hydrolyzed to its active form of mycophenolic acid (Lee et al., 1990) and inhibits both isoforms of inosine 5-monophosphate dehydrogenase (IMPDH), the rate limiting enzyme in the *de novo* synthesis of guanosine nucleotides. MMF therefore counts as a noncompetitive and reversible inhibitor with a 5-fold higher affinity to IMPDH2 than the type 1 isoform. Whereas IMPDH2 was induced predominantly in activated leukocytes and organotypic hippocampal slice cultures (OHSC), the type 1 isoform was constitutively expressed in most cell types (Allison and Eugui, 2000; Gu et al., 2003; Ebrahimi et al., 2012). MMF application resulted in specific inhibition of proliferating leukocytes *via* IMPDH2 (Jonsson and Carlsten, 2002). In astrocytes and microglia, MMF inhibited the proliferation and reduced the release of inflammatory cytokines like IL 1ß, TNF α, and NO (Miljkovic et al., 2002; Dehghani et al., 2010). In accordance, treatment with MMF in excitotoxically damaged OHSC showed a brain cytoprotective effect in addition to a reduction in glia proliferation (Dehghani et al., 2003; Ebrahimi et al., 2012) and increased survival of long range axonal projections (Oest et al., 2006). Direct effects on neuronal cells were not described since MMF failed to affect neuronal survival in NMDA damaged primary neuronal cell cultures (Dehghani et al., 2010). Thus, MMF probably affects the glial cells directly or rather the interactions between glial cells and neurons. Interestingly, MMF mediated effects showed a temporal pattern since MMF was protective after lesion in a specific time window of 12–36 h in OHSC and significantly reduced the extent of neuronal damage when administered continuously in the first 12 h after injury (Ebrahimi et al., 2012). MMF mediated brain cytoprotection was abolished when the treatment was started later, between 24 and 48 h (Ebrahimi et al., 2012).

In accordance to the Stroke Therapy Academic Industry Roundtable (STAIR) recommendations, the evaluation of brain cytoprotection took place in different time scales for MMF treatment in OHSC (Lyden et al., 2021). Furthermore, microglia independent effects were investigated and the expression dynamics of IMPDH2 in primary microglia and astrocytes after lipopolysaccharide (LPS) stimulation analyzed.

MATERIALS AND METHODS

Ethics Statement

All animal experiments were performed in accordance with the Policy on Ethics and the Policy on the Use of Animals in Neuroscience Research as indicated in the directive 2010/63/EU of the European Parliament and of the Council of the European Union on the protection of animals used for scientific purposes and were approved by the local authorities for care and use of laboratory animals (State of Saxony-Anhalt, Germany, permission number: I11M18, date: 01.12.2012).

Organotypic Hippocampal Slice Cultures

Organotypic hippocampal slice cultures were prepared under aseptic conditions from 8 to 9 days old Wistar rats as described before (Grabiec et al., 2017). Briefly, the frontal pole and the cerebellum were removed and the brains were placed in preparation medium, consisting of minimum essential medium (Invitrogen) and 1% (w/v) L-glutamine (Invitrogen), at 4°C and pH 7.35. Brains were sliced horizontally into 350 μm thick sections (Vibratome VT 1200 S; Leica Microsystem, Wetzlar, Germany). Approximately six to eight OHSC were obtained from each brain. After preparation, slices were transferred into culture inserts (Sarstedt, Nümbrecht, Germany) and incubated with 1 ml of culture medium. The medium consisted of 50 ml minimum essential medium (Invitrogen), 25 ml Hank's balanced salt solution (HBSS, Thermo Fisher), 25 ml heat inactivated horse serum (Invitrogen), 2 ml L-glutamine (Invitrogen), 1 μg/ml insulin (Boehringer, Mannheim, Germany), 1.2 mg/ml glucose (Merck Millipore), 0.1 mg/ml streptomycin and penicillin and 0.8 μg/ml vitamin C (Sigma) at pH 7.4. OHSC were incubated for 6 days at 35°C with 5% CO_2 and the culture medium was changed every second day.

After 6 days OHSC treatment with 50 μM N-methyl-D-aspartate (NMDA, Merck) was performed for 4 h. The OHSC (**Figure 1**) were randomly assigned to the different treatment groups and treated according to the respective protocols. Microglia were depleted from OHSC using the bisphosphonate clodronate (Clo, Bonefos®, Bayer Vital GmbH, Leverkusen, Germany). Sections were incubated with 100 μg/ml Clo in the respective treatment groups for 6 days starting directly after preparation. At the end of experiments the sections were rinsed with 0.1 M phosphate buffer (PB) and then fixed with 4% (w/v) paraformaldehyde (PFA, AppliChem, Darmstadt, Germany) and stored at 4°C.

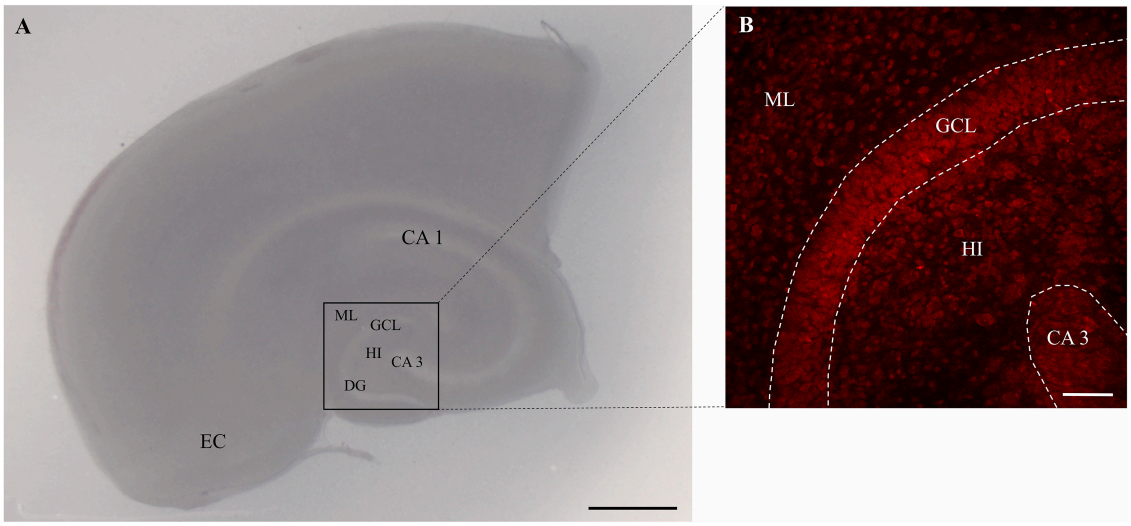

FIGURE 1 | Image of rat OHSC. **(A)** OHSC in culture with intact cytoarchitecture. The entorhinal cortex (EC), cornu ammonis (CA) subfields CA 1 and CA 3, the hilus region (HI) and the dentate gyrus (DG) with the molecular layer (ML) and the granule cell layer (GCL) are highlighted. Scale bar = 1 mm. Panel **(B)** represents the region of interest in the OHSC. The morphology is visualized by the use of PI staining (red). The dotted areas show the GCL and the CA3 regions. Scale bar = 50 μm.

Control

Control OHSC (n = 34) were treated with culture medium only till fixation (**Figures 2A**, **3A**, **4A**).

N-Methyl-Aspartate

On day 6 OHSC (n = 35) were lesioned with NMDA (50 μM; Sigma Aldrich) for 4 h and were further incubated with culture medium until the time of fixation (**Figures 2A**, **3A**, **4A**). The same treatment was done for all NMDA damaged groups.

Mycophenolate Mofetil Time Window

Different concentrations of MMF were tested before (Dehghani et al., 2003; Ebrahimi et al., 2012). To analyze the brain cytoprotective time window, damaged OHSC were treated with MMF (100 μg/ml) at different time intervals. MMF was applied between 8–24 h (n = 12), 8–36 h (n = 43), and 12–36 h (n = 6) after starting with NMDA treatment (**Figure 2A**).

Clodronate

Microglia depleted OHSC were supplied with culture medium. Fixation was performed after 24 h (n = 3), 36 h (n = 5), 48 h (n = 3), and 72 h (n = 4) (**Figures 3A**, **4A**). The same treatment was conducted with 100 μg/ml Clo for all Clo treated groups.

Continuous Mycophenolate Mofetil Treatment in *N*-Methyl-Aspartate Lesioned Organotypic Hippocampal Slice Cultures

Treatment with MMF (100 μg/ml) to NMDA damaged OHSC was performed on day 6. Fixation was carried out after 24 h (n = 11), 36 h (n = 14), 48 h (n = 6), and 72 h (n = 7) (**Figures 3A**, **4A**).

N-Methyl-Aspartate Mediated Damage in Microglia Depleted Organotypic Hippocampal Slice Cultures

Fixation was performed after 24 h (n = 12), 36 h (n = 16), 48 h (n = 12) and 72 h (n = 16) after NMDA damage (**Figures 3A**, **4A**).

Continuous Treatment With Mycophenolate Mofetil in *N*-Methyl-Aspartate Damaged Microglia Depleted Organotypic Hippocampal Slice Cultures

N-methyl-aspartate treatment was followed by application of MMF (100 μg/ml). Fixation was performed after 24 h (n = 40), 36 h (n = 39), 48 h (n = 38), and 72 h (n = 19) (**Figures 3A**, **4A**).

Primary Cell Cultures

Primary microglia and astrocytes were isolated from cerebral cortices of neonatal wild type rats as described before (Dehghani et al., 2003). Briefly, brains were treated with 0.5 mg/ml DNAse (Worthington, Bedford, MA, United States) and 4 mg/ml trypsin (Merck Millipore, Burlington, MA, United States) in Hank's balanced salt solution (Invitrogen). Primary cells were cultured in DMEM (Invitrogen) with 10% (w/v) FBS (Invitrogen) and 1 ml streptomycin/penicillin (Invitrogen) as described before (Grabiec et al., 2012). Microglia or astrocytes were seeded into 6 well plates (250,000 cells/well) and incubated in DMEM (Invitrogen) with 2% (w/v) fetal bovine serum for 24 h prior to treatment. Depending on the group, the cells were treated with lipopolysaccharide (LPS, 10 ng/ml, Sigma Aldrich, Deisenhofen, Germany) or left untreated (CTL).

Western Blot Analyses

For western blot analyses cells were collected 0, 6, 8, 12, 16, and 24 h after treatment, respectively. The cells were taken up in lysis buffer and stored at −80°C as described before (Grabiec et al., 2019). Protein concentrations were determined using the method of Bradford (Pierce™ BCA Protein Assay

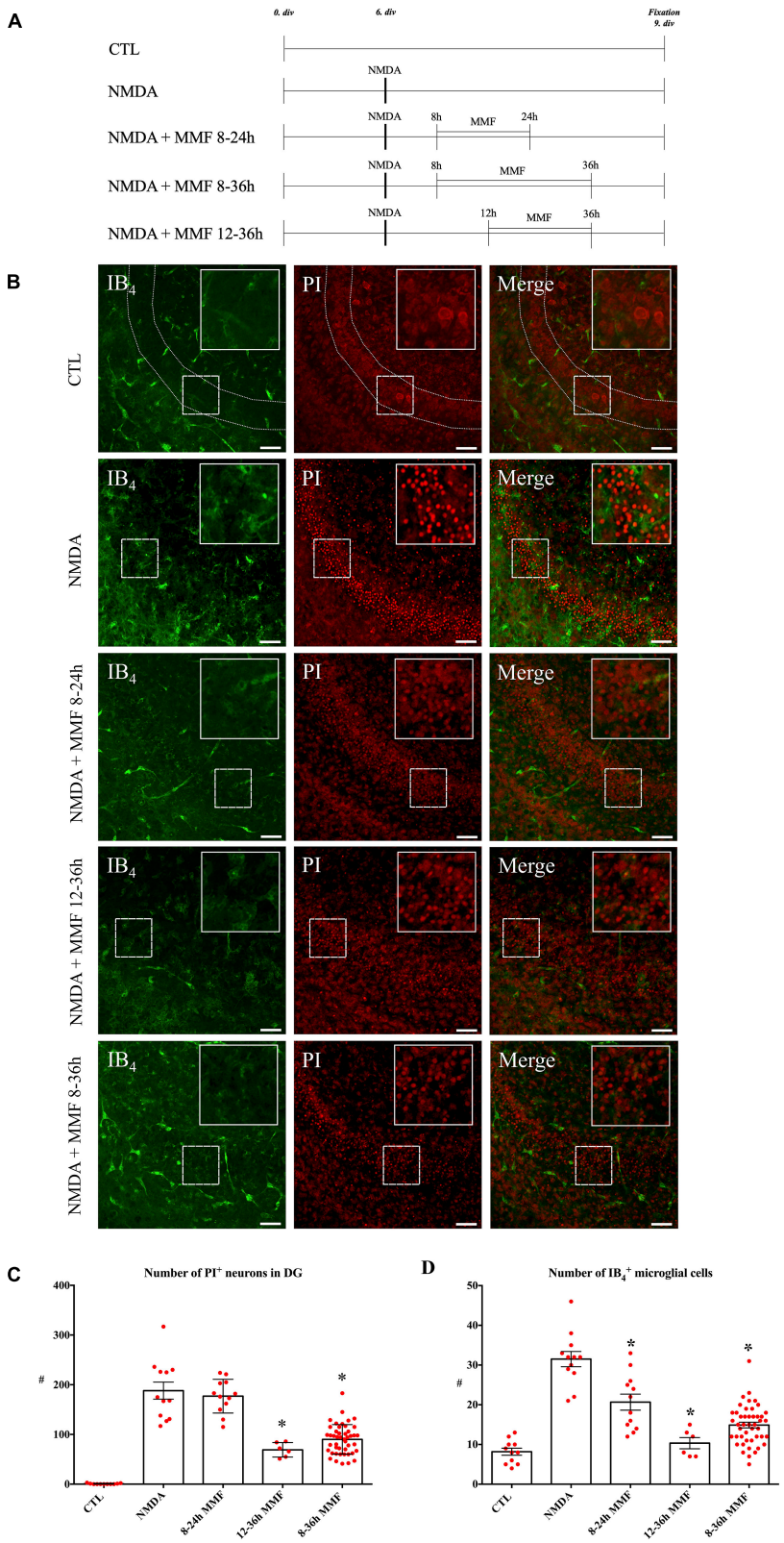

FIGURE 2 | Effects of MMF application in a specific time window in NMDA damaged OHSC fixed at 9 div. **(A)** Treatment protocol. **(B)** CLSM images stained with PI (degenerating neurons, red) and IB_4 (microglial and vessels, green) in overview and in higher magnification of the labeled area. Control (CTL, $n = 5$) OHSC showed a

(Continued)

FIGURE 2 | well preservation of the hippocampal formation with almost no PI positive pyknotic nuclei and only a few ramified IB_4 positive microglia. OHSC treated with NMDA (n = 13) (50 μM) for 4 h had massive accumulation of PI positive degenerating neurons and amoeboid IB_4 positive microglia. Treatment with MMF (100 μg/ml) in defined time windows resulted in a reduction of PI positive neurons between 12 and 36 h (n = 6) and 8 and 36 h (n = 43) but not between 8 and 24 h (n = 12) after NMDA damage. In all time windows, there was a reduction in the number of microglia. Quantitative analyses of the mean numbers of panel **(C)** PI positive degenerating neurons (*$p < 0.05$ vs. NMDA) and **(D)** IB_4 positive microglia (*$p < 0.05$ vs. NMDA). The asterisk denotes significant results regarding the respective measurement indicated with the bar. The values are served as a mean with standard error of the mean. Scale bars = 50 μm.

Kit, Thermo Fisher Scientific, Barrington IL, United States) (Bradford, 1976) and 10 μg protein was loaded onto a 12.5% (w/v) sodium dodecyl sulfate–polyacrylamide gel. After gel electrophoresis, the proteins were blotted onto nitrocellulose membranes (Protran 0.45 μm, Amersham, Freiburg, Germany) and non-specific protein binding sites were blocked for 30 min with roti block solution (Carl Roth, Karlsruhe, Germany). The nitrocellulose membranes were incubated with the antibody against IMPDH2 (**Table 1**) [diluted 1:2000 in roti block solution containing 0.2% (v/v) Tween 20] until the next day at 4°C. After incubation with horseradish peroxidase conjugated antibodies (**Table 1**) the chemiluminescent (Luminata Forte, Merck) signal was detected with Fusion X (VWR, Radnor, PA, United States). For semi quantitative analysis, the relative signal intensities of the immunoreactive bands were determined and the IMPDH2 intensity was normalized to the ß-actin (**Table 1**) intensity. Fusion FX7 with FusionCapt Advance Solo software (VWR) was used for analysis.

Immunofluorescence, Microscopy, and Image Acquisition

To visualize neuronal cell death OHSC were stained with 5 μg/ml of propidium iodide (**Figure 1B**; PI, Merck) 2 h before fixation. Microglia were labeled with fluorescein isothiocyanate (FICT)-conjugated isolectin B_4 (IB_4, Vector Laboratories, Burlingame, CA, United States) diluted 1:50 in PBS/Triton for 24 h. Before staining, the OHSC were incubated in normal goat serum (NGS, Sigma Aldrich, 1:20) in PB (0.2 M) for 30 min. Thereafter the sections were washed with PBS/Triton and water before the OHSC were covered with the DAKO fluorescence medium (DAKO, Hamburg, Germany). The OHSC were imaged with a confocal laser scanning microscope (LSM 710 Meta, Carl Zeiss AG, Göttingen, Germany). PI was visualized with monochromatic light at 543 nm and an emission bandpass filter of 585–615 nm. IB_4 was detected with monochromatic light at 488 nm and an emission bandpass filter of 505 to 530 nm. The images were taken using a z-stack with a section distance of 2 μm. On average, 13–17 optical sections were obtained from each OHSC. For PI and IB_4 analyses, only the three middle sections of an OHSC were evaluated at 200-fold magnification with a resolution of 1024×1024 pixels. The number of PI and IB_4 positive cells was determined by the use of self-written script in MATLAB (MathWorks, Natick, MA, United States).

Statistical Analysis

Statistical analysis was performed with Prism 6 (GraphPad Software, San Diego, CA, United States). The analysis for the normal distribution was performed using D'Agnostino and Pearson and Shapiro–Wilk normality test. For statistical analysis, Mann Whitney test was performed as a non-parametric test. Further, the one-way ANOVA was used followed by Bonferroni's test for multiple comparisons between the groups which yielded identical results. The data were presented as mean and SEM. Differences were considered significant at $p \leq 0.05$. All experiments were carried out in at least three independent biological replicates.

RESULTS

Mycophenolate Mofetil Mediated Effects in Organotypic Hippocampal Slice Cultures Begin Within 8 h of Injury and Last Over 24 h

Control OHSC showed a well-preserved cytoarchitecture, and only very few PI positive cells were observed (**Figures 2A–C**, CTL: 0.64 PI positive cells/GCL). Microglia showed a ramified morphology and were located mostly in the molecular layer of the DG (**Figures 2B,D**, CTL: 8.18 IB_4 positive cells/GCL). NMDA treatment led to a massive accumulation of PI positive neurons in DG (**Figures 2B,C**, NMDA: 188.1 PI positive cells/GCL), and the number of IB_4 positive microglia increased significantly (**Figures 2B,D**, NMDA: 31.5 IB_4 positive cells/GCL).

When compared to the NMDA group, MMF treatment from 8 h to 24 h (NMDA + MMF 8–24 h: 177.0 PI positive cells/GCL) showed no significant reduction in the number of PI positive neurons (**Figures 2B,C**) but significantly reduced the number of microglia (**Figures 2B,D**, 22.9 IB_4 positive cells/GCL vs. NMDA, $p<0.01$). MMF treatment from 12–36 h (NMDA + MMF 12–36 h: 69.0 PI positive cells/GCL vs. NMDA, $p < 0.001$) post-injury showed a significant reduction of PI positive neurons (**Figures 2B,C**) and microglia (**Figures 2B,D**, 11.5 IB_4 positive cells/GCL vs. NMDA $p < 0.0001$). Similarly, MMF application in the time-window of 8–36 h (NMDA + MMF 8–36 h: 90.1 PI positive cells/GCL vs. NMDA, $p < 0.0001$) significantly reduced the number of PI positive cells (**Figures 2B,C**) and microglia when compared to the NMDA group (**Figures 2B,D**, NMDA + MMF 8–36 h: 14.9 IB_4 positive cells/GCL vs. NMDA, $p < 0.001$). There was no significant difference in the number of PI positive neurons or IB_4 positive microglia between the time windows 8–36 h and 12–36 h (**Figures 2C,D**, $p > 0.05$).

Consistent Microglia Dependent Brain Cytoprotective Effects of Mycophenolate Mofetil at 24, 36, 48, and 72 h After Injury

To study the temporal development of the brain cytoprotective effect of MMF, the extent of the damage and the number of

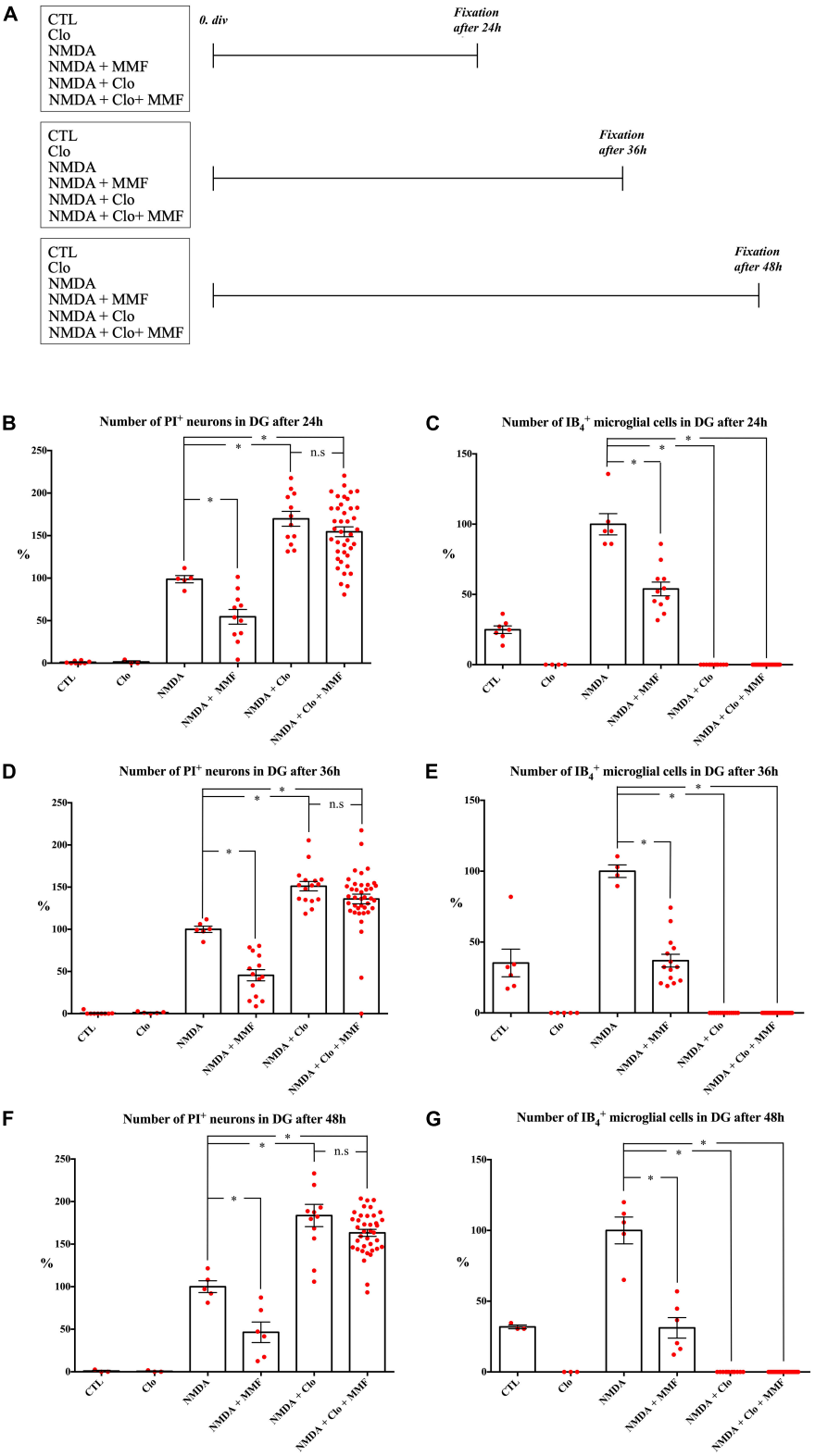

FIGURE 3 | Effects of continuous treatment with MMF for OHSC fixed at 24, 36, and 48 h after injury with and without (Clo) microglia. **(A)** Treatment protocol. The slices were fixed 24, 36, or 48 h after NMDA damage. Quantitative analysis of PI positive degenerating neurons after **(B)** 24 h, **(D)** 36 h, and **(F)** 48 h and microglia after **(C)** 24 h, **(E)** 36 h, and **(G)** 48 h. The asterisk denotes significant results regarding the respective measurement indicated with the bar (*$p < 0.05$ vs. NMDA, n.s. $p > 0.05$ vs. NMDA + Clo). The values are served as a mean with standard error of the mean.

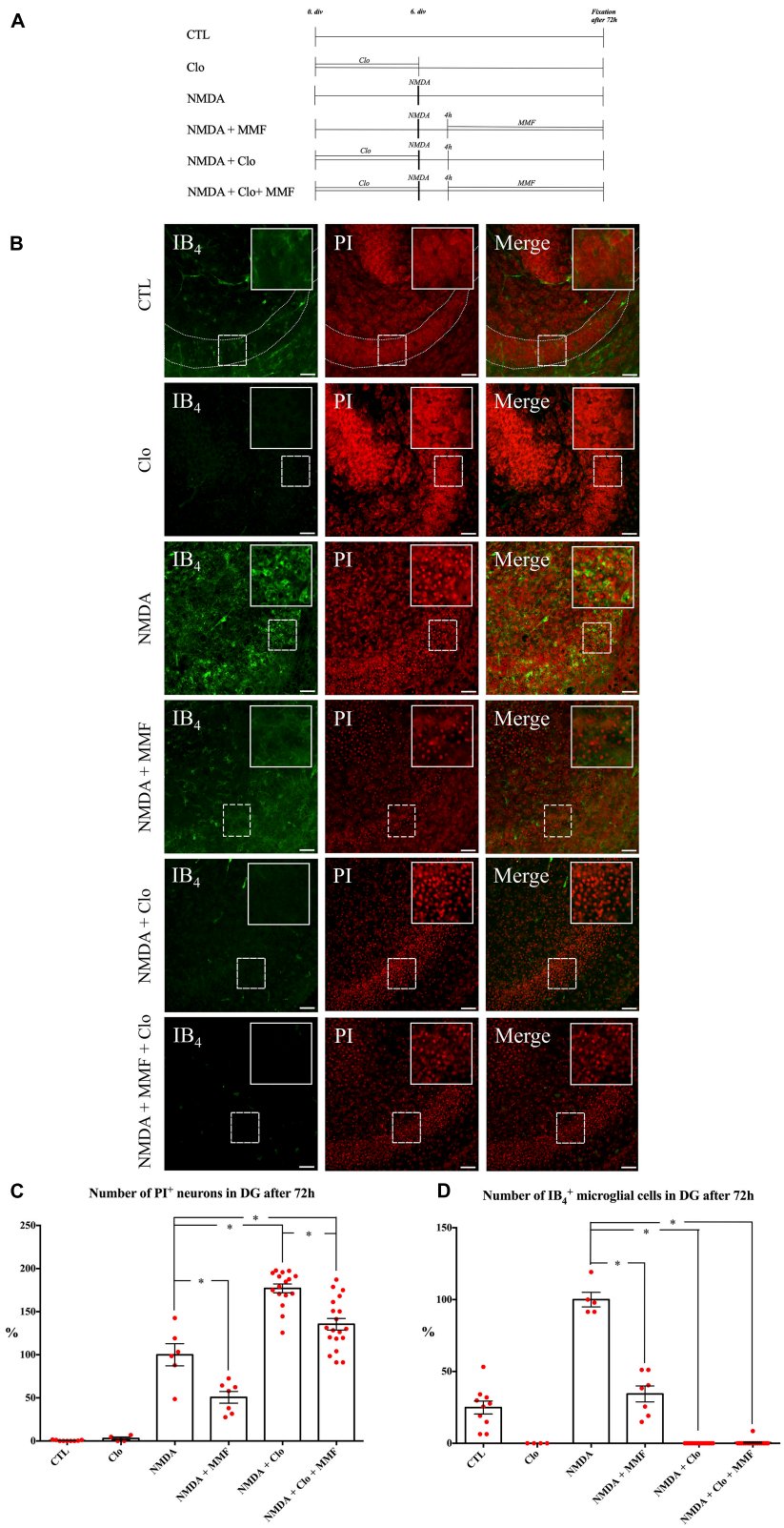

FIGURE 4 | Effects of continuous MMF treatment for OHSC fixed at 72 h after injury with and without microglia **(A)** Treatment protocol. **(B)** CLSM images stained with PI (degenerating neurons, red) and IB_4 (microglial cells vascular vessels, green) in overview and in higher magnification of the labeled area. In comparison to

(Continued)

FIGURE 4 | control (CTL, $n = 9$), treatment with NMDA for 4 h (NMDA, $n = 6$) led increase in number of PI positive degenerating neurons. Treatment with MMF (NMDA + MMF, $n = 7$) in a period between 4 and 72 h after the injury resulted in a reduction of PI positive degenerated neurons. Incubation with 100 μg/ml Clo for 6 days resulted in successful depletion of microglia from OHSC in the respective groups (Clo, $n = 4$; NMDA + Clo, $n = 16$; NMDA + Clo + MMF, $n = 19$). Additional application of MMF in this period led to reduction of PI positive degenerated neurons in microglia depleted OHSC (NMDA + Clo + MMF). Depletion of microglia led to an increase in number of damaged cells (NMDA + Clo, NMDA + Clo + MMF). Quantitative analyses of the mean numbers of panel **(C)** PI positive degenerating neurons (*$p < 0.05$ vs. NMDA or NMDA + Clo) and **(D)** IB_4 positive microglia (*$p < 0.05$ vs. NMDA). The asterisk denotes significant results regarding the respective measurement indicated with the bar. The values are served as a mean with standard error of the mean. Scale bars = 50 μm.

TABLE 1 | Antibodies: western blot analysis.

Name	Company	Number	Dilution	Antibody ID
IMPDH 2	Proteintech Group, Rosemont, IL, United States	12948-1-AP	1:2000	
Goat anti-rabbit IgG, HRP conjugated	Vector Laboratories	PI-1000	1:20000	AB_2336198
Horse anti-mouse IgG, HRP conjugated	Vector Laboratories	PI-2000	1:10000	AB_2336177
ß-actin	Cell Signaling, Boston, United States	3700	1:5000	AB_2242334

microglia were analyzed at different fixation times (**Figures 3**, **4**), namely after 24 h (**Figures 3A–C**), 36 h (**Figures 3A,D,E**), 48 h (**Figures 3A,F,G**), and 72 h (**Figures 4B–D**). Across the different time points, all OHSC controls (CTL) showed a well-preserved cytoarchitecture in DG with only a few isolated PI positive cells and indifferent ramified morphology of the microglia (**Figure 4**, **Supplementary Figures 1–3**, and **Table 2**). After injury with NMDA, a significant accumulation of PI positive neurons in DG, particularly after 24, 36, 48, and 72 h, was observed in all NMDA treated groups (**Figures 3B,D,F**, **4C** and **Table 2**). Additionally, a significant increase in the number of IB_4 positive microglia was observed at all time points, with a peak after 36 h (**Figures 3C,E,G**, **4D**, NMDA, **Supplementary Figure 4**, and **Table 2**). Treatment with MMF (NMDA + MMF) after 24 h showed a significant reduction in degenerated PI positive neuronal cells/GCL, that remained stable after 36, 48, and 72 h (**Figures 3**, **4**, **Supplementary Figures 1–3**, and **Table 2**). The number of IB_4 positive microglia was also significantly reduced at all time points (**Figures 3**, **4**, NMDA + MMF and **Table 2**). Although 24 h after MMF treatment, the number of microglia was slightly higher than in the OHSC controls (**Supplementary Figure 4**). Already after 36 h as well as at the subsequent time points, an adaptation to the control level in the number of microglia was observed (**Figures 3C,E,G**, **4B,D**, **Supplementary Figure 4**, NMDA + MMF, and **Table 2**). In an analogous manner, there were already fewer amoeboid microglia, partially also with ramified morphology, after 24 h consistently over the further time points (**Supplementary Figures 1–3**). There was a significant strong correlation between the number of PI and IB_4 positive cells (correlation coefficient 219 = 0.631 [0.485, 0.743], **Supplementary Figure 5**).

Mycophenolate Mofetil Showed Microglia-Independent Brain Cytoprotective Effects

In addition, the effects of MMF were assessed at the same time points after depletion of microglia by clodronate (Clo). Treatment with Clo only led to analogous results on PI positive cells as obtained for CTL across all time points. Additionally, a complete reduction was observed in the number of microglia (**Figures 3C,E,G**, **4B,D**, **Supplementary Figures 1–3**, and **Table 2**). Treatment with NMDA in OHSC after microglia depletion led to a significant increase in neuronal damage (**Table 2**) that strongly exceeded the injury as observed in the presence of microglia. This observation was consistent for all analyzed time points (**Figures 3**, **4** and **Table 2**). Thereby, the maximum was already reached after 24 h (**Figures 3B,C**, **Supplementary Figure 4**, and **Table 2**). After additional treatment with MMF, no significant differences were found in comparison to the NMDA + Clo group after 24 h (**Figure 3C**), 36 h (**Figure 3E**), and 48 h (**Figure 3G**). However, 72 h after the injury a significant reduced number of PI positive degenerated neurons was detected in the DG (**Figures 4B,C** and **Table 2**).

Inosine 5-Monophosphate Dehydrogenase 2 Expression in Primary Microglia and Astrocytes

The expression of IMPDH2 was investigated in primary microglia (**Figure 5A**) or astrocyte (**Figure 5B**) cell cultures at different time points. IMPDH2 was detected with a single band at 56 kDa after 6, 8, 12, and 24 h (**Supplementary Figure 6**). In relation to ß-actin, no changes were observed after stimulation with LPS for all examined time points in microglia and astrocytes ($p > 0.05$, **Figures 5A,B**). Furthermore, a LPS independent increase in IMPDH2 expression was evident in the primary microglia cell cultures after approximately 12 h (**Figure 5A**) and in the primary astrocyte cultures after 16 and 24 h (**Figure 5B**).

DISCUSSION

Acute damage to the CNS, such as TBI or stroke, often leads to permanent limiting deficits (Carandang et al., 2006; Feigin et al., 2014). Whereas primary damage is the result of acute and usually immediate injury, secondary damage progresses over hours and days and is a consequence of various complex processes, including excitotoxicity, overproduction of free radicals, and inflammation (Leker et al., 2002; Werner and Engelhard, 2007). During secondary damage, microglia and astrocytes act as important cellular players and contribute to

TABLE 2 | Brain cytoprotective effects of continuous MMF treatment at different points in time with or without depletion of microglia.

Treatment	n	Standard deviation PI	PI no. (%)	Mean Diff. % (95% CI)†, ‡. *,**	Standard deviation IB_4	IB_4 no. (%)	Mean Diff. % (95% CI)†,*,**
24 h							
CTL	8	1.42	3.6 (1.1)	$p = 0.0016$* 98.9 (50.98–144.30)†	7.15	13.6 (24.9)	$p = 0.0012$* 75.0 (63.30–86.77)†
Clo	3	2.42	4.0 (1.4)	$p = 0.0357$* 98.6 (37.56–157.10)†	0.0	0.0 (0.0)	$p = 0.0095$* 100 (86.31–113.54)†
NMDA	5	9.57	286.2 (100)		18.57	44.2 (100)	
NMDA + MMF	11	28.72	160.7 (54.5)	$p = 0.0087$* 45.5 (0.39–88.05)†	16.15	23.8 (53.9)	$p = 0.0004$* 46.9 (35.33–56.73)†
NMDA + Clo	12	30.13	485.8 (169.8)	$p = 0.0003$* 69.8 (27.76–114.30)†	0.0	0.0 (0.0)	$p < 0.0001$* 100 (89.38–110.47)†
NMDA + Clo + MMF	40	36.27	442.2 (154.5)	$p = 0.0008$* 54.5 (17.23–94.32)† 15.2 (−7.91 to 38.39)‡ $p = 0.2167$**	0.0	0.0 (0.0)	$p < 0.0001$* 100 (90.68–109.17)† $p > 0.9999$**
36 h							
CTL	9	1.736	3.2 (0.7)	$p = 0.0002$* 99.3 (60.76–138.00)†	23.87	18.5 (35.2)	$p = 0.0095$* 64.8 (48.77–80.76)†
Clo	5	1.066	5.0 (1.3)	$p = 0.0043$* 98.7 (54.38–143.10)†	0.0	0.0 (0.0)	$p = 0.0079$* 100 (83.38–116.62)†
NMDA	6	9.088	286.1 (100)		8.87	52.5 (100)	
NMDA + MMF	14	24.72	130.1 (45.5)	$p < 0.0001$* 54.5 (18.77–90.26)†	16.85	19.4 (36.9)	$p = 0.0007$* 63.13 (49.08–77.18)†
NMDA + Clo	16	22.14	432.5 (151.1)	$p < 0.0001$* 51.1 (16.07–89.19)†	0.0	0.0 (0.0)	$p = 0.0002$* 100 (86.15–113.85)†
NMDA + Clo + MMF	39	35.66	399.2 (135.9)	$p = 0.0002$* 35.9 (3.80–68.04)† 15.2 (−4.09 to 34.51)‡ $p = 0.0892$**	0.0	0.0 (0.0)	$p < 0.0001$* 100 (86.98–113.02)† $p > 0.9999$**
48 h							
CTL	3	1.841	2.0 (1.3)	$p = 0.0357$* 98.7 (32.9–164.47)†	2.35	16 (32.5)	$p = 0.0357$* 67.5 (50.62–84.33)†
Clo	3	1.228	5.4 (0.9)	$p = 0.0357$* 99.1 (33.36–164.91)†	0.0	0.0 (0.0)	$p = 0.0357$* 100 (83.14–116.86)†
NMDA	5	15.45	230.4 (100)		21.19	49.2 (100)	
NMDA + MMF	6	29.52	107.0 (46.5)	$p = 0.0087$* 53.56 (5.95–101.16)†	17.75	15.3 (31.2)	$p = 0.0043$* 68.84 (56.63–81.03)†
NMDA + Clo	12	45.18	423.1 (183.6)	$p = 0.0023$* 83.6 (41.78–125.48)†	0.0	0.0 (0.0)	$p = 0.0002$* 100 (89.28–110.72)†
NMDA + Clo + MMF	38	25.30	376.1 (163.3)	$p < 0.0001$* 63.3 (25.85–100.65)† 20.4 (−0.27 to 41.02)‡ $p = 0.0714$**	0.0	0.0 (0.0)	$p < 0.0001$* 100 (90.42–109.58)† $p > 0.9999$**
72 h							
CTL	9	0.6651	1.2 (0.5)	$p = 0.0004$* 99.5 (67.34–131.70)†	14.08	11.7 (24.9)	$p = 0.0007$* 75.1 (63.06–87.16)†
Clo	4	3.491	7.3 (2.9)	$p = 0.0095$* 97.1 (57.67–136.48)†	0.0	0.0 (0.0)	$p = 0.0079$* 100 (85.24–114.76)†
NMDA	6	31.56	246.8 (100)		11.36	47 (100)	
NMDA + MMF	7	17.86	125.0 (50.6)	$p = 0.014$* 49.4 (15.40–83.33)†	14.71	16.1 (34.3)	$p = 0.0025$* 65.7 (52.77–78.54)†
NMDA + Clo	16	20.51	436.9 (177.0)	$p < 0.0001$* 77.0 (47.78–106.23)†	0.0	0.0 (0.0)	$p < 0.0001$* 100 (88.64–111.36)†
NMDA + Clo + MMF	19	29.39	334.2 (135.4)	$p = 0.0258$* 35.4 (6.79–63.97)† 41.6 (23.85–59.38)‡ $p < 0.0001$**	1.95	0.0 (0.0)	$p < 0.0001$* 100 (88.493–110.61)† $p > 0.9999$**

Sample size, standard deviation, and mean values for all treatments.
**Mann-Whitney Test vs. NMDA.*
†One-way ANOVA vs. NMDA.
‡t-test vs. NMDA + Clo.
***Mann-Whitney Test vs. NMDA + Clo.*

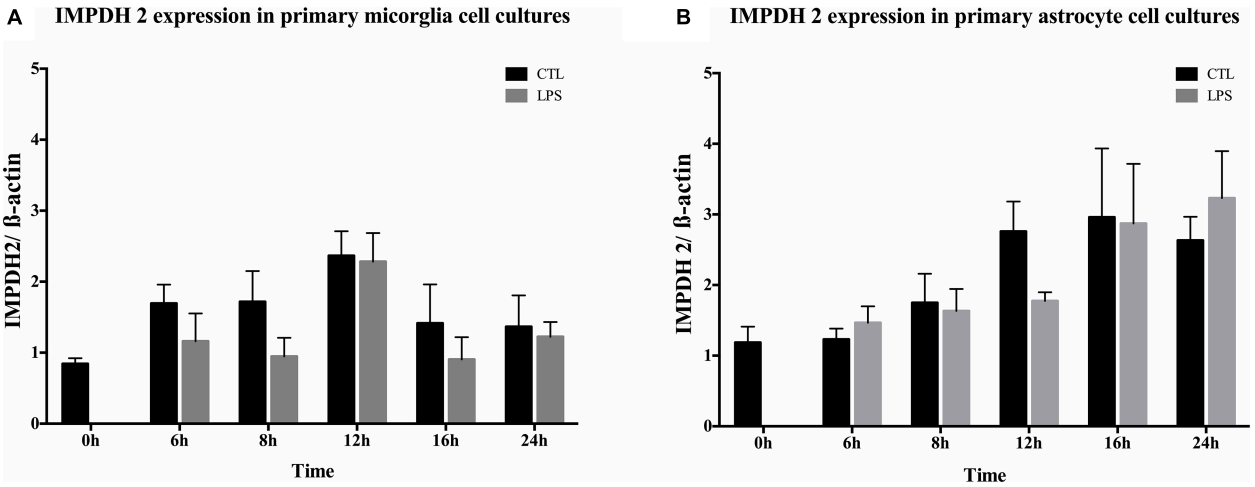

FIGURE 5 | Inosine 5-monophosphate dehydrogenase 2 (IMPDH2) expression in primary microglia and astrocytes. Quantitative analysis of IMPDH2 and ß-actin expression in primary microglia **(A)** and astrocytes **(B)** over time ($n = 3$). IMPDH2 was present at all times in both primary cell lines. Treatment of primary microglia and astrocytes with LPS (10 ng/ml) had no significant effect ($p > 0.05$) on the expression.

the neuroinflammatory response (Morshead and van der Kooy, 1990). However, depending on its severity, the inflammation might lead to further damage of already vulnerable neurons, but could also impact functions that are important for their survival (Dirnagl et al., 1999; Ebrahimi et al., 2010). A promising way for therapeutic intervention might be the blockade of defined intrinsic immunological actions after injury (Chamorro et al., 2016). Immunosuppression has nonetheless some disadvantages, like increased risk of infection (Husain and Singh, 2002). For this reason, it is crucial to limit the interventional time to minimize its side effects.

Modulation of Neuroinflammation as a Brain Cytoprotective Approach

Treatment with the immunosuppressant MMF, a competitive inhibitor of key enzyme in purine metabolism namely IMPDH2, was reported to significantly reduce the neuronal cell death after excitotoxic lesions in OHSC (Dehghani et al., 2003). OHSC represent an established model for intrinsic study of glia cells, neurons and their interactions without the influence of peripheral migrating immune cells or blood flow (Grabiec et al., 2017). A temporal relationship was previously described for MMF resulting in brain cytoprotective effects, saving further cell types and the structure in OHSC (Ebrahimi et al., 2012). A brain cytoprotective time window was found for MMF between 12 and 36 h after injury. However, due to negative effects of immunosuppression, the onset and necessary duration of MMF treatment needed to be further evaluated. Furthermore, it is assumed that the earlier an effective protection is started, the better the neuronal survival. This raised the question whether an earlier start and timely limited treatment may also be protective. Especially in the context of stroke, infections are a feared complication partly due to the so-called stroke-induced immunodepression (Klehmet et al., 2009; Hoffmann et al., 2017). Therefore, the application of therapeutics with immune interfering capabilities should occur as early as possible and for a limited period of time. In addition, new interventional procedures such as thrombectomy led to ever wider clinical therapeutic time windows beyond the 6 h for initiation of therapeutic measures (Nogueira et al., 2018). Therefore, the establishment of temporally appropriate brain cytoprotective approaches is becoming increasingly important.

Recent studies involving immunosuppressive agents indicate brain cytoprotective effects by influencing glia cells function similar to MMF (Zawadzka and Kaminska, 2005; Erlich et al., 2007). Treatment with immunosuppressant FK506 significantly reduced the lesion volume in induced cerebral infarction (Sharkey and Butcher, 1994; Zawadzka and Kaminska, 2005) and affected the activity of microglia as well as astrocyte and cytokine production *in vitro* and *in vivo* (Muramoto et al., 2003; Zawadzka and Kaminska, 2005). These findings are in accordance with MMF data, showing the modulating action of microglia, astrocytes, and cytokine production (Dehghani et al., 2010). Brain cytoprotective effect of immunosuppressant FK506 was also demonstrated in OHSC (Lee et al., 2010). Roscovitine, an inhibitor of CDK5 with additional immunosuppressive effects reduced neuronal loss, glial activation, as well as microglia proliferation, NO release, and neurologic deficits after brain trauma or stroke (Di Giovanni et al., 2005; Hilton et al., 2008; Menn et al., 2010). Treatment with rapamycin, a further immunosuppressant, increased neural survival thus improving the functional recovery and reduced the number of microglia/macrophages after TBI (Erlich et al., 2007; Lipton and Sahin, 2014). In most cases, the substances in the studies were administered in a very early period after injury, mostly within the first few hours. Further temporal aspects of the application were not considered, although it is necessary for the clinical practice. In a several studies, a specific brain cytoprotective time window was demonstrated. For example, FK506 showed a brain cytoprotective time window *in vivo* within the first 120 min but

not if applied later in an occlusion model (Arii et al., 2001; Furuichi et al., 2003). A better characterization of the so called windows of opportunity is needed *in vitro* and *in vivo*. The aspect of a therapeutic time-defined approach gains more and more importance due to the necessity of standardized preclinical study settings (Feuerstein et al., 2008; Lyden et al., 2021).

The Brain Cytoprotective Effect of Mycophenolate Mofetil Depends on the Time of Application

In our previous work, MMF showed a protective time window of 12–36 h in OHSC (Ebrahimi et al., 2012). Continuous treatment up to 12 h after the injury led to a reduction in a number of damaged neurons and microglia. Later onset of MMF treatment was no longer linked to brain cytoprotective effects. While treatment between 24–48 h after injury failed to demonstrate any benefits, a brain cytoprotective effect was identified for treatment duration of up to 12 and 36 h (Ebrahimi et al., 2012). In this regard, the investigation of an earlier start of MMF treatment in the context of new clinical therapeutic interventions and a lower risk of systematic immunosuppressive effect may contribute to an immunomodulatory brain cytoprotective approach (Hug et al., 2009; Fugate et al., 2014; Nogueira et al., 2018). Nonetheless, the time window could be better defined and questions about the necessary treatment duration answered. Hence, this study demonstrated a reduction in damaged neurons in a wider and earlier time window of 8–36 h after injury, but not in a time window of 8–24 h. These results led to two conclusions: (i) Starting MMF treatment should occur in the early phase within the first 8 h of injury in order to achieve better results. (ii) Treatment should last longer than 24 h. In agreement, selected patients underwent thrombectomy had a benefit from the therapy when started at 6–24 h (Nogueira et al., 2018; Lyden et al., 2021). Furthermore, after a short treatment a plasma concentration of approximately 100 μg/ml period is certainly achievable without a risk of general immunosuppressive effects as observed after prolonged MMF therapy. Due to fluctuating plasma concentrations of MMF, area under the curve (AUC) was established as a relevant parameter for bioavailability and therapeutic drug monitoring. The ideal AUC has been reported to be 40–60 μg × h/mL (Ferreira et al., 2020) after renal transplantation and about 30–40 μg × h/mL after lung transplantation (Yabuki et al., 2020). However, it should be noted that the bioavailability in these studies was chosen to establish sufficient immunosuppression with few side effects. These concentrations are therefore slightly below the 100 μg/ml used here, although those were collected in the context of a therapy existing over a longer period of time. The therapeutic use of MMF described here refers to a much shorter period of time and is not intended to cause a permanent immune suppression. A short therapeutic period with a higher AUC for immunomodulation would therefore certainly be conceivable. Furthermore, the increasingly established use of interventional therapies such as mechanical thrombectomies (Nogueira et al., 2018) offers the possibility to apply drugs exactly at the desired site and thus to achieve significantly higher concentrations without systematic effect. Taken together, the here used MMF concentration was chosen based on a realistic scenario and represents an achievable tissue concentration also *in vivo*. Possible limitations might be the fluctuating plasma levels, a more complex pharmacokinetics due to unclear perfusion conditions in the penumbra, a changing blood brain barrier and an increasing isolation of the lesion by glial cells.

Mycophenolate mofetil treatments for a short interval from 8 to 24 h led to a reduction in microglia number. This observation was consistent with previous results from an *in vitro* study, in which treatment for longer than 4 h significantly reduced the number of microglia (Ebrahimi et al., 2012). Although increased apoptosis by MMF application was observed in microglia cell culture (Dehghani et al., 2003). MMF treatment reduced the proliferation rate of astrocytes and microglia in OHSC without changing the number of apoptotic cells (Ebrahimi et al., 2012). Thus, the reduced number of microglia can be attributed to a reduction of proliferation. Notably, the observed brain cytoprotective effect was not always correlated with a reduced number of microglia. Decreased microglia number in a treatment window of 8–24 h remained without significant brain cytoprotective evidence. Therefore, a reduced number and proliferation of microglia in the early phase after the injury appear as a consequence of MMF treatment, but presumably without causality for the brain cytoprotective effects.

Microglia Dependency of Mycophenolate Mofetil Mediated Effects

In general, after CNS injury, increased stimulation through so-called pattern-recognition receptors (PRRs) results in "activation" of microglia with subsequent increased proliferation, migration, and chemotaxis, as well as increased release of cytokines (Deczkowska et al., 2018; Jiang et al., 2020; Ferro et al., 2021). The active form of microglia exerted its effects through increased phagocytic activity, secretion of proinflammatory cytokines, NO, proteases, arachidonic acid derivatives, and expression of several receptors (Simon et al., 2017; Subhramanyam et al., 2019; Takeda et al., 2021). MMF was found to influence cytokine release and NO production in microglia and macrophages. However, effects on astrocytes were observed as well (Miljkovic et al., 2002; Dehghani et al., 2010; Xu et al., 2022). Microglia were depleted from OHSC by clodronate to evaluate the impact of these cells on brain cytoprotective effects. Lesion of almost microglia free OHSC significantly exacerbates NMDA induced damage (Kohl et al., 2003). The results are in line with the increasingly accepted position that microglia, next to their neurotoxic properties, possess many cytoprotective attributes. Often the microglia clearance of CNS debris was misinterpreted as "killing" of neuronal cells. However, it is a more essential function for the maintenance of homeostasis (Derecki et al., 2012; Ferro et al., 2021; Xu et al., 2022). Moreover, microglia had the potential to suppress existing inflammation and to stimulate regenerative processes (Rasley et al., 2006; Thored et al., 2009). This point is particularly illustrated by the fact that after complete microglia depletion the brain cytoprotective effect of MMF at 24, 36,

and 48 h were lost. Furthermore, a significant reduction in damaged neurons was also observed after 72 h in microglia depleted OHSC, indicating the involvement of additional cell types, mainly astrocytes in MMF related effects. MMF was found to affect cytokine release and proliferation in astrocytes and influence cell migration and scar formation in scratch assay (Miljkovic et al., 2002; Ebrahimi et al., 2012). A direct effect on neurons seems unlikely (Dehghani et al., 2010). Microglia very likely mediate the major impact on brain cytoprotection in an early phase of injury. This pattern of MMF effects consisting of an early microglia-mediated phase and a possible late astrocytic phase completed the findings from previous study (Ebrahimi et al., 2012). Excitingly, a brain cytoprotective effect was already found 24 h after injury and subsequent fixation. However, no protective effect was observed after application of MMF in a time window of 8–24 h only and fixation after 72 h. Interestingly, MMF treatment for a short period might not be sufficient to prevent a renewed progression of inflammation and secondary damage. However, a prolonged treatment with MMF in a time window of 8–36 h led to satisfactory results. Thus, there might be a critical phase in which a sufficiently long MMF application would be necessary to achieve a consistent protective effect. Our results fit well to time-dependent data obtained from a genetic characterization of microglia after TBI in rats with upregulation of chemotactic genes and downregulation of anti-inflammatory genes 2 days after trauma (Izzy et al., 2019). Furthermore, it is consistent with the implied observations on IMPDH2 expression in microglia and astrocytes.

IMPDH2 in Glia Cells Seem to Be a Main Target of Mycophenolate Mofetil

After acute neuronal injury, microglia and astrocytes began to proliferate. This is a hallmark of gliosis in several CNS pathologies, including stroke and TBI (Iadecola and Anrather, 2011; Jassam et al., 2017). IMPDH is a major rate limiting enzyme involved in the *de novo* purine biosynthesis and directly affects the proliferation of cells (Allison et al., 1993; Pua et al., 2017). MMF inhibited IMPDH due to the replacement of the nicotinamide adenine dinucleotide (NAD) cofactor (Sintchak et al., 1996) and reduced the guanosine pool, which in turn inhibited proliferation (Allison and Eugui, 2000). Inhibition of IMPDH results primarily in depletion of guanosine monophosphate (GMP) and consequently also of intercellular guanosine triphosphate (GTP) and deoxyguanosine triphosphate (dGTP) (Allison et al., 1993; Gu et al., 2003). Guanosine as well as deoxyguanosine in turn show an allosteric function of 5-phosphoribosyl-1-pyrophosphate (PRPP) synthetase and ribonucleotide reductase which in turn affect the entire purine metabolism and thus the replication of DNA and cell cycle. This inhibition of *de novo* synthesis followed by a reduced intracellular concentration of guanosine nucleotides seems to be one of the determining mechanisms behind the reduction of cytokines in microglia and astrocytes and thus to play a role in the observed brain cytoprotective effects. In a combined treatment with guanosine and MMF in the damaged OHSC, the brain cytoprotective effect was abrogated (Ebrahimi et al., 2012). These results are also consistent with reduced proliferation rates, cytokine, and NO production shown in microglia and astrocytes, which where antagonized by guanosine (Dehghani et al., 2010). Sappanone A (SA), a highly selective inhibitor of IMPDH2, led to a reduction in microglia activation and cytokine production (Liao et al., 2017). Furthermore, SA significantly reduced GTP levels in BV2 cells, and the neuroinflammatory effects were attenuated after application of an IMPDH2 siRNA (Liao et al., 2017). The close link between metabolism and immunological cellular responses, proliferation as well as cell differentiation seems to be an important basis to understand the complex inflammatory reactions. MMF was reported to modulate the activities of Myc *via* NDRG1 in endothelial cells (Domhan et al., 2008). This activity was closely linked to the regulation of cell growth, proliferation, and differentiation (Secombe et al., 2004). In a gastric cancer cell line, treatment with MMF led to an alteration of several cyclins and cyclin kinases at the transcriptional level, indicating an influence on the PI3K/AKT/mTOR pathway (Dun et al., 2013). This could explain the changed expression of genes involved in glutaminolysis, nucleotide synthesis and glycolysis in Jurkat T cells by MMF (Fernandez-Ramos et al., 2017; Zhu and Thompson, 2019). Furthermore, a reduction of HIF-1alpha and Myc but not of Akt and mTORC1 was demonstrated and an independent regulation of Myc and HIF-1alpha by MMF was suggested (Fernandez-Ramos et al., 2017). In human CD4 T cells, an alteration of the Akt/mTOR as well as STAT5 signaling pathway was noticed (He et al., 2011). In addition to the reduction of GTP by MMF, a moderate decrease in adenosine triphosphate (ATP) concentration was detected within a short time in T cells, which in turn might activate AMPK as an energetic sensor (Fernandez-Ramos et al., 2017) and conceivably modulate mTORC1 (Saxton and Sabatini, 2017). The relationship between nucleotide metabolism, the cell cycle, in terms of proliferation and the release of neuroinflammatory cytokines in neuronal injury needs to be further characterized. Previously, the expression of IMPDH2 was demonstrated in OHSC (Ebrahimi et al., 2012). Since microglia belong to the monocytic cell lineage, it was likely that IMPDH2 is particularly expressed in these cells (Ginhoux et al., 2010; Ginhoux and Jung, 2014). Hence, in this study, the expression of IMPDH2 in primary microglia and astrocytes was detected in accordance to an earlier report (Liao et al., 2017). LPS stimulation in primary microglia as well as astrocytes did not result in a quantitative increase of IMPDH2 in comparison to the control which was observed after stimulation of lymphocytes (Dayton et al., 1994). However, there was a general increased amount of IMPDH2 in primary microglia after 12 h in culture. Primary astrocytic culture showed an increase in IMPDH2 after 16 h as well as after 24 h. Among others, early proliferation of microglia accompanied by delayed astrocytic proliferation in cell culture might explain this increase. This would also be consistent with the early microglia-mediated effect and the late microglia-independent effect by MMF. As LPS treatment did not lead to any altered expression, IMPDH2 might be regulated in its kinetics or dependent on protein-protein interactions (Jain et al., 2004). Furthermore, the activation of toll like receptor (TLR) 4 misses to alter the IMPDH2 expression (Liao et al., 2017).

CONCLUSION

The application of brain cytoprotective therapeutics for a short period of time and early after neuronal damage is a fundamental prerequisite of an immunomodulating approach. MMF led to a reduction of neuronal damage in OHSC when the treatment was started within the first 8 h of injury and lasted for a period of at least 24 h. MMF showed a brain cytoprotective effect at 24, 36, 48, and 72 h after injury. In addition, no protection was detectable at 24, 36, and 48 h after depleting microglia, indicating an early microglia-dependent phase and a late microglia-independent phase for MMF effects. It is very likely that microglia mediate the major impact for MMF brain cytoprotective effects but the role of astrocytes should be considered particularly in the late phase. The IMPDH2 as a target of MMF was detected in primary microglia as well as in astrocytes. Summarizing our results, MMF might be a potential candidate in the treatment of acute lesions of the CNS.

DATA AVAILABILITY STATEMENT

The datasets presented in this study can be found in online repositories. The names of the repository/repositories and accession number(s) can be found in the article/**Supplementary Material**.

ETHICS STATEMENT

All animal experiments were performed in accordance with the Policy on Ethics and the Policy on the Use of Animals in Neuroscience Research as indicated in the directive 2010/63/EU of the European Parliament and of the Council of the European Union on the protection of animals used for scientific purposes and were approved by the local authorities for care and use of laboratory animals (State of Saxony-Anhalt, Germany, permission number: I11M18, date: 01.12.2012).

AUTHOR CONTRIBUTIONS

FD, UH, and JK conceptualized and designed the study and wrote the manuscript. JK, UH, TH, CG, MS, SL, and BA conducted the research. JK, UH, and TH analyzed the data. All authors provided critical revisions to the manuscript.

FUNDING

This research was partly funded by the HaPKoM-Program of the Medical Faculty Martin-Luther-University Halle-Wittenberg.

ACKNOWLEDGMENTS

We thank Candy Rothgänger-Strube and Liudmila Litvak for technical assistance.

SUPPLEMENTARY MATERIAL

The Supplementary Material for this article can be found online at: https://www.frontiersin.org/articles/10.3389/fnagi.2022.863598/full#supplementary-material

REFERENCES

Ahmad, A., Crupi, R., Campolo, M., Genovese, T., Esposito, E., and Cuzzocrea, S. (2013). Absence of TLR4 reduces neurovascular unit and secondary inflammatory process after traumatic brain injury in mice. *PLoS One* 8:e57208. doi: 10.1371/journal.pone.0057208

Allison, A. C., and Eugui, E. M. (2000). Mycophenolate mofetil and its mechanisms of action. *Immunopharmacology* 47, 85–118. doi: 10.1016/s0162-3109(00)00188-0

Allison, A. C., Kowalski, W. J., Muller, C. D., and Eugui, E. M. (1993). Mechanisms of action of mycophenolic acid. *Ann. N. Y. Acad. Sci.* 696, 63–87. doi: 10.1111/j.1749-6632.1993.tb17143.x

Arii, T., Kamiya, T., Arii, K., Ueda, M., Nito, C., Katsura, K.-I., et al. (2001). Neuroprotective effect of immunosuppressant FK506 in transient focal ischemia in rats: therapeutic time window for FK506 in transient focal ischemia. *Neurol. Res.* 23, 755–760. doi: 10.1179/016164101101199135

Bradford, M. M. (1976). A rapid and sensitive method for the quantitation of microgram quantities of protein utilizing the principle of protein-dye binding. *Anal. Biochem.* 72, 248–254. doi: 10.1006/abio.1976.9999

Burda, J. E., and Sofroniew, M. V. (2014). Reactive gliosis and the multicellular response to CNS damage and disease. *Neuron* 81, 229–248. doi: 10.1016/j.neuron.2013.12.034

Carandang, R., Seshadri, S., Beiser, A., Kelly-Hayes, M., Kase, C. S., Kannel, W. B., et al. (2006). Trends in incidence, lifetime risk, severity, and 30-day mortality of stroke over the past 50 years. *JAMA* 296, 2939–2946. doi: 10.1001/jama.296.24.2939

Chamorro, A., Dirnagl, U., Urra, X., and Planas, A. M. (2016). Neuroprotection in acute stroke: targeting excitotoxicity, oxidative and nitrosative stress, and inflammation. *Lancet Neurol.* 15, 869–881. doi: 10.1016/S1474-4422(16)00114-9

Chamorro, A., Meisel, A., Planas, A. M., Urra, X., van de Beek, D., and Veltkamp, R. (2012). The immunology of acute stroke. *Nat. Rev. Neurol.* 8, 401–410. doi: 10.1038/nrneurol.2012.98

Dayton, J. S., Lindsten, T., Thompson, C. B., and Mitchell, B. S. (1994). Effects of human T lymphocyte activation on inosine monophosphate dehydrogenase expression. *J. Immunol.* 152, 984–991.

Deczkowska, A., Amit, I., and Schwartz, M. (2018). Microglial immune checkpoint mechanisms. *Nat. Neurosci.* 21, 779–786. doi: 10.1038/s41593-018-0145-x

Dehghani, F., Hischebeth, G. T. R., Wirjatijasa, F., Kohl, A., Korf, H.-W., and Hailer, N. P. (2003). The immunosuppressant mycophenolate mofetil attenuates neuronal damage after excitotoxic injury in hippocampal slice cultures. *Eur. J. Neurosci.* 18, 1061–1072. doi: 10.1046/j.1460-9568.2003.02821.x

Dehghani, F., Sayan, M., Conrad, A., Evers, J., Ghadban, C., Blaheta, R., et al. (2010). Inhibition of microglial and astrocytic inflammatory responses by the immunosuppressant mycophenolate mofetil. *Neuropathol. Appl. Neurobiol.* 36, 598–611. doi: 10.1111/j.1365-2990.2010.01104.x

Derecki, N. C., Cronk, J. C., Lu, Z., Xu, E., Abbott, S. B., Guyenet, P. G., et al. (2012). Wild-type microglia arrest pathology in a mouse model of Rett syndrome. *Nature* 484, 105–109. doi: 10.1038/nature10907

Di Giovanni, S., Movsesyan, V., Ahmed, F., Cernak, I., Schinelli, S., Stoica, B., et al. (2005). Cell cycle inhibition provides neuroprotection and reduces glial proliferation and scar formation after traumatic brain injury. *Proc. Natl. Acad. Sci. U.S.A.* 102:8333. doi: 10.1073/pnas.0500989102

Dirnagl, U., and Endres, M. (2014). Found in translation: preclinical stroke research predicts human pathophysiology, clinical phenotypes, and therapeutic outcomes. *Stroke* 45, 1510–1518. doi: 10.1161/STROKEAHA.113.004075

Dirnagl, U., Iadecola, C., and Moskowitz, M. A. (1999). Pathobiology of ischaemic stroke: an integrated view. *Trends Neurosci.* 22, 391–397. doi: 10.1016/s0166-2236(99)01401-0

Domhan, S., Muschal, S., Schwager, C., Morath, C., Wirkner, U., Ansorge, W., et al. (2008). Molecular mechanisms of the antiangiogenic and antitumor effects of mycophenolic acid. *Mol. Cancer Ther.* 7, 1656–1668. doi: 10.1158/1535-7163.Mct-08-0193

Dun, B., Sharma, A., Xu, H., Liu, H., Bai, S., Zeng, L., et al. (2013). Transcriptomic changes induced by mycophenolic acid in gastric cancer cells. *Am. J. Transl. Res.* 6, 28–42.

Ebrahimi, F., Hezel, M., Koch, M., Ghadban, C., Korf, H. W., and Dehghani, F. (2010). Analyses of neuronal damage in excitotoxically lesioned organotypic hippocampal slice cultures. *Ann. Anat.* 192, 199–204. doi: 10.1016/j.aanat.2010.06.002

Ebrahimi, F., Koch, M., Pieroh, P., Ghadban, C., Hobusch, C., Bechmann, I., et al. (2012). Time dependent neuroprotection of mycophenolate mofetil: effects on temporal dynamics in glial proliferation, apoptosis, and scar formation. *J. Neuroinflammation* 9:89. doi: 10.1186/1742-2094-9-89

Erlich, S., Alexandrovich, A., Shohami, E., and Pinkas-Kramarski, R. (2007). Rapamycin is a neuroprotective treatment for traumatic brain injury. *Neurobiol. Dis.* 26, 86–93. doi: 10.1016/j.nbd.2006.12.003

Feigin, V. L., Forouzanfar, M. H., Krishnamurthi, R., Mensah, G. A., Connor, M., Bennett, D. A., et al. (2014). Global and regional burden of stroke during 1990-2010: findings from the Global Burden of Disease Study 2010. *Lancet* 383, 245–254. doi: 10.1016/s0140-6736(13)61953-4

Fernandez-Ramos, A. A., Marchetti-Laurent, C., Poindessous, V., Antonio, S., Petitgas, C., Ceballos-Picot, I., et al. (2017). A comprehensive characterization of the impact of mycophenolic acid on the metabolism of Jurkat T cells. *Sci. Rep.* 7:10550. doi: 10.1038/s41598-017-10338-6

Ferreira, P. C. L., Thiesen, F. V., Pereira, A. G., Zimmer, A. R., and Froehlich, P. E. (2020). A short overview on mycophenolic acid pharmacology and pharmacokinetics. *Clin. Transplant.* 34:e13997. doi: 10.1111/ctr.13997

Ferro, A., Auguste, Y. S. S., and Cheadle, L. (2021). Microglia, cytokines, and neural activity: unexpected interactions in brain development and function. *Front. Immunol.* 12:703527. doi: 10.3389/fimmu.2021.703527

Feuerstein, G. Z., Zaleska, M. M., Krams, M., Wang, X., Day, M., Rutkowski, J. L., et al. (2008). Missing steps in the STAIR case: a Translational Medicine perspective on the development of NXY-059 for treatment of acute ischemic stroke. *J. Cereb. Blood Flow Metab.* 28, 217–219. doi: 10.1038/sj.jcbfm.9600516

Fugate, J. E., Lyons, J. L., Thakur, K. T., Smith, B. R., Hedley-Whyte, E. T., and Mateen, F. J. (2014). Infectious causes of stroke. *Lancet Infect. Dis.* 14, 869–880. doi: 10.1016/S1473-3099(14)70755-8

Furuichi, Y., Katsuta, K., Maeda, M., Ueyama, N., Moriguchi, A., Matsuoka, N., et al. (2003). Neuroprotective action of tacrolimus (FK506) in focal and global cerebral ischemia in rodents: dose dependency, therapeutic time window and long-term efficacy. *Brain Res.* 965, 137–145. doi: 10.1016/S0006-8993(02)04151-3

Ginhoux, F., Greter, M., Leboeuf, M., Nandi, S., See, P., Gokhan, S., et al. (2010). Fate mapping analysis reveals that adult microglia derive from primitive macrophages. *Science* 330, 841–845. doi: 10.1126/science.1194637

Ginhoux, F., and Jung, S. (2014). Monocytes and macrophages: developmental pathways and tissue homeostasis. *Nat. Rev. Immunol.* 14, 392–404. doi: 10.1038/nri3671

Grabiec, U., Hohmann, T., Ghadban, C., Rothgänger, C., Wong, D., Antonietti, A., et al. (2019). Protective effect of N-Arachidonoyl Glycine-GPR18 signaling after excitotoxical lesion in murine organotypic hippocampal slice cultures. *Int. J. Mol. Sci.* 20:1266. doi: 10.3390/ijms20061266

Grabiec, U., Hohmann, T., Hammer, N., and Dehghani, F. (2017). Organotypic hippocampal slice cultures as a model to study neuroprotection and invasiveness of tumor cells. *J. Vis. Exp.* 126:e55359. doi: 10.3791/55359

Grabiec, U., Koch, M., Kallendrusch, S., Kraft, R., Hill, K., Merkwitz, C., et al. (2012). The endocannabinoid N-arachidonoyldopamine (n.d.) exerts neuroprotective effects after excitotoxic neuronal damage via cannabinoid receptor 1 (CB(1)). *Neuropharmacology* 62, 1797–1807. doi: 10.1016/j.neuropharm.2011.11.023

Gu, J. J., Tolin, A. K., Jain, J., Huang, H., Santiago, L., and Mitchell, B. S. (2003). Targeted disruption of the inosine 5'-monophosphate dehydrogenase type I gene in mice. *Mol. Cell Biol.* 23, 6702–6712. doi: 10.1128/mcb.23.18.6702-6712.2003

Hailer, N. P. (2008). Immunosuppression after traumatic or ischemic CNS damage: it is neuroprotective and illuminates the role of microglial cells. *Prog. Neurobiol.* 84, 211–233. doi: 10.1016/j.pneurobio.2007.12.001

He, X., Smeets, R. L., Koenen, H. J., Vink, P. M., Wagenaars, J., Boots, A. M., et al. (2011). Mycophenolic acid-mediated suppression of human CD4+ T cells: more than mere guanine nucleotide deprivation. *Am. J. Transplant.* 11, 439–449. doi: 10.1111/j.1600-6143.2010.03413.x

Hilton, G. D., Stoica, B. A., Byrnes, K. R., and Faden, A. I. (2008). Roscovitine reduces neuronal loss, glial activation, and neurologic deficits after brain trauma. *J. Cereb. Blood Flow Metab.* 28, 1845–1859. doi: 10.1038/jcbfm.2008.75

Hoffmann, S., Harms, H., Ulm, L., Nabavi, D. G., Mackert, B. M., Schmehl, I., et al. (2017). Stroke-induced immunodepression and dysphagia independently predict stroke-associated pneumonia – The PREDICT study. *J. Cereb. Blood Flow Metab.* 37, 3671–3682. doi: 10.1177/0271678X16671964

Hug, A., Dalpke, A., Wieczorek, N., Giese, T., Lorenz, A., Auffarth, G., et al. (2009). Infarct volume is a major determiner of post-stroke immune cell function and susceptibility to infection. *Stroke* 40, 3226–3232. doi: 10.1161/STROKEAHA.109.557967

Husain, S., and Singh, N. (2002). The impact of novel immunosuppressive agents on infections in organ transplant recipients and the interactions of these agents with antimicrobials. *Clin. Infect. Dis.* 35, 53–61. doi: 10.1086/340867

Iadecola, C., and Anrather, J. (2011). The immunology of stroke: from mechanisms to translation. *Nat. Med.* 17, 796–808. doi: 10.1038/nm.2399

Izzy, S., Liu, Q., Fang, Z., Lule, S., Wu, L., Chung, J. Y., et al. (2019). Time-dependent changes in microglia transcriptional networks following traumatic brain injury. *Front. Cell. Neurosci.* 13:307. doi: 10.3389/fncel.2019.00307

Jain, J., Almquist, S. J., Ford, P. J., Shlyakhter, D., Wang, Y., Nimmesgern, E., et al. (2004). Regulation of inosine monophosphate dehydrogenase type I and type II isoforms in human lymphocytes. *Biochem. Pharmacol.* 67, 767–776. doi: 10.1016/j.bcp.2003.09.043

Jassam, Y. N., Izzy, S., Whalen, M., McGavern, D. B., and El Khoury, J. (2017). Neuroimmunology of Traumatic brain injury: time for a paradigm shift. *Neuron* 95, 1246–1265. doi: 10.1016/j.neuron.2017.07.010

Jiang, C. T., Wu, W. F., Deng, Y. H., and Ge, J. W. (2020). Modulators of microglia activation and polarization in ischemic stroke (Review). *Mol. Med. Rep.* 21, 2006–2018. doi: 10.3892/mmr.2020.11003

Jonsson, C. A., and Carlsten, H. (2002). Mycophenolic acid inhibits inosine 5'-monophosphate dehydrogenase and suppresses production of pro-inflammatory cytokines, nitric oxide, and LDH in macrophages. *Cell Immunol.* 216, 93–101. doi: 10.1016/s0008-8749(02)00502-6

Klehmet, J., Harms, H., Richter, M., Prass, K., Volk, H. D., Dirnagl, U., et al. (2009). Stroke-induced immunodepression and post-stroke infections: lessons from the preventive antibacterial therapy in stroke trial. *Neuroscience* 158, 1184–1193. doi: 10.1016/j.neuroscience.2008.07.044

Kohl, A., Dehghani, F., Korf, H. W., and Hailer, N. P. (2003). The bisphosphonate clodronate depletes microglial cells in excitotoxically injured organotypic hippocampal slice cultures. *Exp. Neurol.* 181, 1–11. doi: 10.1016/s0014-4886(02)00049-3

Lee, K. H., Won, R., Kim, U. J., Kim, G. M., Chung, M. A., Sohn, J. H., et al. (2010). Neuroprotective effects of FK506 against excitotoxicity in organotypic hippocampal slice culture. *Neurosci. Lett.* 474, 126–130. doi: 10.1016/j.neulet.2010.03.009

Lee, W. A., Gu, L., Miksztal, A. R., Chu, N., Leung, K., and Nelson, P. H. (1990). Bioavailability improvement of mycophenolic acid through amino ester derivatization. *Pharm. Res.* 7, 161–166. doi: 10.1023/a:1015828802490

Leker, R. R., Shohami, E., and Constantini, S. (2002). Experimental models of head trauma. *Acta Neurochir. Suppl.* 83, 49–54. doi: 10.1007/978-3-7091-6743-4_9

Liao, L. X., Song, X. M., Wang, L. C., Lv, H. N., Chen, J. F., Liu, D., et al. (2017). Highly selective inhibition of IMPDH2 provides the basis of antineuroinflammation therapy. *Proc. Natl. Acad. Sci. U.S.A.* 114, E5986–E5994. doi: 10.1073/pnas.1706778114

Lipton, J. O., and Sahin, M. (2014). The neurology of mTOR. *Neuron* 84, 275–291. doi: 10.1016/j.neuron.2014.09.034

Lyden, P., Buchan, A., Boltze, J., and Fisher, M. (2021). Top priorities for cerebroprotective studies-A paradigm shift: report from STAIR XI. *Stroke* 52, 3063–3071. doi: 10.1161/strokeaha.121.034947

Maas, A. I., Stocchetti, N., and Bullock, R. (2008). Moderate and severe traumatic brain injury in adults. *Lancet Neurol.* 7, 728–741. doi: 10.1016/S1474-4422(08)70164-9

Menn, B., Bach, S., Blevins, T. L., Campbell, M., Meijer, L., and Timsit, S. (2010). Delayed treatment with systemic (S)-roscovitine provides neuroprotection and inhibits in vivo CDK5 activity increase in animal stroke models. *PLoS One* 5:e12117. doi: 10.1371/journal.pone.0012117

Miljkovic, D., Samardzic, T., Cvetkovic, I., Mostarica Stojkovic, M., and Trajkovic, V. (2002). Mycophenolic acid downregulates inducible nitric oxide synthase induction in astrocytes. *Glia* 39, 247–255. doi: 10.1002/glia.10089

Morshead, C. M., and van der Kooy, D. (1990). Separate blood and brain origins of proliferating cells during gliosis in adult brains. *Brain Res.* 535, 237–244. doi: 10.1016/0006-8993(90)91606-h

Muramoto, M., Yamazaki, T., Nishimura, S., and Kita, Y. (2003). Detailed in vitro pharmacological analysis of FK506-induced neuroprotection. *Neuropharmacology* 45, 394–403. doi: 10.1016/s0028-3908(03)00168-0

Nedergaard, M., and Dirnagl, U. (2005). Role of glial cells in cerebral ischemia. *Glia* 50, 281–286. doi: 10.1002/glia.20205

Nogueira, R. G., Jadhav, A. P., Haussen, D. C., Bonafe, A., Budzik, R. F., Bhuva, P., et al. (2018). Thrombectomy 6 to 24 Hours after Stroke with a Mismatch between Deficit and Infarct. *N. Engl. J. Med.* 378, 11–21. doi: 10.1056/NEJMoa1706442

Oest, T. M., Dehghani, F., Korf, H. W., and Hailer, N. P. (2006). The immunosuppressant mycophenolate mofetil improves preservation of the perforant path in organotypic hippocampal slice cultures: a retrograde tracing study. *Hippocampus* 16, 437–442. doi: 10.1002/hipo.20182

Pua, K. H., Stiles, D. T., Sowa, M. E., and Verdine, G. L. (2017). IMPDH2 is an intracellular target of the Cyclophilin A and Sanglifehrin A complex. *Cell Rep.* 18, 432–442. doi: 10.1016/j.celrep.2016.12.030

Rasley, A., Tranguch, S. L., Rati, D. M., and Marriott, I. (2006). Murine glia express the immunosuppressive cytokine, interleukin-10, following exposure to *Borrelia burgdorferi* or *Neisseria meningitidis*. *Glia* 53, 583–592. doi: 10.1002/glia.20314

Saxton, R. A., and Sabatini, D. M. (2017). mTOR Signaling in Growth. *Metab. Dis. Cell* 169, 361–371. doi: 10.1016/j.cell.2017.03.035

Secombe, J., Pierce, S. B., and Eisenman, R. N. (2004). Myc: a weapon of mass destruction. *Cell* 117, 153–156. doi: 10.1016/s0092-8674(04)00336-8

Sharkey, J., and Butcher, S. P. (1994). Immunophilins mediate the neuroprotective effects of FK506 in focal cerebral ischaemia. *Nature* 371, 336–339. doi: 10.1038/371336a0

Simon, D. W., McGeachy, M. J., Bayır, H., Clark, R. S., Loane, D. J., and Kochanek, P. M. (2017). The far-reaching scope of neuroinflammation after traumatic brain injury. *Nat. Rev. Neurol.* 13, 171–191. doi: 10.1038/nrneurol.2017.13

Sintchak, M. D., Fleming, M. A., Futer, O., Raybuck, S. A., Chambers, S. P., Caron, P. R., et al. (1996). Structure and mechanism of inosine monophosphate dehydrogenase in complex with the immunosuppressant mycophenolic acid. *Cell* 85, 921–930. doi: 10.1016/s0092-8674(00)81275-1

Subhramanyam, C. S., Wang, C., Hu, Q., and Dheen, S. T. (2019). Microglia-mediated neuroinflammation in neurodegenerative diseases. *Semin. Cell Dev. Biol.* 94, 112–120. doi: 10.1016/j.semcdb.2019.05.004

Takeda, H., Yamaguchi, T., Yano, H., and Tanaka, J. (2021). Microglial metabolic disturbances and neuroinflammation in cerebral infarction. *J. Pharmacol. Sci.* 145, 130–139. doi: 10.1016/j.jphs.2020.11.007

Thored, P., Heldmann, U., Gomes-Leal, W., Gisler, R., Darsalia, V., Taneera, J., et al. (2009). Long-term accumulation of microglia with proneurogenic phenotype concomitant with persistent neurogenesis in adult subventricular zone after stroke. *Glia* 57, 835–849. doi: 10.1002/glia.20810

Werner, C., and Engelhard, K. (2007). Pathophysiology of traumatic brain injury. *Br. J. Anaesth.* 99, 4–9. doi: 10.1093/bja/aem131

Xu, L., Wang, J., Ding, Y., Wang, L., and Zhu, Y.-J. (2022). Current knowledge of microglia in traumatic spinal cord injury. *Front. Neurol.* 12:796704. doi: 10.3389/fneur.2021.796704

Yabuki, H., Matsuda, Y., Watanabe, T., Eba, S., Hoshi, F., Hirama, T., et al. (2020). Plasma mycophenolic acid concentration and the clinical outcome after lung transplantation. *Clin. Transplant.* 34:e14088. doi: 10.1111/ctr.14088

Zawadzka, M., and Kaminska, B. (2005). A novel mechanism of FK506-mediated neuroprotection: downregulation of cytokine expression in glial cells. *Glia* 49, 36–51. doi: 10.1002/glia.20092

Zhu, J., and Thompson, C. B. (2019). Metabolic regulation of cell growth and proliferation. *Nat. Rev. Mol. Cell Biol.* 20, 436–450. doi: 10.1038/s41580-019-0123-5

Conflict of Interest: The authors declare that the research was conducted in the absence of any commercial or financial relationships that could be construed as a potential conflict of interest.

Publisher's Note: All claims expressed in this article are solely those of the authors and do not necessarily represent those of their affiliated organizations, or those of the publisher, the editors and the reviewers. Any product that may be evaluated in this article, or claim that may be made by its manufacturer, is not guaranteed or endorsed by the publisher.

Copyright © 2022 Kleine, Hohmann, Hohmann, Ghadban, Schmidt, Laabs, Alessandri and Dehghani. This is an open-access article distributed under the terms of the Creative Commons Attribution License (CC BY). The use, distribution or reproduction in other forums is permitted, provided the original author(s) and the copyright owner(s) are credited and that the original publication in this journal is cited, in accordance with accepted academic practice. No use, distribution or reproduction is permitted which does not comply with these terms.

frontiers in Neuroscience

ORIGINAL RESEARCH
published: 07 November 2019
doi: 10.3389/fnins.2019.01180

Opposite Effects of Neuroprotective Cannabinoids, Palmitoylethanolamide, and 2-Arachidonoylglycerol on Function and Morphology of Microglia

*Urszula Hohmann†, Markus Pelzer†, Joshua Kleine, Tim Hohmann, Chalid Ghadban and Faramarz Dehghani**

Department of Anatomy and Cell Biology, Medical Faculty, Martin Luther University Halle-Wittenberg, Halle (Saale), Germany

OPEN ACCESS

Edited by:
Johannes Boltze, University of Warwick, United Kingdom

Reviewed by:
Livio Luongo, Second University of Naples, Italy
Meliha Karsak, University Medical Center Hamburg-Eppendorf, Germany
Natsuo Ueda, Kagawa University, Japan

***Correspondence:**
Faramarz Dehghani
Faramarz.Dehghani@medizin.uni-halle.de

†These authors have contributed equally to this work

Specialty section:
This article was submitted to Neurodegeneration, a section of the journal Frontiers in Neuroscience

Received: *15 May 2019*
Accepted: *18 October 2019*
Published: *07 November 2019*

Citation:
Hohmann U, Pelzer M, Kleine J, Hohmann T, Ghadban C and Dehghani F (2019) Opposite Effects of Neuroprotective Cannabinoids, Palmitoylethanolamide, and 2-Arachidonoylglycerol on Function and Morphology of Microglia. Front. Neurosci. 13:1180. doi: 10.3389/fnins.2019.01180

Various studies performed in cultured cells and in *in vivo* models of neuronal damage showed that cannabinoids exert a neuroprotective effect. The increase in cannabinoids and cannabinoid like substances after stroke has been postulated to limit the content of neuronal injury. As well-accepted, inflammation, and neuronal damage are coupled processes and microglial cells as the main intrinsic immunological effector within the brain play a central role in their regulation. Treatment with the endocannabinoid, 2-arachidonoylglycerol (2-AG) or the endocannabinoid-like substance, palmitoylethanolamide (PEA) affected microglial cells and led to a decrease in the number of damaged neurons after excitotoxical lesion in organotypic hippocampal slice cultures (OHSC). 2-AG activated abnormal cannabidiol (abn-CBD) receptor, PEA was shown to mediate neuroprotection via peroxisome proliferator-activated receptor (PPAR)α. Despite the known neuroprotective and anti-inflammatory properties, the potential synergistic effect, namely possible entourage effect after treatment with the combination of these two protective cannabinoids has not been examined yet. After excitotoxical lesion OHSC were treated with PEA, 2-AG or a combination of both and the number of damaged neurons was evaluated. To investigate the role of microglial cells in PEA and 2-AG mediated protection, primary microglial cell cultures were treated with lipopolysaccharide (LPS) and 2-AG, PEA or a combination of those. Thereafter, we measured NO production, ramification index, proliferation and PPARα distribution in microglial cells. While PEA or 2-AG alone were neuroprotective, their co-application vanished the protective effect. This behavior was independent of microglial cells. Furthermore, PEA and 2-AG had contrary effects on ramification index and on NO production. No significant changes were observed in the proliferation rate of microglial cells after treatment. The expression of PPARα was not changed upon stimulation with PEA or 2-AG, but the distribution was significantly altered. 2-AG and

PEA mediated neuroprotection was abolished when co-applied. Both cannabinoids exert contrary effects on morphology and function of microglial cells. Co-application of both cannabinoids with different targets did not lead to a positive additive effect as expected, presumably due to the contrary polarization of microglial cells.

Keywords: 2-arachidonoylglycerol, palmitoylethanolamide, peroxisome proliferator-activated receptor, neuroprotection, microglial cells

INTRODUCTION

Traumatic brain injury affects a high number of young adults and their hospitalization is still a significant public challenge (Meaney et al., 2014). During neuronal damage a complex series of mechanisms becomes activated (Dirnagl et al., 2003; Kunz et al., 2010). Energy failure leads to calcium overload, depolarization of neurons and release of neurotransmitters with consecutive excitotoxicity, induced through overstimulation from excitatory receptors like NMDA receptor. This cascade is followed by activation of proteolytic enzymes and release of reactive oxygen species, damaging mitochondria, followed by apoptosis and neuronal death (Bruce et al., 1995; Kunz et al., 2010). Injured neuronal tissue releases pro-inflammatory cytokines leading to migration of inflammatory cells to the damaged site and inflammation (Jassam et al., 2017). Microglial cells play a crucial role during this process of secondary neuronal damage since they are the immunocompetent cells of the central nervous system (Kettenmann et al., 2011).

Cannabinoids positively affect cellular and molecular processes during ischemic, excitotoxical, or traumatic brain injury and were shown to be protective in different models mostly via microglial cells. All kind, plant-derived (isolated from *Cannabis sativa*), endo- (animal-derived) and synthetic cannabinoids were shown to affect neuronal damage (Kreutz et al., 2007, 2009; Mechoulam and Shohami, 2007; Koch et al., 2011a,b; Grabiec et al., 2012; Fernández-Ruiz et al., 2015; Guida et al., 2017; Belardo et al., 2019; Impellizzeri et al., 2019). Using the model of excitotoxically lesioned OHSC the number of damaged neurons was significantly reduced after treatment with endocannabinoids, like *N*-arachidonoyl dopamine, 2-arachidonoylglycerol (2-AG) or PEA associated with altered microglial cell number but not the phytocannabinoid, Δ-9-tetrahydrocannabinol (Kreutz et al., 2007; Koch et al., 2011a; Grabiec et al., 2012).

2-AG was shown to induce protection after neuronal lesion and to reduce the amount of tumor necrosis factor α released from LPS activated microglial cells (Facchinetti et al., 2003). Both, PEA and 2-AG are produced in the central nervous system and upregulated after neuronal damage (Kondo et al., 1998; Panikashvili et al., 2001; Franklin et al., 2003) and were shown to exhibit neuroprotection in several *in vivo* and *in vitro* models (Koch et al., 2011a; Beggiato et al., 2018; Herrera et al., 2018). Anti-inflammatory effects of PEA were associated with PPARα activation (LoVerme et al., 2005; Koch et al., 2011a; Citraro et al., 2013), and induction of PPARα expression was related in parallel to protective effects (Genovese et al., 2008; Koch et al., 2011a). A recent study demonstrated the presence of PPARα in different brain regions on neurons, astrocytes and microglial cells (Warden et al., 2016). Effects of 2-AG were abolished by O-1918 and cannabidiol (CBD), both antagonists of the abn-CBD sensitive receptor (abn-CBDR) (Kreutz et al., 2009). Evidence for functional abn-CBDR in the brain was pharmacologically found on microglial cells (Franklin and Stella, 2003; Walter et al., 2003; Kreutz et al., 2009). Consequently, 2-AG mediated protection depends on the presence of microglial cells as confirmed by microglial cells depletion (Kohl et al., 2003; Kreutz et al., 2009).

2-AG mediated protective properties were demonstrated in a variety of animal models of degenerative neurological disorders including multiple sclerosis, Parkinson's disease, and Alzheimer's disease (Scotter et al., 2010; Pertwee, 2014; Mounsey et al., 2015) and *in vitro* in astrocytes exposed to oxygen-glucose deprivation (Wang et al., 2015, 2018). 2-AG is the most abundant endocannabinoid in the brain and known to bind and activate CB_1 and CB_2 receptors. The treatment with exogenous 2-AG attenuated neuronal damage *in vivo* partly via CB_1 and mimicked the effects reported after aplication of synthetic CB_2 agonists. Some effects were absent in $CB_1^{-/-}$ mice (Mechoulam and Shohami, 2007; Magid et al., 2019). Furthermore, Carrier et al. (2004) observed that 2-AG affected microglial cells via CB_2. However, in rat OHSC and after NMDA damage effects of 2-AG were not blocked by CB_1 or CB_2 antagonists but inhibited by abnormal cannabidiol sensitive receptor (abn-CBDR) antagonists. These results make an involvement of CB_1 or CB_2 in 2-AG mediated neuroprotection unlikely (Kreutz et al., 2009). Application of PEA improved neuronal survival *in vitro* in primary mouse cortical astrocyte-neuron co-cultures (Beggiato et al., 2018) and in cortical neurons after hypoxia (Portavella et al., 2018). PEA possessed further beneficial properties in animal models of degenerative neurological disorders including vascular dementia (Siracusa et al., 2017). PEA and anandamide, if administrated together reduced the pain response 100-fold more potently than both substances alone and induced stronger vascular effects (Calignano et al., 1998; Ho et al., 2008). Such a co-application of two active cannabinoids increased their efficacy via the so called entourage effect, which is an endogenous cannabinoid molecular regulation route (Ben-Shabat et al., 1998). Ben-Shabat et al. (1998) demonstrated for the first time, that two inactive compounds, namely 2-linoleoylglycerol and 2-palmitoylglycerol potentiate the binding of 2-AG to the CB_1 and thereby its effects. Additionally, 2-linoleoylglycerol significantly inhibited the inactivation of 2-AG. Similarly, PEA was reported to prevent the inactivation of anandamide (Jonsson et al., 2001;

Abbreviations: 2-AG, 2-arachidonoylglycerol; abn-CBD, abnormal cannabidiol; abn-CBDR, abn-CBD-sensitive receptor; CB, cannabinoid receptor; CBD, cannabidiol; div, day *in vitro*; iNOS, inducible nitric oxide synthase; LPS, lipopolysaccharide; NMDA, *N*-methyl-D -aspartate, NO, nitric oxide; OHSC, organotypic hippocampal slice cultures; PEA, palmitoylethanolamide; PPAR, peroxisome proliferator-activated receptor.

Ho et al., 2008) indicating possible entourage effect. Microglial cells, the main immune cell of the central nervous system, has a ramified morphology and is stationary, surveying its surrounding if in an undamaged and non-inflammatory state (Smith et al., 2012). In pathologies, like neuropathic pain CB_2 expression increased in parallel to appearance of activated microglial cells. CB_2 ligands significantly alleviated the pain indicating that microglial cells are a main target of cannabinoids (Zhang et al., 2003; Luongo et al., 2010). During neuronal damage microglial cells become amoeboid, migrate to the lesion site, proliferate and can be affected by cannabinoids, as for example PEA potentiates microglial cell motility (Franklin et al., 2003; Vinet et al., 2012). Microglial cells mediate neuroprotection, but can also contribute to the damage, e.g., by upregulation of iNOS, an enzyme producing toxic amounts of NO from L-arginine (Garry et al., 2015). 2-AG was shown to induce the iNOS expression and NO production (Lipina and Hundal, 2017) and to stimulate NO release in invertebrate immune cells via CB_1 (Stefano et al., 2000). Contrary, NO donors were found to be neuroprotective (Kakizawa et al., 2007). Little is known about the influence of endocannabinoids on arginase, which inhibits the production of NO as a competing regulatory enzyme in the arginase-NO-synthase regulatory system in microglial cells. In peripheral immune cells Δ-9-tetrahydrocannabinol and AM1241, an CB_2 agonist induced arginase 1 expression (Hegde et al., 2010; Ma et al., 2015).

Earlier studies consistently reported about increased levels of endocannabinoids, such as PEA or 2-AG after neuronal injury. A question is raised why the secondary neuronal damage can't be prevented despite the high presence of neuroprotective substances. Since both endocannabinoids 2-AG and PEA if applied exogenously were shown to be neuroprotective via abn-CBDR or PPARα respectively, we asked whether the neuroprotective potential of both is additive. To assess a potential entourage effect between 2-AG and PEA on neuroprotective properties OHSC were excitotoxically lesioned and treated with PEA, 2-AG or combination of both. As mentioned, PEA and 2-AG target microglial cells. Therefore, their effects on function and morphology of primary microglial cells were investigated in untreated or LPS stimulated cultures. Ramification index, NO production, proliferation index, and temporal PPARα distribution were determined overtime.

MATERIALS AND METHODS

All experiments involving animal material were performed in accordance with the directive 2010/63/EU of the European Parliament and the Council of the European Union (22.09.2010) and approved by local authorities of the State of Saxony-Anhalt (permission number: I11M18, date: 01.12.2012) protecting animals and regulating tissue collection used for scientific purposes.

Materials

2-Arachidonylglycerol (2-AG, 10 nM, stock solved in DMSO; Tocris, Minneapolis, MN, United States, cat No. 1298), Clodronate (100 μg/ml, stock solved in Aqua; Bayer Vital GmbH GB; PZN: 04299668), Palmitoylethanolamide (PEA, 10 nM, stock solved in DMSO, Tocris, cat No. 0879), LPS (10 ng/ml, stock solved in Aqua; Sigma-Aldrich, cat No. L8274) and NMDA (50 μM, stock solved in Aqua bidest., Sigma-Aldrich, cat No. M3262) were used and applied to the culture medium according to treatment protocol.

Cell Culture

Primary microglia astrocyte co-cultures were prepared from 1 day old Wistar rats and cultured, as described earlier (Kohl et al., 2003; Grabiec et al., 2012). Briefly brains were treated with 0.5 mg/mL DNAse (Worthington, Bedford, MA, United States) and 4 mg/mL trypsin (Merck Millipore, Billerica, MA, United States) solved in Hank's balanced salts solution (Invitrogen, Carlsbad, CA, United States). Cells were cultured in DMEM (Invitrogen, cat No. 41965-062) with 10% FBS (Invitrogen, cat No. 10500-062) and 1 ml streptomycin/penicillin (Invitrogen). After 10 days microglial cells were isolated from astrocytic monolayer and seeded into well plates.

For immunocytochemical analysis 50,000 cells were placed on glass cover slips coated with poly-L-lysin and allowed to attach for 3 h. Cannabinoids were applied for 48 h to determine the microglial cells morphology. Bromodeoxyuridine (BrdU) (0.01 mM, Sigma-Aldrich) was added to the culture medium 16 h before the fixation to assess proliferation. Intracellular distribution of PPARα was analyzed 1, 6, and 24 h after treatment. The cells were fixed with 4% paraformaldehyde (Sigma-Aldrich, Munich, Germany) for 10 min and stored in 0.02M PBS at 4°C for further analysis.

For NO measurement supernatant of 50,000 cells treated for 72 h with cannabinoids was collected and stored at −80°C until further analysis.

Organotypic Hippocampal Slice Cultures (OHSC)

Organotypic hippocampal slice cultures were prepared from 7 to 9 day old Wistar rats as reported earlier (Grabiec et al., 2012, 2017; Hagemann et al., 2013; Hohmann et al., 2017, 2019) and kept at 35°C in a fully humidified atmosphere with 5% (v/v) CO_2. Culture medium was changed every other day. After 6 days *in vitro* experiments were started. All slices despite the control groups were treated with NMDA (50 μM) for 4 h. OHSC were treated with PEA (10 nM) or 2-AG (10 nM) or their combination for 72 h. The NMDA treated set of excitotoxically damaged OHSC was supplemented with 2-AG, PEA or combination of both or left untreated to asses an effect on neuronal damage in region of dentate gyrus.

To investigate the role of microglial cells OHSC were incubated with 100 μg/ml clodronate from 1 to 6 day *in vitro* (div). Clodronic acid, a bisphosphonate, affects only cells of the monocytic lineage and leads to apoptosis of microglia and macrophages (Kohl et al., 2003) (**Figures 1**, **2A**).

All slice cultures were treated with propidium iodide (PI; Merck Millipore, cat No. 537059) 2 h prior to fixation to visualize

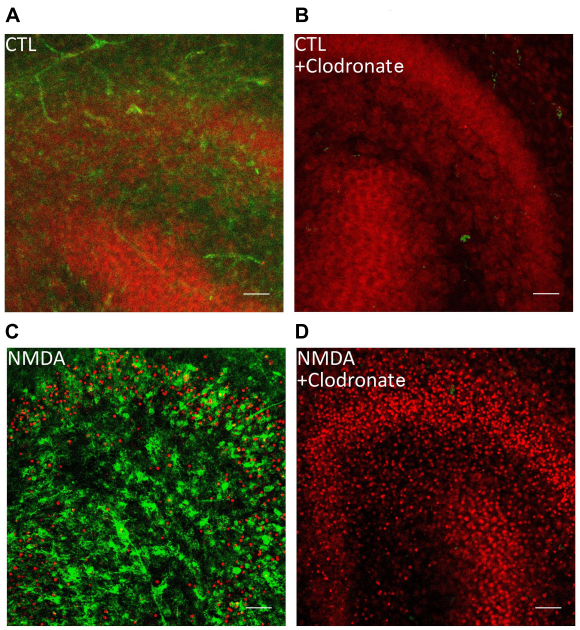

FIGURE 1 | Clodronate depletes microglial cells from OHSC. **(A)** PI labeled control OHSC with dentate gyrus and CA3. No PI positive nuclei (red) and ramified IB_4 (green) labeled microglial cells are visible. **(B)** Application of clodronate to CTL slices removed IB_4 positive microglial cells without damaging the neurons. **(C)** Treatment with NMDA led to massive increase in PI positive cells and IB_4 positive microglia. **(D)** Depletion of microglial cells led to exacerbation of neuronal damage after NMDA treatment in OHSC. Scale bar = 50 μm.

degenerated neurons (Ebrahimi et al., 2010; Grabiec et al., 2012, 2017; Hezel et al., 2012).

Immuno-, Lectinhistochemistry and Staining

All antibodies and lectins and conditions used are listed in **Table 1**. For labeling of incorporated BrdU fixed microglial cells were incubated with 2 mol/l HCl for 1 h, washed three times with PBS/Triton and pre-incubated with normal horse serum (Gibco BRL, Life Technologies, Eggenstein, Germany, cat No. 31874, dilution 1:20) in PBS/Triton. Afterward anti-BrdU antibody (**Table 1**) was applied for 1 h, followed by incubation with Alexa 488 conjugated goat anti-mouse antibody for 1 h. Cells were washed three times with PBS/Triton and incubated with 4′,6-diamidino-2-phenylindole (DAPI, Sigma-Aldrich, Munich, Germany, cat No. D9542).

Organotypic hippocampal slice cultures were stained with Alexa 488 conjugated IB_4 (Molecular Probes). All fluorescence stained slides were washed with PBS/Triton and Aqua dest. before covering with mounting medium (DAKO, Agilent Technologies, Inc., Santa Clara, CA, United States).

For measurement of ramification index biotin labeled IB_4 was used. To measure the PPARα distribution, an anti-PPARα antibody was applied as characterized before (Koch et al., 2011a). After washing with PBS, biotinylated goat anti-rabbit antibody

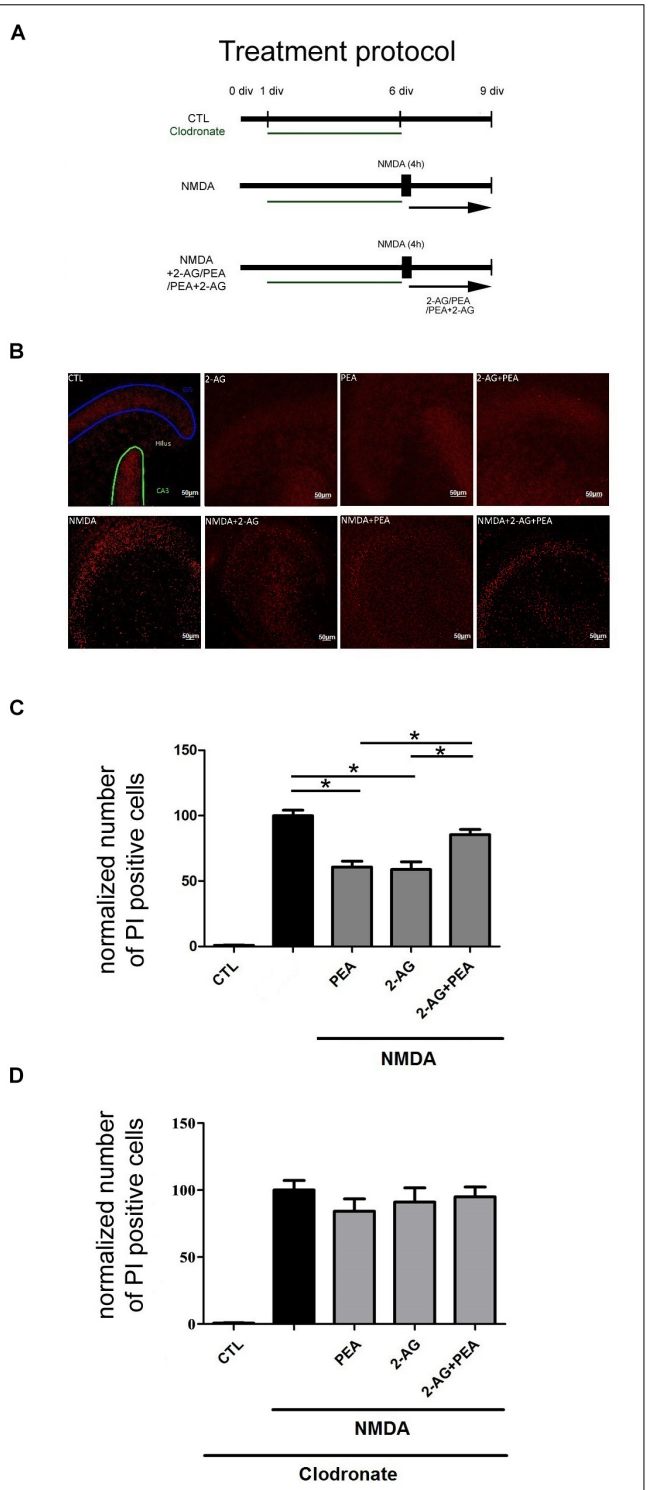

FIGURE 2 | Effects of 2-AG and PEA in excitotoxically damaged OHSC. 2-AG and PEA did not further decrease the number of PI positive degenerated neurons in comparison to OHSC treated with 2-AG or PEA alone. **(A)** Treatment protocol. Control OHSC (CTL), were kept in culture medium and served as negative controls. The NMDA treated group function as positive control (NMDA). For microglial cells depleted groups clodronate (green) was applied from 1 div until 6 div. Cannabinoids were added alone on day 6 *in vitro*

(Continued)

FIGURE 2 | Continued
(div) to OHSC or following 4 h incubation with NMDA (NMDA+2-AG/PEA/PEA+2-AG). The fixation was performed on 9 div. **(B)** Representative images of the dentate gyrus in OHSC stained with PI (in red). After NMDA damage a massive increase in the number of damaged neurons occurred in comparison to control group (CTL), PEA, and 2-AG significantly reduced the neurodegeneration, but combination of both did not significantly reduce the number of PI positive nuclei. Dentate gyrus (GD) is highlighted in blue, Cornu ammonis (CA) 3 in green. Scale bar = 50 μm. **(C)** Quantitative analysis of PI positive nuclei in treated groups. The number of PI positive neurons increased significantly after treatment with NMDA (n_{NMDA} = 42) in comparison to control group (n_{CTL} = 42). 2-AG, PEA alone or combination of both had no effect on viability of OHSC (n_{PEA} = 12, n_{2-AG} = 12, $n_{2-AG+PEA}$ = 10). Treatment with PEA ($n_{NMDA+PEA}$ = 23) or 2-AG ($n_{NMDA+2-AG}$ = 20) of excitotoxically damaged OHSC reduced significantly the number of PI positive cells. The combination of 2-AG and PEA after NMDA damage induced no significant protective effect ($n_{NMDA+2-AG+PEA}$ = 34). **(D)** Treatment of microglia depleted OHSC with NMDA induced a massive neuronal damage (n_{CTL} = 15, n_{NMDA} = 18). The application of PEA, 2-AG or combination of both to clodronate treated NMDA damaged OHSC had no significant effect on the number of PI positive cells ($n_{CLO+NMDA+2-AG}$ = 12, $n_{CLO+NMDA+PEA}$ = 12, $n_{CLO+NMDA+2-AG+PEA}$ = 14). Statistics was performed using a One-Way ANOVA with Bonferroni *post hoc* analysis and significance was chosen for $p < 0.05$. The asterisk denotes significant results regarding the respective measurement indicated with the bar. The values are served as a mean with standard error of the mean.

was applied for 1 h. The following subsequent steps were the same as for IB_4 staining: the cells were washed tree times with PBS and incubated with ExtrAvidin-Peroxidase for 1 h. After washing with PBS and Tris buffer, the slides were stained with 3,3′-Diaminobenzidine (DAB) (Sigma-Aldrich, cat No. D8001) and covered with Entallan (Merck Millipore, Darmstadt, Germany, cat No. 107960).

Microscopy and Analysis

For analysis of proliferation index, ramification index and PPARα staining five areas per cover slip were recorded with Leica DMi8 (Wetzlar, Germany) or Axioplan (Zeiss, Oberkochen, Germany) microscopes.

Proliferation index was represented as the ratio of BrdU positive cells to all DAPI positive cells. The BrdU positive cells were counted using image J v1.46r (National Institutes of Health, Laboratory for Optical and Computational Instrumentation, University of Wisconsin, Madison, WI, United States).

To evaluate the ramification of microglial cells, the surface of microglia was stained with IB_4 and the outlining of the cell was divided by the smallest convex hull around the cell. Values close to 1 correspond to strongly amoeboid cells while lower numbers represent ramified cells. The analysis was performed automatically using a self-written MatLab script (The MathWorks, Natick, MA, United States).

Next, the translocation of PPARα from the cytoplasm to the nucleus or vice versa was assessed after treatment with cannabinoids. PPARα staining was performed and manually evaluated by counting cells that showed a nuclear or/and cytoplasmic staining or were free of PPARα labeling. Results are presented as proportion of cells with a specific expression pattern relative to the total number of cells. For the calculation of the standard error of the mean in these experiments we used bootstrapping to calculate empirical standard deviations. Therefore all measurements were used and resampled 10,000 times. Afterward, the proportion of nuclear, cytoplasmic, nuclear+cytoplasmic location or no expression was calculated for each resampling and an empirical standard deviation and standard error of the mean was calculated.

The imaging of the fixed OHSC was performed using a confocal laser scanning microscope (LSM 510 Meta, Zeiss) with an excitation wavelength of 488 nm for IB_4 and 543 nm for PI. Emission was detected using a band-pass filter with $\Delta\lambda$ = 510–550 nm (IB_4) and $\Delta\lambda$ = 610–720 nm (PI). The dentate gyrus was visualized with a 20x objective, as a z-stack with a step width of 2 μm (Grabiec et al., 2012). The number of PI positive death cells in the obtained image stacks was analyzed using the maximal intensity projection and quantified using a self-written Matlab script.

Nitrite Assay

A standard solution was prepared by solving sodium nitrite in medium up to concentrations of 100, 50, 25, 12.5, 6.25, 3.125, and 1.5625 μM. The measured values were used for calculation of a standard curve. 50 μl of the standard solutions or 50 μl of the collected samples were analyzed in duplicate. After applying 50 μl of Griess reagent (Sigma-Aldrich) the extinction was measured after 15 min at 540 nm in a microplate reader (SynergyTM Mx, BioTek Instruments, Winooski, VT, United States). The nitrite concentrations for the samples were interpolated from the standard curves.

Statistical Analysis

Statistics was performed using the one-way ANOVA with Bonferroni post-test and significance was chosen for $p < 0.05$. All *p*-values refer to the respective controls of the same parameter of the same cell line or to the treatment with agonist for the respective receptor. All groups were normalized to the positive

TABLE 1 | Antibodies.

Name	Company	Number	Dilution	Antibody ID
Biotinylated goat anti-rabbit antibody	Sigma-Aldrich	B7389	1:100	
BrdU	DAKO	M0744	1:100	
Alexa 488 conjugated IB_4	Molecular Probes, Life Technologies, Eggenstein, Germany	I21411	1:500	AB_2314662
Biotin labeled IB_4	Vector Laboratories, Burlingame, CA, United States	B-1205	1:100	AB_2314661
ExtrAvidin-Peroxidase	Sigma-Aldrich	E2886	1:100	
PPARα	Thermo Fisher, Waltham, MA, United States	PA1-822A	1:500	AB_2165595

control. Statistics for cellular PPARα was performed using a Chi Square test and significance was chosen for $p < 0.05$. The values are served as a mean with standard error of the mean. The asterisk denotes significant results regarding the respective measurement indicated with the bar.

RESULTS

2-AG and PEA Do Not Further Decrease the Number of PI Positive Degenerated Neurons

The application of NMDA led to an increase in the number of PI positive cells in OHSC (100.0 ± 4.24%) in comparison to control group (0.86 ± 0.28%, **Figures 2B,C**).

Treatment of NMDA lesioned OHSC with PEA (60.64 ± 4.52%) or 2-AG (58.78 ± 5.94%) induced a significant reduction of neuronal damage. Combination of 2-AG and PEA (85.46 ± 3.92%) in excitotoxically damaged OHSC did not decrease the number of dead cells in a significant manner (**Figures 2B,C**). Notably the values were not significantly different when compared to NMDA group, but significantly higher when compared to NMDA+2-AG or NMDA+ PEA groups.

Depletion of Microglial Cells Leads to Loss of Neuroprotection

The application of NMDA to microglia depleted OHSC (**Figure 1**) led to a significant increase in the number of PI positive cells (100.0 ± 7.12%) in comparison to control group (0.74 ± 0.17%, **Figure 2D**). The depletion of microglial cells was controlled through IB_4 staining (**Figure 1**).

Neither the application of PEA (84.19 ± 9.29%) nor 2-AG (91.04 ± 10.68%) to NMDA damaged microglia depleted OHSC induced a significant neuroprotective effect. Also, the combination of 2-AG and PEA (94.93 ± 7.42%) to excitotoxically damaged microglia depleted OHSC showed any significant effect on the number of dead neurons (**Figure 2D**).

Effects of 2-AG and PEA Treatment on Ramification Index

Application of PEA (0.72 ± 0.01) or 2-AG (0.75 ± 0.02) had no impact on ramification index in comparison to control group (0.73 ± 0.01). Treatment with LPS (0.89 ± 0.01) led to a more amoeboid morphology of cells. Co-application of LPS and PEA reduced the ramification index significantly (0.76 ± 0.03) making cells more ramified. Incubation with 2-AG did not change the ramification index (0.84 ± 0.01) in comparison to LPS. However, PEA and 2-AG application together with LPS induced significant reduction in ramification index (0.76 ± 0.02) (**Figures 3A,C**).

Effects of 2-AG and PEA on Nitrite Concentration

Application of PEA (0.19 ± 0.1%), 2-AG (0.14 ± 0.06%), or PEA+2-AG (0.76 ± 0.30%) did not change the nitrite concentration in comparison to control group (0.48 ± 0.22%). Treatment with LPS (100.0 ± 2.24%) led to an increased concentration of nitrite. Whereas co-application of LPS and PEA reduced the nitrite concentration significantly (81.06 ± 4.6%), incubation with 2-AG increased the nitrite concentration (128.2 ± 5.52%) in comparison to LPS. The same increase was detected for application of 2-AG+ PEA+ LPS (134.5 ± 7.11%) (**Figure 3E**).

Effect of 2-AG and PEA on Proliferation of Primary Microglial Cells

After incubation with LPS (0.07 ± 0.01), PEA (0.13 ± 0.04), or 2-AG (0.12 ± 0.05) no significant changes in proliferation were detected in comparison to control group (0.097 ± 0.02). The results for PEA+2-AG (0.07 ± 0.02); LPS+PEA (0.07 ± 0.019); LPS+2-AG (0.09 ± 0.05); and LPS+PEA+2-AG (0.07 ± 0.03) were not significantly altered after treatment (**Figures 3B,D**). The overall test showed no significant differences between the groups.

PPARα Distribution and Cellular Localization After Incubation With 2-AG and PEA

The evaluation of the localization of the PPARα receptor was significantly altered for treated groups overtime (1, 6, 24 h) (**Figures 4A–E**). The positive staining was localized in the cytoplasm and in the nucleus. The subcellular location was scored in 483 (1 h), 362 (6 h), and 337 (24 h) cells by light microscopy and presented as percentage. Each independent experiment was repeated at least three times ($n = 3$). The number of cells expressing nuclear as compared to cytoplasmic PPARα was significantly different between groups. Treatment with PEA; 2-AG; and LPS induced a significant shift in PPARα distribution after 1 and 6 h from nuclear to cytoplasmic and from cytoplasmic to nuclear localization. PEA and LPS changed significantly the localization of the receptor after 24 h (**Figures 4A–C**). The distribution was significantly different between 2-AG (Nucleus, N: 36%, Cytoplasm, C:21%, Both, B:33%, No signal, None:10%) and 2-AG co-applied with PEA (N:50%, C:4%, B:43%, None:4%) after 1 h, between PEA (N:49%, C:11%, B:38%, None:2%) and 2-AG+PEA (N:22%, C:11%, B:51%, None:16%) after 6 h and between PEA (N:51%, C:3%, B:36%, None:10%) or 2-AG (N:11%, C:7%, B:83%, None:0%) and 2-AG+PEA (N:29%, C:2%, B:66%, None:2%) after 24 h. PEA ($N_{1\ h}$:51%, $C_{1\ h}$:5%, $B_{1\ h}$:17%, $None_{1\ h}$:27%; $N_{6\ h}$:61%, $C_{6\ h}$:7%, $B_{6\ h}$:18%, $None_{6\ h}$:14%), 2-AG ($N_{1\ h}$:67%, $C_{1\ h}$:3%, $B_{1\ h}$:29%, $None_{1\ h}$:1%; $N_{6\ h}$:30%, $C_{6\ h}$:11%, $B_{6\ h}$:34%, $None_{6\ h}$:26%) and PEA+2-AG ($N_{1\ h}$:54%, $C_{1\ h}$:14%, $B_{1\ h}$:20%, $None_{1\ h}$:12%; $N_{6\ h}$:21%, $C_{6\ h}$:21%, $B_{6\ h}$:35%, $NS_{6\ h}$:23%) changed significantly the localization of PPARα after 1 and 6 h in combination with LPS (vs. LPS; $N_{1\ h}$:25%, $C_{1\ h}$:15%, $B_{1\ h}$:53%, $None_{1\ h}$:7%; $N_{6\ h}$:67%, $C_{6\ h}$:10%, $B_{6\ h}$:20%, $None_{6\ h}$:3%). No effect could be observed for LPS+PEA (N: 22%, C: 3%, B: 69%, None: 6%) in comparison to LPS (N: 28%, C: 2%, B: 56%, None: 14%) after 24 h, but 2-AG (N: 27%, C: 2%, B: 69%, None: 2%) and 2-AG+PEA (N: 20%, C: 0%, B: 80%, None: 0%) if co-applied

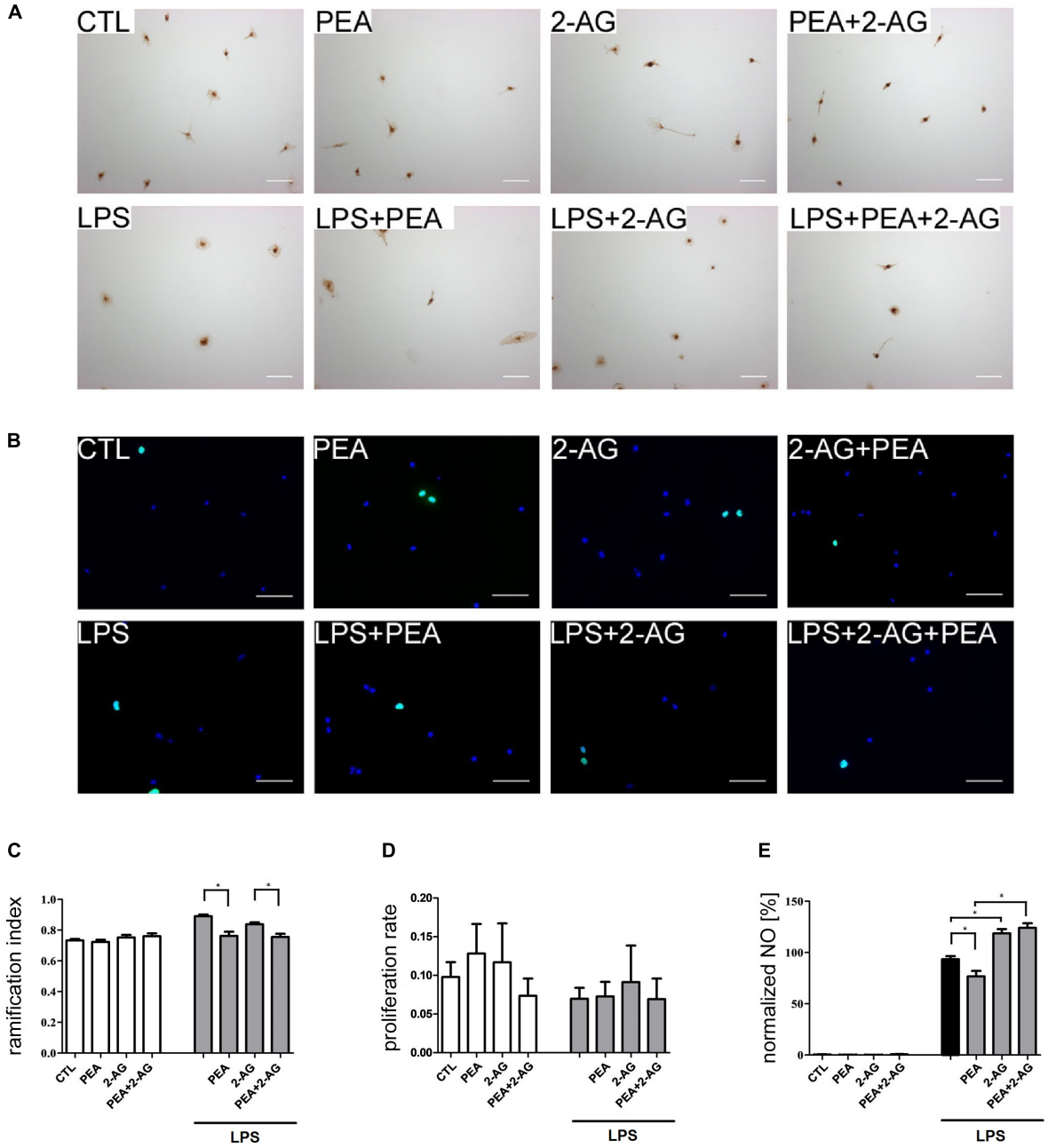

FIGURE 3 | Effect of 2-AG and PEA on ramification index, proliferation index and nitrite concentration of primary rat microglia. Representative pictures of stained microglia for **(A)** ramification index (IB_4) and **(B)** proliferation rate (BrdU in green, DAPI in blue). Scale bar = 50 μm. **(C)** Effects of 2-AG and PEA on ramification index. Application of LPS (n_{LPS} = 22) led to an increase in the ramification index in comparison to control group (CTL; n_{CTL} = 22). Whereas PEA co-applied with LPS ($n_{LPS+PEA}$ = 23) reduced the ramification index significantly, 2-AG ($n_{LPS+2-AG}$ = 23) had no effect. 2-AG, PEA, or combination of both applied alone (n_{PEA} = 19, n_{2-AG} = 22, $n_{2-AG+PEA}$ = 22) had no effect on ramification index. The combination of LPS, 2-AG and PEA ($n_{LPS+2-AG+PEA}$ = 22) led to decrease in the ramification index in comparison to the groups treated with LPS and 2-AG. **(D)** No effect of 2-AG and PEA with/or without LPS on proliferation of primary microglia cells could be observed (n_{CTL} = 12, n_{LPS} = 12, n_{PEA} = 11, n_{2-AG} = 11, $n_{2-AG+PEA}$ = 12, $n_{LPS+PEA}$ = 12, $n_{LPS+2-AG}$ = 11, $n_{LPS+2-AG+PEA}$ = 12). **(E)** Effects of 2-AG and PEA on nitrite concentration after 72 h. PEA, 2-AG, or PEA combined with 2-AG had no effect on the nitrite concentration in primary microglia (n_{CTL} = 18, n_{PEA} = 18, n_{2-AG} = 18, $n_{2-AG+PEA}$ = 18). After administration of LPS, nitrite concentration increased significantly. PEA co-applied with LPS ($n_{LPS+PEA}$ = 18) decreased the NO production in comparison to LPS (n_{LPS} = 18). 2-AG+LPS ($n_{LPS+2-AG}$ = 18) and also 2-AG+PEA+LPS ($n_{LPS+2-AG+PEA}$ = 18) treated microglia produced significantly more NO in comparison to LPS. Statistics was performed using a one-way ANOVA test with Bonferroni correction and significance was chosen for $p < 0.05$. The asterisk denotes significant results regarding the respective measurement indicated with the bar. The values are served as a mean with standard error of the mean.

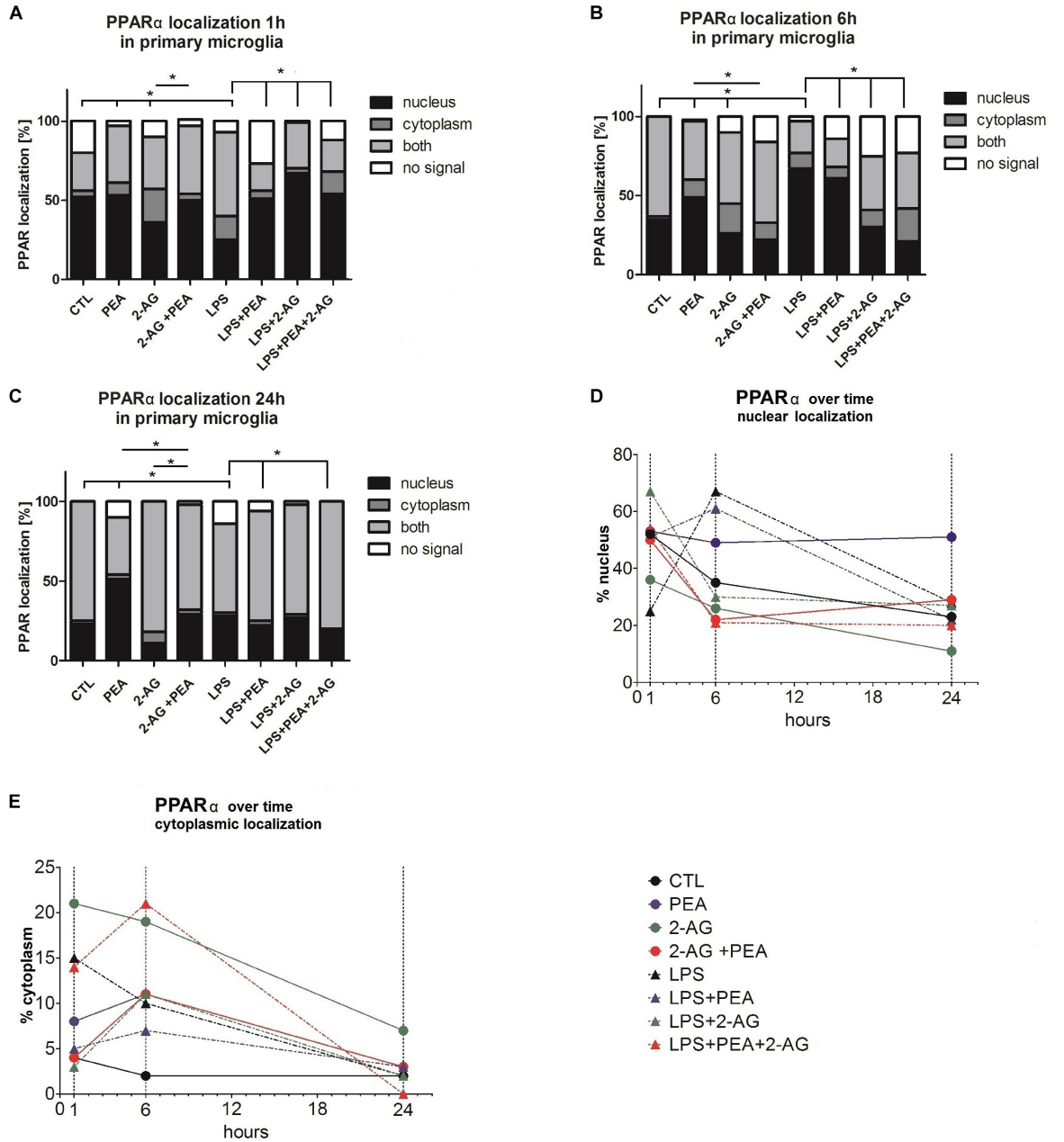

FIGURE 4 | PPARα subcellular distribution and cellular localization after incubation with 2-AG and PEA in primary microglial cells. The localization of PPARα was analyzed over time by the use of staining **(A–C)** 1, 6, and 24 h after treatment, **(D)** nuclear, **(E)** cytoplasmic localization (1, 6, and 24 h after treatment). The number of cells which did not or expressed PPARα in the nucleus or/and cytoplasm was counted. In graphs **(A–E)** the subcellular location was scored in 483 (1 h), 362 (6 h), and 337 (24 h) cells by light microscopy and presented as percentage. Each independent experiment was repeated at least three times. The same data are displayed in two different ways to point out the differences in the distribution **(A–C)** between the time points for cytoplasmic and nuclear localization **(D,E)**. Statistics was performed using a Chi Square test and significance was chosen for $p < 0.05$. The asterisk denotes significant results regarding the respective measurement indicated with the bar. The values are served as a mean with standard error of the mean.

with LPS altered significantly the distribution (**Figures 4A–C** and **Table 2**).

Lipopolysaccharide alone induced a shift to nuclear localization after 6 h, whereas LPS+PEA+2-AG after 6 h led to more cytoplasmic expression, similar to 2-AG and PEA alone (**Figures 4D,E**).

DISCUSSION

Reduction of neuronal damage in injured patients is a main contributor to sustain quality of life, for this reason its improvement and new approaches are needed. Evidence has accumulated that endocannabinoids can be beneficial for

TABLE 2 | PPARα subcellular distribution and cellular localization after incubation with 2-AG and PEA in primary microglial cells.

	Mean	SEM	Mean	SEM	Mean	SEM	Mean	SEM	Mean	SEM	Mean	SEM	Mean	SEM
Localization	**CTL**		**PEA**		**2-AG**		**2-AG+PEA**		**LPS**		**LPS+PEA**		**LPS+2-AG**		**LPS+2-AG+PEA**	
1 h																
Nucleus	0.53	0.01	0.39	0.01	0.30	0.01	0.34	0.01	0.18	0.01	0.26	0.02	0.65	0.01	0.38	0.01
Cytoplasm	0.04	0.00	0.06	0.00	0.18	0.01	0.03	0.01	0.10	0.00	0.03	0.01	0.03	0.00	0.10	0.00
Both	0.24	0.01	0.26	0.01	0.28	0.01	0.29	0.01	0.36	0.01	0.09	0.01	0.29	0.01	0.14	0.01
No signal	0.20	0.01	0.03	0.00	0.09	0.00	0.03	0.01	0.05	0.00	0.14	0.01	0.01	0.00	0.09	0.00
6 h																
Nucleus	0.35	0.01	0.51	0.01	0.22	0.01	0.20	0.01	0.51	0.01	0.53	0.01	0.27	0.01	0.18	0.01
Cytoplasm	0.02	0.00	0.12	0.01	0.16	0.01	0.10	0.01	0.08	0.01	0.06	0.01	0.10	0.01	0.18	0.01
Both	0.63	0.01	0.39	0.01	0.37	0.01	0.45	0.01	0.16	0.01	0.16	0.01	0.31	0.01	0.29	0.01
No signal	0.00	0.00	0.02	0.00	0.08	0.01	0.14	0.01	0.02	0.00	0.12	0.01	0.24	0.01	0.20	0.01
24 h																
Nucleus	0.23	0.01	0.50	0.01	0.13	0.01	0.30	0.01	0.30	0.01	0.18	0.01	0.35	0.01	0.23	0.01
Cytoplasm	0.03	0.00	0.03	0.00	0.08	0.01	0.03	0.00	0.03	0.00	0.03	0.01	0.03	0.00	0.00	0.00
Both	0.75	0.01	0.35	0.01	0.95	0.01	0.68	0.01	0.60	0.01	0.55	0.01	0.90	0.01	0.90	0.01
No signal	0.00	0.00	0.10	0.01	0.00	0.00	0.03	0.00	0.15	0.01	0.05	0.01	0.03	0.00	0.00	0.00

Rounded mean values (two positions) and SEM.

treatment of patients with brain injury (Fernandez-Ruiz et al., 2010). Cannabinoids, as shown before have different targets and are potential therapeutics, but first it is necessary to better understand the molecular and cellular mechanisms of cannabinoid action.

The Protective Effects of 2-AG and PEA Are Abolished, When Both Are Applied Together

In this study, we focused on excitotoxicity, a main factor of neuronal damage as described before (Kunz et al., 2010; Lau and Tymianski, 2010). To investigate the intrinsic responses and to exclude interfering influences such as blood flow and infiltrating peripheral immune cells the well-established model of excitotoxic lesioned OHSC was chosen. Both, PEA and 2-AG were shown to be protective with microglia participation in NMDA lesioned OHSC before. In our previous studies we extensively examined the involvement of cannabinoid receptors in PEA and 2-AG mediated actions. Whereas PEA and the synthetic PPARα agonist Wy-14,643 protected dentate gyrus granule cells, treatment with the PPARα antagonist GW6471 blocked PEA-mediated neuroprotection. Selective activation or inhibition of PPARγ displayed no positive effect (Koch et al., 2011a). Interestingly, 2-AG induced neuroprotection was inhibited by cannabidiol (CBD) and O-1918 and mimicked by abn-CBD indicating the involvement of abn-CBDR. The 2-AG effects were not blocked by the specific CB_2 receptor antagonist (AM630). Depletion of microglial cells abolished the neuroprotection mediated by 2-AG or abn-CBD raising the hypothesis that the neuroprotective effects of 2-AG were abn-CBDR and microglia dependent (Kreutz et al., 2007, 2009). The abn-CBDR is a pharmacologically characterized non-CB_1/non-CB_2 receptor and has been first described on endothelial cells of rat mesenteric blood vessels (Járai et al., 1999; Pertwee et al., 2010), and has not been identified yet. PEA, 2-AG or their analogs were also protective in other models like moderate traumatic injury and reduced neuroinflammation (Panikashvili et al., 2001; Genovese et al., 2008; D'Agostino et al., 2012; Esposito et al., 2012; Mounsey et al., 2015; Guida et al., 2017; Belardo et al., 2019; Impellizzeri et al., 2019). In PPARα$^{-/-}$ mice PEA induced neuroprotection after spinal cord trauma was abolished, however involvement of further PPARs was suggested (Paterniti et al., 2013). The application of PEA was found to trigger the synthesis of 2-AG in human and canine plasma and enhance its effects on transient receptor potential cation channel subfamily V member 1 (TRPV1) in HEK-293 cells (Petrosino et al., 2016). In striatum PEA triggered the synthesis of 2-AG via GPR55 (Musella et al., 2017). These effects were referred to an entourage effect, which might be mediated through TRPV1 activation or inhibition of fatty acid amide hydrolase, with PEA as its substrate or activation of GPR55 (Jonsson et al., 2001; Smart et al., 2002). A further possible explanation is an allosteric modulation, which could explain that 2-AG and PEA abolished their neuroprotective properties in the OHSC model and reduced ramification index at PEA level. While TRPV1 was not found in OHSC, GPR55

was expressed in slices and was associated with neuroprotection (Grabiec et al., 2012; Kallendrusch et al., 2013). Consequently, GPR55 might be involved in the PEA mediated actions observed here. Furthermore, PEA was also shown to enhance the CB_2 expression via PPARα activation in macrophages (Guida et al., 2017). Increased number of CB_2 next to abn-CBDR can be activated by 2-AG and induce further effects. PEA at cellular level reduced ramification index, making cells more ramified whereas 2-AG had no impact on morphology of microglial cells. The decrease in neuroprotection mediated by co-treatment with both cannabinoids might be attributable to their effects on cellular level, especially on microglial cells, the conductor of the neuroprotective properties of 2-AG and PEA. An entourage effect with PEA as enhancer of the anti-inflammatory and anti-nociceptive activity of other endogenous compounds by potentiating their affinity for a receptor or by inhibiting their metabolic degradation (Skaper and Facci, 2014) is missing in OHSC in the context of neuroprotection.

Effects of PEA and 2-AG Are Microglia Dependent

Neuroprotective capabilities of microglial cells include synaptic stripping, induction of neurogenesis, phagocytosis, and maintenance of central nervous system homeostasis (Chen and Trapp, 2016). On the other hand microglial cells are also able to suppress neuroinflammation, protect nerve tissue by producing anti-inflammatory and tissue-repairing cytokines and factors (Colton, 2009). Microglial cells can contribute to neuronal damage via inflammation and release of cytotoxic substances as described earlier and are associated with neurodegenerative diseases, cognitive dysfunction in aging and dementia, epilepsy, and other conditions leading to brain inflammation and neuronal lesion (Ekdahl et al., 2003; Smith et al., 2012; Chhor et al., 2013). Cannabinoids were shown to interact with microglial cells in further pathological states and to change the morphology, activation and number of the cells (Zhang et al., 2003; Luongo et al., 2010; Guida et al., 2017).

After microglia depletion in OHSC with the bisphosphonate clodronate PEA and 2-AG lost their neuroprotective effects supporting the hypothesis that 2-AG, PEA exert their neuroprotective effects via microglial cells. PEA was shown before to induce migration and increase of motility of BV2 microglial cell line (Franklin et al., 2003; Guida et al., 2017). Notably, microglial cells produce both 2-AG and PEA (Muccioli et al., 2007; Muccioli and Stella, 2009) and their levels were found to be increased after focal cerebral ischemia (Franklin et al., 2003).

PEA and 2-AG Mediate Opposite Effects on Nitric Oxide Synthesis in Primary Microglial Cells

Endocannabinoids, which are in part produced by microglia, affect the ability of microglia cells to proliferate, phagocytize, and produce NO (Stella, 2009). NO production occurs enzymatically via a conversion of L-arginine to L-citrulline by NO synthase, competing with arginase for L-arginine as a substrate. iNOS is not expressed in healthy brain tissue under physiological conditions but its expression can be induced in astrocytes and microglial cells through trauma. iNOS induction starts several hours before NO is generated and involves transcription of mRNA and novel protein synthesis. iNOS is mainly expressed under inflammatory conditions and after transient ischemic periods and is known as an antimicrobial defense mechanism of the immune system (Vincent et al., 1998). The increase in NO driven by iNOS might be neurotoxic as it forms reactive nitrogen oxide species like peroxynitrite (Garry et al., 2015). It was reported that 2-AG alone stimulates the release of NO from human immune and vascular tissues and from invertebrate immune cells via CB_1 activation (Stefano et al., 2000). Contrary, in our study 2-AG or PEA applied alone had no effect on NO production by microglial cells after 72 h. However, LPS in combination with 2-AG increased NO concentration, although 2-AG was protective after NMDA damage. PEA was able to reduce NO production by microglial cells after LPS treatment. In accordance to this study PEA significantly inhibited the NO release induced by LPS in murine macrophage cell line RAW264.7, which was not sensitive to pertussis toxin treatment, indicating a G-protein independent mode of action (Ross et al., 2000). Pre-treatment of LPS-stimulated primary mouse microglial cells with PPARα agonists also resulted in inhibition of NO production (Xu et al., 2005). In similarity to PEA in murine macrophage cell line RAW264.7, WIN55,212, a neuroprotective cannabinoid decreased NO level when applied together with LPS via CB_2 receptor (Ross et al., 2000; Koch et al., 2011b). Furthermore, PEA reduced iNOS expression in spinal cord 6 h after paw edema induction (D'Agostino et al., 2007). The results presented in our study are in accordance with previous investigations and strengthen the hypothesis that PEA mediates neuroprotection via microglial cells. The neuroprotective effects observed here in the OHSC model underline the intrinsic positive effects of cannabinoids as influences through alterations in cerebral blood flow and infiltration of peripheral cells are missing (Grabiec et al., 2017), making the inhibition of NO produced by microglial cells one possible explanation for neuroprotection. In agreement with our work and previous studies LPS induces NO production mainly in microglial cells in models of excitotoxicity or during transient ischemic periods (Nakamura et al., 1999; Genovese et al., 2008; Yao et al., 2017). Further endocannabinoids were shown to decrease iNOS activity in rat microglial cells, e.g., CP55940 exerted a dose-dependent inhibition of interferon gamma /LPS-inducible NO production (Cabral et al., 2001) Little is known about the influence of endocannabinoids on arginase, in peripheral immune cells and in microglial N9 cells Δ-9- tetrahydrocannabinol and CB_2 agonist induced arginase 1 expression, what reduce NO production (Hegde et al., 2010; Ma et al., 2015).

Through combination treatment of both PEA and 2-AG, NO production was significantly elevated and neuroprotective properties were diminished. It leads to the hypothesis that PEA may be neuroprotective through reduction of NO present after brain injury. On the other hand, 2-AG significantly elevated NO production while still exerting neuroprotective effects similar

to NO donors (Kakizawa et al., 2007), 2-AG acts probably via another targets and mechanisms.

Changes in Morphology and Phenotypes of Primary Microglial Cells After Treatment

In vivo, *ex vivo,* and *in vitro* a broad spectrum of differentiation stages of microglial cells has been observed (Dubbelaar et al., 2018). Under physiological conditions microglial cells are ramified and constantly scanning their surroundings (Nimmerjahn et al., 2005). Upon damage or inflammation, they become amoeboid, move to the site of neuronal lesion and remove cell debris. However, this morphological change of microglia upon a shift in activation state does not seem to be uniform, but it can be best mimicked by administration of LPS. The morphology ranges from amoeboid-like shapes during inflammation to highly ramified ones and includes many intermediate forms that are often associated with the activation status of microglial cells (Zhou et al., 2017; Dubbelaar et al., 2018). According to the phenotype microglial cells were often described as anti-inflammatory or neuroprotective or proinflammatory and neurotoxic. However, there is no binary system of phenotypes for microglia and they may possess multiple context dependent properties at the same time (Ransohoff, 2016; Dubbelaar et al., 2018).

In synopsis with NO reduction, the administration of PEA to LPS stimulated microglial cells induced a more ramified morphology; these anti-inflammatory properties of PEA may mediate its neuroprotective effects. 2-AG did not alter the LPS induced amoeboid state of microglial cells but increased the NO concentration, indicating that the neuroprotective properties of 2-AG are mediated through other microglial cell dependent mechanisms than those involving NO. However, *in vivo* and in acute experimental autoimmune encephalomyelitis 2-AG increased the ramification of microglia (Lourbopoulos et al., 2011). In excitotoxically lesioned OHSC 2-AG reduced the number of microglial cells (Kreutz et al., 2007). It is plausible that the absence of changes is model dependent or that 2-AG influenced other properties of microglia, which were not examined in this study, like phagocytosis, motility, and alterations in extracellular signaling.

The combination of 2-AG and PEA induced a ramification of microglial cells in comparison to 2-AG and abolished PEA mediated NO concentration decrease. This may indicate that the anti-inflammatory properties of PEA are lost if co-incubated with 2-AG, since decrease in the number of damaged neurons in OHSC was missing and therefore neuroprotection. 2-AG and PEA exert contrary effects on microglial cells and it is plausible, that co-application of both led to their abolishment. Expected entourage effect is missing in case of this model and those substances.

It will be necessary to verify how 2-AG exerts neuroprotection at a cellular level and whether this process is microglia dependent only, since 2-AG was found protective in isolated neuronal cultures (Zhang and Chen, 2008). Interestingly, proliferation of pure microglial cell cultures was not affected in this study, whereas the number of microglial cells was significantly decreased in dentate gyrus in OHSC after excitotoxical damage and treatment with PEA or 2-AG, this effect was mimicked by PPARα agonists and blocked by its antagonists (Kreutz et al., 2007; Koch et al., 2011a). Since microglial cells in culture proliferate very slowly without astrocytes, it seems plausible that the effects observed in OHSC might be the result of PEA actions on astrocytes, microglia, possibly neurons in the network and/or their cross-talk, since all cell types express the PPARα receptor (Xu et al., 2006; Warden et al., 2016).

PPARα Expression and Localization Changed After Incubation With Cannabinoids

Peroxisome proliferator-activated receptors predominantly are localized in the nucleus, theirs activity is modulated via phosphorylation and PPARα undergoes ligand-dependent nucleo-cytoplasmic shuttling (Burns and Vanden Heuvel, 2007; Umemoto and Fujiki, 2012). The amount of PPARα was shown to increase in microglial cells in nucleus after 6 h and to decrease after 24 h after PEA treatment. PPARs are ligand-activated transcription factors, and their biological role is coupled to the function of their target genes. In immunocytochemical staining a translocation of PPARα into the nucleus was seen. Neuroprotective effects of PEA are known to be mediated by PPARα. On the one hand, the nuclear localization of the receptor induces specific PEA related effects; its shift into the cytoplasm reduces the amount of available receptor in the nucleus. On the other hand the cytoplasmic localization of PPARα may favor the binding of other ligands and mediate different actions (Guida et al., 2017). The lower levels of PPARα in nuclei of microglial cells after simultaneous treatment with 2-AG and PEA with or without LPS might be a possible explanation for the missing neuroprotection in OHSC. It also indicates an interference between 2-AG and PEA signaling pathways with a more dominant role of 2-AG and inhibitory actions on PPARs translocation into the nucleus. Specific activation of central PPARα controls inflammation in the spinal cord as well as in the periphery (D'Agostino et al., 2007), when the amount of receptor decreased no effect could be induced. Additionally, fatty acid oxygenase metabolism products of 2-AG were able to activate PPARα receptor in human undifferentiated epidermal keratinocytes and stimulation of PPARα and its downstream target genes led to cell differentiation (Kömüves et al., 2000; Kozak et al., 2002). It is plausible that 2-AG and PEA interact directly on PPARα receptor in the opposite way.

CONCLUSION

While endocannabinoids are promising regarding treatment of neuronal diseases, and their neuroprotective properties are known for a while, little is known how they are mediated. 2-AG and PEA are both protective agents with different targets. Their positive effect is not enhanced by co-incubation. The understanding of interactions between signaling pathways of

different endocannabinoids will help to elucide the in part conflicting results reported in the literature.

DATA AVAILABILITY STATEMENT

All datasets generated for this study are included in the article/supplementary material.

ETHICS STATEMENT

The animal study was reviewed and approved by the local authorities of the State of Saxony-Anhalt (permission number: I11M18, date: 01.12.2012) protecting animals and regulating tissue collection used for scientific purposes.

AUTHOR CONTRIBUTIONS

FD and UH: conceptualization, supervision, and project administration. MP, UH, TH, and JK: methodology and formal analysis. TH: software and data curation. MP, UH, TH, and FD: validation. MP, UH, JK, TH, and CG: investigation. FD: resources. UH and MP: visualization and writing original draft. UH, TH, JK, and FD: writing review and editing. All authors contributed to the manuscript revision, and read and approved the submitted version.

FUNDING

We acknowledge the financial support within the funding program Open Access Publishing by the German Research Foundation (DFG).

REFERENCES

Beggiato, S., Borelli, A. C., Ferraro, L., Tanganelli, S., Antonelli, T., and Cristina Tomasini, M. (2018). Palmitoylethanolamide blunts activation and improves neuronal survival in primary mouse cortical astrocytes-neuron co-cultures. *J. Alzheimer's Dis.* 61, 389–399. doi: 10.3233/JAD-170699

Belardo, C., Iannotta, M., Boccella, S., Rubino, R. C., Ricciardi, F., Infantino, R., et al. (2019). Oral cannabidiol prevents allodynia and neurological dysfunctions in a mouse model of mild traumatic brain injury. *Front. Pharmacol.* 10:352. doi: 10.3389/fphar.2019.00352

Ben-Shabat, S., Fride, E., Sheskin, T., Tamiri, T., Rhee, M.-R., Vogel, Z., et al. (1998). An entourage effect: inactive endogenous fatty acid glycerol esters enhance 2-arachidonoyl-glycerol cannabinoid activity. *Eur. J. Pharmacol.* 353, 23–31. doi: 10.1016/s0014-2999(98)00392-6

Bruce, A. J., Sakhi, S., Schreiber, S. S., and Baudry, M. (1995). Development of kainic acid and N-methyl-d-aspartic acid toxicity in organotypic hippocampal cultures. *Exp. Neurol.* 132, 209–219. doi: 10.1016/0014-4886(95)90026-8

Burns, K. A., and Vanden Heuvel, J. P. (2007). Modulation of PPAR activity via phosphorylation. *Biochim. Biophys. Acta* 1771, 952–960. doi: 10.1016/j.bbalip.2007.04.018.Modulation

Cabral, G. A., Harmon, K. N., and Carlisle, S. J. (2001). "Cannabinoid-mediated inhibition of inducible nitric oxide production by rat microglial cells: evidence for receptor participation," in *Neuroimmune Circuits, Drugs of Abuse, and Infectious Diseases*, eds H. Friedman, T. W. Klein, and J. J. Madden (Boston, MA: Springer), 207–214. doi: 10.1007/0-306-47611-8_24

Calignano, A., Rana, G., La Giuffrida, A., and Piomelli, D. (1998). Control of pain initiation by endogenous cannabinoids. *Nature* 394, 277–281. doi: 10.1038/28393

Carrier, E. J., Kearn, C. S., Barkmeier, A. J., Breese, N. M., Yang, W., Nithipatikom, K., et al. (2004). Cultured rat microglial cells synthesize the endocannabinoid 2-arachidonylglycerol, which increases proliferation via a CB 2 receptor-dependent mechanism. *Mol. Pharmacol.* 65, 999–1007. doi: 10.1124/mol.65.4.999

Chen, Z., and Trapp, B. D. (2016). Microglia and neuroprotection. *J. Neurochem.* 136, 10–17. doi: 10.1111/jnc.13062

Chhor, V., Le, T., Lebon, S., Oré, M.-V., Celador Lara, I., Josserand, J., et al. (2013). Brain, behavior, and immunity characterization of phenotype markers and neuronotoxic potential of polarised primary microglia *in vitro*. *Brain Behav. Immun.* 32, 70–85. doi: 10.1016/j.bbi.2013.02.005

Citraro, R., Russo, E., Scicchitano, F., Rijn, C. M., Van Cosco, D., Avagliano, C., et al. (2013). Neuropharmacology Antiepileptic action of N - palmitoylethanolamine through CB1 and PPAR- a receptor activation in a genetic model of absence epilepsy. *Neuropharmacology* 69, 115–126. doi: 10.1016/j.neuropharm.2012.11.017

Colton, C. A. (2009). Heterogeneity of microglial activation in the innate immune response in the brain. *J. Neuroimmune. Pharmacol.* 4, 399–418. doi: 10.1007/s11481-009-9164-4

D'Agostino, G., Rana, G., La Russo, R., Sasso, O., Iacono, A., Esposito, E., et al. (2007). Acute intracerebroventricular administration of palmitoylethanolamide, an endogenous peroxisome proliferator-activated receptor-alpha agonist, modulates carrageenan-induced paw edema in mice. *J. Pharmacol. Exp. Ther.* 332, 1137–1143. doi: 10.1124/jpet.107.123265

D'Agostino, G. D., Russo, R., Avagliano, C., Cristiano, C., Meli, R., and Calignano, A. (2012). Palmitoylethanolamide protects against the amyloid- B 25-35-induced learning and memory impairment in mice, an experimental model of alzheimer disease. *Neuropsychopharmacology* 37, 1784–1792. doi: 10.1038/npp.2012.25

Dirnagl, U., Simon, R. P., and Hallenbeck, J. M. (2003). Ischemic tolerance and endogenous neuroprotection. *Trends Neurosci.* 26, 248–254. doi: 10.1016/S0166-2236(03)00071-7

Dubbelaar, M. L., Kracht, L., Eggen, B. J. L., and Boddeke, E. W. G. M. (2018). The kaleidoscope of microglial phenotypes. *Front. Immunol.* 9:1753. doi: 10.3389/fimmu.2018.01753

Ebrahimi, F., Hezel, M., Koch, M., Ghadban, C., Korf, H. W., and Dehghani, F. (2010). Analyses of neuronal damage in excitotoxically lesioned organotypic hippocampal slice cultures. *Ann. Anat.* 192, 199–204. doi: 10.1016/j.aanat.2010.06.002

Ekdahl, C. T., Claasen, J., Bonde, S., Kokaia, Z., and Lindvall, O. (2003). Inflammation is detrimental for neurogenesis in adult brain. *PNAS* 100, 13632–13637.

Esposito, E., Impellizzeri, D., Mazzon, E., Paterniti, I., and Cuzzocrea, S. (2012). Neuroprotective activities of palmitoylethanolamide in an animal model of parkinson ' s disease. *PLoS One* 7:e41880. doi: 10.1371/journal.pone.0041880

Facchinetti, F., Del Giudice, E., Furegato, S., Passarotto, M., and Leon, A. (2003). Cannabinoids ablate release of TNFalpha in rat microglial cells stimulated. *Glia* 41, 161–168. doi: 10.1002/glia.10177

Fernandez-Ruiz, J., Garcia, C., Sagredo, O., Gomez-Ruiz, M., and de Lago, E. (2010). The endocannabinoid system as a target for the treatment of neuronal damage. *Expert Opin. Ther. Targets* 14, 387–404. doi: 10.1517/14728221003709792

Fernández-Ruiz, J., Moro, M. A., and Martínez-Orgado, J. (2015). Cannabinoids in neurodegenerative disorders and stroke / brain trauma: from preclinical models to clinical applications. *Neurotherapeutics* 12, 793–806. doi: 10.1007/s13311-015-0381-7

Franklin, A., Parmentier-batteur, S., Walter, L., Greenberg, D. A., and Stella, N. (2003). Palmitoylethanolamide increases after focal cerebral ischemia and

potentiates microglial cell motility. *J. Neurosci.* 23, 7767–7775. doi: 10.1523/jneurosci.23-21-07767.2003

Franklin, A., and Stella, N. (2003). Arachidonylcyclopropylamide increases microglial cell migration through cannabinoid CB 2 and abnormal-cannabidiol-sensitive receptors. *Eur. J. Pharmacol.* 474, 195–198. doi: 10.1016/S0014-2999(03)02074-0

Garry, P. S., Ezra, M., Rowland, M. J., Westbrook, J., and Pattinson, K. T. S. (2015). The role of the nitric oxide pathway in brain injury and its treatment — From bench to bedside. *Exp. Neurol.* 263, 235–243. doi: 10.1016/j.expneurol.2014.10.017

Genovese, T., Esposito, E., Mazzon, E., Paola, R., Di Meli, R., Bramanti, P., et al. (2008). Effects of palmitoylethanolamide on signaling pathways implicated in the development of spinal cord injury. *J. Pharmacol. Exp. Ther.* 326, 12–23. doi: 10.1124/jpet.108.136903.recent

Grabiec, U., Hohmann, T., Hammer, N., and Dehghani, F. (2017). Organotypic hippocampal slice cultures as a model to study neuroprotection and invasiveness of tumor cells. *J. Vis. Exp.* 126:e55359. doi: 10.3791/55359

Grabiec, U., Koch, M., Kallendrusch, S., Kraft, R., Hill, K., Merkwitz, C., et al. (2012). The endocannabinoid N-arachidonoyldopamine (n.d.) exerts neuroprotective effects after excitotoxic neuronal damage via cannabinoid receptor 1 (CB 1). *Neuropharmacology* 62, 1797–1807. doi: 10.1016/j.neuropharm.2011.11.023

Guida, F., Luongo, L., Boccella, S., Giordano, M. E., Romano, R., Bellini, G., et al. (2017). Palmitoylethanolamide induces microglia changes associated with increased migration and phagocytic activity: involvement of the CB2 receptor. *Sci. Rep.* 7:375. doi: 10.1038/s41598-017-00342-1

Hagemann, C., Fuchs, S., Monoranu, C. M., Herrmann, P., Smith, J., Hohmann, T., et al. (2013). Impact of MACC1on human malignant glioma progression and patients' unfavorable prognosis. *Neuro. Oncol.* 15, 1696–1709. doi: 10.1093/neuonc/not136

Hegde, V. L., Nagarkatti, M., and Nagarkatti, P. S. (2010). Cannabinoid receptor activation leads to massive mobilization of myeloid-derived suppressor cells with potent immunosuppressive properties. *Eur J Immunol.* 40, 3358–3371. doi: 10.1002/eji.201040667.Cannabinoid

Herrera, M. I., Udovin, L. D., Toro-urrego, N., and Kusnier, C. F. (2018). Palmitoylethanolamide ameliorates hippocampal damage and behavioral dysfunction after perinatal asphyxia in the immature rat brain. *Front Neurosci.* 12:145. doi: 10.3389/fnins.2018.00145

Hezel, M., Ebrahimi, F., Koch, M., and Dehghani, F. (2012). Propidium iodide staining: a new application in fluorescence microscopy for analysis of cytoarchitecture in adult and developing rodent brain. *Micron* 43, 1031–1038. doi: 10.1016/j.micron.2012.04.006

Ho, W.-S., Barrett, D., and Randall, M. (2008). " Entourage " effects of N -palmitoylethanolamide and N -oleoylethanolamide on vasorelaxation to anandamide occur through TRPV1 receptors. *Br. J. Pharmocol.* 155, 837–846. doi: 10.1038/bjp.2008.324

Hohmann, T., Feese, K., Greither, T., Ghadban, C., Jäger, V., Dehghani, F., et al. (2019). Synthetic cannabinoids influence the invasion of glioblastoma cell lines in a cell- and receptor-dependent manner. *Cancers* 11, 1–20. doi: 10.3390/cancers11020161

Hohmann, T., Grabiec, U., Ghadban, C., Feese, K., and Dehghani, F. (2017). The influence of biomechanical properties and cannabinoids on tumor invasion. *Cell Adh. Migr.* 11, 54–67. doi: 10.1080/19336918.2016.1183867

Impellizzeri, D., Siracusa, R., Cordaro, M., Peritore, A. F., Gugliandolo, E., D'Amico, R., et al. (2019). N-Palmitoylethanolamine-oxazoline (PEA-OXA): a new therapeutic strategy to reduce neuroinflammation, oxidative stress associated to vascular dementia in an experimental model of repeated bilateral common carotid arteries occlusion. *Neurobiol. Dis* 125, 77–91. doi: 10.1016/j.nbd.2019.01.007

Járai, Z., Wagner, J. A., Varga, K., Lake, K. D., Compton, D. R., Martin, B. R., et al. (1999). Cannabinoid-induced mesenteric vasodilation through an endothelial site distinct from CB1 or CB2 receptors. *Proc. Natl. Acad. Sci. U.S.A.* 96, 14136–14141. doi: 10.1073/pnas.96.24.14136

Jassam, Y. N., Izzy, S., Whalen, M., Mcgavern, D. B., and El Khoury, J. (2017). Review neuroimmunology of traumatic brain injury: time for a paradigm shift. *Neuron* 95, 1246–1265. doi: 10.1016/j.neuron.2017.07.010

Jonsson, K.-O., Vandevoorde, S., Lambert, D. M., Tiger, G., and Fowler, C. J. (2001). Effects of homologues and analogues of palmitoylethanolamide upon the inactivation of the endocannabinoid anandamide. *Br. J. Pharmocology* 133, 1263–1275. doi: 10.1038/sj.bjp.0704199

Kakizawa, H., Matsui, F., Tokita, Y., Hirano, K., Okumura, A., Kojima, S., et al. (2007). Neuroprotective effect of nipradilol, an NO donor, on hypoxic – ischemic brain injury of neonatal rats. *Early Hum. Dev.* 83, 535–540. doi: 10.1016/j.earlhumdev.2006.10.003

Kallendrusch, S., Kremzow, S., Nowicki, M., Grabiec, U., Winkelmann, R., Benz, A., et al. (2013). The G protein-coupled receptor 55 Ligand L - a -lysophosphatidylinositol exerts after excitotoxic lesion. *Glia* 61, 1822–1831. doi: 10.1002/glia.22560

Kettenmann, H., Hanisch, U.-K., Noda, M., and Verkhratsky, A. (2011). Physiology of microglia. *Physiol. Rev.* 91, 461–553. doi: 10.1152/physrev.00011.2010

Koch, M., Kreutz, S., Boettger, C., Benz, A., Maronde, E., Ghadban, C., et al. (2011a). Palmitoylethanolamide protects dentate gyrus granule cells via peroxisome proliferator-activated receptor-alpha. *Neurotox. Res.* 19, 330–340. doi: 10.1007/s12640-010-9166-2

Koch, M., Kreutz, S., Böttger, C., Grabiec, U., Ghadban, C., Korf, H. W., et al. (2011b). The cannabinoid WIN 55,212-2-mediated protection of dentate gyrus granule cells is driven by CB1 receptors and modulated by TRPA1 and Ca v2.2 channels. *Hippocampus* 21, 554–564. doi: 10.1002/hipo.20772

Kohl, A., Dehghani, F., Korf, H., and Hailer, N. P. (2003). The bisphosphonate clodronate depletes microglial cells in excitotoxically injured organotypic hippocampal slice cultures. *Exp. Neurol.* 181, 1–11. doi: 10.1016/S0014-4886(02)00049-3

Kömüves, L. G., Hanley, K., Lefebvre, A.-M., Man, M.-Q., Ng, D. C., Bikle, D. D., et al. (2000). Stimulation of PPAR a promotes epidermal keratinocyte differentiation *In Vivo*. *J. Invest. Dermatol.* 115, 353–360. doi: 10.1046/j.1523-1747.2000.00073.x

Kondo, S., Kondo, H., Nakane, S., Kodaka, T., Tokumura, A., Waku, K., et al. (1998). 2-Arachidonoylglycerol, an endogenous cannabinoid receptor agonist: identification as one of the major species of monoacylglycerols in various rat tissues, and evidence for its generation through Ca2+‡ -dependent and -independent mechanisms. *FEBS Lett.* 429, 152–156. doi: 10.1016/s0014-5793(98)00581-x

Kozak, K. R., Gupta, R. A., Moody, J. S., Ji, C., Boeglin, W. E., Dubois, R. N., et al. (2002). 15-Lipoxygenase metabolism of 2-Arachidonylglycerol. *J. Biol. Chem.* 277, 23278–23286. doi: 10.1074/jbc.M201084200

Kreutz, S., Koch, M., Böttger, C., Ghadban, C., Korf, H. W., and Dehghani, F. (2009). 2-Arachidonoylglycerol elicits neuroprotective effects on excitotoxically lesioned dentate gyrus granule cells via abnormal-cannabidiol-sensitive receptors on microglial cells. *Glia* 57, 286–294. doi: 10.1002/glia.20756

Kreutz, S., Koch, M., Ghadban, C., Korf, H., and Dehghani, F. (2007). Cannabinoids and neuronal damage: differential effects of THC, AEA and 2-AG on activated microglial cells and degenerating neurons in excitotoxically lesioned rat organotypic hippocampal slice cultures. *Exp. Neurol.* 203, 246–257. doi: 10.1016/j.expneurol.2006.08.010

Kunz, A., Dirnagl, U., and Mergenthaler, P. (2010). Acute pathophysiological processes after ischaemic and traumatic brain injury. *Best Pract. Res. Clin. Anaesthesiol.* 24, 495–509. doi: 10.1016/j.bpa.2010.10.001

Lau, A., and Tymianski, M. (2010). Glutamate receptors, neurotoxicity and neurodegeneration. *Pflugers Arch. Eur. J. Physiol.* 460, 525–542. doi: 10.1007/s00424-010-0809-1

Lipina, C., and Hundal, H. S. (2017). The endocannabinoid system: " NO " longer anonymous in the control of nitrergic signalling? *J. Mol. Cell Biol.* 9, 91–103. doi: 10.1093/jmcb/mjx008

Lourbopoulos, A., Grigoriadis, N., Lagoudaki, R., Touloumi, O., Polyzoidou, E., Mavromatis, I., et al. (2011). Administration of 2-arachidonoylglycerol ameliorates both acute and chronic experimental autoimmune encephalomyelitis. *Brain Res.* 1390, 126–141. doi: 10.1016/j.brainres.2011.03.020

LoVerme, J., La Rana, G., Russo, R., Calignano, A., and Piomelli, D. (2005). The search for the palmitoylethanolamide receptor. *Life Sci.* 77, 1685–1698. doi: 10.1016/j.lfs.2005.05.012

Luongo, L., Palazzo, E., Tambaro, S., Giordano, C., Gatta, L., Scafuro, M. A., et al. (2010). 1-(2′,4′-dichlorophenyl)-6-methyl-N-cyclohexylamine-1,4-dihydroindeno[1,2-c] pyrazole-3-carboxamide, a novel CB2 agonist, alleviates neuropathic pain through functional microglial changes in mice. *Neurobiol. Dis.* 37, 177–185. doi: 10.1016/j.nbd.2009.09.021

Ma, L., Jia, J., Liu, X., Bai, F., Wang, Q., and Xiong, L. (2015). Biochemical and Biophysical Research Communications Activation of murine microglial N9 cells is attenuated through cannabinoid receptor CB2 signaling. *Biochem. Biophys. Res. Commun.* 458, 92–97. doi: 10.1016/j.bbrc.2015.01.073

Magid, L., Heymann, S., Elgali, M., Avram, L., Cohen, Y., Liraz-zaltsman, S., et al. (2019). The Role of CB 2 Receptor in the Recovery of Mice after Traumatic Brain Injury. *J. Neurotrauma* 36, 1836–1846. doi: 10.1089/neu.2018.6063

Meaney, D. F., Morrison, B., and Bass, C. D. (2014). The mechanics of traumatic brain Injury: a review of what we know and what we need to know for reducing its societal burden. *J. Biomech. Eng.* 136:021008. doi: 10.1115/1.4026364

Mechoulam, R., and Shohami, E. (2007). Endocannabinoids and traumatic brain injury. *Mol. Neurobiol.* 36, 68–74. doi: 10.1007/s12035-007-8008-6

Mounsey, R. B., Mustafa, S., Robinson, L., Ross, R. A., Riedel, G., Pertwee, R. G., et al. (2015). Increasing levels of the endocannabinoid 2-AG is neuroprotective in the Parkinson ' s disease. *Exp. Neurol.* 273, 36–44. doi: 10.1016/j.expneurol.2015.07.024

Muccioli, G. G., and Stella, N. (2009). Microglia produce and hydrolyze palmitoylethanolamide. *Neuropharmacology* 54, 16–22. doi: 10.1016/j.neuropharm.2007.05.015

Muccioli, G. G., Xu, C., Odah, E., Cudaback, E., Cisneros, J. A., Lambert, D. M., et al. (2007). Identification of a Novel Endocannabinoid-Hydrolyzing Enzyme Expressed by Microglial Cells. *J. Neurosci.* 27, 2883–2889. doi: 10.1523/JNEUROSCI.4830-06.2007

Musella, A., Fresegna, D., Rizzo, F. R., Gentile, A., Bullitta, S., and De Vito, F. (2017). A novel crosstalk within the endocannabinoid system controls GABA transmission in the striatum. *Sci. Rep.* 7, 1–8. doi: 10.1038/s41598-017-07519-8

Nakamura, Y., Si, Q. S., and Kataoka, K. (1999). Lipopolysaccharide-induced microglial activation in culture: temporal profiles of morphological change and release of cytokines and nitric oxide. *Neurosci. Res.* 35, 95–100. doi: 10.1016/s0168-0102(99)00071-1

Nimmerjahn, A., Kirchhoff, F., and Helmchen, F. (2005). Resting microglial cells are highly dynamic surveillants of brain parenchyma *In Vivo*. *Science* 308, 1314–1319.

Panikashvili, D., Simeonidou, C., Ben-shabat, S., Breuer, A., Mechoulam, R., and Shohami, E. (2001). An endogenous cannabinoid (2-AG) is neuroprotective after brain injury. *Nature* 413, 527–531. doi: 10.1038/35097089

Paterniti, I., Impellizzeri, D., Crupi, R., Morabito, R., Campolo, M., Esposito, E., et al. (2013). Molecular evidence for the involvement of PPAR- δ and PPAR- γ in anti-inflammatory and neuroprotective activities of palmitoylethanolamide after spinal cord trauma. *J. Neuroinflammation* 10, 1–13. doi: 10.1186/1742-2094-10-20

Pertwee, R. G. (2014). Elevating endocannabinoid levels: pharmacological strategies and potential therapeutic applications. *Proc. Nutr. Soc.* 73, 96–105. doi: 10.1017/S0029665113003649

Pertwee, R. G., Howlett, A. C., Abood, M. E., Alexander, S. P. H., Marzo, V., Di Elphick, M. R., et al. (2010). International union of basic and clinical pharmacology . LXXIX . cannabinoid receptors and their ligands: beyond CB 1 and CB 2. *Pharmacol. Rev.* 62, 588–631.

Petrosino, S., Moriello, A. S., Cerrato, S., Fusco, M., Puigdemont, A., De Petrocellis, L. X., et al. (2016). The anti-inflammatory mediator palmitoylethanolamide enhances the levels of 2-arachidonoyl-glycerol and potentiates its actions at TRPV1 cation channels. *Br. J. Pharmocol.* 173, 1154–1162. doi: 10.1111/bph.13084

Portavella, M., Rodriguez-espinosa, N., Galeano, P., Blanco, E., and Romero, J. I. (2018). Oleoylethanolamide and Palmitoylethanolamide Protect Cultured Cortical Neurons Against Hypoxia. *Cannabis Cannabinoid Res.* 3, 171–178. doi: 10.1089/can.2018.0013

Ransohoff, R. M. (2016). A polarizing question: do M1 and M2 microglia exist? *Nat. Neurosci.* 19, 987–991. doi: 10.1038/nn.4338

Ross, R. A., Brockie, H. C., and Pertwee, R. G. (2000). Inhibition of nitric oxide production in RAW264.7 macrophages by cannabinoids and palmitoylethanolamide. *Eur. J. Pharmacol.* 401, 121–130. doi: 10.1016/s0014-2999(00)00437-4

Scotter, E. L., Abood, M. E., and Glass, M. (2010). The endocannabinoid system as a target for the treatment of neurodegenerative disease. *Br. J. Pharmocology* 160, 480–498. doi: 10.1111/j.1476-5381.2010.00735.x

Siracusa, R., Impellizzeri, D., Cordaro, M., Crupi, R., and Cuzzocrea, S. (2017). Anti-inflammatory and neuroprotective effects of Co-UltraPEALut in a mouse model of vascular dementia. *Front. Neurol.* 8:233. doi: 10.3389/fneur.2017.00233

Skaper, S. D., and Facci, L. (2014). Mast cells, glia and neuroinflammation: partners in crime? *Immunology* 141, 314–327. doi: 10.1111/imm.12170

Smart, D., Jonsson, K.-O., Vandevoorde, S., Lambert, D. M., and Fowler, C. J. (2002). ' Entourage ' effects of N -acyl ethanolamines at human vanilloid receptors . Comparison of e € ects upon anandamide-induced vanilloid receptor activation and upon anandamide metabolism. *Br. J. Pharmocology* 136, 452–458. doi: 10.1038/sj.bjp.0704732

Smith, J. A., Das, A., Ray, S. K., and Banik, N. L. (2012). Role of pro-inflammatory cytokines released from microglia in neurodegenerative diseases. *Brain Res. Bull.* 87, 10–20. doi: 10.1016/j.brainresbull.2011.10.004

Stefano, G. B., Bilfinger, T. V., Rialas, C. M., and Dale, G. (2000). 2-arachidonyl-glycerol stimulates nitric oxide release from human immune and vascular tissues and invertebrate immunocytes by cannabinoid receptor 1. *Pharmacol. Res.* 42, 317–322. doi: 10.1006/phrs.2000.0702

Stella, N. (2009). Endocannabinoid signaling in microglial cells. *Neuropharmacology* 56, 244–253. doi: 10.1016/j.neuropharm.2008.07.037. Endocannabinoid

Umemoto, T., and Fujiki, Y. (2012). Ligand-dependent nucleo-cytoplasmic shuttling of peroxisome proliferator-activated receptors, PPAR a and PPAR c. *Genes Cells* 17, 576–596. doi: 10.1111/j.1365-2443.2012.01607.x

Vincent, V. A. M., Tilders, F. J. H., and Van Dam, A.-M. (1998). Production, regulation and role of nitric oxide in glial cells. *Mediators Inflamm.* 7, 239–255. doi: 10.1080/09629359890929

Vinet, J., van Weering, H. R., Heinrich, A., Kälin, R. E., Wegner, A., Brouwer, N., et al. (2012). Neuroprotective function for ramified microglia in hippocampal excitotoxicity. *J. Neuroinflamm.* 9:27. doi: 10.1186/1742-2094-9-27

Walter, L., Franklin, A., Witting, A., Wade, C., Xie, Y., Kunos, G., et al. (2003). Nonpsychotropic cannabinoid receptors regulate microglial cell migration. *J. Neurosci.* 23, 1398–1405. doi: 10.1002/glia.20813

Wang, F., Li, M., Li, X., Kinden, R., Zhou, H., Guo, F., et al. (2015). 2-AG protects primary astrocytes exposed to oxygen-glucose deprivation through a blockade of NDRG2 signaling and STAT3 phosphorylation. *Exp. Neurol.* 273, 1–25. doi: 10.1089/rej.2015.1703

Wang, S., Zhang, H., Geng, B., Xie, Q., Li, W., Deng, Y., et al. (2018). 2-arachidonyl glycerol modulates astrocytic glutamine synthetase via p38 and ERK1 / 2 pathways. *J. Neuroinflamm.* 15, 1–10. doi: 10.1186/s12974-018-1254-x

Warden, A., Truitt, J., Merriman, M., Ponomareva, O., Jameson, K., Ferguson, L. B., et al. (2016). Localization of PPAR isotypes in the adult mouse and human brain. *Sci. Rep.* 6, 1–15. doi: 10.1038/srep27618

Xu, J., Chavis, J. A., Racke, M. K., and Drew, P. D. (2006). Peroxisome proliferator-activated receptor- a and retinoid X receptor agonists inhibit inflammatory responses of astrocytes. *J. Neuroimmunol.* 176, 95–105. doi: 10.1016/j.jneuroim.2006.04.019

Xu, J., Storer, P. D., Chavis, J. A., Racke, M. K., Drew, P. D., and Rock, L. (2005). Agonists for the peroxisome proliferator- activated receptor- a and the retinoid X receptor inhibit inflammatory responses of microglia. *J. Neurosci. Res.* 411, 403–411. doi: 10.1002/jnr.20518

Yao, X., Liu, S., Ding, W., Yue, P., Jiang, Q., Zhao, M., et al. (2017). TLR4 signal ablation attenuated neurological de fi cits by regulating microglial M1 / M2 phenotype after traumatic brain injury in mice. *J. Neuroimmunol.* 310, 38–45. doi: 10.1016/j.jneuroim.2017.06.006

Zhang, J., and Chen, C. (2008). Endocannabinoid 2-arachidonoylglycerol protects neurons by limiting COX-2 elevation. *J. Biol. Chem. Biol. Chem.* 283, 22601–22611. doi: 10.1074/jbc.M800524200

Zhang, J., Hoffert, C., Vu, H. K., Groblewski, T., Ahmad, S., Donnell, D. O., et al. (2003). Induction of CB2 receptor expression in the rat spinal cord of neuropathic but not in ¯ ammatory chronic pain models. *Eur. J. Neurosci.* 17, 2750–2754. doi: 10.1046/j.1460-9568.2003.02704.x

Zhou, T., Huang, Z., Sun, X., Zhu, X., Zhou, L., Li, M., et al. (2017). Microglia polarization with M1 / M2 phenotype changes in rd1 mouse model of retinal degeneration. *Front. Neuroanat.* 11:77. doi: 10.3389/fnana.2017.00077

Conflict of Interest: The authors declare that the research was conducted in the absence of any commercial or financial relationships that could be construed as a potential conflict of interest.

Copyright © 2019 Hohmann, Pelzer, Kleine, Hohmann, Ghadban and Dehghani. This is an open-access article distributed under the terms of the Creative Commons Attribution License (CC BY). The use, distribution or reproduction in other forums is permitted, provided the original author(s) and the copyright owner(s) are credited and that the original publication in this journal is cited, in accordance with accepted academic practice. No use, distribution or reproduction is permitted which does not comply with these terms.

International Journal of
Molecular Sciences

MDPI

Article

Nimodipine Exerts Time-Dependent Neuroprotective Effect after Excitotoxical Damage in Organotypic Slice Cultures

Urszula Hohmann [1], Chalid Ghadban [1], Tim Hohmann [1], Joshua Kleine [1], Miriam Schmidt [1], Christian Scheller [2], Christian Strauss [2] and Faramarz Dehghani [1,*]

[1] Medical Faculty, Institute of Anatomy and Cell Biology, Martin Luther University Halle-Wittenberg, 06112 Halle (Saale), Germany; urszula.hohmann@medizin.uni-halle.de (U.H.); chalid.ghadban@medizin.uni-halle.de (C.G.); tim.hohmann@medizin.uni-halle.de (T.H.); joshua.kleine@student.uni-halle.de (J.K.); miriam.schmidt@student.uni-halle.de (M.S.)
[2] Department of Neurosurgery, Medical Faculty, Martin Luther University Halle-Wittenberg, 06120 Halle (Saale), Germany; christian.scheller@klinikum-bremerhaven.de (C.S.); christian.strauss@uk-halle.de (C.S.)
* Correspondence: faramarz.dehghani@medizin.uni-halle.de; Tel.: +49-3455571707

Abstract: During injuries in the central nervous system, intrinsic protective processes become activated. However, cellular reactions, especially those of glia cells, are frequently unsatisfactory, and further exogenous protective mechanisms are necessary. Nimodipine, a lipophilic L-type calcium channel blocking agent is clinically used in the treatment of aneurysmal subarachnoid haemorrhage with neuroprotective effects in different models. Direct effects of nimodipine on neurons amongst others were observed in the hippocampus as well as its influence on both microglia and astrocytes. Earlier studies proposed that nimodipine protective actions occur not only via calcium channel-mediated vasodilatation but also via further time-dependent mechanisms. In this study, the effect of nimodipine application was investigated in different time frames on neuronal damage in excitotoxically lesioned organotypic hippocampal slice cultures. Nimodipine, but not nifedipine if pre-incubated for 4 h or co-applied with NMDA, was protective, indicating time dependency. Since blood vessels play no significant role in our model, intrinsic brain cell-dependent mechanisms seems to strongly be involved. We also examined the effect of nimodipine and nifedipine on microglia survival. Nimodipine seem to be a promising agent to reduce secondary damage and reduce excitotoxic damage.

Keywords: nimodipine; excitotoxicity; nifedipine; neuroprotection; microglia

check for updates

Citation: Hohmann, U.; Ghadban, C.; Hohmann, T.; Kleine, J.; Schmidt, M.; Scheller, C.; Strauss, C.; Dehghani, F. Nimodipine Exerts Time-Dependent Neuroprotective Effect after Excitotoxical Damage in Organotypic Slice Cultures. *Int. J. Mol. Sci.* **2022**, *23*, 3331. https://doi.org/10.3390/ijms23063331

Academic Editor: Bae Hwan Lee

Received: 21 January 2022
Accepted: 16 March 2022
Published: 19 March 2022

Publisher's Note: MDPI stays neutral with regard to jurisdictional claims in published maps and institutional affiliations.

Copyright: © 2022 by the authors. Licensee MDPI, Basel, Switzerland. This article is an open access article distributed under the terms and conditions of the Creative Commons Attribution (CC BY) license (https://creativecommons.org/licenses/by/4.0/).

1. Introduction

Nimodipine has been found to be beneficial in many central nervous system disorders, including stroke, brain injury, cerebral ischemia, epilepsy, dementia and age-related degenerative diseases [1–4]. Nimodipine acts as a potent cerebral vasodilator and binds to cell membranes (K_D(human) = 0.27 nM) and is a more lipophilic molecule than the calcium channel antagonist nifedipine [5]. Furthermore, the tissue concentration after application is three times higher than for nifedipine, indicating differences in crossing the blood–brain barrier [5]. Clinical and in vivo studies with nimodipine have demonstrated protection against ischemic damage [6] and an increased postischemic perfusion. Although this is a possible vascular mechanism for nimodipine's protective effect, an additional direct effect by blocking calcium entry into neurons has also been suggested. In animal models, nimodipine has been shown to induce neuroprotection against glutamate or amyloid β-induced toxicity [7] and has been found to improve dementia [8] and memory in a variety of cognitive tests in aging subjects [9]. Nimodipine has affected neurons in the hippocampus in different studies [2,5,9–15]. Effects in the hippocampus seem to be independent from the vasculature [10]. In most in vitro studies, the effective concentrations of nimodipine

were considerably higher than required for its cerebro-vascular effects; for this reason, nimodipine at therapeutic doses seems not to affect the release of neurotransmitters from neurons in healthy brain tissue [5].

On the cellular level, both microglia and astrocytes were influenced by nimodipine [16–18]. The neuroprotective effect of nimodipine in inflammation-mediated neurodegenerative disease was attributed to the inhibition of microglial activation, since nimodipine significantly inhibited the production of nitric oxide (NO) and further cytokines from lipopolysaccharide (LPS)-stimulated cells [16]. Activated microglia migrate to the lesion site and proliferate [19]. Changes in the number of microglia are associated with neuronal damage. However, both increases in the pro-reparative and decreases in the pro-inflammatory population might induce neuroprotective effects [19]. Furthermore, nimodipine attenuated neurotoxicity induced by interferon (IFN) γ in human astrocytes [17].

Nifedipine, a further calcium antagonist, also displayed neuroprotection but at a lower potency and in much higher concentrations (100 µM) than nimodipine [20]. Nimodipine was neuroprotective, whereas nifedipine exerted no effects in clinical applications and in in vitro models [5,21].

In this study, organotypic hippocampal slice cultures (OHSC), a well-studied model with physiological neuronal cell morphology, and their in vivo-like organization were used to further characterize direct cellular effects of nimodipine [22].

Since nimodipine was neuroprotective against excitotoxical damage in cell culture [11,12], an influence of nimodipine and nifedipine on a neuronal damage model of excitotoxically lesioned OHSC was examined. Furthermore, the effect of calcium antagonists on microglia viability was assessed.

2. Results

2.1. Nimodipine Is Protective When Administered Simultaneously with NMDA

The number of Propidium Iodide (PI)-positive neurons was assessed, and all data were normalized to the N-Methyl-D-Aspartat (NMDA, 10 µM) group. Control slices (CTL) exhibited a good neuronal preservation. Only few PI-positive nuclei were found in the granule cell layer (GCL) of the dentate gyrus (DG) (8.43%/GCL, Figure 1b). Nimodipine (0.1 µM: 10.35%/GCL; 10 µM: 7.96%/GCL; 20 µM: 9.21%/GCL, Figure 1a) alone had no significant effect on the number of PI-positive cells in the GCL.

Lesion of OHSC with 10 µM NMDA resulted in a massive accumulation of PI-positive nuclei in the DG (100%/GCL, Figure 1a,b). Treatment of lesioned OHSC with nimodipine 0.1 µM (102.4%/GCL) parallel to NMDA had no effect on cell degeneration, whereas a higher concentration (1 µM: 52.88%/GCL; 20 µM: 38.83%/GCL) led to a significant reduction in the number of PI-positive cells. Parallel incubation with nifedipine did not influence (0.1 µM: 83.28%/GCL; 1 µM: 119.7%/GCL; 20 µM: 98%/GCL) the neuronal damage.

Application of NMDA (100%/GCL) led to an increase in the number of IB4-positive microglia in comparison to CTL (37.27%/GCL). Combined treatment of nimodipine (0.1 µM: 87.12%/GCL; 1 µM: 82.08%/GCL; 20 µM: 76.67%/GCL) or nifedipine (0.1 µM: 123.9%/GCL; 1 µM: 85.22%/GCL; 20 µM: 74.70%/GCL) with NMDA resulted in no significant changes in the number of IB4-positive cells (Figure 2).

2.2. Nimodipine Showed No Neuroprotective Effects When Applied after Neuronal Damage

Application of nimodipine (0.1 µM: 114.3%/GCL; 1 µM: 71.80%/GCL; 20 µM: 125.8%/GCL) or nifedipine (0.1 µM: 185.5%/GCL; 1 µM: 68.92%/GCL; 20 µM: 129.2%/GCL) 4 h after beginning of the lesion with NMDA did not lead to a reduction in the number of PI-positive cells (Figure 1c). No significant changes in the number of IB4-positive cells was observed when nimodipine (0.1 µM: 111.9/GCL; 1 µM: 82.29%/GCL; 20 µM: 107.5%/GCL) or nifedipine (0.1 µM: 78.76%/GCL; 1 µM: 114.1%/GCL; 20 µM: 102%/GCL) were applied 4 h after beginning of the lesion with NMDA (Figure 2).

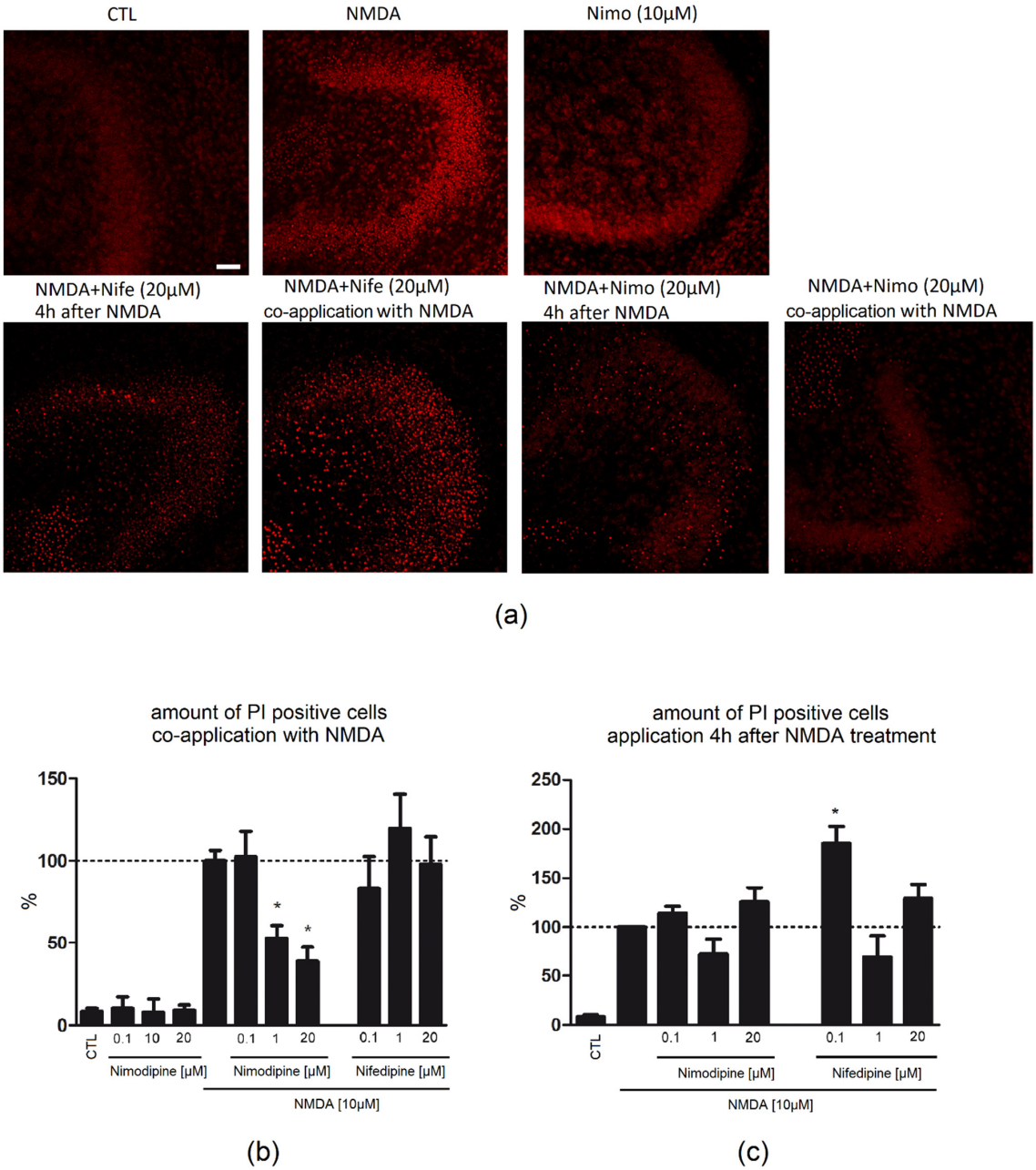

Figure 1. Effect of nimodipine and nifedipine after NMDA damage at different time points of application. Amount of PI-positive damaged neurons after NMDA (10 µM) damage followed by treatment with nimodipine (0.1, 1, 20 µM) or nifedipine (0.1, 1, 20 µM). (**a**) In CTL slices, few PI-positive cells (red) were found, whereas after NMDA treatment, a massive increase in the number of dead cells in GCL of DG was observed. Representative pictures for nimodipine (20 µM) and nifedipine (20 µM)-treated slices after/during neuronal damage (**b**) In the control group, few positive neurons were detected (n_{CTL} = 30). Incubation with NMDA (n_{NMDA} = 20) over 4 h induced a massive increase in the number of damaged cells in the region of interest. Nimodipine, when applied alone to OHSC had no significant effect on the number of PI-positive damaged cells ($n_{0.1\mu M}$ = 6; $n_{10\mu M}$ = 3; $n_{20\mu M}$ = 9). Nimodipine ($n_{0.1\mu M}$ = 5; $n_{1\mu M}$ = 15; $n_{20\mu M}$ = 19) but not nifedipine ($n_{0.1\mu M}$ = 11; $n_{1\mu M}$ = 10; $n_{20\mu M}$ = 7) was protective after NMDA (10 µM) lesion, when applied directly with NMDA. (**c**) Nimodipine ($n_{0.1\mu M\text{-}4\,h}$ = 4; $n_{1\mu M\text{-}4\,h}$ = 8 $n_{20\mu M\text{-}4\,h}$ = 16) and nifedipine ($n_{0.1\mu M\text{-}4\,h}$ = 3, $n_{1\mu M\text{-}4\,h}$ = 4; $n_{20\mu M\text{-}4\,h}$ = 11) applied after 4 h showed no protective effects after NMDA damage in OHSC. All values were normalized to NMDA. Data are presented as mean with SEM. * depict statistically significant results with $p < 0.05$. Scale bar = 50 µM.

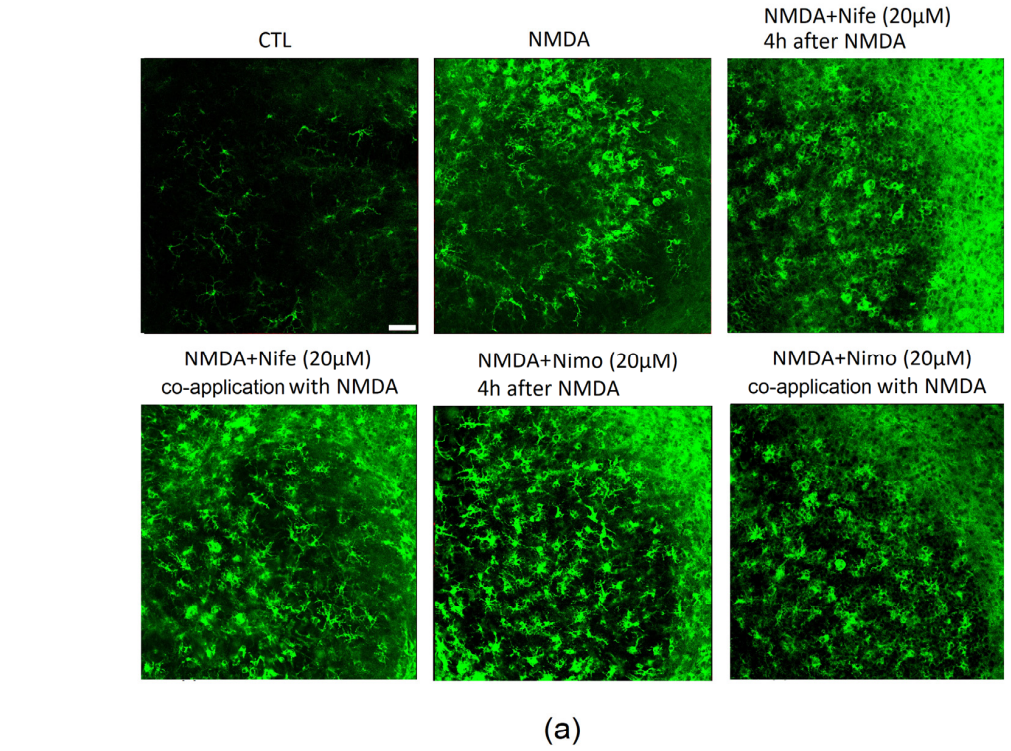

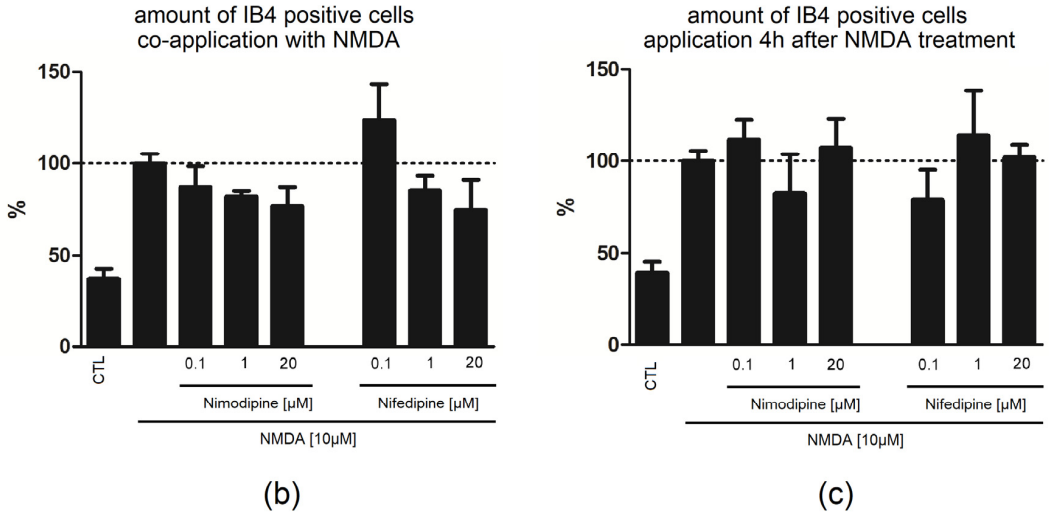

Figure 2. Effects of nimodipine or nifedipine after NMDA damage at different time points of application. Amount of IB4-positive microglia cells after NMDA (10 µM) lesion followed by treatment with nimodipine (0.1, 1, 20 µM) or nifedipine (0.1, 1, 20 µM). (**a**) In CTL slices, few IB4-positive cells (green) were found, whereas NMDA treatment led to a massive increase in the number of IB4-positive cells in GCL of DG. Representative pictures for nimodipine (20 µM) and nifedepine (20 µM)-treated slices after/during neuronal damage (**b**) In the control group, few IB4-positive cells were detected (n_{CTL} = 21). Incubation with NMDA (n_{NMDA} = 35) over 4 h induced a massive increase in the number of IB4-positive cells in the DG. Nimodipine ($n_{0.1\mu M}$ = 5; $n_{1\mu M}$ = 3; $n_{20\mu M}$ = 10) and nifedipine ($n_{0.1\mu M}$ = 5 $n_{1\mu M}$ = 6; $n_{20\mu M}$ = 7) did not significantly affect the number of microglia after NMDA (10 µM) lesion, when applied directly with NMDA. (**c**) Nimodipine ($n_{0.1\mu M\text{-}4\,h}$ = 4; $n_{1\mu M\text{-}4\,h}$ = 4; $n_{20\mu M\text{-}4\,h}$ = 10) and nifedipine ($n_{0.1\mu M\text{-}4\,h}$ = 9, $n_{1\mu M\text{-}4\,h}$ = 4; $n_{20\mu M\text{-}4\,h}$ = 14), when applied 4 h after the induction of injury, showed no significant effects on the number of IB4-positive cells. All values were normalized to those of the NMDA group. Data are presented as mean with SEM. Scale bar = 50 µM.

2.3. Four Hour Preincubation with Nimodipine Is Protective, Whereas 24 h Preapplication of Nimodipine or Nifedipine Had No Effect on Neuronal Damage

Application of nimodipine 4 h before NMDA damage until fixation was protective (0.1 µM: 56.6%/GCL; 1 µM: 58.1%/GCL; 20 µM: 64.38/GCL) in contrast to nifedipine (0.1 µM: 112.2%/GCL; 1 µM: 83.26%/GCL; 20 µM: 88.06%/GCL, Figure 3).

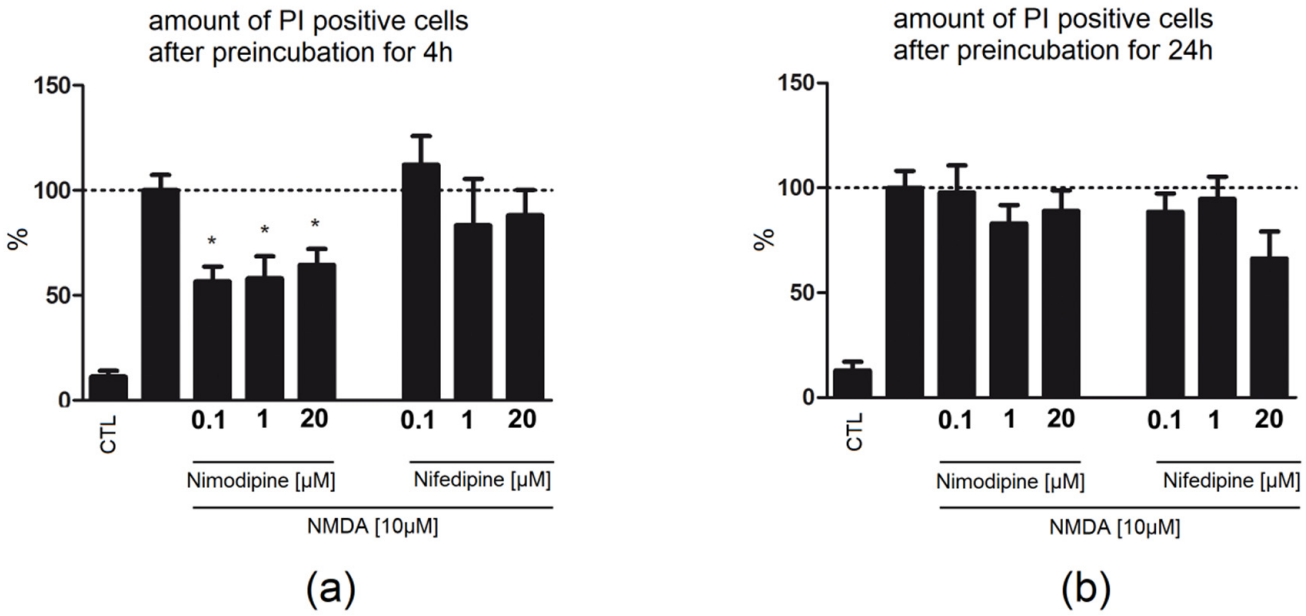

Figure 3. Effect of nimodipine and nifedipine in NMDA-damaged OHSC at different time points of application. Only few cells were positive in the control group ((**a**) n_{CTL} = 18; (**b**) n_{CTL} = 17). Application of NMDA ((**a**) n_{NMDA} = 28; (**b**) n_{NMDA} = 27) for 4 h led to accumulation of PI-positive nuclei in the dentate gyrus. (**a**) Preincubation (4 h) with nimodipine ($n_{0.1\mu M}$ = 8; $n_{1\mu M}$ = 11; $n_{20\mu M}$ = 9) led to significant reduction in the number of damaged neurons in comparison to nifedipine treatment ($n_{0.1\mu M}$ = 9; $n_{1\mu M}$ = 9; $n_{20\mu M}$ = 10) that showed no reduction (**b**) Nimodipine ($n_{0.1\mu M}$ = 19; $n_{1\mu M}$ = 16; $n_{20\mu M}$ = 13) or nifedipine ($n_{0.1\mu M}$ = 18; $n_{1\mu M}$ = 12; $n_{20\mu M}$ = 5), when pre-applied for 24 h before NMDA-damaged OHSC had no significant effect on the number of PI-positive damaged cells. All values were normalized to NMDA. Data are presented as mean with SEM. * depict statistically significant results with $p < 0.05$.

Preincubation for 24 h with nimodipine (0.1 µM: 97.82%/GCL; 1 µM: 83.01%/GCL; 20 µM: 89/GCL) or nifedipine (0.1 µM: 88.53%/GCL; 1 µM: 94.63%/GCL; 20 µM: 66.34%/GCL, Figure 3) for 24 h followed by co-application with NMDA and incubation after the lesion until fixation did not lead to reduction in the number of PI-positive cells.

2.4. Application of Nimodipine Had No Effect on Microglia Cell Death

Nimodipine (0.1 µM:0.21; 1 µM: 0.07; 20 µM: 0.15) or nifedipine (0.1 µM:0.32; 1 µM: 0.04; 20 µM: 0.0) displayed no statistically resolvable effect on microglial cell death in primary cell culture, whereas clodronate (CLO: 0.79) depleted microglia significantly in comparison to CTL (0.04) (Figure 4).

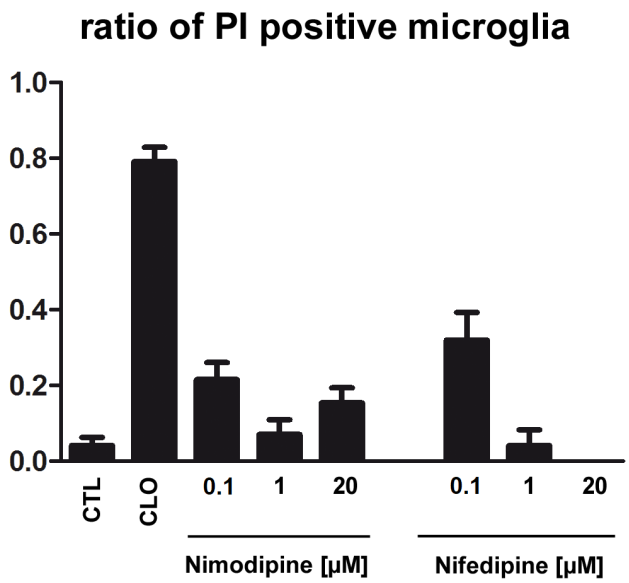

Figure 4. Effects of nimodipine or nifedipine on microglia cell death. The application of nimodipine ($n_{0.1\mu M}$ = 21; $n_{1\mu M}$ = 15; $n_{20\mu M}$ = 17) or nifedipine ($n_{0.1\mu M}$ = 13; $n_{1\mu M}$ = 6; $n_{20\mu M}$ = 7) had no effect on cell death in primary microglia (5000). Clodronate (n_{CLO} = 59) increased the number of damaged microglia in comparison to CTL (n_{CTL} = 25) with typical changes in morphology, whereas nimodipine or nifedipine had no effect on cell death. Data from three independent experiments are presented as mean with SEM.

3. Discussion

Nimodipine, a 1,4-dihydropyridine Ca^{2+} channel antagonist, has been used as a neuroprotective agent in subarachnoidal haemorrhage (SAH) against vasospasm [23,24]. Improved clinical outcome of patients seems to be associated with additional Ca^{2+} channel independent mechanisms such as inhibition of vasospasm, increase in fibrinolytic activity, neuroprotection, reduction of spreading, depolarization and inhibition of microthromboembolism [6,25]. Furthermore, in various in vivo and in vitro models of cerebral ischemia, nimodipine was found to be protective [4,6].

3.1. Nimodipine but Not Nifedipine Is Protective in OHSC

Whereas the primary injury cannot be reversed, the secondary injury, as a result of destructive and self-propagating biological changes in cells and tissues leads to further dysfunction and cell death after hours to weeks [26]. The therapeutic actions focus on deceleration and containment of cellular and molecular mechanisms during the secondary injury [27]. However, effective drugs are missing.

In this study, organotypic hippocampal slice cultures (OHSC), a well-studied model with unaltered morphology of neuronal cells and their in vivo-like organization, was used.

In order to simulate neuronal damage, NMDA was applied to OHSC to induce excitotoxicity. Excitotoxicity is a complex process triggered by glutamate receptor activation that results in Ca^{2+} overload, which activates various intracellular mechanisms, enzymes and free radicals, leading to degeneration of dendrites and cell death [28]. It has recently become clear that there exists a number of subtypes of apoptosis and an overlap between apoptosis, necrosis and autophagy. Cells can die via different mechanisms with partially high mechanistic overlap and with some forms of induced cell death cascades being reversible, even in late stages [29]. Excitotoxic neuronal death as observed in OHSC is characterized by a continuum of necrotic, apoptotic, and autophagic events [30], which can be visualized by PI labelling [31]. The degradation of neurons is associated with an inflammatory response from glia cells and peripheral immune cells [27]. From a mechanistic point of view, calcium antagonists might be promising agents counteracting excitotoxicity.

In our study, nimodipine but not nifedipine reduced the secondary damage in OHSC if co-applied with NMDA. Findings on nimodipine (2–5 μM) are in accordance with previous studies showing protective effects in hippocampal neurons against glutamate excitotoxicity [12,32,33]. While NMDA receptor activation is a primary contributor to excitotoxic injury, the relative contribution of voltage-dependent calcium channels to excitotoxicity may differ depending on particular type of neuron. An antagonist that selectively blocks one of the different glutamate receptors or Ca^{2+} channels may therefore exhibit differential effectiveness in protecting different populations of neurons [28]. Consistent with this idea, nimodipine at various concentrations was shown to protect against injury generated by exogenous application of NMDA or glutamate to cultured hippocampal neurons [11]. In the OHSC model, simultaneous application of nimodipine with damaging NMDA was protective in concentrations of 1 and 20 μM. Nifedipine showed no protective effect. It seems plausible that further unknown mechanisms next to calcium antagonisation exist for nimodipine-mediated neuroprotection that are absent for nifedipine.

Several studies reported on reductions of L-type calcium currents by nimodipine in hippocampal CA1 neurons [2,13,14,34]. Furthermore, and in agreement with this study, investigations in in vitro and animal models indicated neuroprotection against glutamate or amyloid β-induced toxicity [7] and in focal ischemia (MCA occlusion) [5]. In mesencephalic neuron–glia cultures and in NGF-differentiated PC-12 cells, nimodipine had neuroprotective effects [16,20]. In line with our findings, Nuglisch and colleagues reported on the neuroprotective effect of nimodipine independent of cerebral vasodilation and suggested direct actions on neurons or glial cells [35]. Nimodipine (10 μM) was found to completely block synaptic activity, significantly reduce the toxicity induced by 0.1 mM magnesium, and protect hippocampal cultures from excitotoxicity [12]. Notably, higher nimodipine concentrations might express nonselective effects or inhibit further channels or targets [12]. In rat cortical synaptosomes, nimodipine at 0.5 to 25 μM inhibited the release of endogenous glutamate that was correlated with the inhibition of Ca^{2+} uptake [5].

In substantia nigra but not in the tegmental area, both nimodipine and nifedipine improved survival of dopaminergic neurons after 4 weeks of application [36]. Furthermore, nimodipine but not nifedipine ameliorated survival of Neuro2a cells [37], and nimodipine rescued Neuro2a cells from ethanol-, heat- and mechanically induced cell death in a dose-dependent manner [38]. In the majority of models, nimodipine but not nifedipine showed positive effects on neuronal survival.

Still, there is some controversy about nifedipine-mediated neuroprotection. Some authors observed for nifedipine protective effects after acute axotomy [36], in dopaminergic neurons [39] and in pancreatic β-cells [40,41]. In addition, nifedipine but not nimodipine was found to exhibit antioxidant properties [42,43]. In our model, nifedipine (0.1 μM) increased the number of damaged neurons if applied 4 h after neuronal damage, and there is no clear explanation for this effect. It was shown before that nifedipine in smaller doses was toxic in patients [44]. It was also shown that nifedipine alters lipid concentration, and that lipids are mediators of neurotoxic effects of astrocytes, which may be the mechanism behind nifedipine toxicity in this model. However, the mechanism behind nifedipine-mediated toxicity 4 h after NMDA damage is unclear [45,46]. Despite protective properties of nifedipine due to the blockade of calcium channels, nimodipine seems to involve additional and other mechanisms [5,6]. The data hint to a possible variable expression of targets between cell and tissue types; as well, the region of the central nervous system seems to be crucial.

3.2. The Absence of Functional Blood Vessels in OHSC and the Neuroprotective Effect of Nimodipine but Not Nifedipine Strengthens the Presence of Other Intrinsic Targets

Nimodipine blocks the flux of extracellular calcium through L-type voltage-gated calcium channels. Voltage-dependent calcium channels (VDCCs) are widely distributed throughout the body and regulate the excitability and secretion in a diverse range of cell

types. L-type calcium channels (LTCC) are expressed in the smooth muscles of vascular system on neurons and astrocytes [47,48].

In vivo applied nimodipine (0.1 μM) did not increase the recovery of dentate granule cells after 10 min of anoxia and did not reduce the decrease in ATP in dentate gyrus and CA1 [10]. Mechanisms behind neuroprotection for both calcium antagonists are not sufficiently clarified. Intravenous administration of nimodipine increased the firing rates of rabbit CA1 neurons, whereas nifedipine had no effect [21]. Conversely, nifedipine (1 μM) also reduced calcium spike potentials in young guinea pig CA1 [49] and rat CA3 neurons [50].

3.3. The Application Time of Nimodipine Is Crucial

Nimodipine was protective in OHSC when applied 4 h before damage or simultaneously to NMDA treatment, whereas 24 h preapplication of nimodipine or treatment 4 h after damage had no effect on neuronal damage. Preischemic application (1 h prior to ischemia) of nimodipine (0.1 or 0.3 mg/kg) was earlier reported to reduce the neuronal damage in the hippocampal CA1 subfield without affecting the postischemic local cerebral blood flow [35]. In that study, neuronal necrosis in the pyramidal cells of the hippocampus (CA3 and CA4 subfields) was only marginal and stayed unaffected from treatment with nimodipine [35]. In line with our findings, nimodipine-administered postischemic failed to preserve neurons from damage in a four-vessel occlusion model of global ischemia in rats [35]. These results show that nimodipine is able to protect neurons against ischemic damage if preincubated for a short time (1 h). Pretreatment with nimodipine before intracranial transection of the facial nerve led to an increased neuronal survival in the facial nucleus [51]. In addition, in mesencephalic neuron–glia cultures, pretreatment (30 min) with nimodipine (10 and 30 μM) reduced the degeneration of dopaminergic neurons after LPS (5 ng/mL) treatment [16]. Furthermore, nimodipine conferred neuroprotection in PC-12 cells only in a narrow therapeutic time window within the first 5 h [20]. In addition and in a model of intracranial facial nerve transection, nimodipine when administrated for 3 days preoperatively and 1 month postoperatively increased the number of surviving neurons [51]. Our results in OHSC support a concept of nimodipine-mediated protection in a temporally close vicinity to the injury. In our model, a 4 h pre-incubation or co-application with NMDA was followed by incubation with nimodipine until the fixation significantly reduced neuronal damage, but a pre-incubation 24 h before damage or application 4 h after starting the injury remained without any positive effects. Nimodipine might be qualified by these findings as a protective agent for elective neurosurgical procedures and should be considered in the planning of such interventions.

3.4. Effect of Nimodipine on Glia Cells

Among glia cells, microglia initiate the inflammatory response following various brain injuries, and once activated, migrate to the lesion site, proliferate and are the source of immunomodulatory molecules. Microglia-mediated attenuation in inflammation and oxidative stress is believed to protect neurons [19]. Nimodipine seem to act via multiple cellular targets. In the absence of microglia, nimodipine-mediated neuroprotection was abolished in dopaminergic neurons after damage [16] indicating direct effects on microglia. Nimodipine was also shown to block microglia phagocytosis but without interfering with inflammation or neuronal cell death mechanisms and was sufficient to enhance neuronal survival during inflammation [52]. However, nimodipine (5, 10, and 25 μM), when added in vitro to macrophages collected from splanchnic artery occlusion shock rats, significantly enhanced their phagocytic activity [53]. Nonetheless, microglia and macrophages differ in their inflammatory profile during injury as shown before [54].

The expression of LTCC, a target of nimodipine, was shown to be induced in activated microglia [55]. However, the effects on calcium household seem not to be responsible for nimodipine-mediated neuroprotection. Therefore, the possible role of microglia was investigated. Here, the effects of nimodipine and nifedipine on microglia viability and

the number of IB4-positive cells after NMDA damage in OHSC were analysed. Both substances did not affect cell death of primary microglia or the number of microglia in OHSC in comparison to NMDA. In previous studies, the activation of microglia was inhibited after incubation with nimodipine, due to reduction in the production of nitric oxide (NO), tumour necrosis factor α (TNF α), interleukin-1ß and prostaglandin E2 from LPS-stimulated microglia [16]. Nimodipine was found to inhibit cell death triggered by amyloid ß in primary microglia and interleukin-1ß release from microglia (challenged with ATP 1 mM, LPS 1 µg/mL) [56]. Microglia cells were shown to express NMDA-receptors, but it is still a matter of debate if those are functional [19,57,58]. Microglia were shown to express NMDA receptors in the murine and human central nervous system, and these receptors triggered microglia activation in vitro and secretion of neurotoxic factors [58]. Conversely, pretreatment with NMDA antagonists did not affect production of NO or intracellular Ca^{2+} elevation induced by TNF, the mRNA expression of pro- or anti-inflammatory markers, or phagocytic activity of rodent microglial cells [57]. Further reports confirmed that microglial cells do not express functional NMDA in the rodent brain [19,59,60]. Taken together, it seems unlikely that stimulation with NMDA of primary microglia would change the effect on cellular death, since in OHSC after NMDA treatment, a massive increase in microglia numbers was observed [61,62].

In addition, nifedipine-mediated protection was associated with a reduction in proinflammatory cytokines from microglia in substantia nigra [36,63]. However, microglia pass through spatial, temporal, and functional diversity during homeostasis but also in diseases [64]. Possibly, microglial cells from various brain regions respond differently to nimodipine or nifedipine treatment. It is also plausible that nimodipine interact with microglia and change their function. In addition, direct interactions with neurons cannot be ruled out; however, blocking of calcium entry into neurons was observed by both nimodipine and nifedipine.

In human astrocytes, nimodipine significantly suppressed toxic secretions after treatment with interferon (IFN)-γ. Earlier results indicate that nimodipine-mediated protection involves microglia or/and astrocytes, since nimodipine improved neuroinflammation-induced memory deficits after systemic infusion of LPS [65]. Nimodipine, if applied before intracranial transection of the facial nerve, led to an increased amount of microglia, macrophages and activated astrocytes in the facial nucleus [51]. In agreement with this data, continuous nimodipine treatment led to higher glial fibrillary acid protein-immunoreactivity in astrocytes after resection of the facial and hypoglossal nerves [66]. Both studies indicate long-term effects of nimodipine on astrocytes and microglia.

The modulation of neuroinflammatory responses due to LTCC in activated microglia and astrocytes needs further examination, and it is still not fully clear how nimodipine effects are mediated. However, this study showed that nimodipine seems to be a powerful agent which reduces excitotoxic damage and restricts spreading of secondary damage.

Few studies analysed the mechanisms of nimodipine actions in the CNS. After spinal cord injury, nimodipine-treated rats showed improvements in gliosis, CGRP+ fibre sprouting, and an increased KCC2 expression in lumbar motor neurons [67]. Furthermore, nimodipine downregulated lncRNA nuclear paraspeckle assembly transcript 1, upregulated miR-27a, downregulated microtubule associated protein tau, inhibited brain tissue cell apoptosis and enhanced brain cell activity, resulting in improved outcomes and cognitive performance [68]. The effects of nifedipine were not assessed in the mentioned studies. Nimodipine-mediated neuroprotection seems therefore to be a result of actions on glia cells and neurons.

4. Materials and Methods

All experiments involving animal material were performed in accordance with Directive 2010/63/EU of the European Parliament and the Council of the European Union (22 September 2010).

4.1. Primary Cell Cultures and Cell Lines

Primary microglia were detached from microglia–astrocyte co-cultures prepared from cerebral cortices of neonatal wild-type mice as described before (Grabiec et al., 2019). Brains were removed, and cells were dissociated after treatment with 4mg/mL trypsin (Merck Millipore, Burlington, MA, USA) and 0.5 mg/mL DNAse (Worthington, Bedford, MA, USA) in Hank's balanced salts solution (Invitrogen, Carlsbad, CA, USA). This procedure resulted in the growth of a confluent astrocyte monolayer with attached microglia cells on top. Microglia cells were isolated from the monolayer by gentle shaking, and a purity of approximately 99% was reached.

Murine primary cells were cultured in medium consisting of DMEM (Invitrogen) with 10% FBS (Invitrogen) and 1 mL streptomycin/penicillin.

The microglial cells (5.000) were seeded into 24-well plates and treated with nimodipine (Bayer, Leverkusen, Germany, 0.1 µM, solved in ethanol), nifedipine (Bayer, 0.1 µM, solved in ethanol) or clodronate (10 µg/mL solved in water, Bayer for 24 h). For cell death analyses, propidium iodide (PI, 5 µg/mL, Sigma Aldrich, St. Louis, MO USA) was added 2 h before the fixation with 4% paraformaldehyde (PFA).

Cells were incubated with nucleic acid stain Sytox Green (Invitrogen, 1:10.000) and covered with DAKO fluorescent mounting medium (DAKO Diagnostika GmbH, Hamburg, Germany).

4.2. Organotypic Hippocampal Slice Cultures (OHSC)

OHSC were obtained from 5-day-old BL6J wild-type mice and prepared as published before [61,69–71]. After decapitation and dissection of the brains, the cerebellum and frontal pol were removed. Up to six 350 µM thin slices were obtained after cutting on vibratome VT 1200S (Leica, Wetzlar, Germany). The OHSC were incubated on inserts (Sarstedt, Nümbrecht, Germany) in culture medium (pH = 7.3) consisting of 47% MEM (Invitrogen, Carlsbad, CA, USA), 25% Hank's balanced salt solution (HBSS), 25% normal horse serum (Invitrogen), 1% glutamine, 0,45% glucose (Braun, Melsungen, Germany), 1% penicillin/streptomycin (Invitrogen), and 0.8 µg/mL ascorbic acid (Invitrogen). The culture dishes were incubated at 35 °C in fully humidified atmosphere with 5% CO_2. OHSC were divided into different experimental groups and treated with nimodipine or nifedipine in concentrations 0.1, 1 and 20 µM and NMDA (10 µM) (Figure 5). For detection of degenerating neuronal nuclei, 5 µg/mL PI was added 2 h prior to fixation. Afterwards, 4% PFA was applied for at least 24 h. For isolectin B4 (IB4, Vector laboratories, Burlingame, CA, USA) staining, OHSC were placed into a 24-well plate and washed with phosphate buffered saline (PBS) containing 0.03% (*v*/*v*) Triton X-100 (PBS-T) for 10 min. OHSC were then incubated with normal goat serum (diluted 1:20 in PBS-T) for 30 min and stained with FITC-conjugated IB4 diluted 1:50 in PBS-T containing 0.05% (*v*/*v*) bovine serum albumin (Sigma Aldrich) for 16 h. Thereafter, OHSC were washed with PBS/Triton for 10 min and then for 5 min with Aqua dest, and finally coverslipped with DAKO fluorescent mounting medium (DAKO Diagnostika GmbH, Hamburg, Germany). OHSC were analysed with Zeiss (LSM 700, Zeiss, Göttingen, Germany) and Leica (Leica DMi8, Leica, Wetzlar, Germany) confocal laser scanning microscopes. For detection of PI labelled degenerating neurons, monochromatic light at 543 nm and an emission bandpass filter of 585–615 nm was used. For visualization of IB4-labelled microglia, monochromatic light at 488 nm with a dichroic beam splitter (FT 488/543) and an emission band pass filter of 505–530 nm were used. PI and IB4-positive cells were counted in the granule cell layer (GCL) of the dentate gyrus (cells/GCL) using a MatLab script.

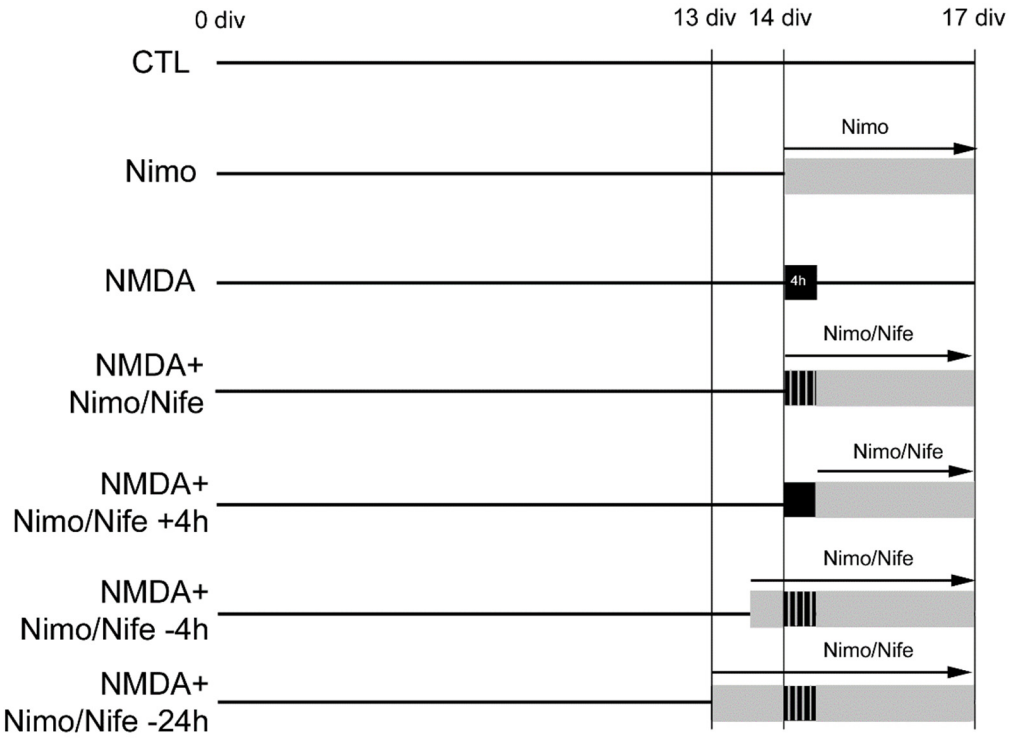

Figure 5. Treatment of murine OHSC. Murine OHSC were excitotoxically lesioned on 14 div. Next to the negative control (CTL) and positive control group damaged with NMDA (10 μM) for 4 h, one set of OHSC was treated simultaneously with NMDA (10 μM) and nimodipine (Nimo) or nifedipine (Nife). Further groups of OHSC were pretreated with nimodipine or nifedipine for 4 or 24 h before lesion.

5. Conclusions

Since the excitotoxical damage was reduced after treatment with nimodipine, this substance might be a useful treatment option for a broad spectrum of neuronal injuries. Some aspects about nimodipine actions are crucial: first, the time of the application, and second, the concentration. Further, L-type channel blockers such as nifedipine are not protective in OHSC; for this reason, the mechanism of nimodipine seems to be unique.

Author Contributions: Conceptualization, U.H., F.D., C.S. (Christian Strauss) and C.S. (Christian Scheller); methodology, T.H.; software, U.H.; validation, U.H., C.G., T.H., J.K. and M.S.; formal analysis, U.H.; investigation, U.H., C.G., T.H., J.K. and M.S.; resources, F.D. and C.S. (Christian Strauss); data curation, U.H. and T.H.; writing—original draft preparation, U.H.; writing—review and editing, U.H., F.D., T.H. and C.S. (Christian Strauss); visualization, U.H.; supervision, U.H. and F.D.; project administration, U.H. and F.D. All authors have read and agreed to the published version of the manuscript.

Funding: This research received no external funding.

Institutional Review Board Statement: The animal study was reviewed and approved by the local authorities of the State of Saxony–Anhalt (permission number: I11M18, date: 01 December 2012), protecting animals and regulating tissue collection used for scientific purposes.

Informed Consent Statement: Not applicable.

Data Availability Statement: All datasets generated for this study are included in the article.

Conflicts of Interest: The authors declare no conflict of interest.

References

1. Meyer, F.B.; Anderson, R.E.; Sundt, T.M.; Sharbrough, F.W. Selective Central Nervous System Calcium Channel Blockers—A New Class of Anticonvulsant Agents. *Mayo Clin. Proc.* **1986**, *61*, 239–247. [CrossRef]
2. Scriabine, A.; Schuurman, T.; Traber, J. Pharmacological basis for the use of nimodipine in central nervous system disorders. *FASEB J.* **1989**, *3*, 1799–1806. [CrossRef]
3. Sandin, M.; Jasmin, S.; Levere, T. Aging and cognition: Facilitation of recent memory in aged nonhuman primates by nimodipine. *Neurobiol. Aging* **1990**, *11*, 573–575. [CrossRef]
4. Horn, J.; De Haan, R.J.; Vermeulen, M.; Luiten, P.G.; Limburg, M. Nimodipine in animal model experiments of focal cerebral ischemia: A systematic review. *Stroke* **2001**, *32*, 2433–2438. [CrossRef]
5. Scriabine, A.; Van den Kerckhoff, W. Pharmacology of Nimodipine—A Review. *Ann. N. Y. Acad. Sci.* **1988**, *522*, 698–706. [CrossRef]
6. Carlson, A.P.; Hänggi, D.; Macdonald, R.L.; Shuttleworth, C.W. Nimodipine Reappraised: An Old Drug with a Future. *Curr. Neuropharmacol.* **2019**, *18*, 65–82. [CrossRef]
7. Weiss, J.H.; Pike, C.J.; Cotman, C.W. Rapid Communication: Ca^{2+} Channel Blockers Attenuate β-Amyloid Peptide Toxicity to Cortical Neurons in Culture. *J. Neurochem.* **2008**, *62*, 372–375. [CrossRef]
8. Fritze, J.; Walden, J. Clinical findings with nimodipine in dementia: Test of the calcium hypothesis. *J. Neural Transm. Suppl.* **1995**, *46*, 439–453.
9. Moyer, J.R.; Thompson, L.; Black, J.P.; Disterhoft, J. Nimodipine increases excitability of rabbit CA1 pyramidal neurons in an age- and concentration-dependent manner. *J. Neurophysiol.* **1992**, *68*, 2100–2109. [CrossRef]
10. Kass, I.S.; Cottrell, J.E.; Chambers, G. Magnesium and Cobalt, not Nimodipine, Protect Neurons against Anoxic Damage in the Rat Hippocampal Slice. *Anesthesiology* **1988**, *69*, 710–715. [CrossRef]
11. Abele, A.E.; Scholz, K.P.; Scholz, W.K.; Miller, R.J. Excitotoxicity induced by enhanced excitatory neurotransmission in cultured hippocampal pyramidal neurons. *Neuron* **1990**, *4*, 413–419. [CrossRef]
12. McLeod, J.R.; Shen, M.; Kim, D.J.; Thayer, S.A. Neurotoxicity mediated by aberrant patterns of synaptic activity between rat hippocampal neurons in culture. *J. Neurophysiol.* **1998**, *80*, 2688–2698. [CrossRef]
13. Black, J.; Disterhoft, J.F.; Yeh, J.Z. Dihydropyridine effects on non-inactivating calcium currents in CA1 neurons. *Soc. Neurosci. Abstr.* **1990**, *16*, 510.
14. O'Dell, T.J.; Alger, B.E. Single calcium channels in rat and guinea pig hippocampal neurons. *J. Physiol.* **1991**, *436*, 739–767. [CrossRef]
15. O'Regan, M.H.; Kocsis, J.D.; Waxman, S.G. Nimodipine and nifedipine enhance transmission at the Schaffer collateral CA1 pyramidal neuron synapse. *Exp. Brain Res.* **1991**, *84*, 224–228. [CrossRef]
16. Li, Y.; Hu, X.; Liu, Y.; Bao, Y.; An, L. Nimodipine protects dopaminergic neurons against inflammation-mediated degeneration through inhibition of microglial activation. *Neuropharmacology* **2009**, *56*, 580–589. [CrossRef]
17. Hashioka, S.; Klegeris, A.; McGeer, P.L. Inhibition of human astrocyte and microglia neurotoxicity by calcium channel blockers. *Neuropharmacology* **2012**, *63*, 685–691. [CrossRef]
18. Leisz, S.; Simmermacher, S.; Prell, J.; Strauss, C.; Scheller, C. Nimodipine-dependent protection of schwann cells, astrocytes and neuronal cells from osmotic, oxidative and heat stress is associated with the activation of AKT and CREB. *Int. J. Mol. Sci.* **2019**, *20*, 4578. [CrossRef]
19. Kettenmann, H.; Hanisch, U.-K.; Noda, M.; Verkhratsky, A. Physiology of Microglia. *Physiol. Rev.* **2011**, *91*, 461–553. [CrossRef]
20. Lecht, S.; Rotfeld, E.; Arien-Zakay, H.; Tabakman, R.; Matzner, H.; Yaka, R.; Lelkes, P.I.; Lazarovici, P. Neuroprotective effects of nimodipine and nifedipine in the NGF-differentiated PC12 cells exposed to oxygen-glucose deprivation or trophic withdrawal. *Int. J. Dev. Neurosci.* **2012**, *30*, 465–469. [CrossRef]
21. Thompson, L.; Deyo, R.; Disterhoft, J. Nimodipine enhances spontaneous activity of hippocampal pyramidal neurons in aging rabbits at a dose that facilitates associative learning. *Brain Res.* **1990**, *535*, 119–130. [CrossRef]
22. Grabiec, U.; Hohmann, T.; Hammer, N.; Dehghani, F. Organotypic Hippocampal Slice Cultures As a Model to Study Neuroprotection and Invasiveness of Tumor Cells. *J. Vis. Exp.* **2017**, *126*, e55359. [CrossRef] [PubMed]
23. Murray, G.D.; Teasdale, G.M.; Schmilz, H.; Schmitz, H. Nimodipine in traumatic subarachnoid haemorrhage: A re-analysis of the HIT I and HIT II trials. *Acta Neurochir.* **1996**, *138*, 1163–1167. [CrossRef]
24. Vergouwen, M.D.; Vermeulen, M.; Roos, Y.B. Effect of nimodipine on outcome in patients with traumatic subarachnoid haemorrhage: A systematic review. *Lancet Neurol.* **2006**, *5*, 1029–1032. [CrossRef]
25. Macdonald, R.L. Origins of the concept of vasospasm. *Stroke* **2016**, *47*, e11–e15. [CrossRef]
26. Dirnagl, U.; Simon, R.P.; Hallenbeck, J.M. Ischemic tolerance and endogenous neuroprotection. *Trends Neurosci.* **2003**, *26*, 248–254. [CrossRef]
27. Ricker, J.H.; Arenth, P.M. Traumatic brain injury. *Funct. MRI Appl. Clin. Neurol. Psychiatry* **2006**, *26*, 197–206.
28. Mattson, M.P. Excitotoxicity. *Stress Physiol. Biochem. Pathol.* **2019**, *3*, 125–134. [CrossRef]
29. D'Arcy, M.S. Cell death: A review of the major forms of apoptosis, necrosis and autophagy. *Cell Biol. Int.* **2019**, *43*, 582–592. [CrossRef]
30. Wang, Y.; Qin, Z.-H. Molecular and cellular mechanisms of excitotoxic neuronal death. *Apoptosis* **2010**, *15*, 1382–1402. [CrossRef]
31. Ebrahimi, F.; Hezel, M.; Koch, M.; Ghadban, C.; Korf, H.-W.; Dehghani, F. Analyses of neuronal damage in excitotoxically lesioned organotypic hippocampal slice cultures. *Ann. Anat.-Anat. Anz.* **2010**, *192*, 199–204. [CrossRef]

32. Porter, N.M.; Thibault, O.; Thibault, V.; Chen, K.-C.; Landfield, P.W. Calcium Channel Density and Hippocampal Cell Death with Age in Long-Term Culture. *J. Neurosci.* **1997**, *17*, 5629–5639. [CrossRef]
33. Brewer, L.D.; Thibault, O.; Staton, J.; Thibault, V.; Rogers, J.T.; Garcia-Ramos, G.; Kraner, S.; Landfield, P.W.; Porter, N.M. Increased vulnerability of hippocampal neurons with age in culture: Temporal association with increases in NMDA receptor current, NR2A subunit expression and recruitment of L-type calcium channels. *Brain Res.* **2007**, *1151*, 20–31. [CrossRef]
34. Regan, L.J.; Sah, D.W.; Bean, B.P. Ca^{2+} channels in rat central and peripheral neurons: High-threshold current resistant to dihydropyridine blockers and ω-conotoxin. *Neuron* **1991**, *6*, 269–280. [CrossRef]
35. Nuglisch, J.; Karkoutly, C.; Mennel, H.D.; Roßberg, C.; Krieglstein, J. Protective Effect of Nimodipine against Ischemic Neuronal Damage in Rat Hippocampus without Changing Postischemic Cerebral Blood Flow. *J. Cereb. Blood Flow Metab.* **1990**, *10*, 654–659. [CrossRef]
36. Daschil, N.; Humpel, C. Nifedipine and nimodipine protect dopaminergic substantia nigra neurons against axotomy-induced cell death in rat vibrosections via modulating inflammatory responses. *Brain Res.* **2014**, *1581*, 1–11. [CrossRef]
37. Herzfeld, E.; Speh, L.; Strauss, C.; Scheller, C. Nimodipine but Not Nifedipine Promotes Expression of Fatty Acid 2-Hydroxylase in a Surgical Stress Model Based on Neuro2a Cells. *Int. J. Mol. Sci.* **2017**, *18*, 964. [CrossRef]
38. Herzfeld, E.; Strauss, C.; Simmermacher, S.; Bork, K.; Horstkorte, R.; Dehghani, F.; Scheller, C. Investigation of the Neuroprotective Impact of Nimodipine on Neuro2a Cells by Means of a Surgery-Like Stress Model. *Int. J. Mol. Sci.* **2014**, *15*, 18453–18465. [CrossRef]
39. Ma, Z.; Zhou, Y.; Xie, J. Nifedipine Prevents Iron Accumulation and Reverses Iron-Overload-Induced Dopamine Neuron Degeneration in the Substantia Nigra of Rats. *Neurotox. Res.* **2012**, *22*, 274–279. [CrossRef]
40. Syeda, K.; Mohammed, A.M.; Arora, D.K.; Kowluru, A. Glucotoxic conditions induce endoplasmic reticulum stress to cause caspase 3 mediated lamin B degradation in pancreatic β-cells: Protection by nifedipine. *Biochem. Pharmacol.* **2013**, *86*, 1338–1346. [CrossRef]
41. Arora, D.K.; Mohammed, A.M.; Kowluru, A. Nifedipine prevents etoposide-induced caspase-3 activation, prenyl transferase degradation and loss in cell viability in pancreatic β-cells. *Apoptosis* **2012**, *18*, 1–8. [CrossRef] [PubMed]
42. Üstün, M.; Gürbilek, M.; Ak, A.; Vatansev, H.; Duman, A. Effects of magnesium sulfate on tissue lactate and malondialdehyde levels in experimental head trauma. *Intensiv. Care Med.* **2001**, *27*, 264–268. [CrossRef] [PubMed]
43. Yao, K.; Ina, Y.; Nagashima, K.; Ohmori, K.; Ohno, T. Antioxidant Effects of Calcium Antagonists in Rat Brain Hohogenates. *Biol. Pharm. Bull.* **2000**, *23*, 766–769. [CrossRef] [PubMed]
44. Ramoska, E.; Spiller, H.A.; Myers, A. Calcium channel blocker toxicity. *Ann. Emerg. Med.* **1990**, *19*, 649–653. [CrossRef]
45. Houston, M.C.; Olafsson, L.; Burger, M.C. Effects of Nifedipine GITS and Atenolol Monotherapy on Serum Lipis, Blood Pressure, Heart Rate, and Weight in Mild to Moderate Hypertension. *Angiol. J. Vasc. Dis.* **1991**, *42*, 681–690.
46. Guttenplan, K.A.; Weigel, M.K.; Prakash, P.; Wijewardhane, P.R.; Hasel, P.; Rufen-Blanchette, U.; Münch, A.E.; Blum, J.A.; Fine, J.; Neal, M.C.; et al. Neurotoxic reactive astrocytes induce cell death via saturated lipids. *Nature* **2021**, *599*, 102–107. [CrossRef]
47. Ortner, N.J.; Striessnig, J. L-type calcium channels as drug targets in CNS disorders. *Channels* **2016**, *10*, 7–13. [CrossRef]
48. Latour, I.; Hamid, J.; Beedle, A.M.; Zamponi, G.W.; Macvicar, B.A. Expression of voltage-gated Ca^{2+} channel subtypes in cultured astrocytes. *Glia* **2003**, *41*, 347–353. [CrossRef]
49. Higashi, H.; Sugita, S.; Matsunari, S.; Nishi, S. Calcium-dependent potentials with different sensitivities to calcium agonists and antagonists in guinea-pig hippocampal neurons. *Neuroscience* **1990**, *34*, 35–47. [CrossRef]
50. Gähwiler, B.; Brown, D. Muscarine affects calcium-currents in rat hippocampal pyramidal cells in vitro. *Neurosci. Lett.* **1987**, *76*, 301–306. [CrossRef]
51. Mattsson, P.; Aldskogius, H.; Svensson, M. Nimodipine-induced improved survival rate of facial motor neurons following intracranial transection of the facial nerve in the adult rat. *J. Neurosurg.* **1999**, *90*, 760–765. [CrossRef]
52. Neher, J.J.; Neniskyte, U.; Zhao, J.-W.; Bal-Price, A.; Tolkovsky, A.M.; Brown, G.C. Inhibition of Microglial Phagocytosis Is Sufficient to Prevent Inflammatory Neuronal Death. *J. Immunol.* **2011**, *186*, 4973–4983. [CrossRef]
53. Sturniolo, R.; Altavilla, D.; Berlinghieri, M.C.; Squadrito, F.; Caputi, A.P. Splanchnic artery occlusion shock in the rat: Effects of the calcium entry blockers nimodipine and verapamil. *Circ. Shock* **1988**, *24*, 43–53.
54. Zarruk, J.G.; Greenhalgh, A.D.; David, S. Microglia and macrophages differ in their inflammatory profile after permanent brain ischemia. *Exp. Neurol.* **2018**, *301*, 120–132. [CrossRef]
55. Espinosa-Parrilla, J.F.; Martínez-Moreno, M.; Gasull, X.; Mahy, N.; Rodríguez, M. The L-type voltage-gated calcium channel modulates microglial pro-inflammatory activity. *Mol. Cell. Neurosci.* **2015**, *64*, 104–115. [CrossRef]
56. Sanz, J.M.; Chiozzi, P.; Colaianna, M.; Zotti, M.; Ferrari, D.; Trabace, L.; Zuliani, G.; Di Virgilio, F. Nimodipine inhibits IL-1ß release stimulated by amyloid ß from microglia. *Br. J. Pharmacol.* **2012**, *167*, 1702–1711.
57. Murakawa-Hirachi, T.; Mizoguchi, Y.; Ohgidani, M.; Haraguchi, Y.; Monji, A. Effect of memantine, an anti-Alzheimer's drug, on rodent microglial cells in vitro. *Sci. Rep.* **2021**, *11*, 6151. [CrossRef]
58. Kaindl, A.M.; Degos, V.; Peineau, S.; Gouadon, E.; Chhor, V.; Loron, G.; Le Charpentier, T.; Josserand, J.; Ali, C.; Vivien, D.; et al. Activation of microglial N-methyl-D-aspartate receptors triggers inflammation and neuronal cell death in the developing and mature brain. *Ann. Neurol.* **2012**, *72*, 536–549. [CrossRef]
59. Wendt, S.; Wogram, E.; Korvers, L.; Kettenmann, H. Experimental Cortical Spreading Depression Induces NMDA Receptor Dependent Potassium Currents in Microglia. *J. Neurosci.* **2016**, *36*, 6165–6174. [CrossRef]

60. Takeda, A.; Shinozaki, Y.; Kashiwagi, K.; Ohno, N.; Eto, K.; Wake, H.; Nabekura, J.; Koizumi, S. Microglia mediate non-cell-autonomous cell death of retinal ganglion cells. *Glia* **2018**, *66*, 2366–2384. [CrossRef]
61. Grabiec, U.; Koch, M.; Kallendrusch, S.; Kraft, R.; Hill, K.; Merkwitz, C.; Ghadban, C.; Lutz, B.; Straiker, A.; Dehghani, F. The endocannabinoid N-arachidonoyldopamine (NADA) exerts neuroprotective effects after excitotoxic neuronal damage via cannabinoid receptor 1 (CB1). *Neuropharmacology* **2012**, *62*, 1797–1807. [CrossRef]
62. Ebrahimi, F.; Koch, M.; Pieroh, P.; Ghadban, C.; Hobusch, C.; Bechmann, I.; Dehghani, F. Time dependent neuroprotection of mycophenolate mofetil: Effects on temporal dynamics in glial proliferation, apoptosis, and scar formation. *J. Neuroinflamm.* **2012**, *9*, 89. [CrossRef]
63. Colonna, M.; Butovsky, O. Microglia Function in the Central Nervous System during Health and Neurodegeneration. *Annu. Rev. Immunol.* **2017**, *35*, 441–468. [CrossRef]
64. Masuda, T.; Sankowski, R.; Staszewski, O.; Prinz, M. Microglia Heterogeneity in the Single-Cell Era. *Cell Rep.* **2020**, *30*, 1271–1281. [CrossRef]
65. Hopp, S.C.; D'Angelo, H.M.; E Royer, S.; Kaercher, R.M.; Crockett, A.M.; Adzovic, L.; Wenk, G.L. Calcium dysregulation via L-type voltage-dependent calcium channels and ryanodine receptors underlies memory deficits and synaptic dysfunction during chronic neuroinflammation. *J. Neuroinflamm.* **2015**, *12*, 56. [CrossRef]
66. Guntinas-Lichius, O.; Martinez-Portillo, F.; Lebek, J.; Angelov, D.N.; Stennert, E.; Neiss, W.F. Nimodipine maintains in vivo the increase in GFAP and enhances the astroglial ensheathment of surviving motoneurons in the rat following permanent target deprivation. *J. Neurocytol.* **1997**, *26*, 241–248. [CrossRef]
67. Guo, F.; Zheng, X.; He, Z.; Zhang, R.; Zhang, S.; Wang, M.; Chen, H.; Wang, W. Nimodipine Promotes Functional Recovery after Spinal Cord Injury in Rats. *Front. Pharmacol.* **2021**, *12*, 2521. [CrossRef]
68. Li, J.W.; Ren, S.H.; Ren, J.R.; Zhen, Z.G.; Li, L.R.; Hao, X.D.; Ji, H.M. Nimodipine improves cognitive impairment after subarachnoid hemorrhage in rats through incRNA NEAT1/miR-27a/MAPT axis. *Drug Des. Dev. Ther.* **2020**, *14*, 2295–2306. [CrossRef]
69. Hohmann, T.; Grabiec, U.; Ghadban, C.; Feese, K.; Dehghani, F. The influence of biomechanical properties and cannabinoids on tumor invasion. *Cell Adhes. Migr.* **2017**, *11*, 54–67. [CrossRef]
70. Grabiec, U.; Hohmann, T.; Ghadban, C.; Rothgänger, C.; Wong, D.; Antonietti, A.; Groth, T.; Mackie, K.; Dehghani, F. Protective Effect of N-Arachidonoyl Glycine-GPR18 Signaling after Excitotoxical Lesion in Murine Organotypic Hippocampal Slice Cultures. *Int. J. Mol. Sci.* **2019**, *20*, 1266. [CrossRef]
71. Hohmann, U.; Pelzer, M.; Kleine, J.; Hohmann, T.; Ghadban, C.; Dehghani, F. Opposite Effects of Neuroprotective Cannabinoids, Palmitoylethanolamide, and 2-Arachidonoylglycerol on Function and Morphology of Microglia. *Front. Neurosci.* **2019**, *13*, 1180. [CrossRef] [PubMed]

5.1 Hinweis zur vorliegenden Genehmigung der Verlage

Die folgenden Artikel wurden unter den Bedingungen der Creative Commons Attribution (CC BY)-Lizenz veröffentlicht (https://creativecommons.org/licenses/by/4.0/), welche eine uneingeschränkte Nutzung, Verbreitung und Vervielfältigung in jedem Medium unter Angabe der Autoren (siehe Artikel) und Quellen erlaubt.

1. **Kleine J**, Leisz S, Ghadban C, Hohmann T, Prell J, Scheller C, Strauss C, Simmermacher S, Dehghani F (**2021**) Variants of Oxidized Regenerated Cellulose and Their Distinct Effects on Neuronal Tissue. Int. J. Mol. Sci. 2021,22,11467. https://doi.org/ 10.3390/ijms222111467
   Richtlinien des Journals:
   https://www.mdpi.com/openaccess *(17.01.2024)*
   Beitrag als Autor:
   Im folgenden Artikel war in an der methodischen Konzipierung und Gestaltung der Studie sowie der Verfassung und Editierung des Manuskripts beteiligt. Führte die Untersuchungen durch und analysierte die Daten.

2. **Kleine J,** Hohmann U, Hohmann T, Ghadban C, Schmidt M, Laabs S, Alessandri B and Dehghani F (**2022**) Microglia-Dependent and Independent Brain Cytoprotective Effects of Mycophenolate Mofetil During Neuronal Damage. Front. Aging Neurosci. 14:863598. doi: 10.3389/fnagi.2022.863598
   Richtlinien des Journals:
   https://www.frontiersin.org/about/open-access *(17.01.2024)*
   Beitrag als Autor:
   Im folgenden Artikel war in an der Konzipierung und Gestaltung der Studie sowie der Verfassung des Manuskripts beteiligt. Führte die Untersuchungen durch und analysierte die Daten.

3. Hohmann U, Pelzer M, **Kleine J**, Hohmann T, Ghadban C and Dehghani F (**2019**) Opposite Effects of Neuroprotective Cannabinoids, Palmitoylethanolamide, and 2-Arachidonoylglycerol on Function and Morphology of Microglia. Front. Neurosci. 13:1180. doi: 10.3389/fnins.2019.01180
   Richtlinien des Journals:
   https://www.frontiersin.org/about/open-access *(17.01.2024)*
   Beitrag als Autor:
   Im folgenden Artikel war in an der methodischen und formalen Analyse der Daten sowie der Untersuchungen beteiligt. Weiter war ich an dem Verfassen des Manuskriptes beteiligt.

4. Hohmann U, Ghadban C, Hohmann T, **Kleine J**, Schmidt M, Scheller C, Strauss C, Dehghani, F **(2022)** Nimodipine Exerts Time-Dependent Neuroprotective Effect after Excitotoxical Damage in Organotypic Slice Cultures. Int. J. Mol. Sci. 2022, 23,3331. https://doi.org/10.3390/ ijms23063331
   Richtlinien des Journals:
   https://www.mdpi.com/openaccess *(17.01.2024)*
   Beitrag als Autor:
   Im folgenden Artikel war in an der Überprüfung und Untersuchung der Daten beteiligt.

6. Erklärungen

Ich erkläre, dass ich mich an keiner anderen Hochschule einem Promotionsverfahren unterzogen bzw. eine Promotion begonnen habe.

Ich erkläre, die Angaben wahrheitsgemäß gemacht zu haben und die wissenschaftliche Arbeit an keiner anderen wissenschaftlichen Einrichtung zur Erlangung eines akademischen Grades eingereicht zu haben.

Ich erkläre an Eides statt, dass ich die Arbeit selbstständig und ohne fremde Hilfe verfasst habe. Alle Regeln der guten wissenschaftlichen Praxis wurden eingehalten; es wurden keine anderen als die von mir angegebenen Quellen und Hilfsmittel benutzt und die den benutzten Werken wörtlich oder inhaltlich entnommenen Stellen wurden als solche kenntlich gemacht.

Münster, den 01.10.2024
Joshua Kleine

Tierversuche

Alle Tierversuche wurden in Übereinstimmung mit der Richtlinie über Ethik- und Verwendungsrichtlinien der Richtlinie 2010/63/EU des Europäischen Parlaments und des Rates der Europäischen Union durchgeführt. Die Präparate wurden von den örtlichen Behörden für die Pflege und Verwendung von Labortieren genehmigt (Genehmigungsnummern: K11M1, I11M27, I11M18,).

Die Tierversuche in vivo (Abb. 5 und Abb. 6) mit MMF erfolgten in Zusammenarbeit mit dem Institut für Neurochirurgische Pathophysiologie der Universitätsmedizin der Johannes Gutenberg-Universität Mainz (Langenbeckstr. 1, 55131 Mainz, Versuchsleiter: Dr. sc. nat. ETH Beat Alessandri). Die Genehmigung nach § 8 Abs. 1 des Tierschutzgesetzes für den Versuch erfolgte unter dem Titel „Therapeutisches Wirkungsfenster des Immunsuppressivums Mykophenolat Mofetil (MMF) auf entzündliche Prozesse und Narbenbildung nach fokaler zerebraler Kontusion bei der Ratte“ (G 18-1-52, NTP-ID: 00022727-1-7).

Abbildungen

Die Abbildung 2 wurde unter den Bedingungen der Creative Commons Attribution (CC BY)-Lizenz veröffentlicht (https://creativecommons.org/licenses/by/4.0/), welche eine uneingeschränkte Nutzung, Verbreitung und Vervielfältigung in jedem Medium unter Angabe der Autoren (siehe Artikel) und Quellen erlaubt.

Wang, H., Li, J., Zhang, H., Wang, M., Xiao, L., Wang, Y., et al. (2023a). Regulation of microglia polarization after cerebral ischemia. Front Cell Neurosci 17, 1182621. doi: 10.3389/fncel.2023.1182621.

Angaben des Journals https://www.frontiersin.org/about/open-access *(17.01.2024)*

7. Danksagungen

Ich möchte mich herzlich bei Herrn Prof. Dr. Faramarz Dehghani für die exzellente Betreuung meiner Doktorarbeit bedanken. Lieber Faramarz, vielen Dank für dein hervorragendes Heranführen an das wissenschaftliche Arbeiten und Denken, die vielen konstruktiven Gespräche und Kritiken, sowie deine Bereitschaft als ein Mentor in jeglicher Hinsicht, sowohl wissenschaftlich als auch menschlich.

Mein Dank gilt auch Herrn Prof. Dr. Julian Prell, der sich bereitwillig für die Zweitbetreuung meiner Arbeit erklärt hat. Weiter möchte ich mich beim Herrn Prof. Dr. Christian Strauss und seinem Team, insbesondere Herr Dr. Sebastian Simmermacher und Frau Dr. Sandra Leisz, für die gute Zusammenarbeit und Kooperation unserer Projekte bedanken.

Mein großer Dank gilt Frau Dr. Urszula Hohmann. Liebe Ula, Danke für die Betreuung all die Jahre in Hinblick auf mein wissenschaftliches Arbeiten über viele nicht wissenschaftlichen Themen hinaus. Auch möchte ich mich bei Herrn Dr. Tim Hohmann bedanken, insbesondere bei statistischen Fragen sowie bei analytischen Problemen.

Ein weiterer Dank gilt Chalid Ghadban, der mich mit großer Geduld bei meinen ersten Versuchen im Labor begleitet hat. Vielen Dank für die vielen guten Gespräche.

Auch möchte ich mit bei Herrn Dr. Beat Alessandri, Josef Olbrich und Herrn Prof. Dr. Oliver Kempski für die Zusammenarbeit bei den *in vivo* Versuchen mit MMF bedanken.

Vielen Dank an Miriam Schmidt, Sebastian Laabs, Markus Pelzer, Christoph Walsleben, Kerstin Feese, Carolin Vogel, Agnes Dorn und all die vielen weiteren Wegbegleiter während der Jahre, die zu einer einmaligen kollegialen und freundschaftlichen Arbeitsgruppe beigetragen haben.